

# Analysing the role of surface aging on the impact of microplastic pollution in soil matrices

A thesis presented for the degree of  
Doctor of Philosophy

Dominic Savage

Lancaster Environment Centre

Lancaster University

2024



LEVERHULME  
TRUST

Material  
Social  
Futures

*“.. In our obscurity, in all this vastness, there is no hint that help will come from elsewhere to save us from ourselves.”*

*Carl Sagan*

It is up to us.

# Contents

Table Of Contents	iii
Declaration	viii
Acknowledgements	ix
Abstract	xi
List Of Figures	xx
List Of Tables	xxiii
Glossary of Terms	xxiv
Training in Material Social Futures	xxvi
<b>1 Introduction</b>	<b>1</b>
1.1 Research questions . . . . .	1
1.1.1 Graphical outline of research questions . . . . .	2
1.2 Plastics, Society, & the Environment . . . . .	3
1.2.1 A Brief Introduction . . . . .	3
1.2.2 A Brief History . . . . .	5
1.2.3 A Brief Future . . . . .	7
<b>2 Materials and Methods</b>	<b>9</b>
2.1 Materials used in this research . . . . .	9
2.1.1 Plastic sheets . . . . .	9

2.1.2	Powders . . . . .	9
2.2	X-ray Photoelectron Spectroscopy (XPS) . . . . .	11
2.2.1	Background . . . . .	11
2.2.2	Interpreting spectra . . . . .	13
2.3	Plasma surface treatment . . . . .	16
2.3.1	Background . . . . .	16
2.3.2	Reaction mechanisms . . . . .	18
2.3.3	Plasma surface treatment & modification . . . . .	18
2.3.4	Methodology . . . . .	20
2.4	Accelerated photoaging . . . . .	20
2.5	Scanning Electron Microscopy (SEM) . . . . .	22
2.6	Cryomilling . . . . .	23
2.7	Contact Angle (CA) analysis . . . . .	24
<b>3</b>	<b>Assessing what is known about the fate of plastic pollution in terrestrial matrices</b>	<b>27</b>
	Graphical Abstract . . . . .	27
3.1	The emergence of soil pollution as a major theme in microplastics research . . . . .	28
3.2	Plastic is a novel anthropogenic pollutant in terrestrial ecosystems . . . . .	28
3.2.1	Mechanisms for plastic dispersion . . . . .	29
3.2.2	Accumulation in the environment . . . . .	30
3.3	Hazards associated with microplastic accumulation . . . . .	32
3.3.1	Physical harms . . . . .	33
3.3.2	Additive leaching . . . . .	33
3.3.3	Impacts on microbial diversity . . . . .	34
3.3.4	Plant health . . . . .	34
3.3.5	Interactions with other chemicals in the environment . . . . .	34
3.3.6	Effects on soil properties . . . . .	35
3.3.7	Impacts on the carbon cycle, and other nutrient cycles . . . . .	35
3.4	Mechanisms for plastic degradation in soils . . . . .	36
3.4.1	Photodegradation . . . . .	36
3.4.2	Mechanical stress . . . . .	39
3.4.3	Bio-degradation . . . . .	39

3.4.4	Accelerating polymer aging for research . . . . .	40
3.5	Conclusion . . . . .	41
<b>4</b>	<b>Plasma degradation: A novel, general, and rapid aging protocol for microplastic research in the environment</b>	<b>44</b>
	Graphical Abstract . . . . .	44
	Abstract . . . . .	45
4.1	Introduction . . . . .	45
4.2	Methodology . . . . .	49
4.2.1	Materials & Preparation . . . . .	49
4.2.2	Accelerated Photoaging . . . . .	50
4.2.3	Plasma degradation . . . . .	50
4.2.4	XPS . . . . .	51
4.2.5	SEM . . . . .	51
4.2.6	Water Contact Angle measurements . . . . .	51
4.2.7	Data analysis . . . . .	52
4.3	Results & Discussion . . . . .	53
4.3.1	Control materials . . . . .	53
4.3.2	Changes in polymer stoichiometry introduced as a result of aging . . . . .	57
4.3.3	Impacts of plasma treatment and accelerated photodegradation on polymer surface chemistry . . . . .	59
4.3.4	Physical surface changes . . . . .	63
4.3.5	Contact angles measured on aged polymer surfaces . . . . .	66
4.3.6	Optimisation of methodology . . . . .	69
4.3.7	Characterisation of aged microplastic powders . . . . .	72
4.3.8	Comparing to more common microplastic aging methods . . . . .	75
4.3.9	Recommendations for environmental studies . . . . .	76
4.4	Conclusion . . . . .	77
<b>5</b>	<b>Simulating polymer surface aging effects on environmental nutrient sorption dynamics</b>	<b>78</b>
	Graphical Abstract . . . . .	78

Abstract . . . . .	79
5.1 Introduction . . . . .	79
5.2 Methodology . . . . .	81
5.2.1 Preparation . . . . .	81
5.2.2 Accelerated Photoaging . . . . .	81
5.2.3 Preparation of bark extract solution . . . . .	82
5.2.4 Bark extract stoichiometric reference . . . . .	82
5.2.5 Conditioning of polymer samples in bark extract solution . . . . .	83
5.2.6 Plasma Aging . . . . .	83
5.2.7 Surface conditioning with nutrient salt solutions . . . . .	83
5.2.8 XPS Analysis . . . . .	84
5.2.9 Statistical analysis . . . . .	84
5.3 Results & Discussion . . . . .	85
5.3.1 Conditioning film adsorption analysis . . . . .	85
5.3.2 Adsorption characteristics of bark-derived dissolved organic matter on photoaged polymer surfaces . . . . .	90
5.3.3 Phosphate adsorption analysis . . . . .	96
5.3.4 Nitrate adsorption analysis . . . . .	98
5.3.5 Ammonium adsorption analysis . . . . .	100
5.3.6 G6P adsorption analysis . . . . .	102
5.3.7 Spectral analysis of concentrated nutrient sorption on Pristine and Plasma-aged polymer surfaces . . . . .	103
5.4 Conclusion . . . . .	108
<b>6 Investigating the impact that surface aging of microplastics has on key soil health metrics</b>	<b>110</b>
Graphical Abstract . . . . .	110
Abstract . . . . .	111
6.1 Introduction . . . . .	111
6.2 Methodology . . . . .	114
6.2.1 Soil preparation . . . . .	114
6.2.2 Microplastic and positive control materials . . . . .	115

6.2.3	Plasma aging of microplastics . . . . .	115
6.2.4	Soil sample preparation & incubation . . . . .	116
6.2.5	EC and pH measurements . . . . .	117
6.2.6	Aggregate stability . . . . .	117
6.2.7	Microbial activity assessment . . . . .	118
6.2.8	Available nitrogen analysis . . . . .	120
6.2.9	Available phosphorus analysis . . . . .	120
6.2.10	Statistical analysis . . . . .	120
6.3	Results & Discussion . . . . .	121
6.3.1	Soil drying characteristics . . . . .	121
6.3.2	EC & pH . . . . .	123
6.3.3	Soil microbial activity . . . . .	125
6.3.4	Available phosphorus . . . . .	126
6.3.5	Available nitrogen . . . . .	127
6.3.6	Fast wetting of soil aggregates . . . . .	129
6.3.7	Slow wetting of soil aggregates . . . . .	130
6.4	Conclusion . . . . .	132
<b>7</b>	<b>Discussion, conclusion, &amp; further work</b>	<b>134</b>
	<b>Appendices</b>	<b>139</b>
<b>A</b>	<b>A Short Guide To Plastics For SMEs</b>	<b>139</b>
<b>B</b>	<b>Understanding the role of Corporate Social Responsibility in addressing the plastic crisis</b>	<b>146</b>
<b>C</b>	<b>Web Of Science Queries</b>	<b>155</b>
	<b>Bibliography</b>	<b>156</b>

# Declaration

This thesis has not been submitted in support of an application for another degree at this or any other university. Many ideas and experiments presented in this thesis were a product of discussions with my academic supervisory team, further developed through training with academics, technical staff, and other researchers, and occasionally from discussions with other researchers. The data collection, analysis, and writing included herein is the sole product of my own efforts, with the counsel of my academic team, except where otherwise explicitly stated.

# Acknowledgements

This research was funded by The Leverhulme Trust, through the Material Social Futures (MSF) doctoral training academy organised by PIs Prof. Richard Harper and Prof. Rob Short. Within the MSF academy training in Futures Thinking was enabled by Dr Emily Spiers, training in Political Ecology was made possible by Dr Rosanna Carver, and training in Business Ethics & Society (MNGT 622) was facilitated by Dr Sarah Gregory. Thank you for enriching my education, and broadening my perspectives. Thank you to Louise Bush, Rachel Lyon, Stacey Lofthouse, and Jennifer Thompson for being responsive to administrative queries during my PhD.

This project was further made possible by the supervision, valued insight, and expert guidance of Dr Ben Surridge, Prof. Rob Short, Dr Alex Robson, Prof. Crispin Halsall, and Dr Alison Stowell. Thank you for listening patiently to all of my ideas, helping me discern the innovative from the ill-advised, for giving me the space to explore and define the research objectives, and enabling me to lead on this project.

I would also like to wholeheartedly acknowledge and thank Dr Clare Benskin, Dr Catherine Wearing, Dr Vassil Karkolovski, Dr Hugh Tuffen, Dave Hughes, Tim Gregson, Alessio Quadrelli, Amy Crisp, Emilee Severe, Chris Cook, Dr Laurine Martocq, Christina McBride-Serrano, Mary Cvetkovic-Jones, Dr Angeliki Kourmouli, Daniel Harvey, Kate Morgan, Kate O'Driscoll, Joanne Shaw, and Binne Tanna for supporting me in various laboratories where I began a novice. With your care and counsel I am novice no longer. Thank you as well to Dr Samuel Jarvis for his support in the operation of the X-ray Photoelectron Spectrometer, and to Dr Sara Baldock for operating the SEM, and for her guidance in the interpretation, and analysis of SEM data.

Lastly, I would like to sincerely, wholeheartedly, unabashedly extend my gratitude to Dr Christina Bremer, Dr Alessio Quadrelli, Penelope Quek, Melissa Ross, Jonathan ‘Jono’ Hall, Dr Sam Cusworth, Dr Daniel Routledge, to Dad & Ang, to the family members who supported me on this journey, and to all the other friends and loved ones who made me whole. With love, respect, and admiration, thank you.

# Abstract

Plastics are modern-day super materials, capable of being tailored to virtually every material application imaginable. However, their low cost, resilient nature, and meteoric rise into prolific production has contributed significantly to their widespread pollution of the environment. In recent years citizens and scientists alike have recognised this as an emerging ecological and environmental crisis, and as such keen concern has followed, and significant interest to understand and address this crisis has emerged.

Once present in the environment plastics present a number of novel hazards. Whilst they are resilient to complete mineralisation, they readily break down and fragment into smaller particles known as microplastics and nanoplastics. These tiny particles are promptly dispersed throughout the natural world, making their retrieval and cleanup all but impossible. As a result, understanding what happens to these materials as they age within the environment, and assessing what impact they will have, is essential. This study is naturally an uphill battle for a number of reasons: these materials are highly diverse, owing to their ability to be synthesised readily from a wide variety of monomers in a wide variety of arrangements, their ability to be further adapted with chemical additives, and their uncontrolled degradation in environmental matrices which changes their properties further still.

Because of this, existing research has often focused on the use of so-called ‘pristine’ materials; out-of-the-factory polymers which are easy to obtain, characterise, and categorise. However, whilst this approach is a sensible first step, it leaves a lot of critical understanding out of the picture. More recently, research has progressed to test hypotheses with ‘aged’ materials, as they are more representative of pollution found in the environment. There are a number of common methods for approaching this, but they have their own limitations, and are generally quite slow, making rapid progress on this issue challenging. In very recent studies, new potential tools have been discussed to evaluate hypotheses related to material aging on much faster timescales, such as the use of plasmas.

In this thesis, plasma degradation was pioneered as a proxy for environmental aging in microplastics research. Plasma surface treatment is not a new technology, and indeed polymers have been routinely exposed to plasma in other fields of research to achieve a variety of outcomes. However, its application as a potential aging method to rapidly simulate environmental photodegradation is all but missing. Herein an in-depth analysis and optimisation of plasma degradation for this application was made, with recommendations for sensible implementation of this technique. Overall, it was deemed a rapid alternative method that can *significantly* accelerate the pace of aging-focused studies, whilst remaining a plausible abstraction of photodegradation within appropriately designed methodologies. This technique was demonstrated to have enormous potential in its application to microplastics research.

The optimised aging protocol was then carried forth into two research chapters: the first an analysis of environmental sorption dynamics of common soil nutrients to aged plastic surfaces, using XPS as a method to determine surface adhesion. Results indicated material-specific and aging-specific sorption occurs, however it was concluded that further research was needed to ascertain if nutrient immobilisation is a real concern. The second was a soil incubation study, investigating the impact that the environmental aging of microplastic pollution will have on soil health. These results concluded that even in a low (but representative) concentration of 0.25% w/w microplastics have a small but notable and significant impact on soil health, with some treatments being able to influence phosphorus and ammonium availability, affect soil aggregation, as well as alter pH and EC values within the soil. There was evidence of aging-specific variation, however these data indicated material-specific features were more relevant. These studies demonstrated that plasma surface treatment can be used as an effective and sensible aging protocol for microplastics research in the environment.

# List of Figures

1.1	A visualisation of the outline of this thesis and how it links to the research questions investigated during this PhD . . . . .	2
1.2	Polymerisation of a common monomer, ethene . . . . .	4
1.3	A visualisation of the overlap of broad plastic-related terminology, reproduced from Ford et al [16] under CC BY license. . . . .	5
1.4	Commonly defined size ranges of plastic pollution . . . . .	6
2.1	Particle size distribution resulting from cryomilling of the four materials used throughout this thesis, as percent of total milled mass in microns. As this figure shows the size range varied considerably, so particles in the 125-500 $\mu$ m range were retained and mixed together to create a more comparable set of starting powders. . . . .	10
2.2	A functional schematic of the XPS system used in this study . . . . .	13
2.3	Standard photoemission occurring during XPS where an X-ray photon ejects a core electron (Left); Auger photoemission where a third electron is ejected as a result of the energy released from another electron relaxing into the vacancy left by another electron emission (Right). . . . .	14
2.4	A general interpretation of a survey spectrum for the polymer Nylon 6-6, highlighting how each part of the molecule is observed in the spectrum. CPS on the Y-axis stands for 'Counts Per Second', the number of detected electrons counted per second, and Binding Energy on the X-axis refers to the binding energy of the orbital it was ejected from. . .	14
2.5	A visualisation of how plasma relates to the 3 conventional states of matter, inspired by [44]. . . . .	16

2.6	A visualisation of the diversity of plasma, reproduced from [45] under CC BY license, showing how widely plasma varies based on their microscopic parameters (electron energy $E_e$ and electron density $N_e$ ) . . . . .	17
2.7	Examples of four of the most common plasma mechanisms applied to oxygen, highlighting how plasmas can generate a diverse range of reactive species from air. . . . .	18
2.8	A visualisation of surface degradation during plasma treatment . . . . .	19
2.9	An example chemical scheme for LDPE, highlighting a potential mechanism by which oxygen functional groups, such as peroxy, can be incorporated into polymers through interactions with oxygen radicals generated by free electrons liberated by the strong electric field present in a plasma. . . . .	19
2.10	The spectral irradiance of the solar-filtered Xenon arc lamp utilised in the ATLAS Suntest system operated in chapters 4 and 5. These data were kindly provided by Prof. Crispin Halsall with minimal post-processing. . . . .	21
2.11	A photo of the custom built aluminium matrix for holding flat polymer samples. . . . .	22
2.12	Visualisation of how a contact angle forms for a droplet on a material surface as a result of competing interface tensions. . . . .	25
2.13	An example of a hydrophobic response (L), and a hydrophilic response (R) in contact angle. . . . .	25
2.14	A schematic of the contact angle equipment used for this thesis. A diffuse white light source directs light at the stage, towards the detector behind it. The stage is calibrated to ensure it's level. . . . .	26
3.1	Graphical abstract highlighting key areas of interest in the microplastics literature for this thesis . . . . .	27
3.2	A visualisation of keyword queries of Web of Science for microplastics research studies published each year (1967 - 2022), highlighting the first time a study with relevant keywords was published . . . . .	29
3.3	A chemical scheme showing the process of initiation, where an incoming photon breaks apart a carbon-hydrogen covalent bond. . . . .	37

3.4	A generic chemical scheme showing two key propagation mechanisms during photodegradation, in which a radical of the polymer reacts with diatomic oxygen present in the air to form a peroxy radical. This peroxy radical then reacts with another polymer chain, generating another radical in the process. At the end of both steps new radicals are formed that propagate the degradation of new chains. . . . .	37
3.5	A chemical scheme showing the process of termination, where two radicals react together to form a stable molecule, terminating the photodegradation process. . . . .	37
4.1	A visualisation of this chapter's aims . . . . .	44
4.2	Repeat units of the three polymers that were used in this study . . . . .	50
4.3	Wide scan of a control PS surface showing that the material surface contains only carbon and oxygen, with a 0.32% surface oxygen content. Overall, this indicates a very pure sample with minimal initial oxidation. . . . .	53
4.4	A representative coreline scan of the control PS surface showing a 3.0:1.0 ratio, as would be expected for pristine PS (6 aromatic carbons, 2 aliphatic carbons per molecule). The bright red envelope is the raw data, and fainter lines correspond to the modelling of the chemical environments, fitted to best match the raw data. The Pi-Pi shake up feature is a signature satellite peak resulting from the relaxation of delocalised pi-bond electrons in the phenyl group that is seen in XPS of high-purity PS. . . . .	54
4.5	Wide scan of a control LDPE surface, showing a pure surface with a background oxygen content of <1% oxygen and no impurities. . . . .	55
4.6	A C 1s coreline scan of a control LDPE surface, manually fitted with two realistic components. It shows a dominant aliphatic carbon peak at 284.93 eV with 99.01% of the total area, and a smaller carbon-oxygen peak with 0.99% of the total area. . . . .	55
4.7	A wide scan of a control PLA surface, showing a high-purity PLA sample, with only 0.24% of the surface containing impurities. . . . .	56
4.8	C 1s coreline scan of a control PLA surface, with three manually modelled peaks corresponding to the three distinct carbon environments found in PLA. The fit is good, indicating a high-quality PLA sample with minimal carbon-based impurities. . . . .	56

4.9	Wide scan of a 6-week photoaged PS surface. This spectrum details a surface oxygen concentration of 26.31%, as well as some nitrogen species, both likely introduced through photooxidation of the surface bonds, as well as some silicon species which was assessed to be siloxane contamination. . . . .	58
4.10	Wide scan of a PS surface aged with 60s 100W plasma treatment, showing a surface oxygen content of 18.07%, indicating that plasma treatment led to significant surface oxidation. . . . .	58
4.11	SEM images of long photoaging, PS (images A and B), LDPE (images C and D), PLA (images E and F) ; Control (A, C, and E), 6-week ‘Long’ photoaged (B, D, and F). These surfaces were imaged at 1000x magnification. They show no noticeable changes with treatment. . . . .	63
4.12	SEM images of PS (A-C), LDPE (D-F), PLA (G-I) for Control, 20W 60s plasma aged, and 100W 60s plasma aged going left-to-right respectively. These surfaces were imaged at 1000x magnification. They show no noticeable changes with treatment. . . . .	64
4.13	SEM images of PS (A-C), LDPE (D-F), PLA (G-I) microplastic powders for Control, 100W 5s plasma aged, and 100W 60s plasma aged going left-to-right respectively. These surfaces were imaged at 1000x magnification. They show no noticeable changes with treatment. . . . .	65
4.14	Contact Angle Images of PS (A and B), LDPE (C and D), and PLA (E and F) for Control and ‘Long’ photoaged LR respectively. These images indicate that photoaging does affect surface hydrophobicity, however this did not lead to significant results. . . .	67
4.15	Contact Angle Images of PS (A and B), LDPE (C and D), and PLA (E and F) for Control and 100W 60s aged LR respectively. Plasma treatment qualitatively led to a dramatic change in surface hydrophobic, leading to measured droplets completely flattening across the surface. . . . .	68
4.16	Peak-to-peak normalised C 1s spectra for plasma aged PS at 60s (Red), 300s (Green) and 600s (Blue) plasma durations . . . . .	70
4.17	Peak-to-peak normalised C 1s spectra for plasma aged LDPE at 60s (Red), 300s (Green) and 600s (Blue) plasma durations . . . . .	70
4.18	Peak-to-peak normalised C 1s spectra for 60s plasma aged PS at 20W (Red), 50W (Green) and 100W (Blue) . . . . .	71

4.19	Peak-to-peak normalised C 1s spectra for 60s plasma aged LDPE at 20W (Red), 50W (Green) and 100W (Blue) . . . . .	71
4.20	The drop in quality of the C 1s spectrum for the control PS microplastic powder in this figure was assessed to be a result of charging artefacts that arose due to the challenges of measuring insulating powders, as further visualised in figure 4.21. . . . .	74
4.21	Visual explanation of charging artefacts present in XPS of polymer powders . . . . .	74
5.1	A visualisation of the research hypotheses investigated in this chapter . . . . .	78
5.2	A representative wide scan of the silver foil used to create bark reference spectra before cleaning. The large amount of carbon (63.99% of surface) measured in the pretreatment scan indicates significant surface contamination that needs to be removed in order to use this material reliably. . . . .	85
5.3	A representative wide scan of the silver foil used to create bark reference spectra after plasma cleaning. Overall, adding in a plasma-cleaning step removed a large proportion of the surface contamination, as indicated by the much lower concentration of carbon at 11.98%, making it far more ideal for identifying carbon-based adsorption. . . . .	88
5.4	A representative XPS wide spectrum of the plasma-cleaned silver substrate with dried bark extract, highlighting the wide diversity of different elements present in the bark mixture, making it a strong candidate for used as a treatment to test surface sorption. . . . .	89
5.5	Min-to-max normalised comparison of two examples of C 1s spectra of plasma cleaned Ag Control (Blue) and plasma cleaned Ag with bark incubation (Red), which indicate the emergence of two peaks attributable to the bark extract at 293.0eV, and 296.0eV. . . . .	89
5.6	A long-exposure photoaged PS representative wide scan treated with bark extract. This wide scan shows an oxygen peak of 25.03%, and a carbon peak of 73.10%, making it comparable to the reference spectra seen in chapter 4. There is also the addition of a calcium peak (0.40% at 348.00 eV) and a silicon peak (1.47% at 102.00 eV), indicative of limited but measurable sorption from the mixture. . . . .	91

5.7	A long-exposure photoaged LDPE representative wide scan treated with bark extract. Similarly to those analysed in chapter 4, this long-exposure photoaged LDPE samples has a relatively low level of oxidation compared to the plasma-aged surfaces, and to PS. This sample has only 3.99% surface oxygen, which is assessed to be attributed to the aged material. There is a small amount of silicon adsorbed to the surface (0.22%), but overall it has not changed meaningfully with treatment. . . . .	92
5.8	A long-exposure photoaged PLA representative wide scan treated with the bark extract. The resulting scan similarly showcases a high-quality PLA spectrum, with only 0.53% of non-PLA elements in silicon, indicating minimal sorption from the extract. . . . .	92
5.9	A min-to-max normalised overlay of control PS samples without (Red) and with (Blue) bark extract treatment, indicating no noticeable differences with treatment. This means that there was no noticeable sorption of carbon-based species from the treatment. . . .	93
5.10	A min-to-max normalised overlay of Long Photoaged PS without (Red) and with (Blue) bark extract treatment, indicating minimal differences with treatment. . . . .	93
5.11	A min-to-max normalised overlay of the non-aged Control LDPE without (Red) and with (Blue) bark extract, highlighting that no significant differences were observed in the coreline C1s when treated. . . . .	94
5.12	A min-to-max normalised overlay of Long Photoaged LDPE without (Red) and with (Blue) bark extract, highlighting that no significant differences were observed in the coreline C1s when treated. . . . .	94
5.13	A min-to-max normalised overlay of the non-aged Control PLA without (Red) and with (Blue) bark extract, highlighting some peak broadening occurring. . . . .	95
5.14	A min-to-max normalised overlay of the Long Aged PLA without (Red) and with (Blue) bark extract, highlighting some peak broadening occurring that looks comparable to that seen in the control PLA samples in figure 5.13. . . . .	95
5.15	Offset overlay for pristine (top) and plasma aged (bottom) representative PS spectra treated with $1000\text{mgPL}^{-1}$ $\text{Na}_2\text{HPO}_4$ , with sodium (yellow), and phosphorus (blue) spectral lines highlighted. . . . .	103
5.16	Offset overlay for pristine (top) and plasma aged (bottom) representative LDPE spectra treated with $1000\text{mgPL}^{-1}$ $\text{Na}_2\text{HPO}_4$ , with sodium (yellow), and phosphorus (blue) spectral lines highlighted. . . . .	104

5.17	Offset overlay for pristine (top) and plasma aged (bottom) representative PLA spectra treated with 1000mgPL <sup>-1</sup> Na <sub>2</sub> HPO <sub>4</sub> , with sodium (yellow), and phosphorus (blue) spectral lines highlighted. . . . .	104
5.18	Offset overlay for pristine (top) and plasma aged (bottom) representative PS spectra treated with 1000mgNL <sup>-1</sup> NaNO <sub>3</sub> , with sodium (yellow), and nitrogen (green) spectral lines highlighted. . . . .	105
5.19	Offset overlay for pristine (top) and plasma aged (bottom) representative LDPE spectra treated with 1000mgNL <sup>-1</sup> NaNO <sub>3</sub> , with sodium (yellow), and nitrogen (green) spectral lines highlighted. . . . .	105
5.20	Offset overlay for pristine (top) and plasma aged (bottom) representative PLA spectra treated with 1000mgNL <sup>-1</sup> NaNO <sub>3</sub> , with sodium (yellow), and nitrogen (green) spectral lines highlighted. . . . .	106
5.21	Offset overlay for pristine (top) and plasma aged (bottom) representative PS spectra treated with 1000mgNL <sup>-1</sup> NH <sub>4</sub> Cl, with chlorine (purple), and nitrogen (green) spectral lines highlighted. . . . .	106
5.22	Offset overlay for pristine (top) and plasma aged (bottom) representative LDPE spectra treated with 1000mgNL <sup>-1</sup> NH <sub>4</sub> Cl, with chlorine (purple), and nitrogen (green) spectral lines highlighted. . . . .	107
5.23	Offset overlay for pristine (top) and plasma aged (bottom) representative PLA spectra treated with 1000mgNL <sup>-1</sup> NH <sub>4</sub> Cl, with chlorine (purple), and nitrogen (green) spectral lines highlighted. . . . .	107
6.1	A visualisation of the research hypotheses investigated in this research chapter . . . . .	110
6.2	A flow diagram visualising and explaining how microbial activity in a soil can be assessed by this method . . . . .	119
6.3	Modelled fit of natural drying from 100% WHC to 0% WHC (grey dashed line), with raw data for each replicate plotted on top (green, blue, and yellow dot markers respectively at their equivalent WHCs) . . . . .	122
6.4	Available phosphorus measurements for n=3 replicates. Error bars represent 1 standard deviation from the mean. Significant differences to negative control are denoted with an asterisk (*, p value ≤0.05), and significant differences to the positive control are denoted with a dagger (†, p value ≤0.05). . . . .	126

6.5	Available Ammonium measurements for n=3 replicates. Error bars represent 1 standard deviation from the mean. Significant differences to negative control are denoted with an asterisk (*, p value $\leq 0.05$ ), and significant differences to the positive control are denoted with a dagger (†, p value $\leq 0.05$ ). . . . .	127
6.6	Available nitrate measurements for n=3 replicates. Error bars represent 1 standard deviation from the mean. Significant differences to negative control are denoted with an asterisk (*, p value $\leq 0.05$ ), and significant differences to the positive control are denoted with a dagger (†, p value $\leq 0.05$ ). . . . .	128
6.7	A photo of a typical treatment after fast wetting . . . . .	129
6.8	Comparison of the aggregate size distributions of different soil treatments after slow wetting; significant differences to negative control are denoted with an asterisk (*, p value $\leq 0.05$ ), and significant differences to the positive control are denoted with a dagger (†, p value $\leq 0.05$ ). . . . .	130
6.9	MWD values for each slow wetting treatment. Error bars represent 1 standard deviation from the mean. Significant differences to negative control are denoted with an asterisk (*, p value $\leq 0.05$ ), and significant differences to the positive control are denoted with a dagger (†, p value $\leq 0.05$ ). . . . .	131

# List of Tables

2.1	Total mass conversion from cryomilling, where Total End Mass is the total amendment mass retained, and Useful End Mass is the total amendment mass in the desired size range of 125 - 500 $\mu\text{m}$ . . . . .	11
2.2	A list of chemical shifts used for peak fitting of the C 1s XPS spectra analysed in this thesis, adapted from [42] and [43] . . . . .	15
2.3	The key cryomilling parameters used in processing of the powdered materials analysed in this thesis . . . . .	23
3.1	Top-level comparison of the key advantages and disadvantages of accelerated aging techniques used in microplastics research to simulate long-term environmental degradation. .	42
4.1	Analysis of surface chemistry for plasma-aged polymers compared with photoaged polymers. These data are all from high-quality spectra that have been charge calibrated, had their peak regions manually fitted, and have been corrected for the low levels of siloxane contamination present on the surface where appropriate. These data reflect high-quality samples of n=1. . . . .	60
4.2	Analysis of component composition of different aged spectra. These data highlight the similarity between the chemical environment generated during plasma exposure compared to photoaging. These data reflect high-quality samples of n=1. . . . .	61
4.3	Contact angle response to the ‘Long’ photoaging treatment. Overall, whilst there was a visible shift in the measured contact angle, no measured differences across these samples were significant to a p-value $\leq 0.05$ , highlighting how inconsistent photoaging can be. .	67

4.4	Contact angle response to plasma aging. The asterisk (*) indicates results significant below a p-value $\leq 0.05$ . This indicates that this method is highly reproducible when it comes to creating a hydrophobic response in polymers. . . . .	68
4.5	Analysis of component composition of different aged spectra for microplastic powders. These data reflect good quality samples of n=1. . . . .	73
5.1	Element-electron orbital peaks (% contribution) measured in the bark extract for each trace element observed. . . . .	87
5.2	Relative peak areas for sodium and phosphate ion adsorption onto pristine and plasma-aged polymer surfaces. Asterisks (*) reflect a significant result of $p \leq 0.05$ compared to the respective control materials. n=3. . . . .	97
5.3	Ratios of sodium and phosphate ion adsorption onto pristine and plasma-aged polymer surfaces. n=3. . . . .	97
5.4	Relative peak areas for sodium and nitrate ion adsorption onto pristine and plasma-aged polymer surfaces. Asterisks (*) reflect a significant result of $p \leq 0.05$ compared to the respective control materials. n=3. . . . .	99
5.5	Ratios of sodium and nitrate ion adsorption onto pristine and plasma-aged polymer surfaces. n=3. . . . .	99
5.6	Relative peak areas for ammonium and chloride ion adsorption onto pristine and plasma-aged polymer surfaces. Asterisks (*) reflect a significant result of $p \leq 0.05$ compared to the respective control materials. n=3. . . . .	101
5.7	Ratios of ammonium and chloride ion adsorption onto pristine and plasma-aged polymer surfaces. n=3. . . . .	101
6.1	Mass of tested soil at 0% WHC, used to model drying behaviour. . . . .	121
6.2	Mass of tested soil at 100% WHC, used to model drying behaviour. . . . .	121
6.3	EC and pH measurements of each soil treatment averaged across all replicates (n=3), expressed as $\pm 1$ standard deviation of this distribution and tested to a p value of $\leq 0.05$ ; significant differences to negative control are denoted with an asterisk (*), and significant differences to the positive control are denoted with a dagger (†). . . . .	123

6.4 Mean absorbance of microbial assay tests for n=3 replicates  $\pm$  standard deviation. Data calibrated with blank values and zeroed to a reagent-only control. Each treatment was tested to a p value of  $\leq 0.05$  with no significant differences found. . . . . 125

## Glossary of Terms

Herein, the following terms, acronyms, initialisms, and abbreviations may be of note to the reader:

- Polymer - A large molecule made up of repeating units of smaller molecules ('monomers')
- Plastic - A class of materials formed on a polymer backbone, that are typically (but not exclusively) synthetic, made of mostly hydrogen and carbon, and containing chemical additives; often mistakenly used interchangeably with 'polymer'
- Additive - A class of chemicals that are 'added' to plastic structures to augment their properties, such as UV-stabilizers which change their susceptibility to ultraviolet radiation; additives are typically loosely bound to the polymer structure in a plastic
- Macroplastic - A large arrangement of continuous plastic, such as a plastic water bottle
- Microplastic (MP) - A particle of plastic that is less than 5mm in diameter. These particles can either be directly engineered to this size ('Primary' microplastics), or the result of degradation ('Secondary' microplastics)
- Nanoplastic (NP) - A particle of plastic that is less than 1 $\mu$ m in diameter
- Nonbiodegradable Polymer - A polymer that is resistant to biodegradation on human timescales
- Bio-based Polymer - A polymer synthesised from biomass-derived feedstocks, as opposed to fossil fuel-based feedstocks
- Biodegradable Polymer - Readily converted into biomass, water, carbon dioxide, and other simple molecules by biological and microbial processes
- XPS - X-ray Photoelectron Spectroscopy; a surface chemical analysis technique, see section 2.2 for more detail
- SEM - Scanning Electron Microscopy; a surface imaging technique, see section 2.5 for more detail
- PS - Polystyrene, a common nonbiodegradable polymer used in packaging
- PLA - Polylactic Acid, a relatively common bio-based polymer often described as biodegradable
- LDPE - Low Density Polyethylene, a common nonbiodegradable polymer commonly used in packaging

- Nurdle - A small bead of plastic used as a raw material in the manufacturing process of plastic items
- FWHM - Full Width Half Maximum, a metric used in the peak fitting of XPS spectra which describes the width of a peak at half of the peak's maximum value
- DOM - Dissolved Organic Matter
- IPA - Isopropyl Alcohol; a commonly used laboratory solvent used for cleaning
- CSR - Corporate Social Responsibility
- Pristine plastic - A 'Pristine' plastic is plastic material that is freshly manufactured, that has not been degraded from use, and has not been exposed to the environment in any meaningful way

## **Training in Material Social Futures**

This highly interdisciplinary research was complemented by a wide array of further study and additional work packages that connect the physical science research demonstrated in chapters 4, 5 and 6 to the broader societal and business contexts in which it is found. This formed a significant element of the time and effort of this PhD (approximately 20% of the funded 3 years), and resulted in two key outputs found in appendices A and B.

# Chapter 1

## Introduction

### 1.1 Research questions

Investigating the impact of plastic waste in the environment is an innately interdisciplinary endeavour. Chapters 1-3 give an introduction to the field and to the research methods. In Chapter 4, the validity and application of a novel accelerated aging technique for microplastics, plasma aging, is assessed. The method is then optimised as a novel method to rapidly simulate environmental aging of plastic waste. This technique was then applied to study sorption effects onto aged polymer surfaces in chapter 5, drawing comparison with photoaging (a commonly used method in the existing literature). This method is then ultimately tested in a soil microcosm experiment in chapter 6.

Broadly, this thesis aims to evaluate the following key questions:

1. How does plasma aging compare to photoaging as a way to rapidly simulate environmental aging?
2. Is plasma aging suitable as an alternative rapid aging method for accelerating microplastics research?
3. Does surface aging of plastic materials impacts nutrient sorption & mobility within environmental matrices?
4. Does surface aging of microplastic pollution in soils affect soil health?

### 1.1.1 Graphical outline of research questions

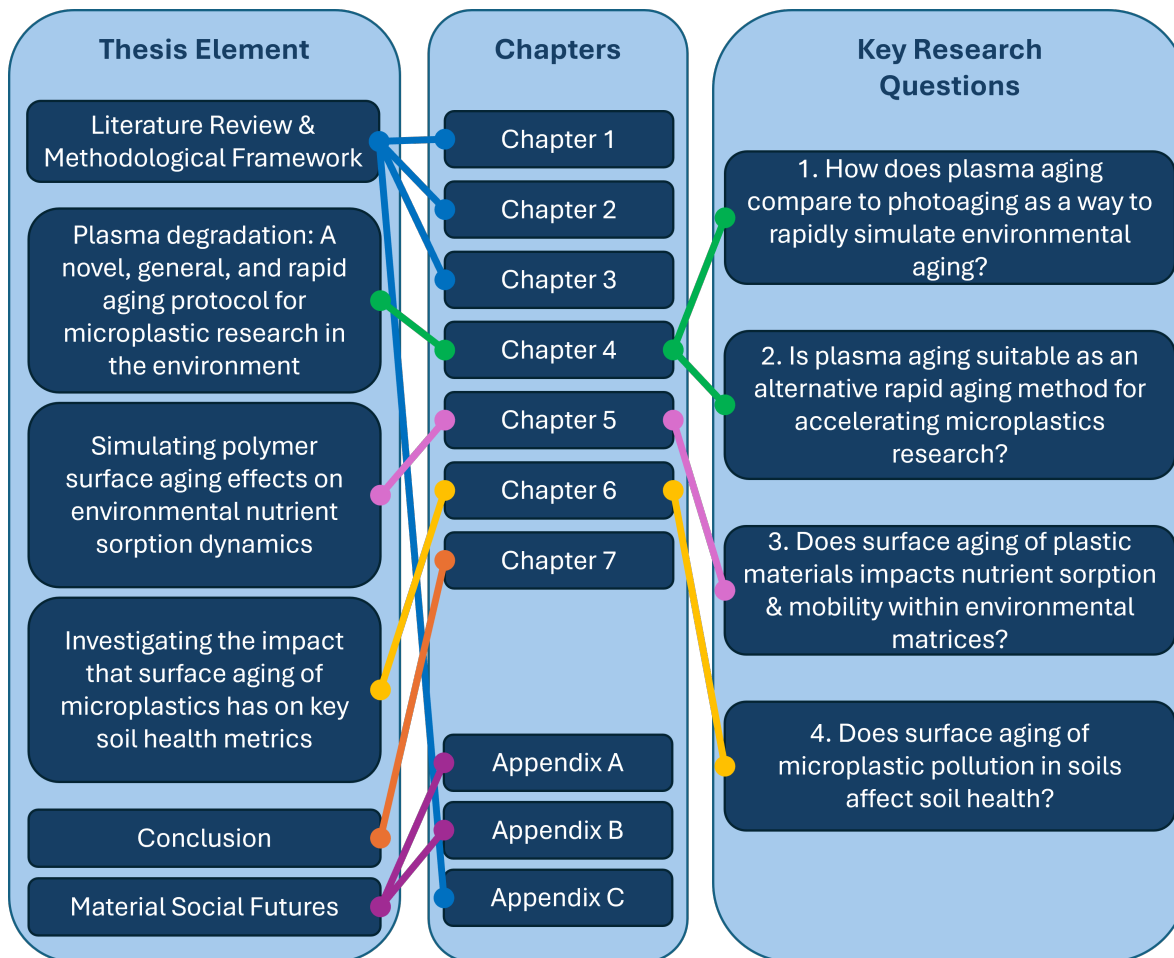


Figure 1.1: A visualisation of the outline of this thesis and how it links to the research questions investigated during this PhD

## 1.2 Plastics, Society, & the Environment

In recent years humanity has transitioned from the stable era of human development known as the Holocene to the uncertain future of the Anthropocene, a shift of geological epochs in which human activity has come to be the dominant influence on our planet [1]. Few materials have defined this transition more completely than plastics. Their unique properties, wide-ranging adaptability, and low cost have found them applied in virtually every facet of modern-day life, and as such they have emerged as one of the most impactful classes of contemporary materials. Consumption has expanded to an estimated 368 million tonnes annually in recent years [2], and there is every indication that this growth will continue. Future projections suggest it will triple by 2050, when it will account for 20% of global oil demand [2][3]. But the desire for convenient, low-cost lifestyles that has made plastics so commonplace, has brought with it immense environmental challenge and an emerging ecological crisis.

Plastics are now known to extensively pollute the natural environment. They have been found in even some of the world's most remote locations, such the mountains ranges of central Asia [4] and suspended in Antarctic waters [5]. The full implications of the sudden emergence of this anthropogenic pollutant remain unclear, but there is evidence of far-reaching consequences, with concerns over their impact on human health [6][7], pressure on biological ecosystems [8], and even potential to influence biogeochemical cycles [9]. Understanding these materials, how they shape society, and how they impact the environment, is an urgent necessity.

### 1.2.1 A Brief Introduction

Plastic is a generic term for a very wide range of different chemicals formed from repeating macromolecules known as 'monomers' which 'polymerise' (figure 1.2) into a long chain (a 'polymer'), and often contain other chemicals called 'additives' [10]. Additives represent a very wide array of organic and inorganic chemicals that can be mixed with polymers, and in almost all cases they are not directly bonded to the polymer structure [11]. Additives serve many purposes, including augmenting the functional properties of a plastic (such as making them more resistant to heat or light), making them more visually attractive, and making them cheaper to produce [11].

Whilst 'plastic' and 'polymer' are often used interchangeably, the more specific term 'polymer' refers exclusively to the repeating molecular pattern. Where appropriate, polymer is preferred nomenclature

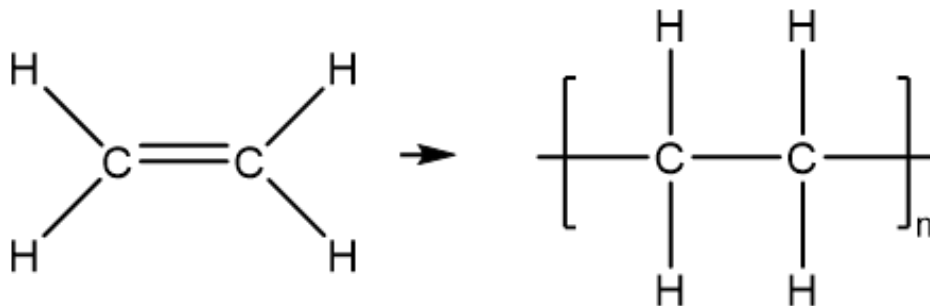


Figure 1.2: Polymerisation of a common monomer, ethene

[10], as ‘plastic’ is applied broadly and imprecisely in modern society, which can lead to confusion. Nevertheless, they are so tightly woven together that even in scientific literature they’re often used interchangeably, and indeed when working across disciplines the term ‘polymer’ can also be ambiguous, as in environmental literature it can be used to refer to individual macromolecules (‘natural polymers’) [12].

Virtually all everyday plastics consist of carbon and hydrogen with some small quantities of other elements, such as oxygen and nitrogen, meaning that by weight they are mostly carbon. Their unmatched ability to adapt to different purposes comes from the addition of small chemical structures known as functional groups, changes in polymer length and branching, their spatial arrangement (otherwise known as their ‘tacticity’), and the addition of chemical additives. The material diversity made possible through the combination of these alterations has led to their widespread use in society.

Commercial polymers are often separated into two origin groups: synthesis from petrochemical stocks (i.e. plastics derived from crude oil and other fossil fuels), and from biomass (i.e. synthesis from plant-based derivatives such as potato starch). Petrochemical-based polymers are far more common, and as such are also often referred to as ‘conventional plastics’ [13]. It is not uncommon for polymers to have multiple synthesis pathways. For example, PET monomers can be created through both oil-based and bio-based routes, producing the exact same polymer at the end of the process [14]. This means that it is entirely possible for the same plastic to be manufactured as a bio-based polymer, a conventional polymer, or a mix, depending on how it was synthesized. Often confused with bio-based polymers, a ‘biodegradable’ polymer is a separate classification, and refers only to its ability to be biologically decomposed, meaning both conventional and bio-based polymers can in theory be biodegradable, as

visualised in figure 1.3. These terms are widely misunderstood, and this lack of understanding often leads to negative outcomes when individual consumers manage their waste [15]. Understanding these nuances is essential when developing scientifically-valid hypotheses, and scientifically-informed policies regarding plastic pollution.

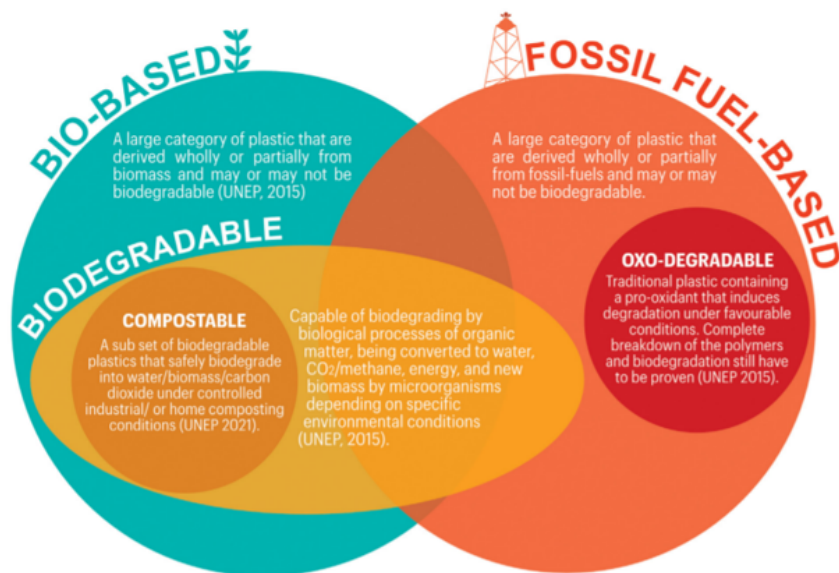


Figure 1.3: A visualisation of the overlap of broad plastic-related terminology, reproduced from Ford et al [16] under CC BY license.

## 1.2.2 A Brief History

Plastics emerged in the late 19th century as a niche chemical curiosity, helping to curb the demand for other natural materials that were in great demand such as ivory and tortoiseshell, which could only be sourced through the near extinction of rare animal species [17]. As the 20th century blossomed and industry boomed, plastics increasingly found roles in emerging technologies, from military radars to musical records [18]. This rapid success empowered technological progress across many different fields, and has transformed day-to-day life in the 21st century. They continue to make many essential products quick to manufacture, cheap to buy, and convenient to use [19]. They serve critical functions in the modern world that society would struggle to replace, such as facilitating many aspects of medical technology that would be all but impossible to substitute with other materials [20]. As a result, plastics are now among the most versatile and most used anthropogenic materials. It is difficult to imagine life without them, and even more difficult to live without them.

Convenience has come at a cost, however. The meteoric rise of these materials occurred without all of the necessary knowledge, infrastructure, or policies in place to effectively manage the end-of-life process. As early as the 1970s alarming studies emerged, demonstrating that these materials inadvertently pollute the natural environment [21]. As the decades progressed it became increasingly clear that this was a widespread problem, with massive levels of pollution being observed in the oceans, leading to disturbing phenomena such as ‘The Great Pacific Garbage Patch’, a large collection of plastic within the Pacific [22]. This problem is not no longer constrained to aquatic matrices, with recent studies finding plastics in soils [23].

Alarmingly, researchers have shown that these plastics are not only present, but accumulate over time in the natural environment [24]. Further still, plastics left in the environment begin to fragment and degrade, fracturing into micro- and nano-sized plastic particles (so-called ‘microplastics’ and ‘nanoplastics’, visualised in figure 1.4) [25].

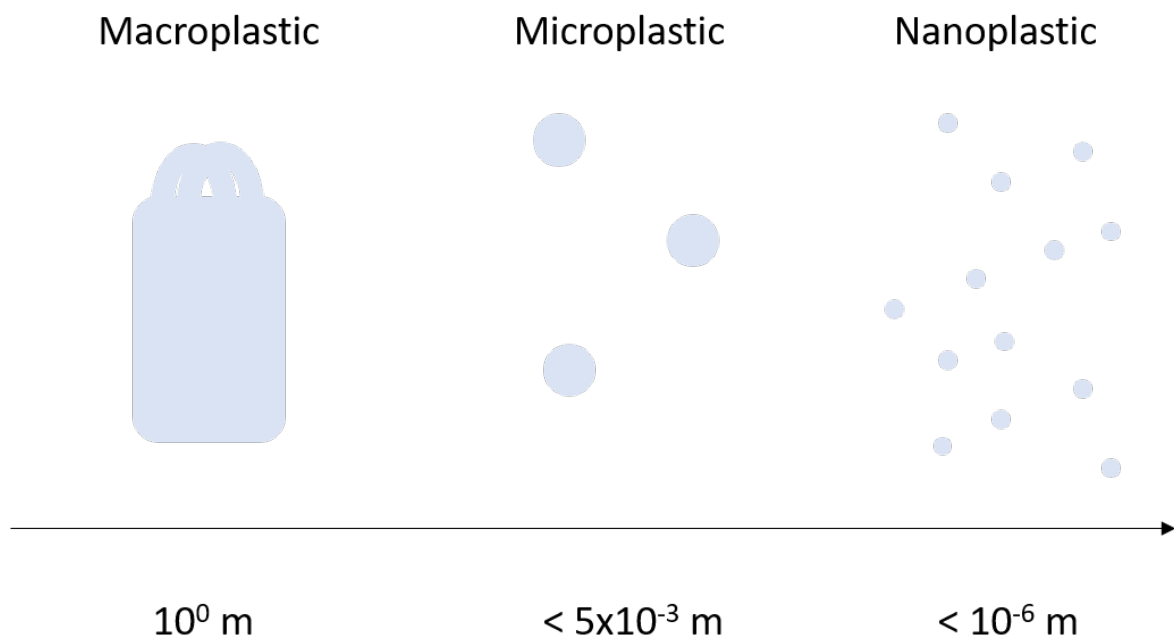


Figure 1.4: Commonly defined size ranges of plastic pollution

These pollutants have been shown to present novel and unintended consequences within the environment, from leaching their additives into their surroundings, to becoming sorption sites for Persistent Organic Pollutants (POPs), antibiotics and heavy metals [26][27][28]. It is geometrically self-evident

that their surface-to-volume ratio increases as material breakdown takes place, and with many of these emerging hazards arising as a result of activity on their surfaces, their uncontrolled fragmentation could see a catastrophic potential to amplify these effects. Additionally, as plastic particles become smaller, identification, quantification, and collection techniques available for research and cleanup become limited. So much as detecting smaller microplastics remains a barrier to restorative action, with most existing techniques having a minimum detectable size limit of a few micrometres [29].

Across their brief history, plastics have transformed the way we live, but they now present humanity with a number of difficult questions about how sustainably we choose to do so, and how we treat our environment. How the next few decades are handled, and what paths are chosen, will have a substantial impact on how this problem evolves.

### 1.2.3 A Brief Future

Plastic consumption is projected to skyrocket in the coming decades, with around 20% of oil expected to be used in the formation of plastics by 2050 [3]. The amount of plastic pollution already in circulation has caused enough concern for some researchers to call for it to be labeled as hazardous [30], and other researchers have described it as a ‘poorly reversible’ form of pollution that may inflict ‘practically irreversible’ damage [31]. Left unchecked, it is widely expected to cause problems for decades to come.

The future of plastic consumption and pollution is an open question, and it is one that will have a critical impact on other environmental crises such as biodiversity loss, and climate change [16][32]. Previously, researchers have speculated about the links between climate change and biodiversity [33], but these two major issues are also entwined with the future of plastic. As such, the decisions and strategies made to address the plastic crisis will have far-reaching implications.

Currently, the zeitgeist is to mediate humanity’s consumption of plastics with two key ideas: improved recycling of consumed materials, and the shift from ‘bad’ plastics (typically thought of as those that are difficult to recycle and made from petrochemicals) to ‘good’ plastics (often signposted as bio-based plastics and biodegradable plastics). These innovations, whilst showing promise, fundamentally cannot be the only solutions humanity has to the crisis, and indeed may reasonably present unintended consequences of their own. Several other ideas have been presented as possible future strategies to minimise the harms of the accumulation of plastic and to make better use of plastic material cur-

rently in circulation. Common strategies include commercial levers, such as working with businesses to adopt more sustainable practices [34], technical levers such as innovative new materials [35], and societal levers such as a cultural shift towards a circular economy [3]. All of these themes could play a role in addressing the plastic crisis.

Rockström et al have argued persuasively that in this era of dominant human activity there are multiple boundaries which humanity is on track to overstep [36], potentially tipping us into ‘undesired states’. It is likely that, in the decades to come, uncontrolled and unaddressed plastic pollution will influence several of these boundaries, and form a major element of the ‘chemical pollution’ threat [37]. Assessing both material and social futures of plastics in parallel is critical to foresee and mitigate their impact on these boundary conditions. Therefore, understanding the impact of plastic pollution is an urgent necessity, and rapid progress in this research field is needed.

As humanity continues to unravel the shift of this new era, clear gaps in our understanding of how the sheer volume of plastic we throw away changes within the environment, how its presence impacts the environment, and what our best tools for quickly assessing the consequences of plastic pollution in the environment look like have become increasingly conspicuous. Additionally, because this crisis was first observed in aquatic environments (and is most visible in aquatic environments) studies looking at their impact in terrestrial matrices are less common, despite being equally critical. This thesis aims to advance understanding in this gap.

## Chapter 2

# Materials and Methods

### 2.1 Materials used in this research

#### 2.1.1 Plastic sheets

Three plastic sheets were used throughout this study, LDPE, PLA, and PS. The highest purity options available for procurement were selected for this research in order to minimise the impact that additives could have on the outcomes. The PLA and PS were transparent plastics, and the LDPE was an off-white plastic. The polymer sheets had different thicknesses, however given the surface-focused nature of these research objectives, this was assessed to have no impact on the experiments conducted herein. All three were procured from Goodfellow Cambridge Ltd.

These materials were chosen specifically for their relevance to the discipline. LDPE is a widely-used polymer with simple chemistry, that sees significant application in agricultural settings, such as being the base of many mulch films [38]. Similarly, PLA is a common ‘biodegradable’ alternative [38]. PS forms the basis of the packaging of many single-use consumer goods, and is a common environmental pollutant [39].

#### 2.1.2 Powders

Three microplastic powders were generated through the cryomilling (section 2.6) of polymer ‘nurdles’. A nurdle is a small bead of plastic used as a raw material in the manufacturing process of plastic items. These nurdles were approximately 2-5mm in diameter pre-milling. Additionally, silica beads

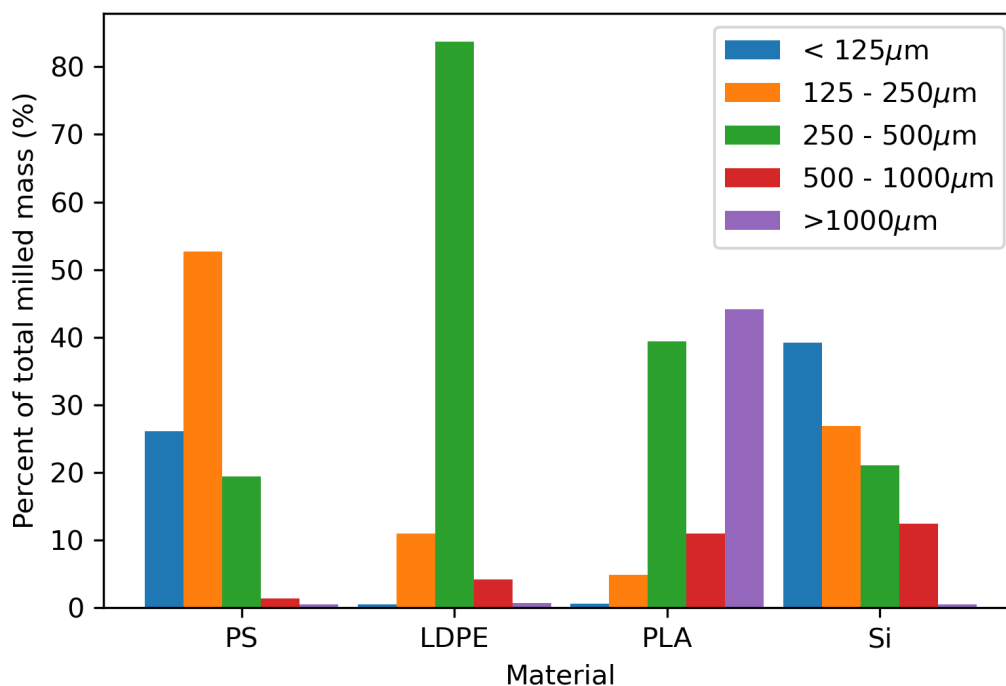


Figure 2.1: Particle size distribution resulting from cryomilling of the four materials used throughout this thesis, as percent of total milled mass in microns. As this figure shows the size range varied considerably, so particles in the 125-500µm range were retained and mixed together to create a more comparable set of starting powders.

were also cryomilled into powders to be used as a positive control material. Silica-based minerals are naturally abundant in the environment [40] and it is also robust to degradation, making it an ideal control material. The highest purity options available for procurement were selected for this research in order to minimise the impact of additives. After cryomilling, these powders were processed using an automatic sieve shaker in a stack of 20cm diameter sieves in the following size ranges: 1000µm, 500µm, 250µm, and 125µm. The resulting size distribution is seen in figure 2.1. To make these powders more comparable, particles of a given material between 125µm and 500µm were retained and mixed together. This size range is a sensible distribution for microplastic particles for soil studies, as microplastic particles in this size range have been commonly found in soil matrices [41]. Additionally, by constraining the particles to this size range, it is possible to more accurately attribute results to the effects of the polymers and their chemistry, as opposed to the impact that the particle size will have, as they are all within the same order of magnitude.

This conversion to ‘useful’ mass is shown in table 2.1. All materials yielded satisfactory results, however there was clear material-specific variation. PLA had a lower useful conversion due to a large fraction of nurdles not milling at all, and silica had a low useful conversion as it milled too well, often generating particles below  $125\mu\text{m}$ .

Table 2.1: Total mass conversion from cryomilling, where Total End Mass is the total amendment mass retained, and Useful End Mass is the total amendment mass in the desired size range of 125 - 500  $\mu\text{m}$

Amendment	Total End Mass (g)	Useful End Mass (g)	% Conversion
PS	23.35	16.83	72.09
LDPE	11.70	11.08	94.68
PLA	30.25	13.37	44.21
Si	23.86	11.43	47.92

## 2.2 X-ray Photoelectron Spectroscopy (XPS)

### 2.2.1 Background

One of the key analytical techniques used in this thesis is X-ray Photoelectron Spectroscopy (XPS). XPS, otherwise known as Electron Spectroscopy for Chemical Analysis (ESCA), is a highly surface sensitive technique that analyses the top few atomic layers of a material surface [42]. By accelerating electrons into a positively-charged anode, high-energy photons (X-rays) are generated. These X-rays are collimated, and directed at the surface of a material with sufficient energy to eject electrons from the surface upon collision via the photoelectric effect. Ejected electrons have variable kinetic energy based on their binding energy (i.e. how strongly bound they are to their atomic nucleus), which is dependent on the chemical environment of that atom.

$$BE = h\nu - (KE + \phi_s) \quad (2.1)$$

Equation 2.1 describes how the binding energy of a given energy state is calculated; an incident photon of energy  $h\nu$  arrives at a material surface, ejecting an electron via the photoelectric effect [42]. The electron has a kinetic energy  $KE$  which then carries it to the detector. The spectrometer work function,  $\phi_s$ , is an instrument-specific value used to correct for the interaction of the ejected photon at the detector.  $\phi_s$  is already known,  $h\nu$  is defined by the X-ray source, and  $KE$  is the measured value.

This allows for the binding energy  $BE$  of the chemical state that the electron was emitted from to be calculated.

$$I = JC\sigma\zeta T\lambda \quad (2.2)$$

The Peak Intensity  $I$  of a detected state (i.e. the area under a peak) is proportional to six main things: 1) the flux of incident X-ray photons  $J$ , 2) the relative concentration of a given chemical state  $C$ , 3) the photoionisation cross-section (i.e. the relative sensitivity) of a given chemical state  $\sigma$ , 4) the spectrometer angular acceptance  $\zeta$ , 5) the spectrometer transmission function  $T$ , and finally the inelastic mean free path  $\lambda$ , as outlined in equation 2.2.  $\lambda$  is a relatively constant value in XPS,  $\zeta$  and  $T$  are constants relating to the spectrometer,  $J$  is another experimental parameter that can typically be varied by an operator, and  $C$  is ultimately the desired information in the spectroscopy of materials. Through the combination of calculations with equations 2.1 and 2.2 the stoichiometry of a surface can be determined.

Whilst X-rays can penetrate deeply into the surface, the ejected electrons are highly interactive, and deeper emissions are reabsorbed quickly. Shallow electron emissions have the fewest opportunities to interact, and are thus able to be ejected from the surface and into the vacuum chamber. The exact sampling depth can be varied by using different anodes, incidence angles, and applied voltages, however the inelastic mean free path of ejected electrons is typically in the order of  $\sim 10\text{-}100\text{\AA}$  [42], meaning only electrons originating within tens of angstroms of the solid surface can leave without energy loss [42]. Therefore whilst ionisation from X-rays can occur deeper into a material, electrons emitted at greater depths experience significant energy loss and are either greatly attenuated, or aren't detected at all.

At a low enough pressure (i.e. in Ultra-High Vacuum (UHV)), these electrons are then able to travel ballistically towards a detector for analysis. As such, XPS operates at very low pressures (typically in the order of  $10^{-7}$  -  $10^{-10}$  Torr) in order to yield high-quality signals. Some scattered electrons are still detected, but as they are attenuated by random collisions, they ultimately do not become a meaningful signal and form the energy background in a spectrum. The simplest implementation of this results in a schematic analogous to figure 2.2, with a sample 'stage', an X-ray source, an electron analyser, a detector, and a computer for analysis.

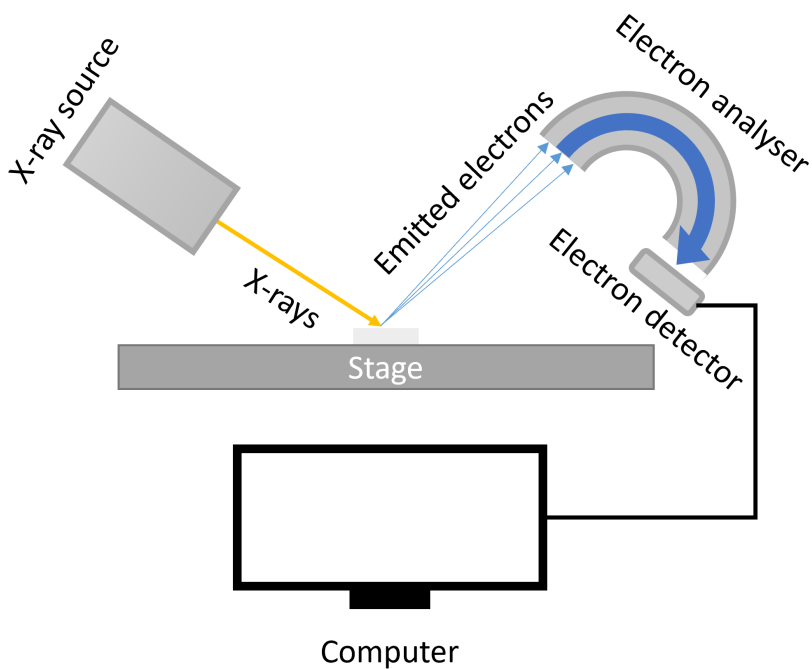


Figure 2.2: A functional schematic of the XPS system used in this study

Separate peaks known as Auger peaks also form part of an XPS spectrum. Auger peaks occur when a higher energy electron relaxes into a vacancy left by an emitted photoelectron, releasing energy, which can then eject a third electron that can be detected [42], as demonstrated in figure 2.3. The kinetic energy of this emission is material-dependent and X-ray independent as it depends only on the relaxation process between different electron states. This makes it a useful additional signature in surface analysis of some materials.

### 2.2.2 Interpreting spectra

Most spectra obtained with XPS are either ‘Survey’ spectra, which scan a wide region of binding energies at a lower resolution in order to detect elemental abundance, or ‘Coreline’ spectra, which are narrow scans of specific peaks at a higher resolution, which are used to identify which chemical states that element is in.

#### Survey spectra

Survey spectra, like the one featured in figure 2.4, feature sharp peaks at different binding energies that are attributable to photoemission from different elemental orbitals, auger peaks, and a broad

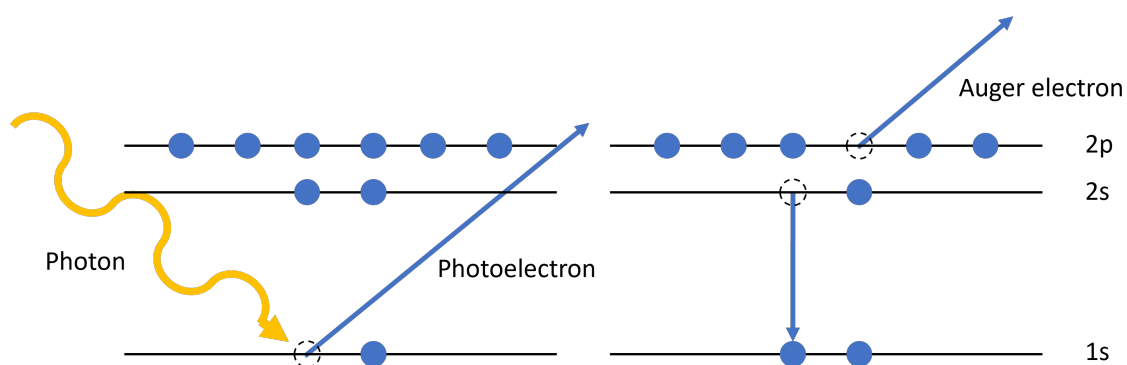


Figure 2.3: Standard photoemission occurring during XPS where an X-ray photon ejects a core electron (Left); Auger photoemission where a third electron is ejected as a result of the energy released from another electron relaxing into the vacancy left by another electron emission (Right).

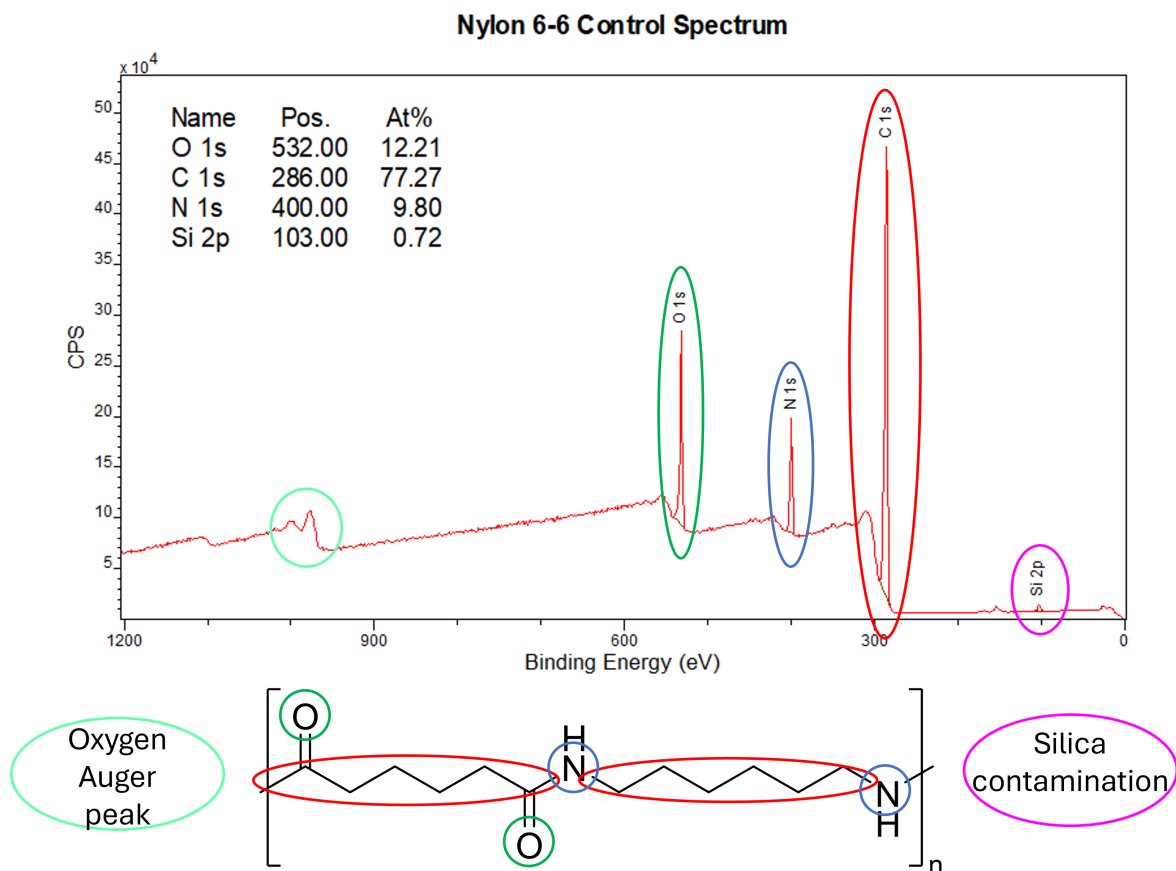


Figure 2.4: A general interpretation of a survey spectrum for the polymer Nylon 6-6, highlighting how each part of the molecule is observed in the spectrum. CPS on the Y-axis stands for 'Counts Per Second', the number of detected electrons counted per second, and Binding Energy on the X-axis refers to the binding energy of the orbital it was ejected from.

background signal arising from scattered electrons. At a given X-ray photon energy, each electronic state has a unique probability of interaction. For carbon, 1s electrons are the most sensitive, whereas for silicon 2p electrons are the most sensitive. Whilst all the peaks in a spectrum contribute to accurate chemical identification, convention is to use the most sensitive elemental peak when performing stoichiometric analysis. Because different elements and different orbitals have different photoionisation cross-sections, spectra have to be calibrated using Relative Sensitivity Factors (RSF) to reflect the relative likelihood of emission. Therefore, the size of a peak is not always a clear indication of the atomic concentration. This is also why different electrons emitted from the same element do not give equally sharp peaks; some are more likely to interact with X-ray photons than others.

Additionally, it is essential to understand in the analysis of polymers that hydrogen is not detected in XPS spectra. This is because hydrogen has only one electron shared in a covalent bond with a low binding energy, and a very small X-ray photoionisation cross-section. As such, XPS analyses omit hydrogen.

### Coreline spectra

Table 2.2: A list of chemical shifts used for peak fitting of the C 1s XPS spectra analysed in this thesis, adapted from [42] and [43]

Functional Group	Binding energy range	Mean chemical shift relative to C-C peak
Aromatic C	284.76 - 284.76 eV	-0.24eV
C-C	284.9 - 285.1 eV	+0.0eV
C-OH	286.4 - 286.6 eV	+1.0eV
O=C-O-[C]	286.5 - 287.0 eV	+1.75eV
C=O	287.8 - 288.0 eV	+2.9eV
O=[C]-O-C	288.9 - 289.1 eV	+4.0eV
HO-C=O	289.1 - 289.5 eV	+4.3eV
CO <sub>3</sub> <sup>2-</sup>	290.2 - 290.6 eV	+5.4eV

Coreline spectra are high-quality data of a given peak in a wide spectrum, such as a C 1s peak. By zooming in on a peak within a survey spectrum, and sampling the region at a much higher resolution, typically  $\leq 0.1\text{eV}$  step size, differences can be observed in the local environment of a given electron. Different chemical environments lead to differences in how strongly an electron is attracted to its bound nucleus, resulting in a subtle ‘chemical shift’ in a characteristic peak. A 1s electron bound to a carbon atom that is bonded only to carbon atoms will have the same binding energy as its neighbours. But a 1s electron bound to a carbon atom on the end of a carboxylic acid is in close proximity to the

oxygen atoms in a C=O double bond and C-OH bond respectively. Oxygen is highly electronegative, so it exerts a greater pull on electrons that it is bonded to, which in turn affects the interactions between outer electrons and core electrons, changing their binding energies. These effects are very small, typically in the order of 0.1 - 10eV. The chemical shifts that were used for the spectral analysis of polymer C 1s peaks in this thesis are seen in table 2.2.

## 2.3 Plasma surface treatment

### 2.3.1 Background

Plasma is a distinct medium that is often described as the fourth state of matter, after solids, liquids and gases. They are found abundantly across the universe as the basis of stars (forming  $\approx 99\%$  of visible matter [44]), and are regularly seen on Earth in the form of lightning and auroras, as shown in figure 2.6. They can also be deliberately formed on Earth, and find their uses in many every-day technologies including emission controls (by reacting plasmas with polluting compounds such as  $\text{NO}_x$  species), electronics manufacturing, and sterilisation [44].

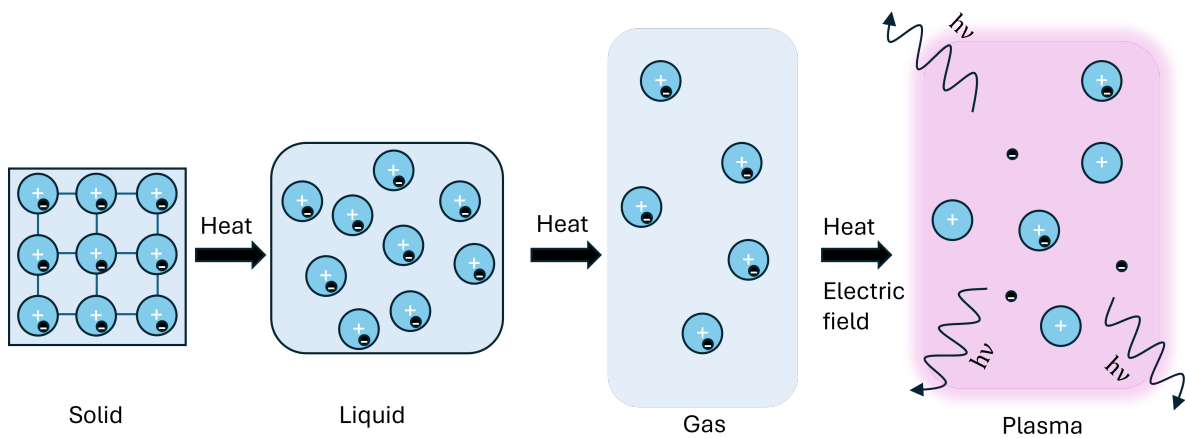


Figure 2.5: A visualisation of how plasma relates to the 3 conventional states of matter, inspired by [44].

As energy is added to a solid it eventually transitions into a liquid, then with more energy into a gas, and adding even more energy results in the gas particles being partially (or totally) ionised, with electrons being removed from the constituent particles; a plasma [45]. This means plasmas are a diverse mixture of ions, free electrons, and electrically-neutral particles (atoms, molecules) [45]. This is

visualised in figure 2.5. Plasmas have a variety of unique properties compared to other states of matter, such as their ability to readily conduct electricity (despite being electrically neutral on a macroscopic scale) [45].

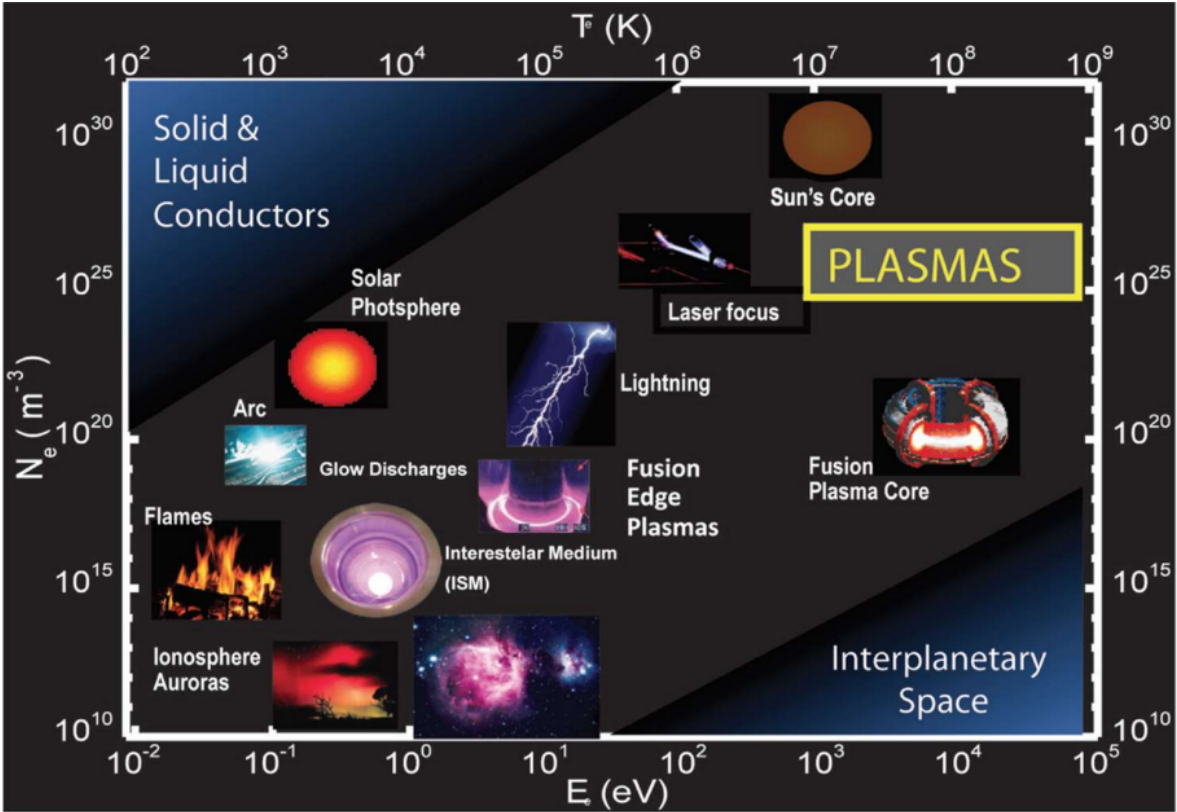


Figure 2.6: A visualisation of the diversity of plasma, reproduced from [45] under CC BY license, showing how widely plasma varies based on their microscopic parameters (electron energy  $E_e$  and electron density  $N_e$ )

They can be categorised into ‘thermal’ (where the constituents reach temperatures in the order of  $10^7 - 10^9^\circ\text{C}$ ) and ‘non-thermal’ (otherwise known as ‘cold’) plasmas, differentiated by whether or not the constituent matter is in thermal equilibrium or not. In the latter, the electronic temperature is relatively high, but the ‘heavy’ components (the atoms, molecules, and ions) are close to room temperature [45]. Cold plasmas can be easily formed within laboratories (so-called ‘technological’ plasmas), and are typically generated through the application of a strong electric field to a gas such as air, argon, or nitrogen. By using an alternating electric field these plasmas can be maintained.

### 2.3.2 Reaction mechanisms

Plasmas are highly reactive media owing to the immense amount of energy available from the applied electric field. When a plasma is ignited electrons liberated from the inlet gas drive excitation, relaxation, ionisation, dissociation of the atoms and molecules, as well as a variety of other mechanisms [46]. These processes generate the diversity of energetic species found in a plasma, from charged particles such as ions, to energetic neutrals like radicals and meta-stable species. A full discussion of these mechanisms is beyond the scope of this thesis, but examples of the most common mechanisms are shown in figure 2.7.

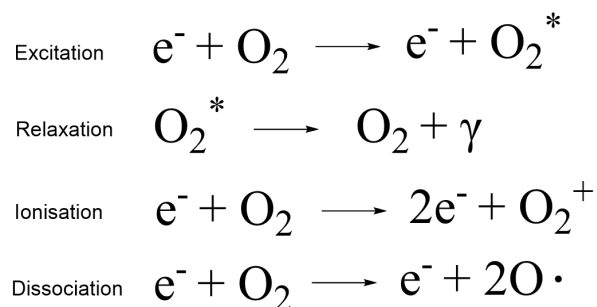


Figure 2.7: Examples of four of the most common plasma mechanisms applied to oxygen, highlighting how plasmas can generate a diverse range of reactive species from air.

### 2.3.3 Plasma surface treatment & modification

Technological plasmas can be tailored for a number of different use cases, making them a versatile tool in material science research. It is commonly found in the preparation of electronic materials and other nanofabrication procedures [47], owing to its ability to etch atomic layers uniformly over time. They are also commonly applied in the preparation of medical implants [45], as plasma treatment can be used to prepare local surface modifications of a material, and recently has even seen application in clinical medicine [48].

For the plasma treatment of polymers, the modifications made to the surface are typically incredibly thin (on the order of nanometers) [49], leaving a distinct plasma-modified layer on top of the unmodified bulk polymer (figure 2.8). This is because the radicals and ions in the plasma are energetic but large, meaning that they can easily break bonds, but cannot penetrate deeply into the material surface. The high-energy photons in the plasma can, but they do not lead to molecular breakdown at the same rate.

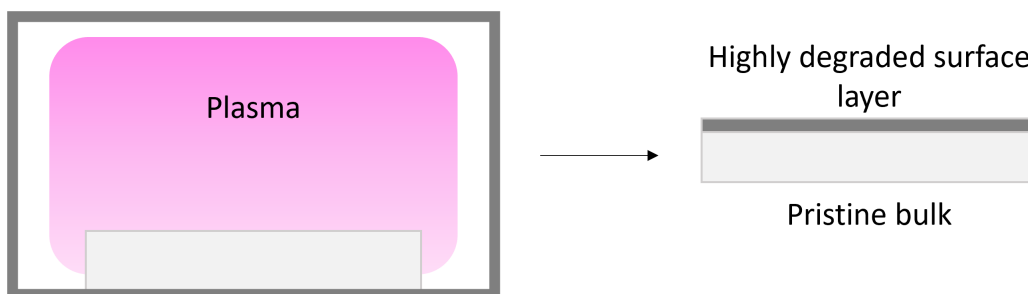


Figure 2.8: A visualisation of surface degradation during plasma treatment

In the case of simple polyolefins, this surface modification leads to oxidation of the polymer chain, as the plasma breaks covalent bonds in the polymer, forming radical intermediates which rapidly recombine with the oxygen in the air, such as the example shown for LDPE in figure 2.9.

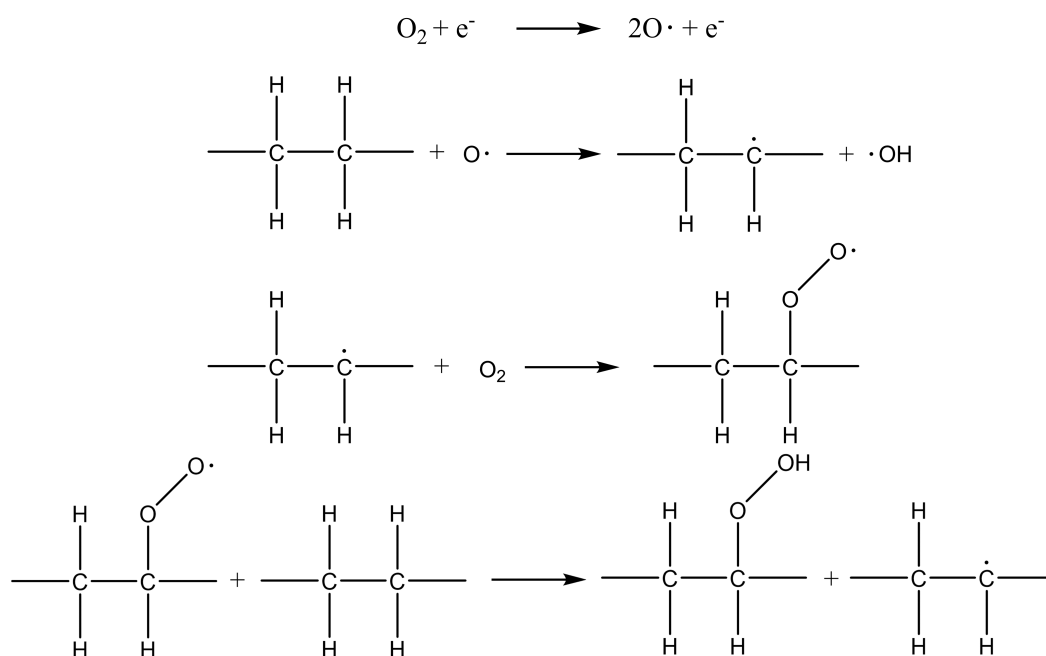


Figure 2.9: An example chemical scheme for LDPE, highlighting a potential mechanism by which oxygen functional groups, such as peroxy, can be incorporated into polymers through interactions with oxygen radicals generated by free electrons liberated by the strong electric field present in a plasma.

### 2.3.4 Methodology

For the plasma treatments utilised in this thesis, a low-pressure air plasma was applied to the polymer surfaces for a short duration, in order to minimise opportunities for thermal degradation and surface etching. The reactor used was a Diener Plasma Technology Zepto Plasma Cleaner, with samples loaded via a metal loading plate. The equipment was pumped down to a nominal pressure of  $5.00 \times 10^{-3}$  Pa prior to loading samples, and after samples had been loaded, to minimise contamination. Air was then passed into the chamber to reach a stable flow at pressures of  $\sim 10 - 15$  Pa. The chamber pressure was monitored using a Leybold Display One Pirani Gauge. This air flow was ignited into a plasma, with an input power of up to 100W, under varied durations and conditions. The chamber was then vented slowly to minimise potential of disruption to these light samples. For the microplastic powders, samples were loaded onto high-walled aluminium foil boats to minimise disruption or spilling caused by surface charging of these light particles. These powders were spread as thinly as possible to ensure even aging, and were shaken and re-aged to ensure even surface aging where appropriate.

## 2.4 Accelerated photoaging

Within microplastics research, one of the most commonly used approaches to test aging effects on polymer surfaces is to use accelerated photoaging. Many studies in recent years have used iterations of this technique, owing to its ease of use, low cost, and extensive literature history [50]. Exposure to solar radiation is well known to oxidise and degrade polymers, and the mechanisms that govern this are explained in greater detail in section 3.4.1, but in essence high-energy solar photons can excite certain bonds within polymers causing them to react with the air, oxidise, and break down.

There are many ways to implement accelerated photoaging techniques, and some standardised methods have been published, such as ASTM's D4329 [51]. Within the microplastics research literature however there is no established methodology, with many researchers opting for different approaches [52][53][54][50]. The approach taken within this research project was to use an ATLAS Suntest CPS+ System to simulate photoaging of the polymer surfaces; a widely-used 'ready-to-go' standard weathering instrument. The chamber and bulb were temperature controlled to prevent over heating of the lamp or melting of the polymer sheets. The bulb present in the chapter was a Xenon Arc lamp fitted with a filter designed to generate a spectrum that mimicked solar radiation. This spectrum can be seen in figure 2.10.

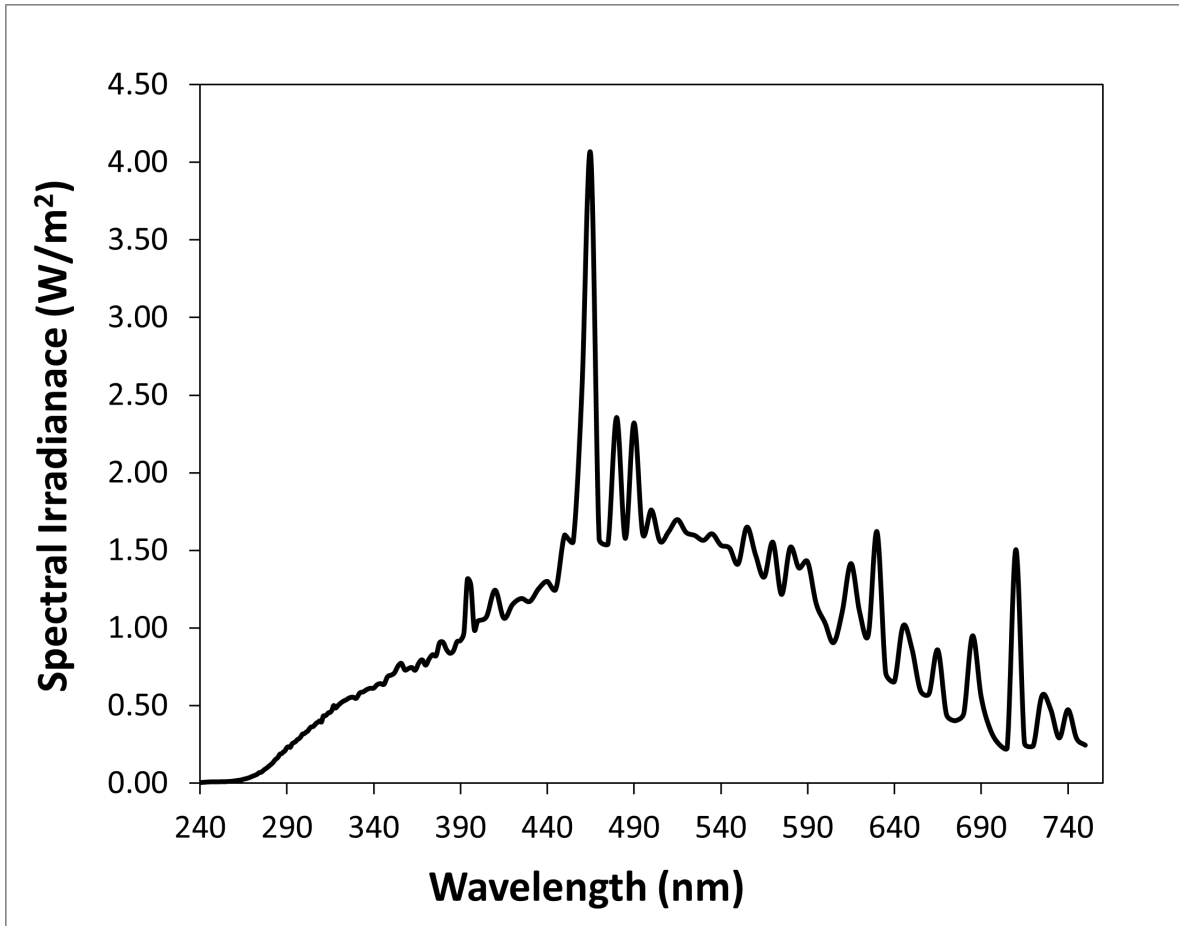


Figure 2.10: The spectral irradiance of the solar-filtered Xenon arc lamp utilised in the ATLAS Suntest system operated in chapters 4 and 5. These data were kindly provided by Prof. Crispin Halsall with minimal post-processing.

For chapters 4 and 5,  $1\text{cm}^2$  sheets of the three polymers used placed in a custom-built aluminium matrix. This matrix was a block of solid aluminium etched to form  $1.5\text{cm}^2$  wells. A solid sheet of aluminium was fastened to the back of this block using two pairs of screws and nuts to ensure it was flush with the block. A photo of this insert is shown in figure 2.11. This enabled the polymer sheets to be left in the open air inside the aging chamber, whilst minimising disruption due to air flow.

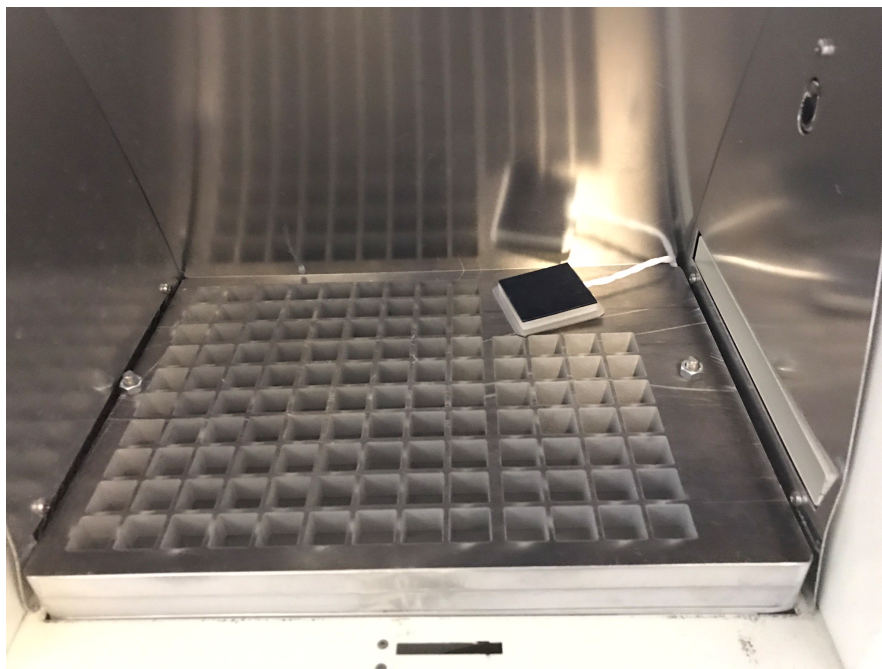


Figure 2.11: A photo of the custom built aluminium matrix for holding flat polymer samples.

## 2.5 Scanning Electron Microscopy (SEM)

SEM is a common surface imaging technique that uses electrons instead of photons to photograph a surface [55]. Because electrons have much shorter wavelengths than optical photons, it is possible to image a surface at much higher resolutions, greatly surpassing the diffraction limit of optical microscopy, with image resolutions down to the nanometer scale being possible [55]. In order to do so, the surface has to be electrically conductive. To image insulating surfaces, such as polymers, a thin ( $\sim 5\text{nm}$ ) layer of a conductive metal, such as gold, is sputtered onto the surface to increase its conductivity without changing the surface topography.

## 2.6 Cryomilling

Cryogenic Milling or ‘Cryomilling’ is a processing technique used to generate fine powders of soft and elastic materials, such as polymers. This process combines a ball mill with a liquid nitrogen feed to keep materials exceptionally cold, making them more brittle and easier to shatter into a powder. The cryomill used in this thesis was a Retsch Cryomill fed with liquid nitrogen from a 60L dewar at a pressure of +1.5Bar. Samples are loaded into a sealed metal cryomill canister with a smooth metal ball bearing, and loaded into the machine. In order to give the ball bearing sufficient space to interact with the material, the canisters were only filled  $\sim 25\%$  full with the input material. An initial precooling period chilled the milling chamber well below room temperature for a fixed duration. Then, the device switches to a milling cycle, and the canister is oscillated at a specified frequency for a specified duration. During operation, the mill is periodically re-cooled with liquid nitrogen during the ‘inter-cooling period’, to mitigate heat generated during milling. The milling cycle and inter-cooling period are then repeated for a given cycle count.

The precooling period was 450s during the first run of a session, and 300s during subsequent runs in the same session, as it was assessed that the mill was sufficiently cool after the first run to require less time. Several tests were conducted to optimise milling parameters for the materials used in this study, with the following material-specific settings reached outlined in table 2.3. Broadly, the polymers responded similarly to each other, but the silica beads required very little milling to form a fine powder.

Table 2.3: The key cryomilling parameters used in processing of the powdered materials analysed in this thesis

Treatment	Cycle length (s)	Inter-cooling time (s)	Cycle count	Frequency (Hz)
PS	180	90	3	25
LDPE	180	90	3	25
PLA	180	90	5	25
Silica beads	30	N/A	1	25

## 2.7 Contact Angle (CA) analysis

When a liquid wets a surface it forms an angle on contact with the surface (as represented by the angle  $\theta$  in figure 2.12). Contact angles vary greatly, and are impacted by the properties of the contact liquid, but also by the physical and chemical characteristics of a surface. This means that dropping a common liquid, like pure water, onto the surface produces simple yet powerful common test for surface hydrophobicity.

Conventionally, this is achieved by placing pure water droplets onto a material surface, and measuring the angle of contact that the base of the droplet forms at the three-phase boundary between the droplet, the substrate, and the air [56]. The angle is typically measured once mechanical equilibrium of the three interfacial surface tensions has been reached (so-called ‘sessile’ contact angle methods). Other methods exist as well, such as the analysis of dynamic contact angles as liquids move over surfaces [57]. These methods are not included in the research found herein, and thus are not detailed further here.

The contact angle relates to the properties of the droplet and the surface via Young’s equation (equation 2.3).

$$\gamma_{LG}\cos(\theta) = \gamma_{SG} - \gamma_{SL} \quad (2.3)$$

Where  $\theta$  is the contact angle formed,  $\gamma_{SG}$  is the solid-gas surface tension,  $\gamma_{SL}$  is the solid-liquid surface tension, and  $\gamma_{LG}$  is the liquid-gas surface tension. This relationship is shown visually for a water droplet in figure 2.12.

Angles greater than 90 degrees are considered as a hydrophobic response, and less than 90 degrees are considered a hydrophilic response, as visualised in figure 2.13.

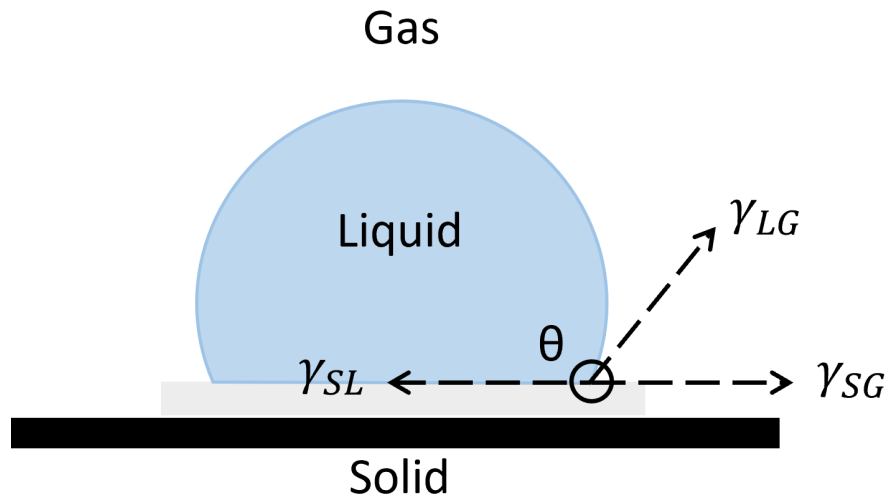


Figure 2.12: Visualisation of how a contact angle forms for a droplet on a material surface as a result of competing interface tensions.

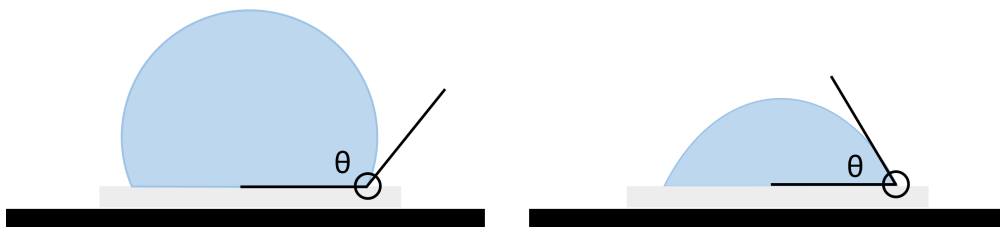


Figure 2.13: An example of a hydrophobic response (L), and a hydrophilic response (R) in contact angle.

For this thesis, an Ossila Goniometer was used to measure contact angles in a simple experimental arrangement shown in figure 2.14. First, the goniometer was levelled using a spirit level, to ensure even contact with the material surface. Then  $5\mu\text{L}$  of Milli-Q water was carefully pipetted onto a given material surface and immediately imaged. The contact angle formed was analysed using Ossila Contact Angle software. This is a sessile contact angle measurement method, and was chosen as it is an effective measure of surface hydrophobicity.

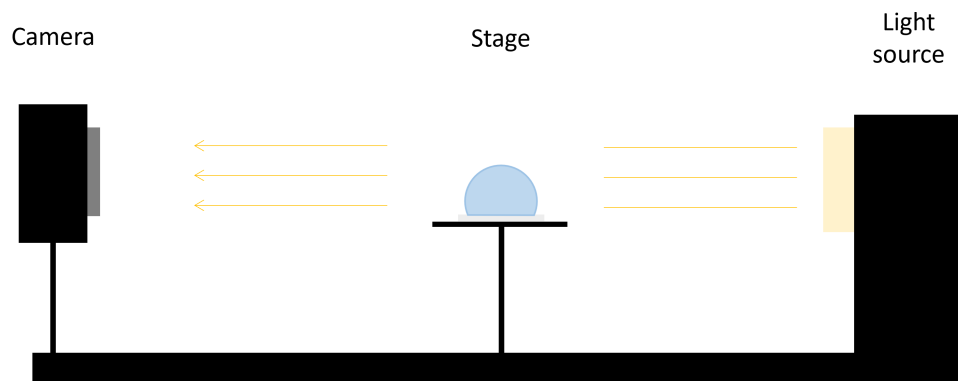


Figure 2.14: A schematic of the contact angle equipment used for this thesis. A diffuse white light source directs light at the stage, towards the detector behind it. The stage is calibrated to ensure it's level.

## Chapter 3

# Assessing what is known about the fate of plastic pollution in terrestrial matrices

### Graphical Abstract

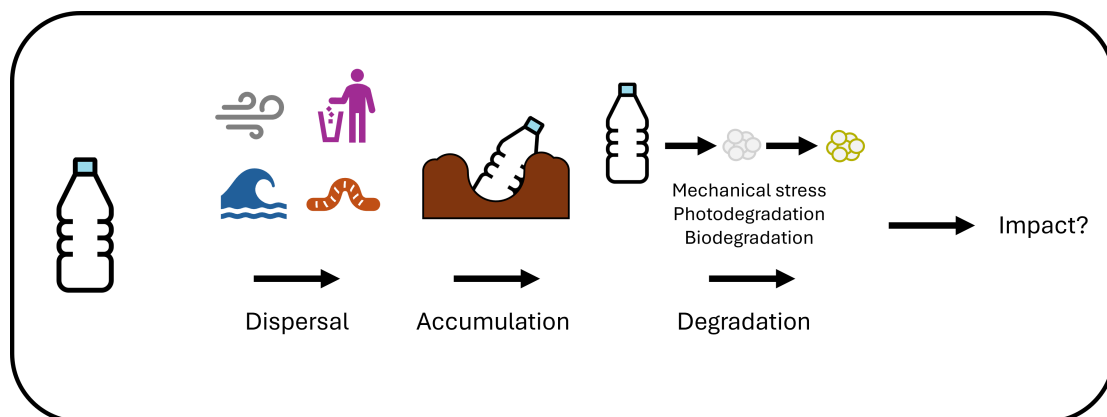


Figure 3.1: Graphical abstract highlighting key areas of interest in the microplastics literature for this thesis

### **3.1 The emergence of soil pollution as a major theme in microplastics research**

It is obvious that plastic waste traces human populations due to consumption, littering, and refuse disposal, however plastics have been observed far beyond cities. A staggering estimated 79% of all plastics ever made are either in landfill, where they are known to leach out from [58], or otherwise polluting the natural environment [59], and if trends continue this is projected to reach a total mass of 12,000Mt by 2050 [59]. In recent years, researchers have become increasingly interested and concerned about these externalities associated with plastic production and consumption, with a dramatic increase in studies citing ‘Microplastic(s)’ as a keyword emerging within the last decade (figure 3.2), compared to the previous half century since the first recorded studies. This sharp observed increase strongly highlights the interest in this field.

To date, the majority of the focus has been on the study of microplastics within aquatic environments, with over 5500 publications being captured in Web of Science query results up to 2022, meaning they hold the lion’s share at 65.1% (5640) of the total 8669 studies returned (details of the queries tailored for this analysis can be found in Appendix C). In comparison, research covering the other major environmental contexts (terrestrial, atmosphere) are lagging behind, with only 17.1% (1483) and 9.4% (814) share of returned studies respectively. The early focus on aquatic debris makes sense, as this is where the first signs of significant plastic pollution emerged, and where some of the most visible signs of the crisis are found, from beached whales found with lethal levels of plastic ingestion [60] to huge ‘garbage patches’ of pollution found in ocean gyres [22]. But the hazards of terrestrial plastic pollution are less visible, obscured by soil, buried in the ground. It is only recently that this issue has become so pressing as to be no longer overlooked.

### **3.2 Plastic is a novel anthropogenic pollutant in terrestrial ecosystems**

With plastics now well on their way to becoming part of the geological record [61], terrestrial matrices are emerging as a critically important long-term sink for plastic pollution. Whilst their emergence as a potential stratigraphic marker of the Anthropocene [62] is concerning, it pales in comparison to

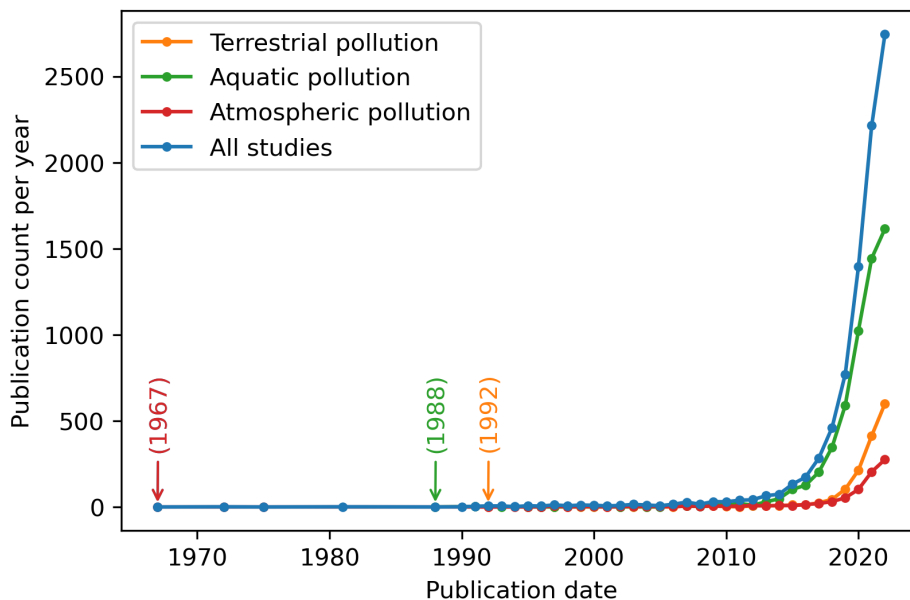


Figure 3.2: A visualisation of keyword queries of Web of Science for microplastics research studies published each year (1967 - 2022), highlighting the first time a study with relevant keywords was published

their accumulation in soil ecosystems around the globe. Soils are critical ecosystems within global biomes, uniquely responsible for governing the vast majority of food resources (an estimated 98.8% of consumed calories) produced today [63], as well as being a key regulator of various ecosystem services essential for maintaining the balance in atmospheric gases that keep the planet breathing [64].

However, with high volumes of anthropogenic pollutants finding their way into the environment this balance is looking increasingly precarious, to the extent that chemical pollution has been established as a planetary boundary threat [36]. It is imperative that researchers develop a clearer understanding of the fate of these materials in order to better ascertain the long-term prospects of their contamination, and assess the risk they present to terrestrial ecosystems. Understanding how they become dispersed into the environment, their residency times, their physical, biological and chemical impacts on soil ecosystems, and their ultimate fate within soil matrices are critical, active research questions.

### 3.2.1 Mechanisms for plastic dispersion

Plastics are typically engineered in configurations with low densities and large surface areas which, when coupled with extensive fragmentation, enables them to be highly mobile within the environment.

These mechanisms can be split out into anthropogenic, biological, and physical processes. This is not an exhaustive list of mechanisms, but it highlights how mobile plastic pollution has become, and how readily it is redistributed.

### **Anthropogenic dispersal**

Microplastic dispersal has been observed to occur through the direct and indirect result of human actions. Littering is one of the most visible mechanisms of plastic dispersal. Despite this, the direct impact due to littering remains largely unquantified [65]. Transportation via cars can lead to microplastic generation through long-term wear on tyres [66]. Management of municipal waste water and sewage can lead to microplastic release into the environment, as filtration mechanisms are not perfect [67][68]. This can be further indirectly introduced to fields through the application of sewage sludge as a form of fertilizer [69].

### **Biological dispersal**

Further dispersal can be the byproduct of biological processes. This can occur through the adhesion to the surfaces of different organisms, such as worms, which then move through the environment [70], leading to vertical transport of microplastics in soils. Biofouling of microplastics can lead to changes in buoyancy, allowing for vertical transport in water columns [71].

### **Physical dispersal**

Physical phenomena are readily able to carry and disperse plastic pollution, and this is well documented. Microplastics are light enough that they are readily carried on currents of air [72][73], potentially leading to their deposition far from their origin. Seasonal floods and monsoons carry and deposit microplastics in certain climates [74]. A substantial fraction of marine plastic pollution is estimated to originate from land-based sources, driven by rivers [75].

## **3.2.2 Accumulation in the environment**

The wide array of dispersion mechanisms outlined above leaves one singular impression: once unconstrained, plastic pollution is highly mobile, and can find its way through the environment into a variety of terrestrial matrices. Because of this, concentrations in soils can be highly variable, depending on their context and role. Further still, as an emerging contaminant these values are often troublesome to

compare, with different units being reported in different studies. Where possible in this section these units have been converted to provide sensible comparisons, however due to the complexity of these measurements this is not always possible. Common representations include reporting Items/particles per unit mass and plastic pollution mass per unit mass, but because of the limitations of quantification techniques, the fact that particle sizes vary wildly, and the fact that the densities of plastic pollutants vary greatly as well, these comparisons are estimations. As time progresses, these values are expected to increase. Existing methods for quantifying these sinks, such as density separation techniques, struggle to assess smaller particle sizes, meaning that existing quantification assessments are likely to be an underestimation, and there is no standardised approach for quantification in soils, which makes comparison of results challenging [76]. Nevertheless, it is an important first step in assessing the extent of the problem.

For uncultivated, uninhabited natural terrestrial matrices, such as national parks, levels of plastic pollution should be low. Despite this, microplastics have still been detected in a number of remote locations. Low levels of microplastics have been identified in Swiss flood plain soils (up to 593 items  $\text{kg}^{-1}$ ) [77], to desert soils in the Iranian plateau at 20 items  $\text{kg}^{-1}$ [78], to the mangrove soils of Brazil where a significantly higher mean value of  $10,782 \pm 7671$  items  $\text{kg}^{-1}$  was observed [79]. Recently, studies have even began emerging identifying microplastic pollution in the so-called ‘Third Pole’, one of the most remote terrestrial regions on Earth nestled in the mountains of central Asia, with measured concentrations in bare soils at the generally low (but measurable) value of  $<200$  items  $\text{kg}^{-1}$  [4]. These studies communicate that plastics are able to accumulate anywhere; it doesn’t necessarily require intentional human activity.

But plastics are also often introduced to soils directly and deliberately. Modern agriculture has taken advantage of the benefits plastics provide, and their appreciable usage in modern agriculture has brought with it the emergence of so-called ‘plasticulture’ [80]. Plastics are used to aid the growth of plants in several ways, such as the use of netting, polytunnels, and through the application of mulch films [81]. This leads to significant plastic waste generated on-site, with researchers estimating 100s of kilograms of waste produced per hectare of typical European farmland each year [82]. In particular, the practice of using mulch films in soils has hugely increased in recent years, with researchers reporting that over 80,000  $\text{km}^2$  of agricultural land are covered in plastic mulch films each year [83]. Typical mulching films last longer than typical crop cycles, and they are incredibly difficult and time consuming

to remove at the end of their use. This process isn't always well managed, leading to plastic films and residues being left in soils [84]. Estimates for residency of plastics vary, and are highly material dependent, but conventional LDPE is expected to last decades, and even examples of LDPE that have been modified to improve their degradability in soil are still expected to take several years to fully break down [65]. As such, agricultural soils are now expected to be a long-term sink for plastic pollution.

Within agricultural soils existing microplastic concentrations have been measured extensively, and vary widely, but with an average of  $\approx 1200$  items  $\text{kg}^{-1}$  [23]. In agricultural soils that have regularly had plastic mulch films deliberately applied, concentrations are expected to be generally higher than those which haven't. A recent study demonstrated that the number of years of mulch film usage is correlated with microplastic concentrations, measuring  $80.3 \pm 49.3$  items  $\text{kg}^{-1}$  after 5 years of mulch film application, increasing to  $1075.6 \pm 346.8$  items  $\text{kg}^{-1}$  observed after 24 years of continuous mulching in Chinese agricultural soils [85]. New technologies, such as biodegradable mulch films, aim to reduce the long-term persistence of these materials by enabling them to break down readily in fields, however this shift presents its own challenges, such as more acute short-term effects [86].

Lastly, in soils found in urban environments, or those used for industrial or waste management purposes, concentrations are unsurprisingly substantially greater. Studies have reported values as great as 12,200 items  $\text{kg}^{-1}$  in urban settings [87]. The most obvious sink for plastic pollution is at the end of waste disposal. Landfills take in a huge volume of plastic waste from municipal sources, depending on local recycling rates, and are arguably the single largest sink for plastic waste in the terrestrial environment. Whilst data on exact microplastic concentrations are somewhat lacking, initial assessments put this value at an unsurprisingly massive value of  $62,000 \pm 23,000$  items  $\text{kg}^{-1}$  [88]. Whilst landfills are not cultivatable soils, and they're expected to be a sink for pollution, landfills are known to leak plastics into surrounding areas [89], and may contribute to airborne concentrations of microplastics [90], so the persistence of plastics in this terrestrial context is still critical to assess.

### **3.3 Hazards associated with microplastic accumulation**

The dispersal and accumulation of these materials demonstrates their widespread pollution of the terrestrial environment, but how concerning is it? Plastics are generally considered to be one of the

safest materials available to the modern world, which is why they are routinely used in Personal Protective Equipment (PPE), food packaging, and medical implants. This leads to a sense that they are harmless, but the reality is the true risks to human health and the environment are still unclear [91]. With each of these applications, the material is tailored to meet a specific need, designed for its use in controlled, well-tested settings. But once released into the environment this control is immediately lost, which leads to unintended consequences.

### **3.3.1 Physical harms**

The most immediate hazard of plastic pollution results from their physical structure. As light, voluminous and resilient materials they are able to get lodged in places they shouldn't be, and become hard to displace. This hazard is most visible with wildlife; they are well-known to be ingested by a wide variety of animals, leading to physical blockages in the guts of large mammals and birds [92] [93], as well as leading to entanglement, injury and suffocation for creatures ensnared by these materials that are unable to escape [94]. They also have the ability to alter physical spaces within the terrestrial environment such as obstructing waterways, which has been raised as a potential flood risk within urban settings [95].

### **3.3.2 Additive leaching**

Plastic pollution also presents an indirect harm due to their complex composition; the pristine polymer backbone of many plastics may be considered nontoxic and harmless, but the chemical additives incorporated into them sometimes aren't. In everyday use this isn't a key concern, but once abandoned in the natural environment these chemicals can leach out over time, as they typically aren't covalently bonded to the polymers, instead worked into the material matrix [96], resulting in them appearing in contexts they weren't designed for. Additives such as phthalates are classified as endocrine disruptors [97], and are known to cause issues in the reproductive health of wildlife even at very low environmentally-relevant concentrations [98]. In marine environments and freshwater environments ecotoxicological studies have demonstrated that additive leaching is harmful [99], and recent studies in a soil context have corroborated this as well [100].

### **3.3.3 Impacts on microbial diversity**

Whilst their robustness may be present a number of challenges, their relative inertness and strength does mean that plastics can be excellent hosts to microbial life. Microorganisms require a robust substrate to grow on, and plastics serve as an excellent medium for this. Over time, microorganisms accumulate and envelope plastic particles, forming a unique assemblage which has come to be known in the literature as a ‘plastisphere’, because the colonies on plastics have been found to be unique in composition when compared to their direct environment [101]. Within marine environments they have been shown to be influenced by the chemistry of the plastic itself, with different bacterial assemblages forming on different plastics, and by different environmental properties such as salinity [102], and in soils there is also some evidence that soil properties such as pH could affect the composition of the plastisphere [103]. Research comparing plastics in two distinct marine environments finds polymer type is not the dominant factor in microbial assemblages, and instead suggests the environment itself is the dominant factor [104], at least for simple hydrocarbons, and the same may be true for terrestrial matrices. Additionally, recent research indicates that the presence of plastic as a substrate may affect the behaviour of biofilms, with bacteria colonising plastic pollution having been shown to have increased rates of horizontal gene transfer (HGT) [105], and HGT is known to play a key role in microbial evolution [106]. In essence, microplastic pollution has shown a substantial ability to affect microbial diversity.

### **3.3.4 Plant health**

Researchers have recently hypothesized that the advent of plastic pollution in soils may have unintended effects on plants in a number of different ways [107]. Research on this topic is emerging, and initial studies have indeed found significant effects on a variety of food crops, with concentrations of 1% w/w of polyethylene and biodegradable polymer mixes leading to negative outcomes for the growth of wheat plants [108], a demonstrated ability to affect the microbial composition of the rhizosphere of wheat plants [109], and negative outcomes on corn plant growth at higher concentrations [110]. Further research is needed, but it is clear that plastic pollution has the potential to perturb plant performance.

### **3.3.5 Interactions with other chemicals in the environment**

Microplastics are well known to become substrates for the sorption of Persistent Organic Pollutants (POPs) such as polychlorinated biphenyls (PCBs), of heavy metals, and of antibiotics within the envi-

ronment [26][27][28][8]. This is an active area of research, and understanding the ability of increasing levels of microplastics to concentrate or amplify other sources of pollution is essential to assessing the overall impact of these materials. This emerging subfield has focused considerably on how microplastics may concentrate these chemical contaminants, and the ecotoxicological risks this presents due to concerns over bio-accumulation [111].

### **3.3.6 Effects on soil properties**

Studies have already demonstrated that microplastic pollution has the potential to alter soil properties under certain conditions. Machado et al have shown impacts of a variety of pristine microplastics in a loamy soil, such as consistent decreases in soil bulk densities and indication that polymer type can influence microbial activity [112], as well as notable changes in other properties such as evapotranspiration, increasing by up to  $\approx 50\%$  with a pristine polyester fiber amendment, as well as leading to a general increase in the water holding capacity of the soils [113]. This is considered a research priority, with calls for additional studies being made in a recent review [114].

### **3.3.7 Impacts on the carbon cycle, and other nutrient cycles**

One final still poorly understood and often overlooked impact of plastic pollution, is their link to the climate crisis. Plastics have significant influence over the carbon cycle, as well as emerging evidence of their ability to alter the cycling of other biogeochemical nutrients.

Plastic is predominantly made of carbon, with around 80% of the weight of most common pure plastics being carbon [115]. Different polymer structures, and different additives give differing stoichiometric considerations, but ultimately once plastics are fully mineralised within the environment they become a flux of the carbon from petrochemical (or biomass-based) stores into the environmental matrix that they assimilate into, either as microbial biomass or respired into  $\text{CO}_2$ . It is not clear if this is the ultimate fate of all plastic pollution, but some polymers are known to readily mineralise into carbon dioxide and dissolved organic carbon through environmental degradation, such as polystyrene [116]. This is also one of the chief concerns of highly-accelerated degradation such as ‘ideal’ biodegradable plastics; they potentially turn petrochemicals and biomass into another  $\text{CO}_2$  flux. Perhaps of greater concern, is that their breakdown can also produce gases with greater global warming potential, such as ethylene and methane [117].

Energy is required in order to produce plastics. Extraction, refining, moulding, transportation, and other industrial processes all have a carbon footprint. These are processes still dominated by fossil fuel energy production, meaning that this impact that plastics can have on the carbon cycle is well understood, and significant [16].

Once introduced to the environment plastics may be able to further indirectly influence the carbon cycle through mechanisms such as ‘priming’ effects [118]. The priming effect is a mechanism by which the input of a nutrient can provide a boost to local microbial activity and ‘prime’ them to break down other organic compounds in their surrounding, therefore creating greater carbon effluxes than would result from the mineralisation of the plastic alone. This has already demonstrated in some environmental contexts [9], and it is possible that this could occur in terrestrial matrices as well.

### **3.4 Mechanisms for plastic degradation in soils**

Even the most resilient polymers breakdown eventually. The environment is a chaotic mix of forces, and materials can be exposed to a wide variety of different stimuli. Solar radiation, physical abrasion, bacterial or fungal colonisation, chemical damage, and thermal stresses, can all be applied in a near-infinite combination yielding different degradation outcomes. These processes can change the properties of plastic pollutants, and over time gradually split polymer chains into oligomers, and then into monomers [119]. Historically, the vast majority of this research focused on studying materials during their ‘useful’ lifetime, and preventing degradation, however as the environmental concerns over plastic pollution have emerged there has been a renewed interest in understanding these mechanisms within environmental contexts. In order to assess the impact and fate of microplastics in soils, it is critical to be aware of these processes.

#### **3.4.1 Photodegradation**

Exposure to solar radiation is well-known to degrade polymers, and has been studied for decades. This process can be broadly explained in three stages:

##### **1. Initiation**

A high-energy photon is absorbed into the material, initiating fission of a covalent bond and causing two radical species to emerge (shown in figure 3.3).

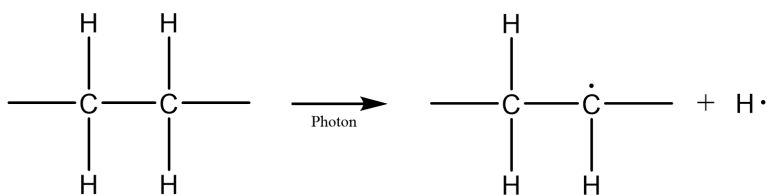


Figure 3.3: A chemical scheme showing the process of initiation, where an incoming photon breaks apart a carbon-hydrogen covalent bond.

## 2. Propagation

Radical species are highly reactive, and readily attack the polymer chain, changing its chemical structure, and generating at least one more radical in the process (shown in figure 3.4).

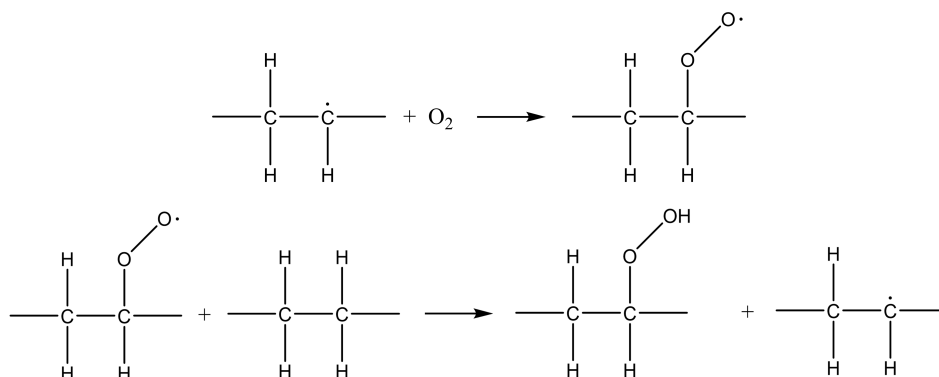


Figure 3.4: A generic chemical scheme showing two key propagation mechanisms during photodegradation, in which a radical of the polymer reacts with diatomic oxygen present in the air to form a peroxy radical. This peroxy radical then reacts with another polymer chain, generating another radical in the process. At the end of both steps new radicals are formed that propagate the degradation of new chains.

## 3. Termination

Radicals react with each other, forming a stable molecule and terminating the process (shown in figure 3.5).

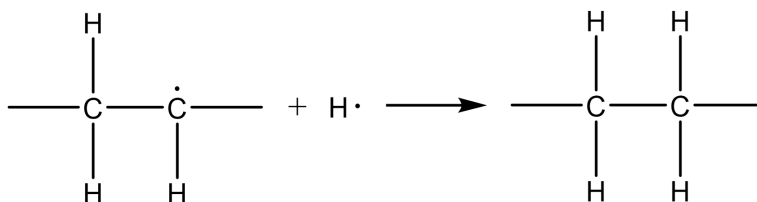


Figure 3.5: A chemical scheme showing the process of termination, where two radicals react together to form a stable molecule, terminating the photodegradation process.

The likelihood of photodegradation occurring depends on the specific polymer structure, as some functional groups and moieties are more photosusceptible than others. However, virtually all polymers are photodegradable, as even if a given polymer has no resonant bonds, chromophores which can readily absorb solar radiation are often introduced as impurities during the manufacturing of polymers, which kick-start this process [120]. Many different radical species can form in polymers, such as primary, secondary and tertiary alkyl radicals, meaning that rates of photolysis can be complex and material dependent. There is a wide variety of specific mechanisms that have been identified in the literature for the photolysis of polymers, such as Norrish Type 1 & Type 2 reactions for ketones, hydrogen abstraction, beta scission, and many more. The full details of this are beyond the scope of this research, but can be found readily in the literature [121][122]. In general, carbon radicals generated from the fission of the covalent bond in step 1 can then react with oxygen in the air to generate oxygen radicals, as oxygen is relatively reactive. This means that long-term degradation leads to measurable oxidation of these materials, and a general increase in oxygen-containing functional groups [123].

Additives can further accelerate or inhibit photolysis, depending on the intention of the material design. Generally, polymers are designed to be resilient to degradation, and as a result there is a large array of additives designed specifically to inhibit photolysis known as ‘UV stabilisers’, encompassing chemicals like Hindered Amine Light Stabilisers (HALS)), which lead to early termination of radical species (so-called ‘radical scavengers’) [124]. However, as uncontrolled environmental degradation occurs additives are known to be able to leach out of plastics [125]. For photo-stabilised polymers, this means that the combination of different environmental exposures can lead to a change in their ability to resist photolysis, as they lose their resistance. This results in a different rate of photolysis in the natural environment when compared to the material studied in its designed environment.

Once in a terrestrial matrix, photolytic mechanisms can become attenuated. Microplastics in soils are almost immediately biofouled, buried under layers of soils or otherwise obscured, which significantly minimises their exposure to solar radiation. Photolysis for other organic chemicals is known to be restricted to the top 0.2-0.4mm for direct photolysis, and the top 2mm of the topsoil for indirect photolysis due to the soil attenuating the radiation [126]. Photolysis is an essential part of polymer degradation, and virtually every polymer will be exposed to some level of photolysis before becoming embedded in a terrestrial matrix. However, it is complex, and will rarely lead to perfect mineralisation of a plastic. This means that when assessing the impacts and fates of plastics, it is essential to consider

the impact that partial photolysis and oxidation will have in this process.

### 3.4.2 Mechanical stress

Mechanical stress of plastics during their useful lifetime has also been well documented in research literature over multiple decades [127][128], but studies on environmental mechanical degradation mechanisms, and how this leads to the formation of microplastics, have only emerged more recently. It has been proposed that mechanical stress is a key mechanism in the generation of microplastics. Shearing forces break bonds and generate macro-radicals, leading a breakdown of the polymer structure [129]. Even seemingly mundane everyday examples, such as using the cap on a plastic water bottle, has been shown to readily generate microplastics [130].

There many physical processes present in nature, driven by the movement of wind, water, soil mass, and the actions of flora and fauna that could drive the generation of microplastics. To date, these mechanisms have not been fully explored, and it is unclear what the dominant mechanical degradation processes are within an environmental context.

### 3.4.3 Bio-degradation

Most soil matrices are rich in microorganisms, which breakdown and repurpose naturally occurring fractions of soil within the environment, and for many materials this is ultimately how they are recycled. However, plastics are chemically novel from the environment's perspective, meaning they are challenging for microorganisms to digest. Many common plastics have long been known to be highly resistant to microbial degradation [131], and modern plastics are often further engineered with microbial-resistant additives to extend their useful lifetime. Despite this, as soon as plastics enter the environment they are still bombarded with biological molecules. Almost immediately, they are coated in a layer of material on their surface often referred to as a 'Conditioning Film' (CF), or 'Eco-corona'; a layer of bio-molecules that initiates biofilm formation [8]. This can be further sorted into a 'hard' core layer, and a 'soft' outer layer, for molecules that are strongly adhered to the surface and loosely bound to the surface respectively [8]. Conditioning films are well-known to be a key driving force for cellular adhesion, but it is not clear whether the formation of hospitable conditioning films affects rates of biodegradation, though it is generally accepted that biofilm formation on a polymer surface is a prerequisite for biodegradation [132].

Once colonies have formed, bacteria and fungi produce enzymes in order to digest surrounding organic material and retrieve their nutrients, and within soil environments it has been proposed that enzymatic hydrolysis of polymer chains is a critical stage in their overall biodegradation [133]. All biodegradable polymers contain hydrolysable bonds and is generally considered to be the most important mechanism in their degradation [119]. Some polymer structures, such as those observed in condensation polymers, may already be suitable for this degradation. However, many polymers have no such sites for hydrolysis, which may explain why they are highly resistant to biodegradation. Other degradation processes could introduce sites for hydrolysis in otherwise robust polymers by shortening the chemical chains, and introducing more accessible functional groups for biodegradation, but this is not well explored. However, whilst some polymers may be shown to degrade by enzymes in a laboratory setting, it does not necessarily translate that it will biodegrade in real-world conditions, which is an important consideration when transitioning understanding of biodegradation out of the laboratory and into the environment [134]. There are several reasons for this. As outlined in Sander et al there are stoichiometric considerations to address [135]. Different colonies of microorganisms have different nutritional requirements, and then different nutrients can be rate limiting. For example, fungi have been found to colonise some plastics, and due to their different stoichiometry they may be preferential in the degradation of plastic polymers, as they require less nitrogen to form biomass [133]. However, to what extent fungi mineralise these substrates is still poorly understood, and is an ongoing question within the research. At the very least the direct mineralisation of many plastics by fungi is expected to be very slow, but may still serve to be a better mechanism for biodegradation of plastics than bacteria as fungi can also make use of their hyphae, effectively connections drawn between different parts of the colony, enabling them to move nutrients around and further help to compensate for the nitrogen needed to breakdown plastic debris.

#### **3.4.4 Accelerating polymer aging for research**

One significant limitation of existing studies investigating plastics in soil matrices is that they have largely focused on the impact of pristine (i.e. new, out of the factory) materials [112][113][136][137]. Section 3.4 demonstrates that this is not realistic of plastic pollution. However, because plastics are resilient materials the degradation of most plastics in the environment is estimated to occur on relatively long human timescales [138], which makes including this element in research significantly time consuming and difficult to achieve. Therefore, it is desirable to simulate advanced aging with

accelerated weathering protocols, such as those compared in table 3.1. These methods can approximate narrow features of aging on quicker timescales, leading to representative aging without having to wait for decades (in which time the materials and additives in circulation could have potentially changed). This subfield within microplastics research is emerging as a keen area of interest, with multiple reviews on the topic published recently [50][139]. There are several ways scientists can approach this.

Mechanical degradation is routinely done in the preparation of microplastic studies. There are two reasons for this: 1) microplastic pollution is often the result of mechanical degradation (so-called ‘secondary’ microplastics, resulting from mechanical degradation in the environment [140]; ‘primary’ microplastics, those designed to microscopic size in the initial instance [140] are necessarily rarer, as their applications are a narrow subsection of plastic use) so in order to prepare microplastics a mechanical degradation step is often required and 2) mechanical aging is extremely quick and straightforward. Common methods seen in the experimental methods include simple mechanical grinding through the use of pestle and mortars [141], and other methods such as cryogenic milling (‘cryomilling’) [142].

Steps are sometimes also taken to accelerate the chemical changes that happen in the environment as a result of photo-oxidation. In general, two broad approaches to mimic environmental photodegradation have emerged as common threads in the literature. The first is to use high-power lamps, treating polymers with a greatly increased flux of photons. This approach can be designed to mimic the solar spectrum, but at a greater power, to achieve a highly-realistic result. Whilst far quicker than natural photodegradation, this process still takes days to months to achieve meaningful results [50].

A second commonly used approach is to bathe plastics in chemical treatments, such as peroxides, and Fenton reagents [143]. This approach can lead to rapid aging in the order of days to weeks [50], however this approach requires plastics be kept in an aqueous mix, often at high temperatures. Other novel methods for microplastic preparation are emerging, such as gamma treatment, and plasma degradation [50], but these methods are unproven, and significant further work is required to assess how fit-for-purpose they are for microplastics research.

## 3.5 Conclusion

Due to the volume of production, their demonstrated mobility in the environment, and ability to fragment into microplastics, it is clear that plastic is an emerging terrestrial pollutant of chief concern.

Table 3.1: Top-level comparison of the key advantages and disadvantages of accelerated aging techniques used in microplastics research to simulate long-term environmental degradation.

	Photo Aging	Chemical Aging	Plasma Aging
Key Advantages	Widely used technique Faster than real-world aging (order of weeks [50]) Directly mimics real-world photodegradation	Much faster degradation (order of days [50]) Relatively easy and cheap to perform (standard lab equipment and cheap reagents)	<i>Exceptionally</i> fast degradation expected (in the order of minutes) [50] Ability to rapidly simulate aging of photo-resistant polymers like PVC [144]
Key Disadvantages	Far slower than the alternative methods	Use of concentrated oxidising chemicals mean this an abstraction of natural degradation	Plasmas have minimal material penetration Use of plasma means this is an abstraction of natural degradation

Once present, they degrade further due to their interactions with their environment, which changes their properties and could potentially change how they interact. Accelerated aging methods enable researchers to simulate these processes more quickly, but these methods can still take considerable time. Emerging methods, such as plasma aging, may be able to achieve significantly more rapid aging, however they remain largely unheard of and unproven within microplastics research. On the basis of this assessment, an analysis of plasma aging as a tool for accelerating microplastics research is highly desirable. This is the objective of chapter 4.

Another common theme in the research explores how plastic pollution interacts with other chemicals in the environment. Previously, this has largely focused on their interactions with other pollutants such as antibiotics and POPs and their potential bioaccumulation. Significant further work is required in order to evaluate their interactions with other chemicals seen in soils, such as soil nutrients. It is unclear what the impact plastic pollution will have on these processes, and to what extent the degradation of polymers could alter these processes. This is the core theme of the research presented in chapter 5.

Ultimately, over time, as plastic pollution persists in soils it becomes a significant fraction of the soil matrix. The long-term implication of this on soil health is a critical gap in the research that has seen considerable recent interest. To date, studies have largely contained themselves to pristine plastics when performing these experiments. This is a sensible first step, however because it is well established that plastic pollution degrades in the environment, a robust understanding of the extent

that polymer aging will have on soil health is essential to concluding an assessment on the long-term impact of plastic pollution. A soil study using pristine and aged microplastics is presented in chapter 6 providing new insights to these questions.

## Chapter 4

# Plasma degradation: A novel, general, and rapid aging protocol for microplastic research in the environment

### Graphical Abstract

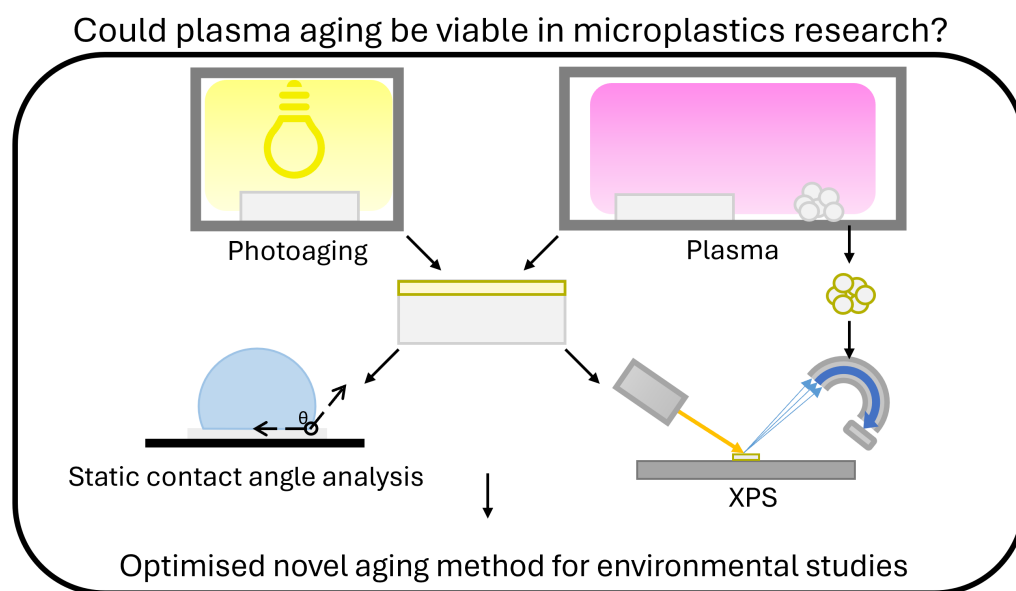


Figure 4.1: A visualisation of this chapter's aims

## Abstract

A comparison of accelerated photoaging and plasma degradation for polystyrene, polylactic acid, and low-density polyethylene was made to evaluate the potential for plasma degradation as an accelerated aging method for microplastics research. Such methods are key to promptly assessing medium- and long-term impacts of these materials, however existing methods have limitations. Plasma degradation promises to be a rapid alternative. Results show that plasma degradation is a suitable match to photodegradation, with the emergence of similar functional groups (carboxyl, carbonyl, alcohol and others) in the plasma-aged surfaces as the photoaged surfaces. Key plasma parameters were then investigated to best match this method of degradation to environmental photoaging. It was found that far shorter exposures (in the order of seconds to minutes) were optimal for microplastics aging when compared with existing literature. In general, the power used to ignite the plasma made some marginal differences in functionalisation of the carbon chain, and a 100W input power setting was optimal for general use. The optimised protocol was then used to successfully age microplastic particles in the 125 - 500  $\mu\text{m}$  size range. Key advantages and limitations were discussed in the context of existing methods, with plasma degradation assessed as better in some key metrics, namely the speed of degradation, and worse in others, such as ease of implementation. Overall, plasma degradation was assessed to be an effective abstraction, both theoretically and empirically, of photodegradation when applied to surface chemistry-focused studies. Plasma degradation, when used appropriately, is a powerful addition to existing aging methods for microplastics research, allowing for greatly accelerated research studies to be conducted.

## 4.1 Introduction

Plastic pollution has emerged in recent decades as one of the defining ecological crises of this generation. First discovered in the early 1970s [21], researchers have now found microplastics the world over [5][65]. It is expected that the addition of significant amounts of these novel pollutants will influence the behaviour of environmental systems, as their properties are dramatically different to existing environmental detritus. Plastics are (in general): stoichiometrically unique within the environment as they are mostly carbon and hydrogen, formed from long-chain molecules with strong chemical bonds, resilient to most forms of natural degradation, typically hydrophobic, resistant to water, very light (and therefore mobile), malleable, and chemically novel to the microbiota that have evolved within

a given environmental matrix. Because of these unique properties, these pollutants result in unique environmental hazards as outlined in section 3.3. In order to inform policies and technologies set to mitigate these issues, the impact of these pollutants needs to be assessed swiftly.

To date, the overall understanding of the impact of plastic pollution on environmental processes is limited, and in particular research covering how their impact changes as they change *over time* within the environment remains largely unexplored. Much existing research has so far tested hypotheses using ‘pristine’ plastics [112][113][136][137]. Researchers typically conduct a mechanical preparation step (such as cutting up the material, or milling), but otherwise leave the materials chemically pristine. Pristine plastics are materials that come directly from a manufacturer or supplier, and they have not seen any meaningful degradation or change in their properties when compared to their synthesis. Because of this, these materials are easy to obtain, categorise, and characterise. However, they are not realistic analogues of plastic waste found in the environment, which is known to be highly degraded both physically and chemically [145]. This means that research which only uses pristine plastics may be missing out on part of the picture, and taking into consideration aging on these effects is essential to seeing the whole picture. In order to do this, researchers need to age plastics.

Plastics begin to age as soon as they are created, but once littered or otherwise discarded, these processes occur in uncontrolled and unpredictable ways. The environment is a chaotic mix of forces, and materials can be exposed to a wide variety of different stimuli, which have the potential to dramatically alter their properties. Solar radiation, physical abrasion, bacterial or fungal colonisation, chemical damage, and thermal stresses, can all be applied in a near-infinite combination yielding different degradation outcomes. Polymers exposed to solar radiation can become less physically resilient [146], mechanical degradation from transportation by wind, water, and animals can fracture these materials, leading to fragmentation and the formation of microplastics [147]. This enables the plastics to be further transported, dispersed, and mixed more readily in terrestrial environments, with smaller particles known to be redistributed through physical and biological means [72][70], becoming intimately intertwined with environmental matrices. Microorganisms also colonise plastics, slowly breaking down polymeric chains through enzymatic hydrolysis [135]. It is reasonable to expect that these shifts due to aging could dramatically impact their interactions within the environment, as transforming clean hydrophobic long-chain polymers into hydrophilic short-chain polymers colonised by microbial life makes their surfaces more active, more interactive with water, and more susceptible to biodegrada-

tion. Oxidation also leads to them changing colour, which has been shown to affect how environmental organisms interact with them [148].

Because natural aging is so chaotic, accurate material characterisation, reproducibility, and identification of causality from this approach is challenging, making it difficult to test hypotheses related to aging in a scientifically-robust manner. Natural aging is also not helpful for assessing the potential impact of future materials, as material innovation happens well within the timescales of natural degradation, meaning materials that are found naturally degraded now are not necessarily the same materials that are in use today. However, there is a middle ground between pristine plastics and natural aging. Researchers can use highly-constrained accelerated aging protocols in the study of plastic pollution [149]. Controlled degradation approximates narrow features of environmental aging, such as tailored changes to surface chemistry, allowing for a direct assessment of the impact of aged materials in a way that is most relevant to a hypothesis.

Within microplastics research, accelerated photoaging and oxidative chemical treatments are by far the most commonly employed methods [50]. Researchers have focused on these methods which cause changes in the polymer surface chemistry, as it is reasonable to expect that changes in the chemical properties are hugely relevant to their environmental impact, such as how increases in oxidation increase the wettability of a surface, given how commonplace water sources are in the natural environment. Whilst faster than natural aging, these processes can still take days to months to yield significant chemical degradation, and improved methods are highly desirable. Existing methods come with unique drawbacks, such as the need for relatively high temperatures used in common chemical aging methods [143], which may lead to unrealistic degradation for some materials in laboratory settings. This is an active field of research, with recent studies published that are further building the understanding of accelerated aging methods [150] and exploring new ways to age polymers quickly in environmentally-relevant ways [151]. Some internationally-recognised standardised protocols exist for assessing weathering in a highly realistic manner, but many researchers have opted for faster protocols that have not been fully developed, standardised, or assessed in suitability. [152]. This makes further reproducibility, comparison of results, and assessment of the true environmental relevance of results challenging. The development of rapid, reproducible, standardised methods is desirable, and being clear about how effective a method is as an abstraction of environmental aging, and how to apply it appropriately, is essential.

One critically under-explored alternative aging method is the treatment of microplastics with plasma. Plasma is a broad classification often referred to as “The fourth state of matter”, which describes a macroscopically neutral, conductive ionised gas comprised of highly energetic free electrons, high-energy photons, ions, and radicals, as well as neutral molecules. Within laboratory conditions plasmas can be formed using a wide variety of parameters, that can be further optimised for different applications [45]. They can be tweaked by using different methods of ignition, different durations, different inlet gases, different strengths of electric fields, and different pressures. Plasma treatment is already known to be able to oxidise polymer surfaces *exceptionally* quickly [153], and this capability has seen application in other fields, such as in the preparation of polymers for surface coatings [154][155]. Plasma can be applied to a polymer surface to approximate photodegradation from solar radiation, as when a plasma ignites it generates a vibrant mix of energetic particles, including UV photons and radical species. This happens because in order to generate a plasma a high-energy electric field is applied across a reaction chamber, and this injection of energy pulls a small fraction of the molecules apart. As natural photolytic processes rely on high-energy photons to generate radicals which then break down plastics, the mix of these immediately available within a plasma make it a reasonable theoretical abstraction of photodegradation.

However, despite its significant potential, only one study has tried to apply plasma-based aging methods as an accelerated aging method in microplastics research [50][144]. Zhou et al successfully aged PVC microplastics in their study and provided evidence that their equipment led to an increase in oxidation of this material [144]. However, due to the complexity and potential variability that plasma has as a degradation method due to the wide variety of possible parameters, further work is required to confidently establish this method as a standardised aging protocol, and analyse its limitations. To date, there has been no decisive attempt to either assess the validity of this technique as an abstraction of environmental aging, or to establish an optimal set of parameters to use for microplastics research.

In this study X-ray Photoelectron Spectroscopy (XPS) was used to identify fine changes in surface chemistry attributed to plasma aging which were compared with a more commonly used photoaging approach, Scanning Electron Microscopy (SEM) was used to confirm whether or not physical changes arose as a result of this treatment, and Contact Angle (CA) measurements were used in order to assess any changes in hydrophobicity. Many environmental impacts of these materials will arise from their contact with the surface (such as microbial attachment and sorption processes), therefore under-

standing how simulated aging affects the material surface chemistry and physicality is essential. Then by testing different parameters of these methods to identify realistic results, an optimised procedure is established. Herein, the role of plasma degradation in microplastics research is analysed and an optimised approach is illustrated.

## 4.2 Methodology

### 4.2.1 Materials & Preparation

Polystyrene (PS), Low-density Polyethylene (LDPE), and Polylactic Acid (PLA) were chosen as the materials for this study. The repeat units of these polymers are shown in figure 4.2. PS and LDPE because they are commonly polluted polymers which degrade relatively slowly, but also have key differences in how they respond to typical photodegradation. PS is a famously photosensitive polymer that is generally manufactured with photostabilisers, and LDPE is a relatively photoresistant polymer. By testing these two polymers it is possible to contrast two uniquely resilient polymers with this aging method. PLA was additionally chosen for this study as it is a commonly-used biodegradable polymer with very different chemistry, making it an ideal contrast for the efficacy of plasma treatment as an aging protocol for biodegradable polymers. These polymers were tested in sheets and in microplastic powders, as both are relevant polluting morphologies, and span the full spectrum of ease of use for research studies; large easy-to-manage macroscopic fractions, and smaller microplastic fractions which are traditionally far more challenging to age due to their lightness, and ability to be disrupted. The former are easier and provide more reliable XPS spectra for calibration of the method, the latter are more relevant to understanding the impact of environmental plastic pollution.

Squares of PS, LDPE and PLA of approximately  $1\text{cm}^2$  in size were cut from sheets of high-purity research-grade polymers sourced from Goodfellow Cambridge Ltd using metal tools cleaned with Isopropyl Alcohol (IPA). These were separated into two groups (Control and Aged) and stored in identical plastic boxes, with care taken to ensure the same face of each polymer sample was always ‘up’ throughout the study. Nurdles of PS, LDPE and PLA were also procured from Goodfellow Cambridge Ltd, and then cryomilled using a Retsch Cryomill. The cryomill was cooled with liquid nitrogen, and microplastic particles were milled to the specifications in section 2.1.2 using the parameters outlined in section 2.6.

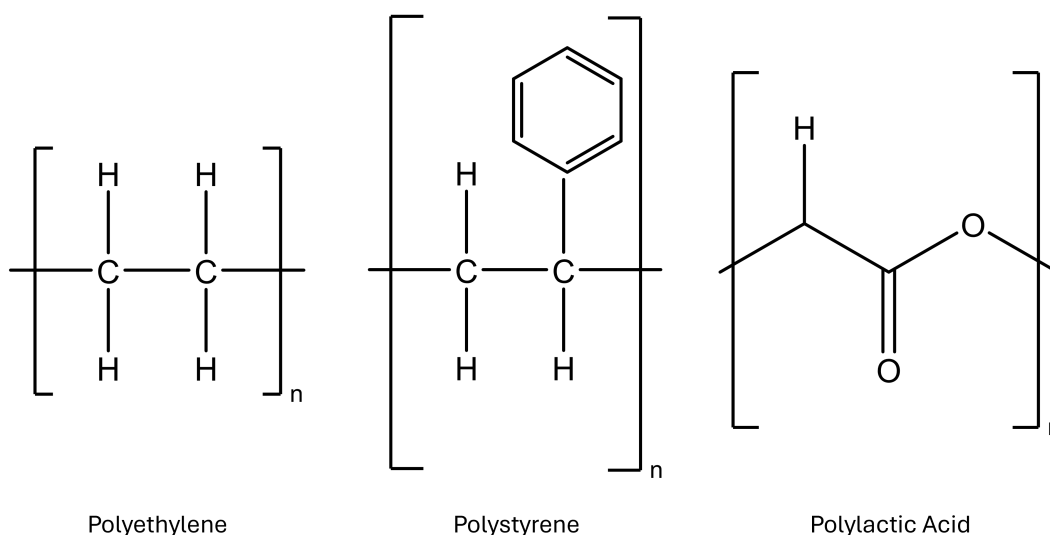


Figure 4.2: Repeat units of the three polymers that were used in this study

#### 4.2.2 Accelerated Photoaging

Squares of PS, LDPE and PLA were subjected to accelerated photoaging using an ATLAS Suntest system, detailed in section 2.4. The spectral irradiance of this equipment is shown in figure 2.10. Samples were loaded into a custom-built aluminium square-well grid, uncovered (as seen in figure 2.11). They were then exposed to a constant photon flux equivalent to  $750\text{Wm}^{-2}$  for durations of 168h, 336h, and 1008h (otherwise referred to as ‘Short’, ‘Medium’, and ‘Long’ durations respectively). Thermal degradation was minimised via the use of an inbuilt cooling fan.

#### 4.2.3 Plasma degradation

‘Aged’ subgroups of the plastic squares were loaded into a Diener Plasma Technology Zepto Plasma Cleaner via a metal loading plate. The equipment was pumped down to base pressure (nominal value of  $5.00 \times 10^{-3}$  Pa) prior to loading samples, and after samples had been loaded, to minimise contamination. Air was then passed into the chamber, reaching stable pressures of  $\sim 10 - 15$  Pa. Air was chosen as the desired inlet gas, as this ‘natural’ mix of gases was assessed to lead to appropriately proportional radical species as found in environmental photoaging. Chamber pressure was monitored using a Leybold Display One Pirani Gauge. This air flow was ignited into a plasma, under varied durations and input powers, as these parameters were assessed to be the most likely to significantly impact the surface chemistry. The input power range was monitored as between 20W and 100W

using the dial on the plasma reactor. Duration was managed using an external electronic timer, with the operator turning the plasma on and off at stated intervals. For the 600s plasma duration a 60s pause was introduced in the middle to keep the chamber cool and minimise thermal degradation. The chamber was then vented slowly to minimise potential of disruption to these light samples, and to ensure the same surface was always maintained upright. For the microplastic powders, samples were loaded onto high-walled aluminium foil boats to minimise disruption or spilling caused by surface charging of these light particles. These powders were spread as thinly as possible to ensure even aging, and were shaken and re-aged once to ensure even surface aging.

#### **4.2.4 XPS**

Square samples were loaded into a Kratos Analytical Axis Supra Plus X-ray Photoelectron Spectrometer, mounted onto standard Kratos Analytical bars using Kapton tape. Powders were similarly mounted with the addition of a metal well plate. The X-ray source was a monochromated Al K- $\alpha$  anode (1.487 keV). XPS analysis was conducted with charge neutralisation enabled, via an inbuilt electron flood gun. Survey scans were taken to analyse the surface stoichiometry in the region of 0 - 1200 eV at a step size of 1eV and a pass energy of 160eV. Coreline spectra for the C 1s peak were also collected to investigate functionalisation of the aliphatic carbon bonds, in the region of 280 - 304 eV binding energy at a step size of 0.1eV and a pass energy of 20eV. For more details on this analysis technique please refer to section 2.2.

#### **4.2.5 SEM**

One replicate of each polymer film treatment was sputtered with a thin film of gold and loaded into a JEOL JSM-7800F Field Emission SEM on double-sided carbon tape in order to assess any changes to physical morphologies. One replicate of each microplastic powder tested was pressed into double-sided carbon tape, sputtered with a 5nm film of gold using a Quorum Technologies Q150RES Rotary Pumped Coater, and loaded into the SEM. I prepared the samples for SEM, Dr Sara Baldock operated the SEM, and then I reviewed and analysed the data.

#### **4.2.6 Water Contact Angle measurements**

A sessile drop contact angle measurement method of water on photoaged and plasma-aged polymer surfaces was tested by pipetting 5 $\mu$ L of deionised water onto the samples. An Ossila Goniometer was

used to observe and measure water droplet contact.  $5\mu\text{L}$  of milli-Q water was carefully pipetted onto a given material surface, left to form a stable, static droplet, and immediately imaged. The contact angle formed was analysed using Ossila Contact Angle software.

#### 4.2.7 Data analysis

XPS data were analysed using CasaXPS, Excel, and Python 3.9 via the Anaconda distribution using the Pandas, Numpy, and Matplotlib libraries. All t-tests conducted in this chapter were completed as two-tail tests at a p value of  $\leq 0.05$ . These tests were performed using Python 3.9 via modules in the Anaconda distribution package (Pandas, SciPy). Within CasaXPS the Kratos library reference values were used when completing sensitivity corrections for the spectra. The textbooks *Handbook Of X-Ray Photoelectron Spectroscopy* [42] and *High Resolution XPS Of Organic Polymers: The Scienta ESCA300 Database* [43] were used as reference manuals for fitting the polymer spectra and for spectral analysis.

## 4.3 Results & Discussion

### 4.3.1 Control materials

Figure 4.3 showcases a representative wide scan of the PS sheet material used in this study. It is clear from this spectrum that the material is of high purity and therefore a good candidate for analysis, as this wide scan shows a sharp carbon peak at 285.0eV, attributed to the polymer chain, and a very small amount of oxygen at 536.0eV, which is likely a result of low-level background oxidation since its production. As there are no other elements present it is clear that there is minimal surface contamination arising from this method and handling procedure, meaning that the sample preparation methodology used did not affect the quality of the data collected.

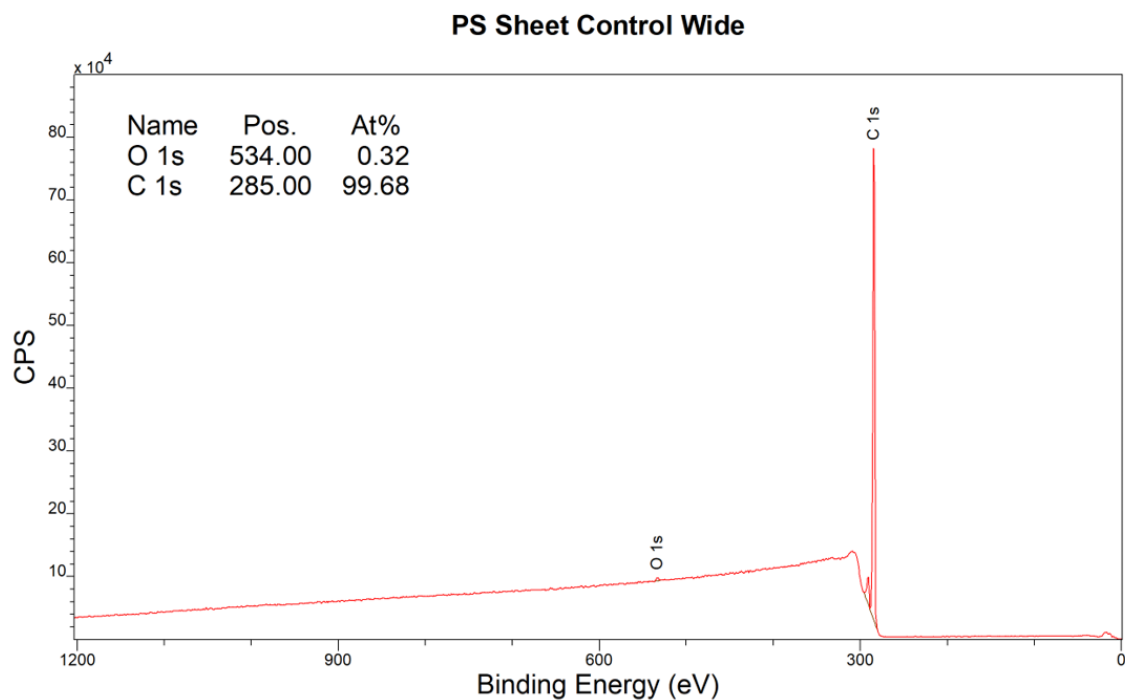


Figure 4.3: Wide scan of a control PS surface showing that the material surface contains only carbon and oxygen, with a 0.32% surface oxygen content. Overall, this indicates a very pure sample with minimal initial oxidation.

Figure 4.4 is the C 1s coreline spectrum for the same material, again highlighting the purity of the material. This spectrum accurately reflects the reference spectrum found in Beamson And Briggs [43], with a broad peak centred near 285eV capturing the aliphatic (285.0eV) and aromatic (284.76eV) components, and pi-pi\* shake up features (292.0eV) arising from interactions of the delocalised electrons in the aromatic ring. These components were fit with the correct ratio (3:1 aromatic:aliphatic for PS), and a small Full Width Half Maximum (FWHM) of 0.84eV, which is further indicative of a high-quality control spectrum, as low FWHM values generally indicate low overall noise in pure materials when looking at coreline spectra.

Figures 4.5, 4.6, 4.7 and 4.8 similarly showcase high-purity polymer sheets that are model examples of their respective reference spectra. These spectra show a strong indication that these materials can be used to reliably identify fine changes in material surface chemistry.

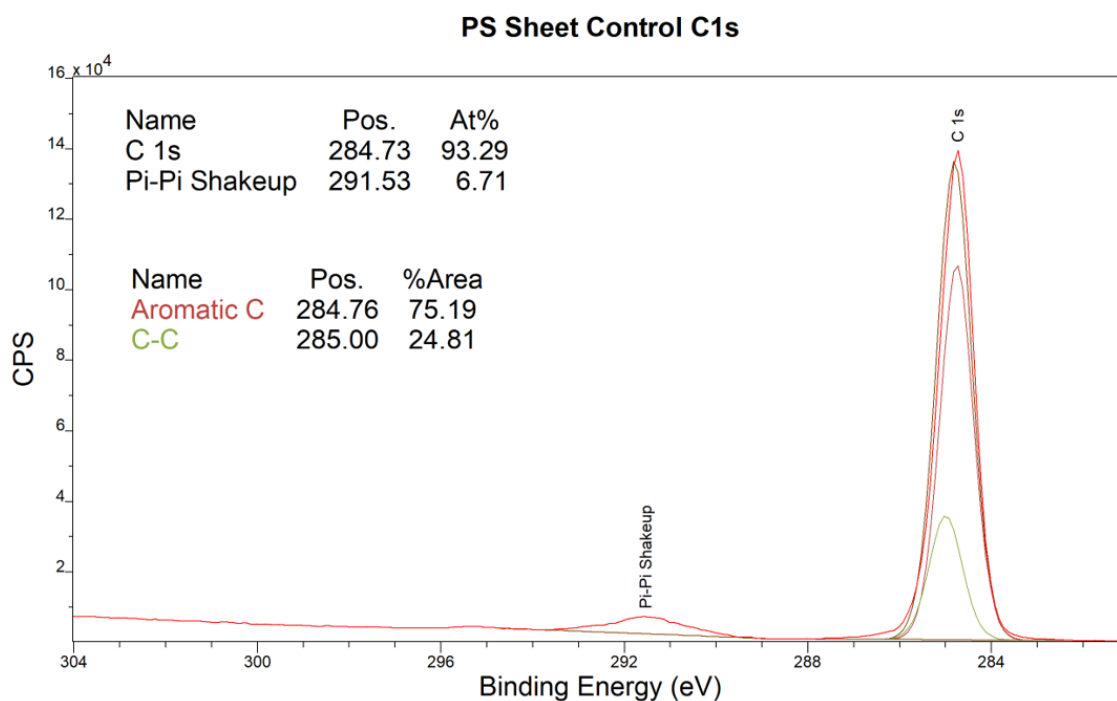


Figure 4.4: A representative coreline scan of the control PS surface showing a 3.0:1.0 ratio, as would be expected for pristine PS (6 aromatic carbons, 2 aliphatic carbons per molecule). The bright red envelope is the raw data, and fainter lines correspond to the modelling of the chemical environments, fitted to best match the raw data. The Pi-Pi shake up feature is a signature satellite peak resulting from the relaxation of delocalised pi-bond electrons in the phenyl group that is seen in XPS of high-purity PS.

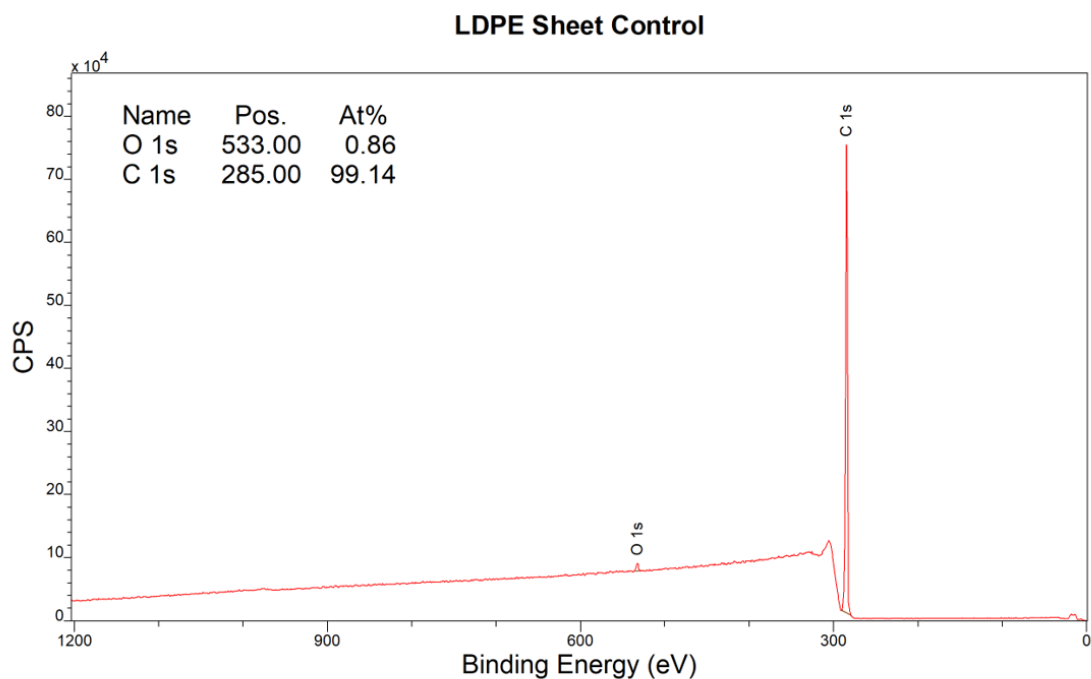


Figure 4.5: Wide scan of a control LDPE surface, showing a pure surface with a background oxygen content of <1% oxygen and no impurities.

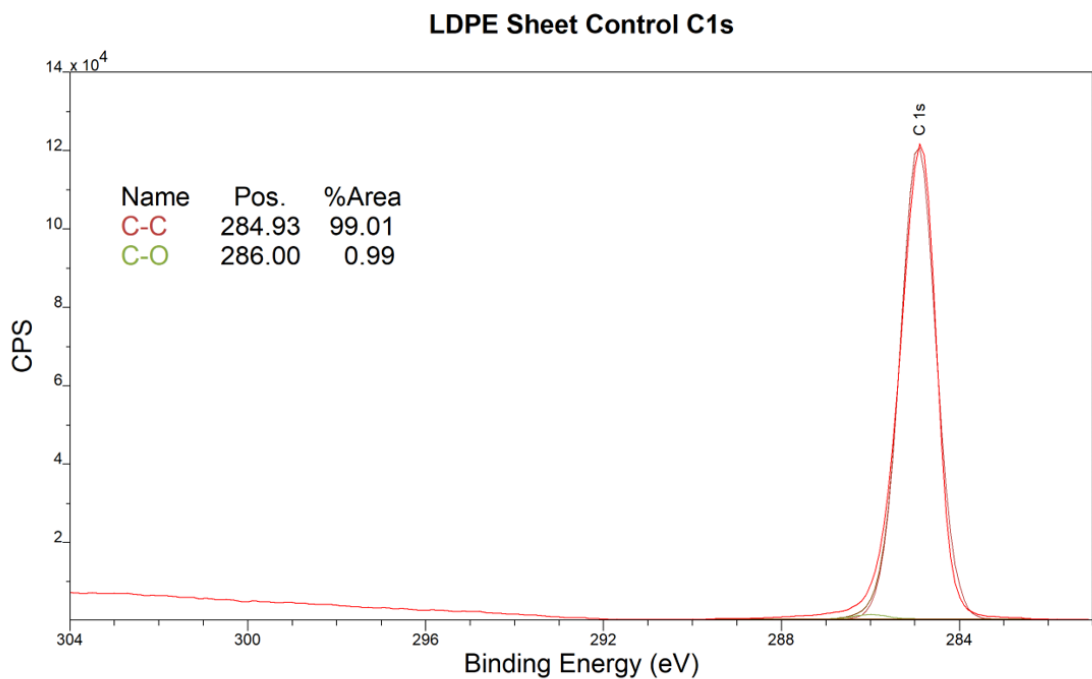


Figure 4.6: A C 1s coreline scan of a control LDPE surface, manually fitted with two realistic components. It shows a dominant aliphatic carbon peak at 284.93 eV with 99.01% of the total area, and a smaller carbon-oxygen peak with 0.99% of the total area.

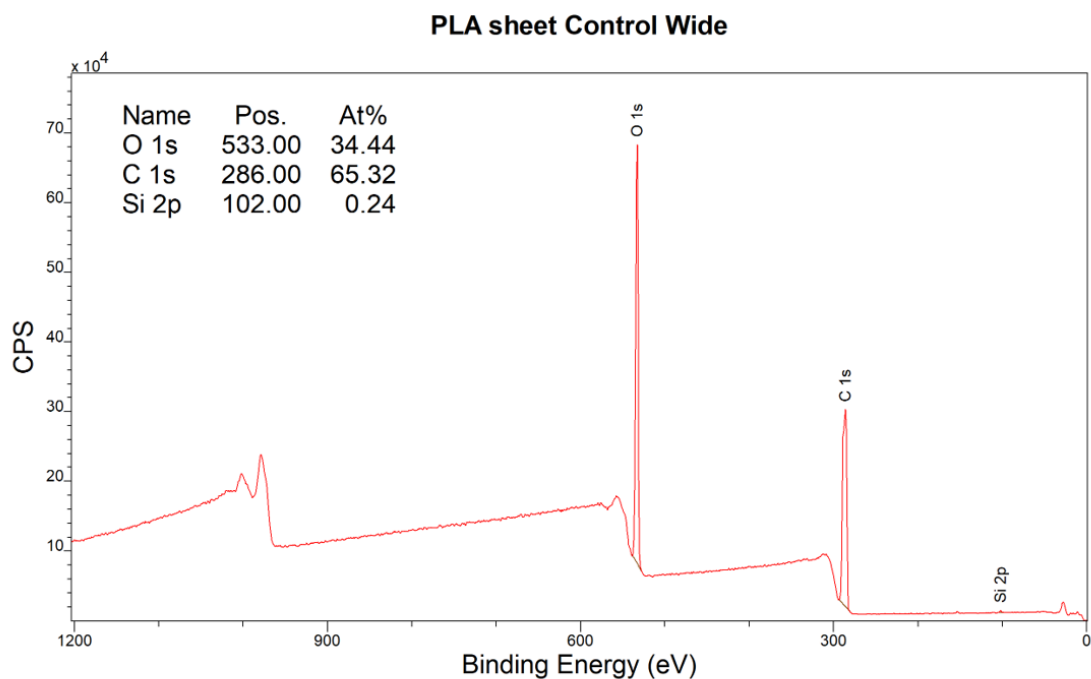


Figure 4.7: A wide scan of a control PLA surface, showing a high-purity PLA sample, with only 0.24% of the surface containing impurities.

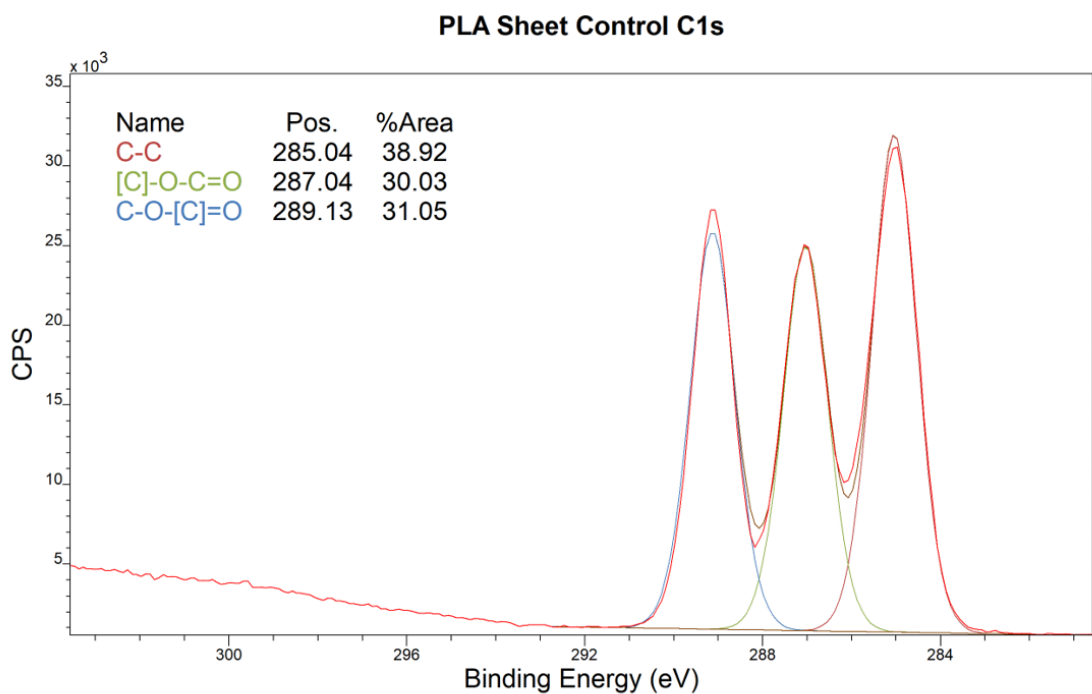


Figure 4.8: C 1s coreline scan of a control PLA surface, with three manually modelled peaks corresponding to the three distinct carbon environments found in PLA. The fit is good, indicating a high-quality PLA sample with minimal carbon-based impurities.

### 4.3.2 Changes in polymer stoichiometry introduced as a result of aging

After application of the aging protocols, the surface stoichiometry of the pristine control materials changed. This is explained mechanistically by high-energy photons initiating fission of the polymer chains, and fission of molecules in the air (generally diatomic oxygen), into radical species that then react with each other, forming new functional groups on the surface of the material in the case of photoaging, and from the strong electric field generating radicals, ions, and high-energy photons which then similarly attack the polymer chain in the case of plasma treatment. More detailed descriptions of these mechanisms can be found in sections 2.3, and 3.4.

The result of this degradation can be observed clearly in PS wide scans showcased in figures 4.9 and 4.10, where peaks attributable to O 1s environments are far more significant, with relative sensitivity-adjusted peak areas of 26.31% and 18.07% respectively. A small amount of nitrogen is observed as well, which is explained by the presence of nitrogen species in the air also forming radicals, but being less able to bond with the polymer chain. There are small peaks of silicon contamination, arising in both the photoaging and plasma aging methods. These are believed to be low levels of siloxane contamination unavoidably being introduced during aging and handling of these materials. Because siloxane is an oxygen-containing contaminant a correction factor was applied to O/C calculations where appropriate. Additionally, some wide spectra captured from plasma aging showed trace amount of other elements, such as the 0.09% sodium peak observed in 4.10. This is similarly expected to be contamination deposited onto the surface due to aging in a plasma reactor that gets used by multiple other operators in a research laboratory, and not something introduced into the carbon chain by the aging method itself.

This initial analysis of the PS wide spectra clearly demonstrates that these aging methods are effective, that they lead to notable changes in surface chemistry with the introduction of sharp oxygen peaks, that the handling and protocols developed in this study result in minimal contamination (spectra are >95% carbon and oxygen), and that high quality XPS spectra can be collected after these techniques have been applied to polymer surfaces. These initial data showcase that the methodology presented is effective for achieving the stated research aims of this chapter.

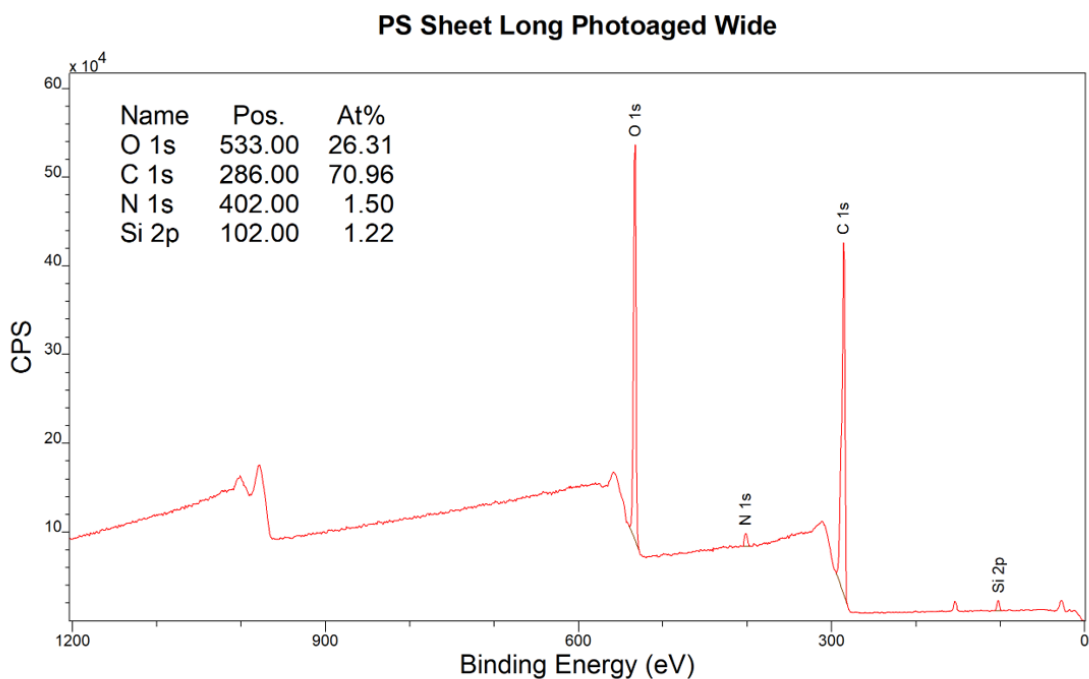


Figure 4.9: Wide scan of a 6-week photoaged PS surface. This spectrum details a surface oxygen concentration of 26.31%, as well as some nitrogen species, both likely introduced through photooxidation of the surface bonds, as well as some silicon species which was assessed to be siloxane contamination.

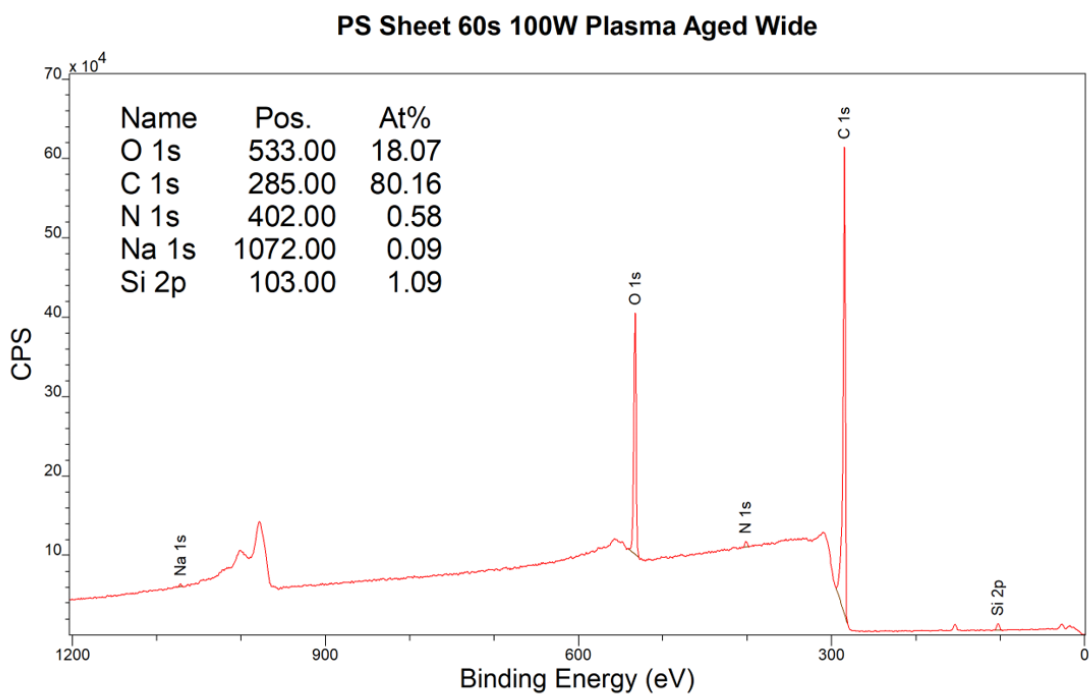


Figure 4.10: Wide scan of a PS surface aged with 60s 100W plasma treatment, showing a surface oxygen content of 18.07%, indicating that plasma treatment led to significant surface oxidation.

### 4.3.3 Impacts of plasma treatment and accelerated photodegradation on polymer surface chemistry

Theoretically, it is clear that air plasma degradation could be an appropriate abstraction for environmental photodegradation due to the presence of high-energy photons and oxygen radicals. This theory was tested in practice using a low-pressure air plasma, and the results in table 4.1 clearly show a strong and consistent surface oxidation resulting from this process. The oxidation looks realistic, as both plasma-aged and photoaged surfaces see an increase in surface oxygen %, and comparison with the ‘Long’ photoaged PS indicates the extent of oxidation with plasma is within the bounds of realistic photodegradation. Once these control materials were exposed to the aging protocols, significant changes in their surface chemistry were observed. Within seconds of plasma exposure polymer surfaces became highly oxidised, in a way that is stoichiometrically similar to photoaging, as both photoaged and plasma-aged surface showcase a significant increase in oxygen content on the surface. After 6 weeks of photoaging, the C 1s spectrum of PS showed clear signs of significant bonding of oxygen into the carbon chain, forming a range of oxygen-based functional groups, including alcohols, ketones, carbonyl groups, carboxyl groups, and some indication of carbonate moieties as well. Each of these different carbon-oxygen structures lead to subtle, measurable shifts in the binding energies of emitted electrons, which were then fitted to the coreline spectra to give an indication of the new chemical environments emerging. In order to fit suspected components to these spectra the carbon spectral signatures found in Beamsom & Briggs [43] were used. A table of the ranges for the chemical shifts used to fit these spectra can be found in section 2.2.2. The ‘Short’ and ‘Medium’ duration photoaging treatments were also analysed, but were found to have minimal changes when compared to the control samples, therefore only the ‘Long’ photoaging results are presented here showcasing the most significant contrasts resulting from photoaging.

In table 4.2 these differences are measured within their coreline spectra. For LDPE, the 6-week accelerated photoaging exposure led to signs of low levels of oxidation of the carbon chain, with over 6% of the C 1s electrons being attributed to alcohol/ketone structures, and a smaller % of environments belonging to carbonyl (1.78%) carboxyl (2.34%) and carbonate (0.44%) appearing in the fit. These same chemical environments appear in the plasma-aged surfaces at higher concentrations of 12.74%, 6.26%, 4.86%, and 0.70% respectively. This is strong evidence that the increase in O/C ratios calculated from the aged polymer wide scans in table 4.1 are resulting in degradation of the carbon chain itself. For

PS the results were more pronounced, with a notably large increase in the carboxyl functionalisation of this structure in the 6-week photoaged sample (14.52% as fitted). The components fitted to the plasma aged PS surface showcased the appearance of the same functional groups but in generally lower concentrations, with the exception of the fitted carbonate peak which is notably greater. This is potentially explained by the more energetic nature of plasma, allowing for exotic functional groups to form more easily. Additionally, there is still a tail at the higher binding energy side of the spectrum that is attributable to Pi-Pi shakeup features found in XPS of aromatic compounds found in both the photoaged and plasma aged surfaces. For the photoaged surface this indicates that the polymer is not fully oxidised yet, but for the plasma-aged surface this is likely better explained by a layer of unoxidised material being nested under a highly oxidised surface layer, as observed in historic studies of plasma modification of polymer surfaces [49].

Table 4.1: Analysis of surface chemistry for plasma-aged polymers compared with photoaged polymers. These data are all from high-quality spectra that have been charge calibrated, had their peak regions manually fitted, and have been corrected for the low levels of siloxane contamination present on the surface where appropriate. These data reflect high-quality samples of n=1.

Polymer	Treatment	O/C Peak Ratio
Polystyrene	Control (Pristine untreated surface)	0.00
	5s 100W Plasma	0.14
	60s 100W Plasma	0.20
	300s 100W Plasma	0.22
	600s 100W Plasma	0.23
	2 week photo-aged	0.02
	6 week photo-aged	0.34
	60s 20W Plasma	0.18
	60s 50W Plasma	0.20
	LDPE	Control (Pristine untreated surface)
5s 100W Plasma		0.12
60s 100W Plasma		0.21
300s 100W Plasma		0.22
600s 100W Plasma		0.22
2 week photo-aged		0.02
6 week photo-aged		0.08
60s 20W Plasma		0.18
60s 50W Plasma		0.21

Table 4.1 shows a clear indication that both of the accelerated aging protocols tested lead to significant increase in oxygen content. Plasma surface degradation leads to a rapid dramatic increase in oxygen content when compared to controls for both PS and LDPE, which is comparable to levels seen in the 6-week accelerated photoaging of the PS samples. It also indicates that changing the input power settings to the plasma reaction has some effect on the overall oxidation, but this impact is

marginal for both LDPE and PS samples.

Table 4.2: Analysis of component composition of different aged spectra. These data highlight the similarity between the chemical environment generated during plasma exposure compared to photoaging. These data reflect high-quality samples of n=1.

Polymer	Treatment	Component	Area % of fitted C 1s peak
Polystyrene	Control	C-C	24.81
	Control	Aromatic C	75.19
	Long Photoaged	C-C	60.87
	Long Photoaged	C-OH/C-O-C	14.42
	Long Photoaged	C=O	8.82
	Long Photoaged	O-C=O	14.52
	Long Photoaged	CO3-	0.08
	Long Photoaged	Pi-Pi	1.23
	Plasma Aged 60s 100W	C-C	77.30
	Plasma Aged 60s 100W	C-OH/C-O-C	8.74
	Plasma Aged 60s 100W	C=O	5.84
	Plasma Aged 60s 100W	O-C=O	3.49
	Plasma Aged 60s 100W	CO3-	3.16
	Plasma Aged 60s 100W	Pi-Pi	1.47
	LDPE	Control	C-C
Control		H-O-C/C-O-C	0.99
Long Photoaged		C-C	89.91
Long Photoaged		C-OH/C-O-C	6.33
Long Photoaged		C=O	1.78
Long Photoaged		O-C=O	2.34
Long Photoaged		CO3-	0.44
Plasma Aged 60s 100W		C-C	75.44
Plasma Aged 60s 100W		C-OH/C-O-C	12.74
Plasma Aged 60s 100W		C=O	6.26
Plasma Aged 60s 100W		O-C=O	4.86
Plasma Aged 60s 100W		CO3-	0.70
PLA		Control	C-C
	Control	[C]-O-C=O	29.99
	Control	C-O-[C]=O	31.14
	Long Photoaged	C-OH/C-O-C	37.41
	Long Photoaged	C=O	30.66
	Long Photoaged	O-C=O	31.93
	Plasma Aged 60s 100W	C-C	61.98
	Plasma Aged 60s 100W	C-OH/C-O-C	12.58
	Plasma Aged 60s 100W	[C]-O-C=O	5.93
	Plasma Aged 60s 100W	C=O	6.84
	Plasma Aged 60s 100W	C-O-[C]=O	5.57
	Plasma Aged 60s 100W	HO-C=O	7.09
	Plasma Aged 60s 100W	CO3-	0.00

A comparison of the control, 6-week photoaged and plasma aged PLA samples is also found in table 4.2. Because PLA is a condensation polymer with a significant amount of oxygen already bonded into its carbon chain, it is not sensible to assess O/C ratios as an expression of the material's degradation, hence why these values are not represented in table 4.1. Instead this assessment is done through a comparison of the C 1s spectra.

Minimal changes in the C 1s of PLA pristine control compared with the 6-week photoaged samples were observed, with each of the chemical environments still present within 1%. Overall, this indicated that the PLA sheets were minimally degraded over the course of this accelerated aging treatment.

Table 4.2 shows that after treatment with plasma the C 1s is notably different. New functional groups have formed in the polymer chain, such as the emergence of a large peak (12.58%) fitted at 286.40eV associated with C-OH/C-O-C bonds, and the emergence of a peak at 287.80eV attributable to a C=O group. Additionally, there is a relatively greater abundance of a simple aliphatic carbon peak, with 61.98% of the C 1s area being attributable to the C-C peak, compared to 38.88% in the PLA control. These features indicate that the carbon chain has degraded significantly.

These observations are best explained by the oxygen-based elements of the carbon chain being the most reactive, and the plasma aging treatment leading to the preferential ablation of these bonds. Ultimately, this a plausible intermediate, as the most highly oxidised components of a polymer surface are the elements which are most able to be mineralised in the natural environment due to their reactivity. However, as the 6-week exposure did not lead to significant degradation it is not possible to confirm how realistic this is. Further work with a significantly extended photoaging treatment that could lead to comparable surface damage of the material would be needed to confirm or reject how realistic this is for the environmental photodegradation of PLA.

#### 4.3.4 Physical surface changes

The SEM images shown in figure 4.11 indicate that the 6-week accelerated photoaging protocol lead to no noticeable physical changes at 1000x magnification for all three materials. The surface damage in figure 4.11E is attributed to tweezer damage when handling, and not an innate feature of the plastic sheet.

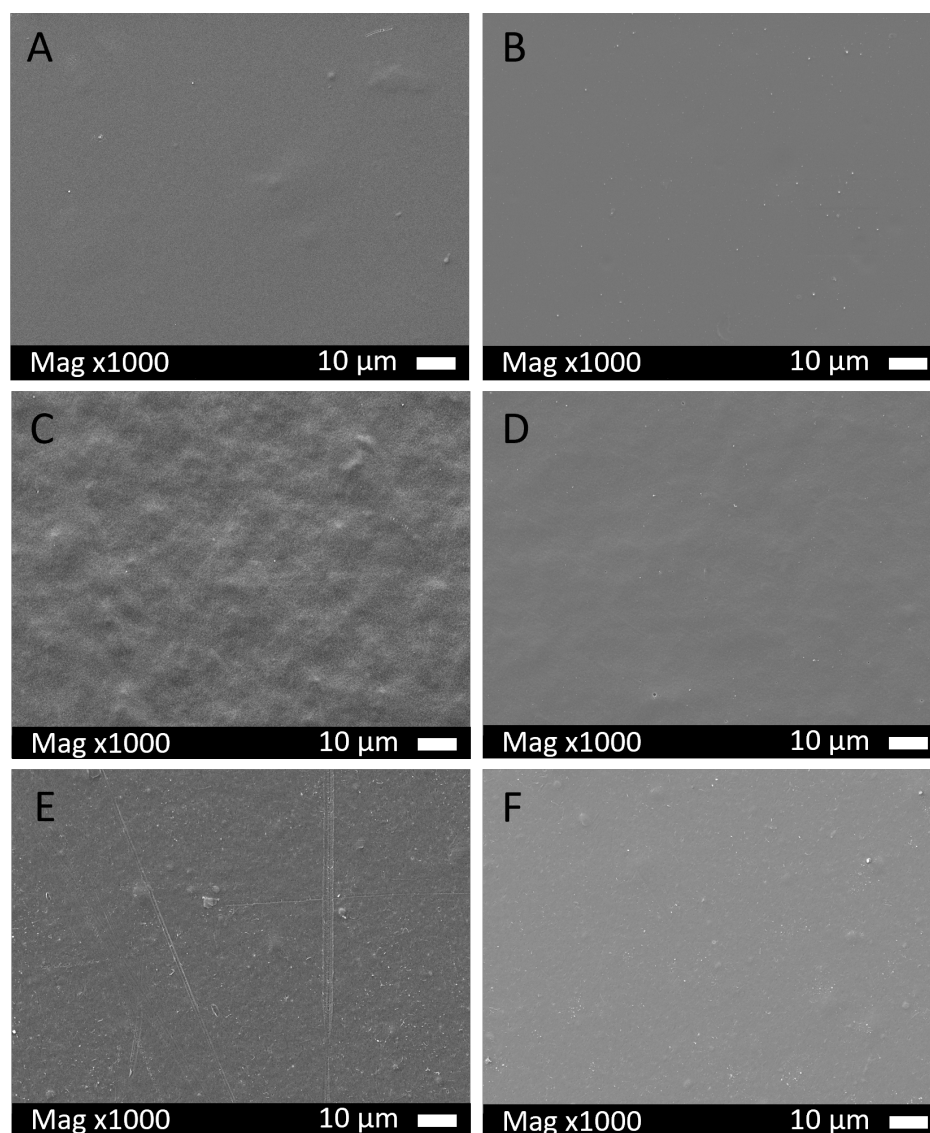


Figure 4.11: SEM images of long photoaging, PS (images A and B), LDPE (images C and D), PLA (images E and F) ; Control (A, C, and E), 6-week 'Long' photoaged (B, D, and F). These surfaces were imaged at 1000x magnification. They show no noticeable changes with treatment.

The SEM images seen in figures 4.12 and 4.13 indicate that the surfaces also showed minimal physical changes at a microscopic scale with a 60s plasma treatment for both the sheets and powders. The damage visible in figure 4.12D-E is again attributable to handling, as polymer surfaces are very soft, and are easily scratched by metal tools. There aren't any systematic changes to the surfaces arising from the treatments. This minimises concerns over surface etching; a well-established process used in other disciplines that can occur when energetic plasmas interact with polymers [156]. This is an expected result, as etching is a relatively slow process, but it is essential to confirm, as it makes it clearer that plasma is an appropriately narrow method focused on oxidative aging, not physical aging of the surface. This outcome agrees with the photoaging results observed in figures 4.11A-F.

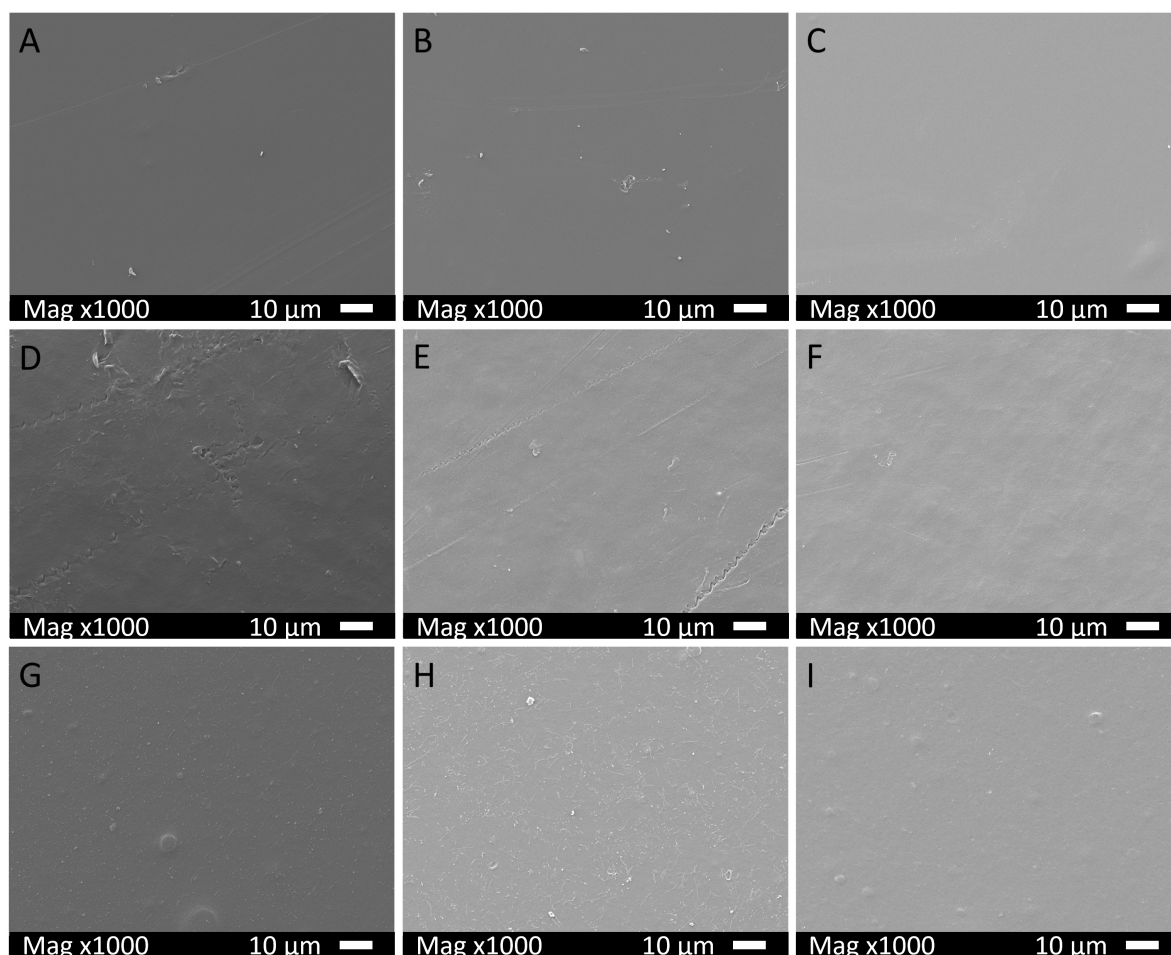


Figure 4.12: SEM images of PS (A-C), LDPE (D-F), PLA (G-I) for Control, 20W 60s plasma aged, and 100W 60s plasma aged going left-to-right respectively. These surfaces were imaged at 1000x magnification. They show no noticeable changes with treatment.

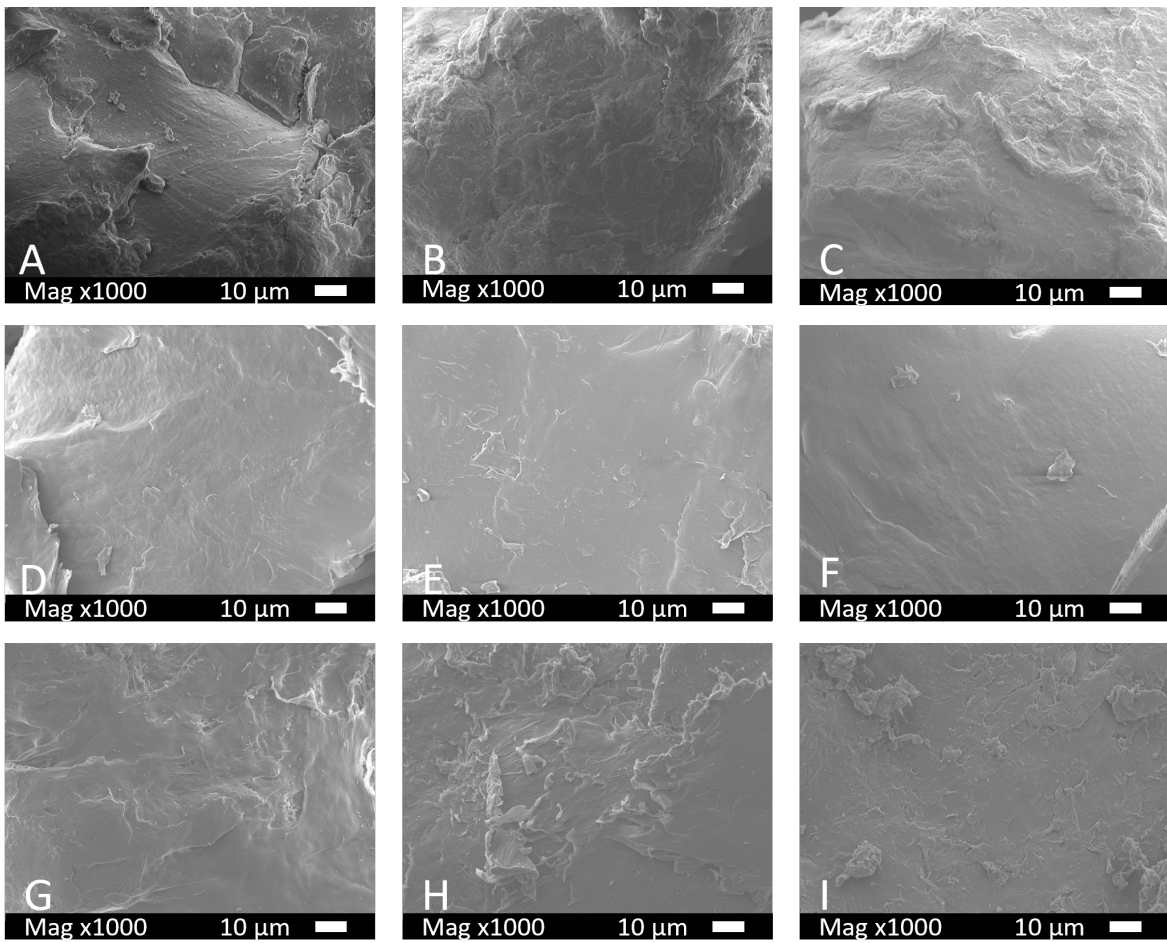


Figure 4.13: SEM images of PS (A-C), LDPE (D-F), PLA (G-I) microplastic powders for Control, 100W 5s plasma aged, and 100W 60s plasma aged going left-to-right respectively. These surfaces were imaged at 1000x magnification. They show no noticeable changes with treatment.

### 4.3.5 Contact angles measured on aged polymer surfaces

Figure 4.14 showcases the contact angle measurements for the ‘Long’ photoaged polymer surfaces. All three polymers indicate some decrease in hydrophobicity, but it is clear that the aged PS had the most noticeable response. This is explained by PS being the most affected by the photoaging process, as indicated by the large increase in oxidation observed in photoaged PS earlier. Whilst they all showcased a difference in their contact angle mean values when compared to their controls, as observed in table 4.3, these differences were not significant to a p-value of  $\leq 0.05$ , therefore caution must be taken when interpreting these results. It is clear, particularly for PS that there is a high degree of variance in the results after photoaging. Given that the samples were analysed after the 6-week photoaging treatment, it is possible small amounts of dust could have accumulated. This also explains why the photoaged control and treated samples have smaller contact angles than their plasma-aged counterparts (table 4.4), which were analysed far more quickly from their preparation date, given the shorter timescales of plasma treatment.

The contact angle response observed in figure 4.15 as a result of plasma treatment is a far more distinct shift in the hydrophobicity of the surfaces, with PS, LDPE and PLA all becoming considerably less hydrophobic. All three plasma-aged plastics showcased a significant difference in their contact angle when compared to their controls at a p-value  $\leq 0.05$ , as observed in table 4.4. This is the expected result for photooxidation, as oxygen-based functional groups such as carbonyl and carboxyl groups are highly polar, which makes them hydrophilic. The response observed in the plasma-aged surfaces was however far more significant compared to the photoaged equivalents. This is generally explained through the increase in oxidation observed in the XPS data, and gives more evidence that the overall surface oxidation occurring during plasma aging is being split between a highly-oxidised surface layer nested on the material bulk, as the 6-week photoaged PS has a greater overall O/C ratio than the plasma-aged PS, but sees a less significant change in contact angle with water.

Table 4.3: Contact angle response to the ‘Long’ photoaging treatment. Overall, whilst there was a visible shift in the measured contact angle, no measured differences across these samples were significant to a p-value  $\leq 0.05$ , highlighting how inconsistent photoaging can be.

Polymer	Angle Formed On Control (Degrees)	Angle Formed On ‘Long’ photoaged (Degrees)
PS	81.72±2.90	46.10±16.98
LDPE	91.91±5.64	80.01±3.94
PLA	70.18±9.82	55.67±3.71

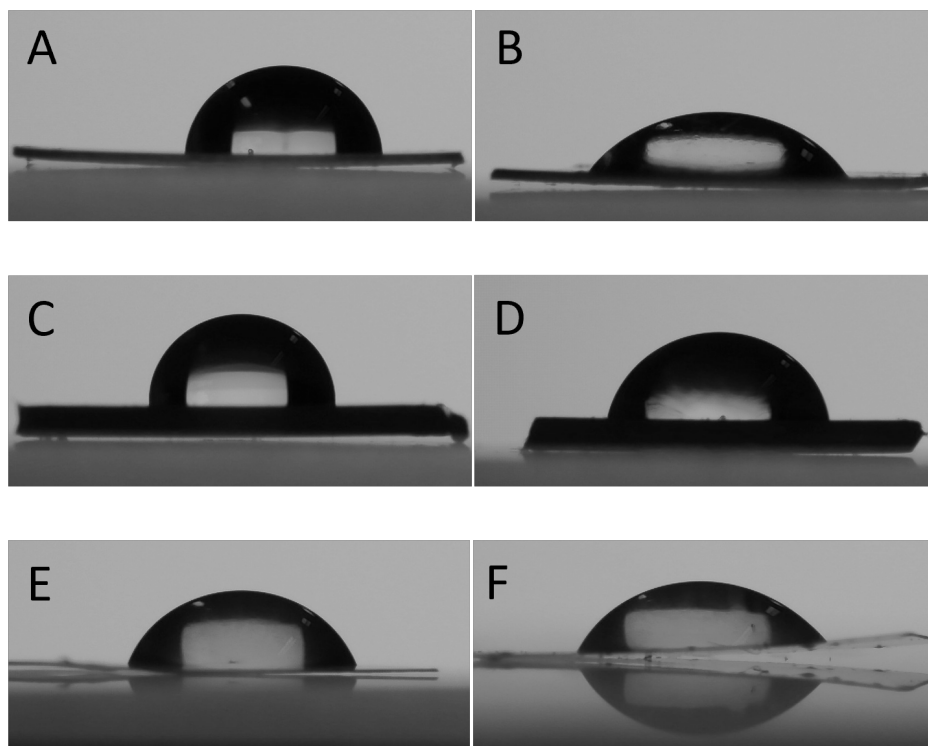


Figure 4.14: Contact Angle Images of PS (A and B), LDPE (C and D), and PLA (E and F) for Control and ‘Long’ photoaged LR respectively. These images indicate that photoaging does affect surface hydrophobicity, however this did not lead to significant results.

Table 4.4: Contact angle response to plasma aging. The asterisk (\*) indicates results significant below a p-value  $\leq 0.05$ . This indicates that this method is highly reproducible when it comes to creating a hydrophobic response in polymers.

Polymer	Angle Formed On Control (Degrees)	Angle Formed On Plasma 60s 100W (Degrees)
PS	$89.16 \pm 3.68$	$12.52 \pm 3.18$ *
LDPE	$93.02 \pm 3.40$	$25.53 \pm 1.97$ *
PLA	$73.08 \pm 4.69$	$29.25 \pm 5.54$ *

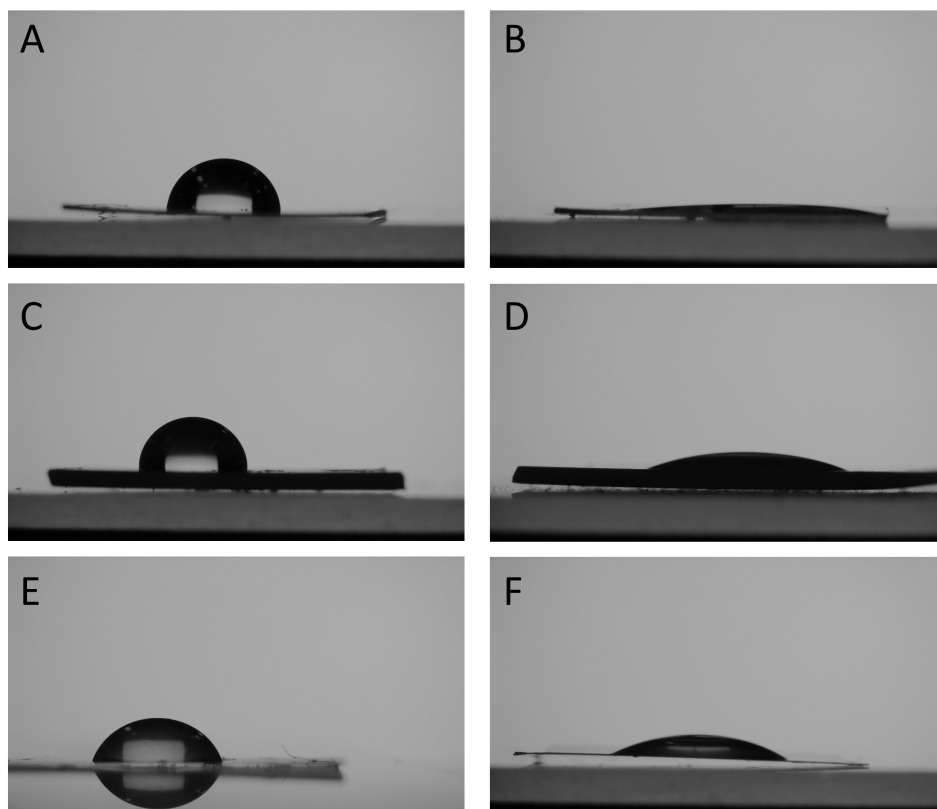


Figure 4.15: Contact Angle Images of PS (A and B), LDPE (C and D), and PLA (E and F) for Control and 100W 60s aged LR respectively. Plasma treatment qualitatively led to a dramatic change in surface hydrophobic, leading to measured droplets completely flattening across the surface.

### 4.3.6 Optimisation of methodology

The method was optimised using the LDPE and PS samples, as these polymers have simpler chemistry and a more straightforward response to the plasma treatment, whilst still providing a contrast between photoresistant and photosusceptible polymers. Moderately longer plasma durations only marginally increased the overall surface oxygen % of the material, such as an increase of O/C ratio of 0.20 to 0.23 when going from 60s to 600s of plasma exposure for PS (Table 4.1). This didn't significantly change the functionalisation of the surface either as indicated in Figures 4.16 and 4.17 by the fact that the peak-to-peak normalised curves are essentially perfect matches, suggesting that longer plasma durations don't necessarily lead to proportionally greater functionalisation when approximating advanced photodegradation, and therefore that short durations are sufficient. From these data, it appears 60s duration is appropriate to achieve functionalisation of polymer chains in a way comparable to accelerated photoaging.

The plasma reactor in use still visibly ignited, albeit weakly, down to 20W. Below this power the plasma struggled to visibly ignite, and data was not collected. A 60s time benchmark was used, and the power was varied. Similarly, changes to plasma power settings appeared to have some marginal effects on the oxygen content of the surfaces at the lowest power of 20W, with an O/C ratio of 0.18 being achieved at 20W for 60s compared to 0.20 at 100W for 60s (Table 4.1), and similarly did not result in noticeable changes for functionalisation of PS and LDPE, as seen in figures 4.18 and 4.19.

It may be possible to further optimise this method through the application of pulsed plasma systems. Pulsed plasma discharge systems are another popular way to generate a cold plasma exposure in which exceptionally short durations of plasmas can be used to modify surfaces rapidly (in the order of ns -  $\mu$ s [45]). By using pulsed plasmas the overall energy imparted can be lower, whilst also giving sufficient time for reactions to occur during the plasma-off period [157]. This could potentially lead to a more realistic analogue of environmental photoaging. Future work could assess the use of pulsed plasmas as a potential further optimisation of this process for environmental studies.

### PS Duration Test Comparison; 60s (Red), 300s (Green), 600s (Blue)

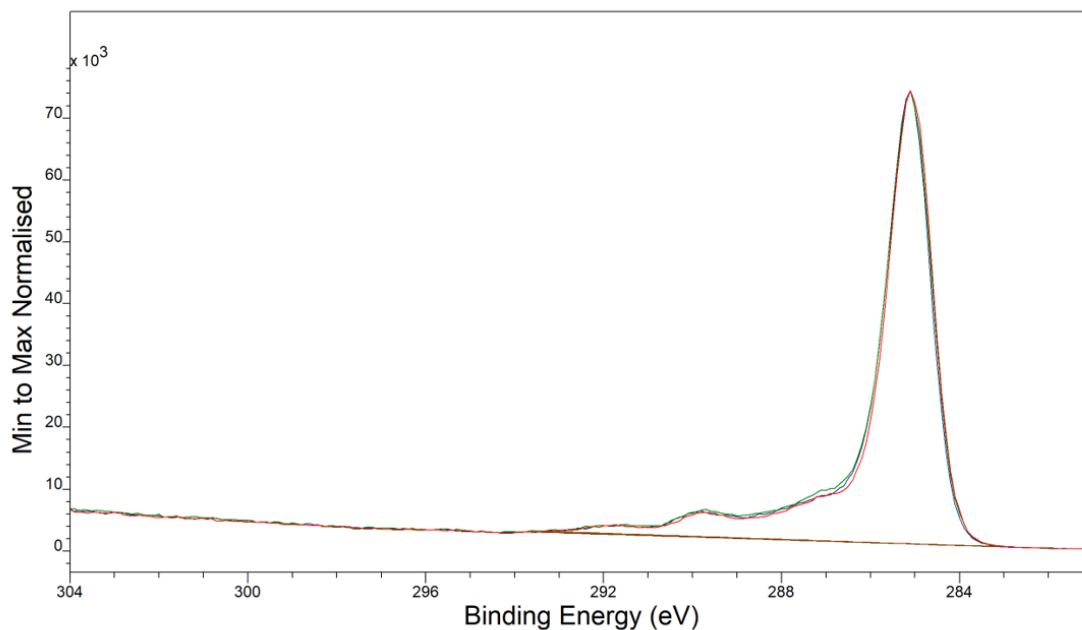


Figure 4.16: Peak-to-peak normalised C 1s spectra for plasma aged PS at 60s (Red), 300s (Green) and 600s (Blue) plasma durations

### LDPE Duration Test Comparison; 60s (Red), 300s (Green), 600s (Blue)

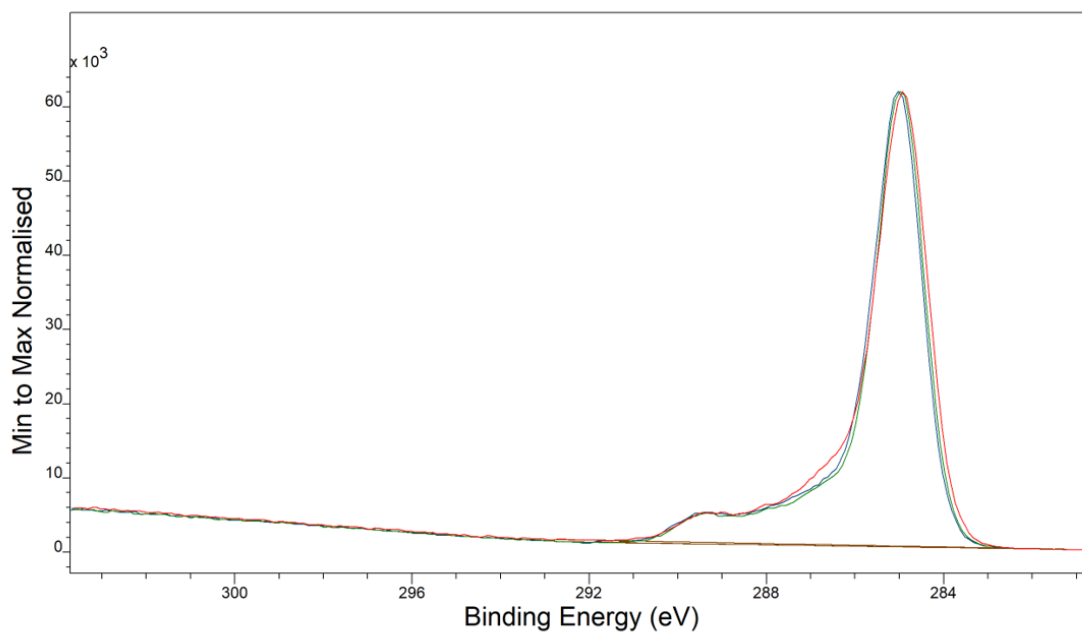


Figure 4.17: Peak-to-peak normalised C 1s spectra for plasma aged LDPE at 60s (Red), 300s (Green) and 600s (Blue) plasma durations

**PS Power Test Comparison; 20W (Red), 50W (Green), 100W (Blue)**

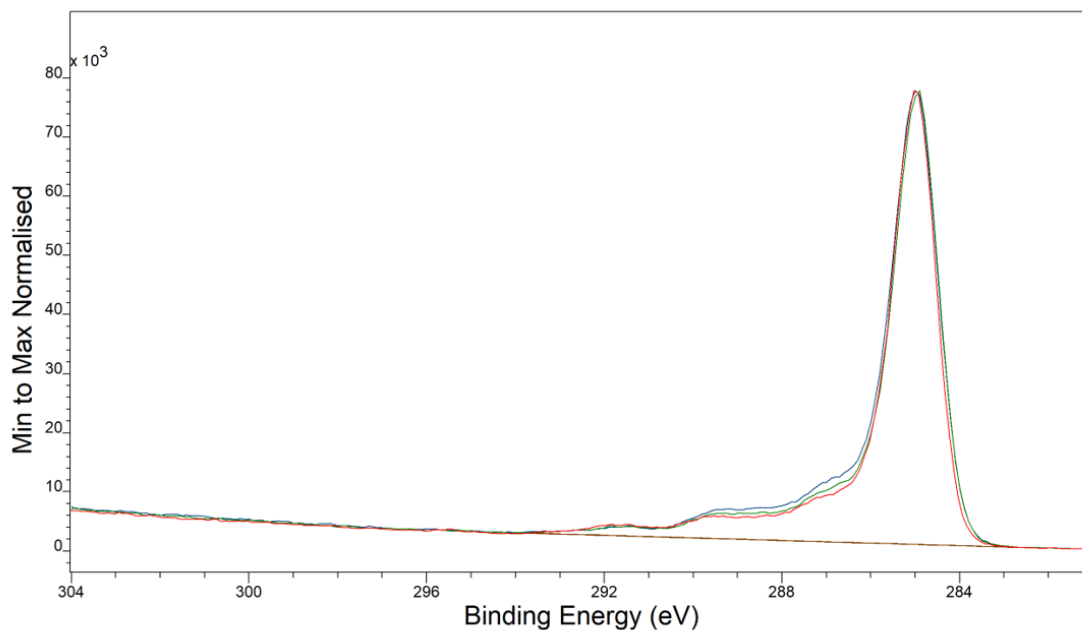


Figure 4.18: Peak-to-peak normalised C 1s spectra for 60s plasma aged PS at 20W (Red), 50W (Green) and 100W (Blue)

**LDPE Power Test Comparison; 20W (Red), 50W (Green), 100W (Blue)**

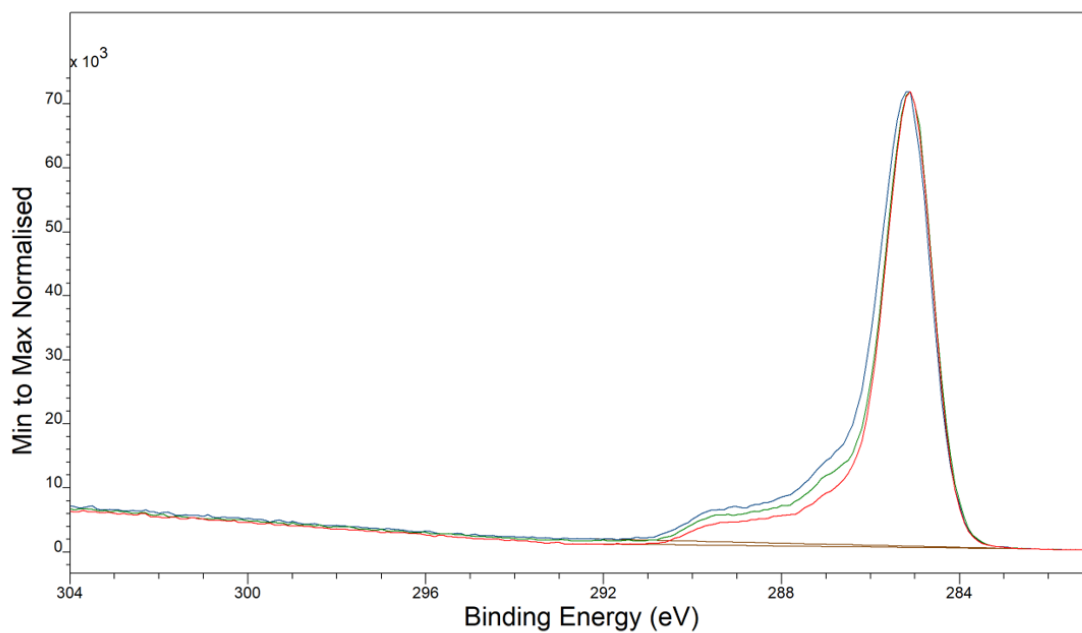


Figure 4.19: Peak-to-peak normalised C 1s spectra for 60s plasma aged LDPE at 20W (Red), 50W (Green) and 100W (Blue)

### 4.3.7 Characterisation of aged microplastic powders

The same plasma aging method was then tested on microplastic powders, a standard morphology of plastic representative of that found within the environment. The microplastic powders raised some distinct challenges when characterised with XPS. It was not possible to obtain perfect charge neutralisation of the samples, resulting in highly-charged coreline spectra. This observation is clearly visible in the PS Microplastic Control C 1s spectrum (figure 4.20), and this trend was observed for all the microplastic C 1s spectra measured.

These erroneous spectra are explained by surface charging arising from the morphology and insulating nature of this material. The X-rays which ionise the polymers can pass through the samples, emitting electrons from any available surface within the powders, but the electron flood gun that serves to neutralise the surface that charges as core electrons are stripped off cannot do this; electrons interact more strongly with the material compared to X-rays, and do not penetrate deep into the powder matrix. This results in some low-level differential charging across powder surfaces, which yields uncharacteristic C 1s spectra, where the core peaks are split by this charging process, as electrons emitted from a charged surface will lose some kinetic energy arising from this electrostatic interaction. This process is visualised in figure 4.21; the X-rays are able to penetrate the powders, exciting electrons on the surfaces of the polymers. Particle A is completely seen by the flood gun, and therefore the removal of the electrons by the X-ray source is compensated for, and no charging occurs. Particle B however is still able to have electrons ejected from its surface that can reach the detector, but is not in view of the flood gun. This means that as electrons are ejected by the X-ray source, positive charge builds up, as electrical insulators like polymers are not able to re-balance their surface charge easily. This positive charge results in an additional interaction that attenuates the kinetic energy of the ejected electron, resulting in a higher measured binding energy for this otherwise comparable electron.

Nevertheless, these charging artefacts ultimately only introduced shifts of a few eV into the spectral peaks. This means that the wide spectra can still be used to get a broad stoichiometric signature for these powders, as a shift of a few eV is not enough to radically change the peak arrangement measured in the wide spectra. The O/C ratios for the control, 5s 100W and 60s 100W plasma aging protocols for PS and LDPE calculated from their wide spectra in the same way as the sheet polymers is found in table 4.5. These data are broadly consistent with the oxidation observed in the plasma aging of the sheets, indicating that this method is effective for the oxidation of microplastic powders. Additionally, the PLA wide scans for the microplastic powders similarly reflected the wide scans of the plasma aged PLA sheets, meaning it was deemed to be equally appropriate for this polymer as well.

Table 4.5: Analysis of component composition of different aged spectra for microplastic powders. These data reflect good quality samples of n=1.

Polymer	Treatment	O/C Peak Ratio
Polystyrene	Control	0.00
	5s 100W	0.08
	60s 100W Plasma	0.16
LDPE	Control	0.00
	5s 100W	0.05
	60s 100W Plasma	0.15

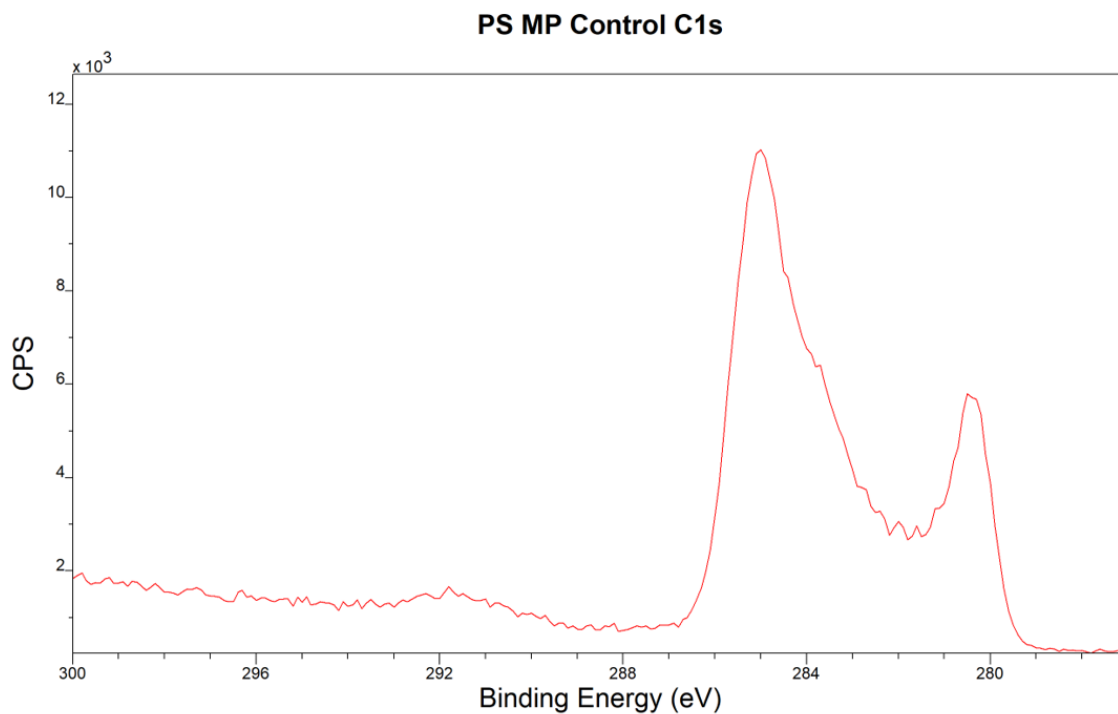


Figure 4.20: The drop in quality of the C 1s spectrum for the control PS microplastic powder in this figure was assessed to be a result of charging artefacts that arose due to the challenges of measuring insulating powders, as further visualised in figure 4.21.

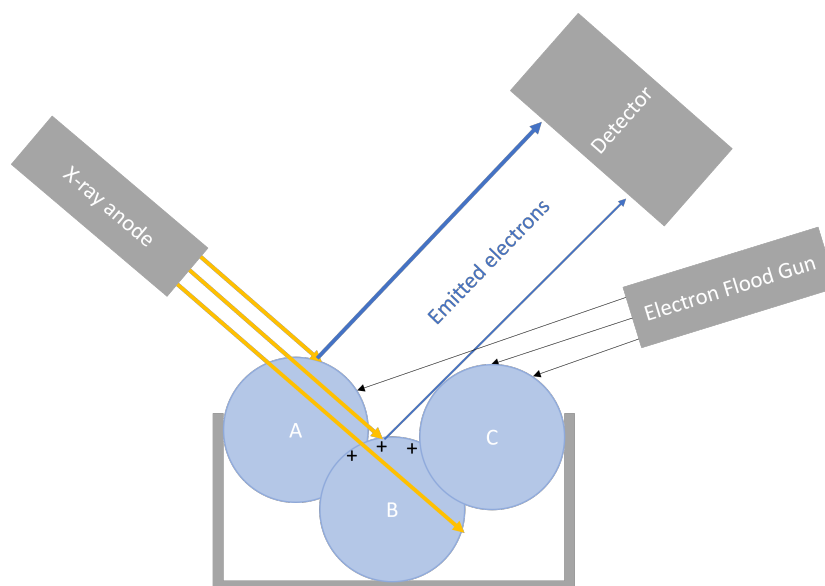


Figure 4.21: Visual explanation of charging artefacts present in XPS of polymer powders

### 4.3.8 Comparing to more common microplastic aging methods

Several techniques have been used to approximate accelerated photoaging in the literature, however two main approaches have been commonly used before: treatments of aggressive oxidising agents, and the use of high-power lamps to accelerate photodegradation. Compared to these two most commonly used aging methods in the literature, the results shown here indicate that plasma degradation stands out uniquely in a number of key dimensions. Photo-initiated oxidation using high-powered lamps instead has been shown in this study to act on timescales of days to months [50], whereas chemical aging treatments are typically in the order of days to weeks [143]. Compared to other environmental aging studies, it is clear that surface oxidation can be achieved rapidly in comparison; because the radical species are generated instantly and in high concentrations within a plasma, degradation is immediate and extreme. Large values of oxidation comparable with highly-aged surfaces occurs within seconds. Plasma treatment can also generate these species at room temperature (so-called ‘cold’ plasmas [45]), mitigating any potential impacts of increased temperatures (such as melting, or changes in tensile strengths) that can be present in other methods [143]. This means that temperature-sensitive polymers, such as polycaprolactone, could be aged with plasma without concerns over temperature changes occurring during the aging process that would happen with these other methods. It also makes it more realistic, as plastics aging naturally in terrestrial soils would never be exposed to these temperatures.

Plasma degradation is also uniquely able to rapidly age chemically-resistant and photo-resistant polymer surfaces, such as PVC [144]. Because of this, plasma degradation offers the ability to test aging-related hypotheses on materials like these that would otherwise be broadly inaccessible with the two most commonly used existing methods seen in this field of research. Lastly, plasma degradation is morphology indifferent; powders, films and fibres are all equally easy to age, and it has been demonstrated here that it is straightforward to do so, with large plastic squares and fine microplastic powders being aged successfully. Because of the wide variability of different plastic pollutants, having a method which is capable of giving consistent aging across different arrangements of the same material is critical for attaining reproducible results when testing aging hypotheses.

The main procedural drawback of plasma aging is that it is highly surface interactive and bulk insensitive. Solar radiation passes through most plastics completely, being attenuated and absorbed at different depths in the material. With a plasma however, degradation processes instead only occur

within the top few atomic layers of a surface [49]. This means that for certain test hypotheses, it may not be an optimal method for approximating environmental aging. For example, hypotheses that are looking to investigate how long-term photodegradation affects structural properties would be ill-advised to use plasma aging over a high-power solar-mimicking lamp, as this process would not yield the same deep structural weaknesses due to its bulk insensitivity. Exposure to long-term solar radiation also often causes polymers to discolour and causes micro-cracking [158], neither of which occur with rapid plasma aging. It is known for example, that the colour of microplastics can influence the feeding habits of certain organisms [148], so any similar attempts to explore these effects of microplastic ingestion resulting from discoloration due to aging under controlled conditions would not be possible with plasma aging; other methods would need to be used.

#### **4.3.9 Recommendations for environmental studies**

Many impacts of microplastics within the environment occur at the surface of these pollutants, thus the use of plasma aging to test the impact of environmental degradation can be appropriate for many experimental designs. However, this technique is not a one-size-fits-all method, requires the acquisition of specialist equipment not commonly found in environmental science laboratories, and some experimental methodologies may not be appropriate for plasma degradation. For example, any deliberate surface exfoliation (such as through milling processes; a common step in the preparation for microplastics in research studies) that occurs after the aging would leave behind a pristine surface, undoing the aging process. This means that mindful methodological sequencing is essential. Overall, care must be taken when designing new experiments around this method to get the most out of it.

With all this considered, the following general recommendations are made for best practice when aging plastics with plasma for environmental impact studies:

1. Duration is best kept short, as surface functionalisation happens immediately, and longer durations may result in noticeable surface etching or heating; from this research a 60 second plasma duration yields a highly degraded surface that can be used for a proxy of advanced aging in microplastics research
2. For short durations power settings have no significant impact on overall oxidation %; for a similar experimental setup using a 100W plasma is recommended, as this setting gave sensible results, and ensures fastest degradation

3. Mindful sequencing is required when preparing materials for an experiment using plasma aging due to its surface sensitivity, and bulk insensitivity; if a milling step is used to simulate mechanical degradation into microplastics, then it is recommended that the plasma treatment is applied last
4. Use conductive wells such as aluminium foil boats when aging microplastic powders to minimise surface charging kicking up particles, as this can result in unintended particle dispersion within the plasma reactor, as observed during early tests for all microplastic powders used in this research

## 4.4 Conclusion

It is clear from the results presented here that plasma degradation is an effective rapid-aging technique for surface-focused microplastics research. Highly degraded surfaces are achieved within seconds, that would otherwise take significantly longer, such as the several weeks required to see comparable oxidation observed in the ‘Long’ photoaged samples in this study. This surface treatment was shown to give rise to comparable surface functionalisation as the photoaging treatment, further indicating that it is a sensible abstraction of photodegradation. Plasma degradation maintains its rapidity across all three materials tested, whereas the traditional photoaging method only led to significant oxidation of PS due to the photosensitivity of this material. Less photosensitive polymers respond well to plasma aging and, as a result, plasma degradation was shown to be a highly desired technique for preparing significantly aged materials that are not photosensitive, such as LDPE. It was also shown to yield a similar hydrodynamic response when compared to photoaging. It allows for a truly rapid simulation of advanced environmental surface aging, which can be used as test for sharp contrasts in a given environmental effect. The optimisation steps taken showed clearly that short durations are ideal for this methodology, and that low input power settings are not needed.

Despite its clear advantages in terms of swiftness, it should not be treated as a one-size-fits-all aging method, and has limitations that must be considered when designing experiments, such as understanding the fact that the aged layer generated is very thin, meaning common mechanical preparation steps used in microplastics research (such as milling) must be performed before plasma treatment is conducted. The treatments of microplastic powders undertaken in this chapter showcase that this is completely feasible, and that this aging method is suitable for the simulated environmental photodegradation of microplastic powders as well.

## Chapter 5

# Simulating polymer surface aging effects on environmental nutrient sorption dynamics

### Graphical Abstract

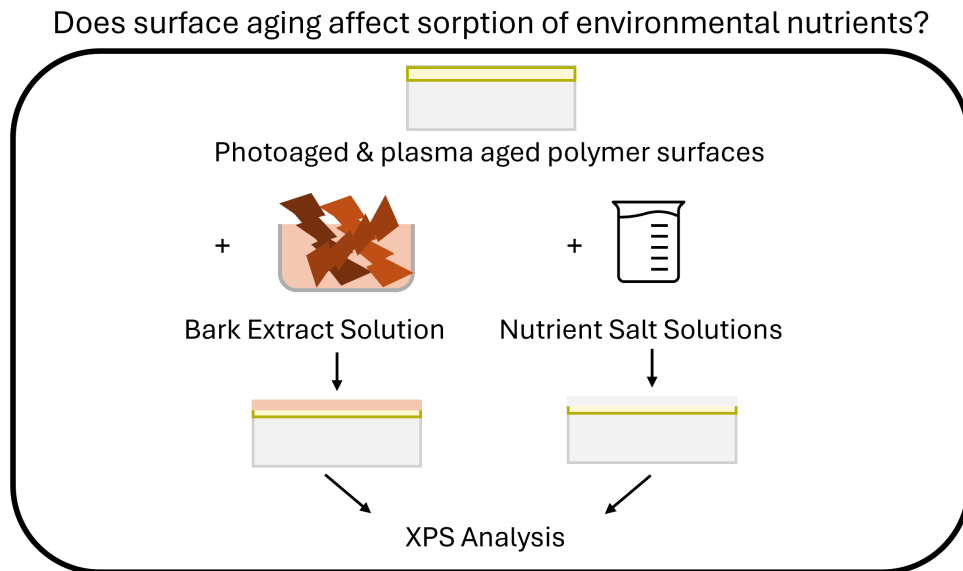


Figure 5.1: A visualisation of the research hypotheses investigated in this chapter

## Abstract

A novel approach was taken using X-ray Photoelectron Spectroscopy to directly monitor surface adsorption of chemical compounds onto pristine and aged polymer surfaces. Initial results of Dissolved Organic Matter (DOM) sorption onto polymers that received accelerated photoaging showed minimal signs of overall sorption, with some very slight material-specific and aging-specific variation, such as consistent adsorption of  $\text{Ca}^{2+}$  ions onto the most photoaged polystyrene samples treated with DOM. In general however, results indicated that even with a significant amount of photodegradation the polymers tested were fairly resistant to surface conditioning and chemical sorption. This observation was then tested in a narrower regime, using specific nutrients ( $\text{NO}_3^-$ ,  $\text{PO}_4^{3-}$ ,  $\text{NH}_4^+$ ) and highly-oxidised plasma-aged surfaces, to identify if this pattern continued. These results showed some nutrient-specific and concentration-specific sorption processes occurring, such as significant adsorption of phosphate and nitrate ions to all aged polymer surfaces. Given the importance of phosphate and nitrate as key forms of P and N that are potentially available to plants and microbial communities, these are important observations. These effects then broadly disappeared when tested with lower concentrations, leaving behind largely unchanged polymer surfaces. These observations highlight that in general both pristine and aged polymer surfaces are relatively resistant to the formation of conditioning films, and that under certain conditions polymer surface aging can lead to immobilisation of nutrient ions.

## 5.1 Introduction

Microplastics are emerging as a concerning novel contaminant within the environment, presenting a variety of challenges within ecosystems. One of these hazards is their ability to absorb and adsorb other chemicals found in their surroundings. Researchers have highlighted that due to their high adsorption capacity MPs present a unique potential to alter adsorption-desorption behaviours of ions in environmental matrices [159]. Perhaps most importantly, as plastics may fragment into smaller and smaller particles in the environment [160], the specific surface area of the material proportionally increases, multiplying their capacity for sorption. Plastic particles have been established as key environmental substrates for sorption of Persistent Organic Pollutants (POPs) such as polychlorinated biphenyls (PCBs), of heavy metals, and of antibiotics [26][27][28][8]. This is an active area of research, and understanding the ability of increasing levels of these novel pollutants to concentrate or amplify other sources of pollution is essential to assessing the overall impact of microplastic pollution in the

environment.

However despite increasing interest in this field in recent years, sparking several reviews and perspectives [161][162][163], this emerging body of work has focused primarily on how microplastics may concentrate other chemical contaminants, and the ecotoxicological risks this presents due to concerns over bio-accumulation resulting from chemicals adsorbing onto microplastic surfaces and being ingested by wildlife [111]. This is indeed a chief concern when assessing the impact of sorption processes connected to microplastics, but it is not the only way these materials present a novel sorption hazard. In particular, virtually nothing is known about their ability to adsorb chemical species essential for plant and soil health, such as nitrate, phosphate, and ammonium ions. It has been proposed that microplastic pollution could directly affect nutrient availability in soils [159], however available research directly assessing this hypothesis is limited. This is critical, because if the increasing amount of microplastic pollution found in agricultural soils across the world is able to consistently act as significant sorption sites for key soil nutrients it could lead to changes in the availability of different nutrient species within soil matrices, lead to nutrient immobilisation, and even potentially alter nutrient cycling.

The availability of nutrients plays a key role in soil health, and fertilizers rich in soil nutrients are frequently added as soil amendments in order to increase fertility and crop yield. It is generally agreed that sorption processes can strongly influence the availability of nutrients in soils, so assessing the ability for novel chemicals that are being introduced to soils to affect these processes is critical. Further, the role that environmental aging will play in the sorption properties of plastics within the environment is unknown. Aging has been identified as a factor that could affect the sorption of organic pollutants to plastic surfaces [164], with several mechanisms being highlighted, such as changes in hydrophobicity that are common in the aging of simple polyolefins contributing to the adsorption of hydrophilic organic pollutants [165]. Therefore in order to accurately assess the sorption behaviour of key soil nutrients to plastic surfaces aging is a critical factor to be considered. When polymers age in the environment their surface chemistry changes, leading to a general increase in carbonyl groups and other highly polar functional groups. As a result of this change, it is plausible that this may lead to electrostatic interactions with nutrient ions dissolved in water within a soil matrix, with the potential to immobilise these nutrients, leading to a deterioration in soil health if the concentration of plastic pollution increases or if the relative aging of existing pollution leads to further adsorption. Because plastic pollution is expected to persist for some time, any ability for plastic pollution to immobilise

soil nutrients is of chief concern, and it is critical to understand the impact of this as soon as possible.

This chapter investigates the role that changes in polymer surface chemistry arising from simulated environmental aging has on the ability for polymers to adsorb Dissolved Organic Matter (DOM) and key soil nutrient species. In the past, adsorption studies have proceeded through inference via isotherms and water concentrations. This approach is effective, but is an indirect measure of adsorption, as it analyses what is left in solution after sorption processes have taken place. In this research study an innovative new approach was pioneered to directly monitor adsorption characteristics by analysing chemical species bound to the surface of plastics via XPS. This allows for a direct unequivocal confirmation of surface-bound adsorption. Two experiments were designed to accomplish this. A more ‘realistic’ approach, mapping a heterogeneous bark extract to photoaged polymer surfaces was first investigated. Early results indicated that these data led to minimal adsorption, so a more focused followup experiment was performed in order to investigate the limits of more specific adsorption in high and realistic concentrations of specific soil nutrient chemical species onto highly oxidised polymer surfaces.

## 5.2 Methodology

### 5.2.1 Preparation

Squares of three polymeric materials (Polystyrene (PS), Polylactic Acid (PLA), Low-density Polyethylene (LDPE)) of approximately  $1\text{cm}^2$  in size were cut from sheets of high-purity research-grade polymers sourced from Goodfellow Cambridge Ltd. This was done using metal tools washed in research-grade isopropyl alcohol (IPA) to remove any organic impurities from the surface of the tools. The squares were then gently washed in IPA to remove any further organic contamination, dried with a nitrogen line, and then separated into pristine and aged batches. The pristine samples were placed into identical plastic boxes, with care taken to ensure the same face of each polymer sample was always ‘up’.

### 5.2.2 Accelerated Photoaging

The aged samples were were subjected to accelerated photoaging using an ATLAS Suntest system, detailed in section 2.4. The spectral irradiance of this equipment is shown in figure 2.10. Samples

were loaded into a custom-built aluminium square-well grid, uncovered (as seen in figure 2.11). In this chapter, samples were exposed to a constant photon flux equivalent to  $750\text{Wm}^{-2}$  in three batches of duration: 1 week, 2 weeks, and 6 weeks (otherwise referred to as ‘Short’, ‘Medium’, and ‘Long’ exposure breakpoints respectively). At the end of a given exposure block, the aged samples were gently removed with clean metal tweezers, carefully keeping track of which side was facing up towards the lamp within the ATLAS chamber, as this face will have received a higher mean dose of solar radiation, placed into identical sample boxes as the control, and stored in the same way prior to analysis.

### 5.2.3 Preparation of bark extract solution

To simulate terrestrial Dissolved Organic Matter (DOM) sorption, a commercially available bag of bark chippings was purchased from Wickes, and then thoroughly mixed with deionised (DI) water in a glass beaker to form an aqueous suspension, at approximately 1:4 bark-to-water ratio. This suspension was left covered overnight in a dry, temperate laboratory in order for DOM to leach from the bark into the deionised water. This mixture was then filtered 5 times: through a coarse 2mm sieve, then vacuum filtered through GF-C and GF-D glass fibre filters, and then through  $0.45\mu\text{m}$  and  $0.2\mu\text{m}$  cellulose nitrate filters, leaving behind a solution of DOM. This approach was taken in order to increase the reproducibility of results, as extracts sourced from natural soils are likely to vary considerably over time, and by location.

### 5.2.4 Bark extract stoichiometric reference

In order to characterise any sorption processes occurring with the bark extract a reference spectrum needed to be obtained to identify a characteristic signature to compare to. In order to do this, an organically clean silver surface was prepared by taking a silver foil sheet, cutting  $1\text{cm}^2$  squares from it, and using a plasma operated at 100W for approximately 20 minutes to lift organic contamination from the surface. The ‘cleaned’ silver surface was then used as an inorganic substrate for the bark extract. Silver was chosen as the reference substrate, as the characteristic peaks of silver within XPS spectra do not overlap with any of the major peaks associated with organic material (such as carbon, nitrogen, phosphorus, calcium, oxygen, sulfur, as well as a range of other additional elements) allowing for clear peak identification. Several drops of the prepared bark extract were pipetted onto the cleaned silver surface, left to dry, and repeated until a visible layer had formed. This sample was then loaded into the XPS using the same methodology as described below for the polymer samples.

### 5.2.5 Conditioning of polymer samples in bark extract solution

Each polymer treatment was placed into a clean unit of a well plate. Metal crocodile clips were washed in IPA, dried, and then fixed to the polymer samples such that the aged surface was tracked and maintained facing upwards. Each polymer treatment was then conditioned in approximately 1cm depth of the bark extract solution for 30 minutes to allow for any DOM to adsorb to the surface and form a ‘hard’ (i.e. strongly associated with the surface [8]) Conditioning Film (CF). After this time, each sample was removed, any loosely bound material was gently rinsed off with a small amount of DI water, and then gently dried with a nitrogen line. These samples were then loaded into the XPS using the method outlined below.

### 5.2.6 Plasma Aging

The plasma aging method reported here is an application of the analysed and optimised process reported in chapter 4. ‘Aged’ subgroups of the polymer squares were loaded into a Diener Plasma Technology Zepto Plasma Cleaner via a metal loading plate. The equipment was pumped down to base pressure (nominal value of  $5.00 \times 10^{-3}$  Pa) prior to loading samples, and after samples had been loaded, to minimise contamination. Air was then passed into the chamber, reaching stable pressures of  $\sim 10 - 15$  Pa. Chamber pressure was monitored using a Leybold Display One sensor. This air flow was ignited into a plasma with an input power of 100W for a duration of 60s. Duration was managed using an external electronic timer. The chamber was then vented slowly to minimise potential of disruption to these light samples, and to ensure the same surface was always maintained upright. More details of this process can be found in sections 2.3 and 4.

### 5.2.7 Surface conditioning with nutrient salt solutions

Each polymer square was transferred to a unit within a clean well plate using metal tweezers, and held in place using metal crocodile clips. Tweezers and clips were routinely wiped down with IPA to minimise organic contamination. Each polymer square was then fully submerged in  $\sim 1$ cm depth of a high-purity nutrient solution for a duration of 1 hour. The solutions used to test adsorption of nitrate, phosphate, and ammonium were high-purity stock standards sourced from Sigma Aldrich. They were suitably diluted with Milli-Q water in volumetric glassware to achieve concentrations of  $1000 \text{mgL}^{-1}$  or  $1 \text{mgL}^{-1}$ , expressed as either N or P for each ion, as required. Glucose-6-phosphate (G6P) was sourced from Fisher Scientific to serve as a proxy for larger labile organic molecules found in the environment,

and was similarly diluted into volumetric glassware to achieve a desired concentration of  $1\text{mgPL}^{-1}$  for comparison. Each polymer treatment was then removed, tapped gently to remove excess moisture, and dried with a high-pressure nitrogen line. Samples were then further dried under a rough vacuum to minimise outgassing during analysis.

### 5.2.8 XPS Analysis

Square samples were loaded into a Kratos Analytical Axis Supra Plus X-ray Photoelectron Spectrometer, mounted onto standard Kratos Analytical bars using Kapton tape. The X-ray source was a monochromated Al K- $\alpha$  anode (1.487 keV). XPS analysis was conducted with charge neutralisation enabled, via an inbuilt electron flood gun. Survey scans were taken to analyse the surface stoichiometry in the region of 0 - 1200 eV at a step size of 1eV and a pass energy of 160eV. Coreline spectra for the C 1s peak were also collected in the region of 280 - 304 eV binding energy at a step size of 0.1eV and a pass energy of 20eV. Measurements of polymer films were completed in triplicate where possible, and in duplicate where stated, due to constraints handling light, fragile samples. For more details on this analysis technique please refer to section 2.2.

### 5.2.9 Statistical analysis

All t-tests conducted in this chapter were completed as two-tail tests at a p value of  $\leq 0.05$ . These tests were performed using Python 3.9 via modules in the Anaconda distribution package (Pandas, SciPy).

## 5.3 Results & Discussion

### 5.3.1 Conditioning film adsorption analysis

#### Characterising the bark extract

In order to explore DOM sorption from the bark extract to the surface of the pristine and aged polymers, a set of reference spectra of the dried bark extract deposited onto a silver foil substrate were taken. To control for the substrate, spectral signatures of the silver were obtained first. Figure 5.2 indicates the pre-cleaned silver foil has a large amount of carbon contamination on its surface. Note that whilst the silver 3d peak at 369.0eV is visibly much larger than the C 1s peak at 285.0eV, silver electrons are far more sensitive to X-ray excitation, with a sensitivity factor over 21 times greater (Ag 3d electrons have a sensitivity correction factor of 5.987, compared to carbon C 1s's factor of 0.278 in the reference library used for this experiment). After correcting for this, the carbon peak in this spectrum is measured at 63.99% of the peak area, to 23.14% of the Ag 3d peak.

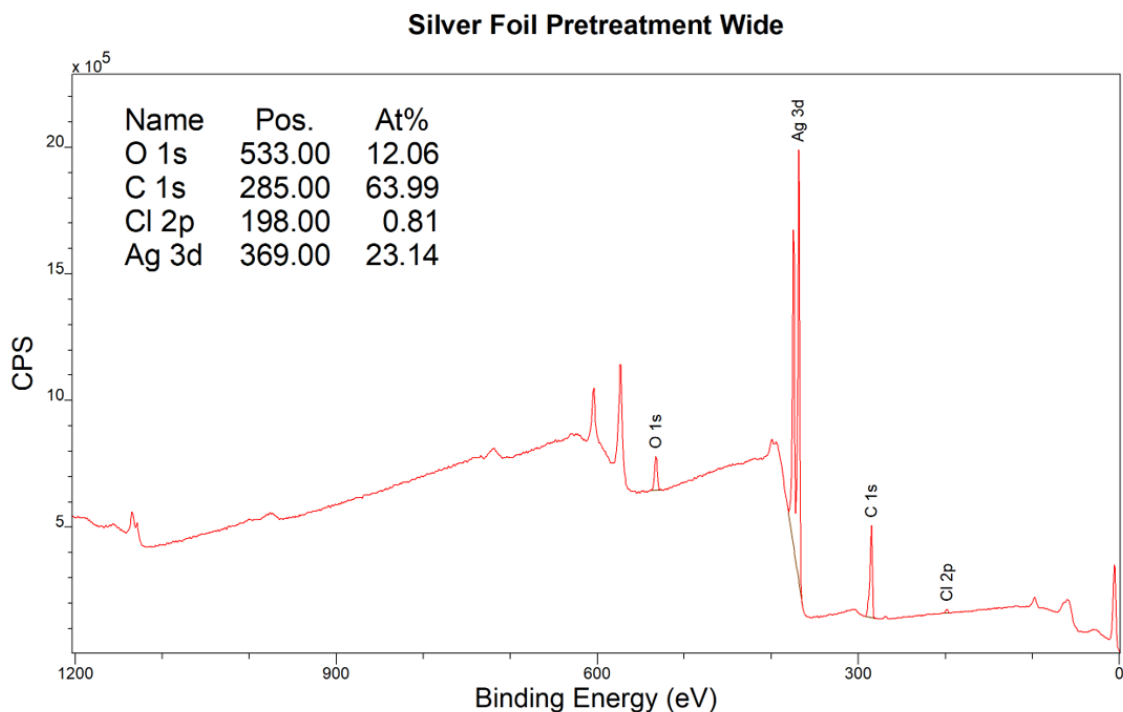


Figure 5.2: A representative wide scan of the silver foil used to create bark reference spectra before cleaning. The large amount of carbon (63.99% of surface) measured in the pretreatment scan indicates significant surface contamination that needs to be removed in order to use this material reliably.

Figure 5.3 showcases representative wide spectra obtained of the cleaned silver surface after the plasma cleaning step. Plasma cleaning was chosen as opposed to other methods, as this method is highly effective at removing soft organic matter from hard metallic surfaces. This surface has much lower concentration of carbon at 11.98%, making it far more ideal as a substrate for identifying adsorption of carbon-based chemical species, as post-cleaning there will be a much lower carbon background signal to compete with. The surface stoichiometry has a large proportion of oxygen at 31.73%, explained by the newly cleaned surface oxidising in air. This would make characterisation of any oxygen-containing compounds challenging if the O 1s coreline spectra were used, so the focus was towards the carbon region. Ideally this surface could be cleaner, but it is significantly better than the silver foil without these cleaning steps.

Figure 5.4 is the same plasma-cleaned silver surface treated with the dried bark extract. This spectrum demonstrates that the bark extract is largely carbon-based, with a large C 1s peak of 52.41% appearing, with some trace amounts of other common lighter elements such as potassium, phosphorus and chlorine. As the Ag3d peak dropped to 0.49%, it is possible to confidently assert that this spectrum is a signature of the bark extract. However it is critical to note that there was variation in the presence and quantities of elements detected when scanning across the surface of the reference materials. This is likely a result of drying dynamics, as when droplets dry they typically do not evaporate uniformly across a surface, a phenomenon widely known as the ‘coffee stain effect’ [166]. In this instance, this likely led to larger molecules, or molecules with a greater affinity for the substrate, being concentrated in different spots of the sample compared to lighter and more mobile chemical species. Therefore, table 5.1 additionally showcases all of the environmentally-relevant elemental peaks detected, with the largest peak area observed. These results highlight the chemical diversity of this extract, which indicate its suitability as an abstraction for environmental DOM. However, as these elements are still in relatively low concentrations, and there was significant variability in measured peaks of trace elements, it was determined that additionally assessing the sorption of dissolved organic matter from this extract with high-resolution coreline C 1s spectra of the treated polymer samples was needed.

Figure 5.5 describes the overlay of the plasma-cleaned silver surface and the bark-treated silver surface, in order to identify characteristic peaks within the carbon environment that could be used as a reference signatures in the high-resolution DOM-on-polymer C 1s spectra. These spectra were min-to-max normalised in order to better determine peaks directly attributable to the bark extract.

Whilst the largest peak sits at 285.0eV, with a broad base, there are two significant characteristic peaks also visible at 293.0eV and 296.0eV that are attributable to the extract. These peaks do not overlap with the peaks associated with the pristine polymer spectra analysed in section 4, and therefore could be used to identify sorption onto the polymer surfaces. These peaks could either be carbon-based chemical species from the bark extract, however it is also possible that this corresponds to K 2p 1/2 and K 2p 3/2 peaks instead, as K 2p and C 1s regions are in close proximity, therefore both possibilities need to be considered when studying the sorption onto the polymer surfaces.

Table 5.1: Element-electron orbital peaks (% contribution) measured in the bark extract for each trace element observed.

Elemental region fitted	Max peak %
N 1s	3.65
Na 1s	3.04
Cl 2p	1.24
P 2p	1.08
Si 2p	8.04
S 2p	2.04
K 2p	2.93
Ca 2p	0.94

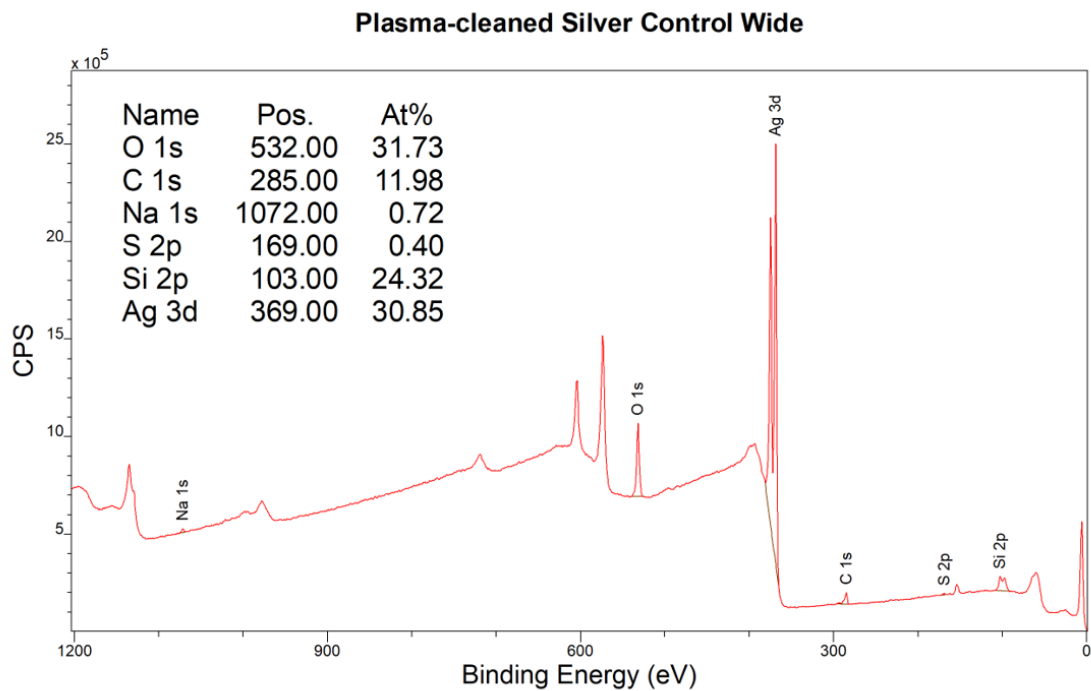


Figure 5.3: A representative wide scan of the silver foil used to create bark reference spectra after plasma cleaning. Overall, adding in a plasma-cleaning step removed a large proportion of the surface contamination, as indicated by the much lower concentration of carbon at 11.98%, making it far more ideal for identifying carbon-based adsorption.

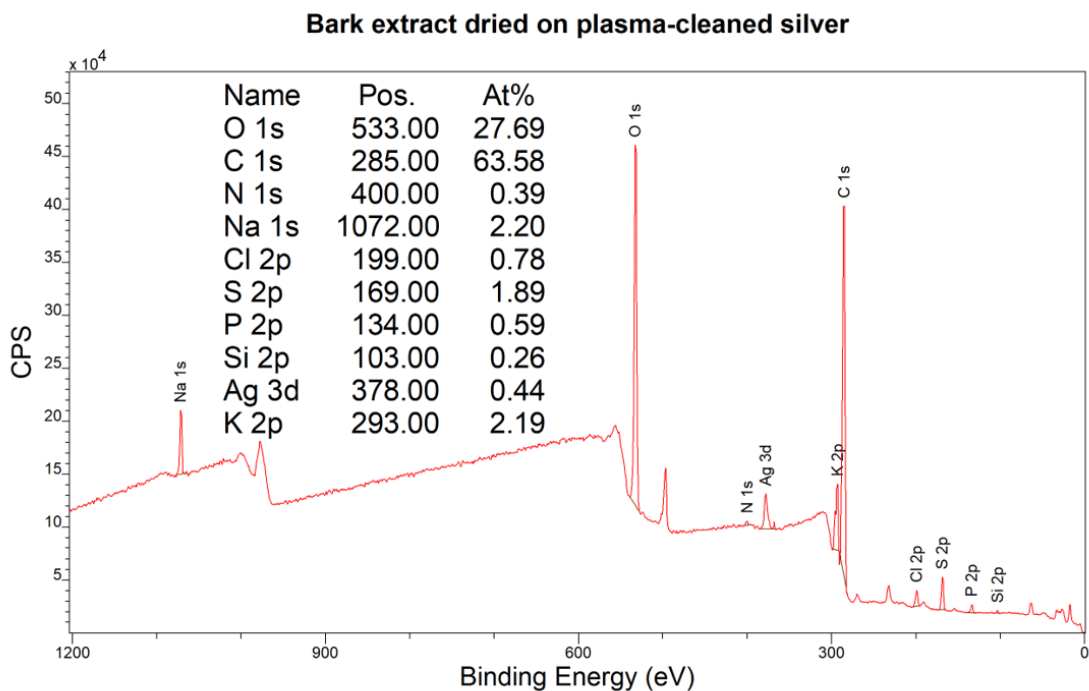


Figure 5.4: A representative XPS wide spectrum of the plasma-cleaned silver substrate with dried bark extract, highlighting the wide diversity of different elements present in the bark mixture, making it a strong candidate for used as a treatment to test surface sorption.

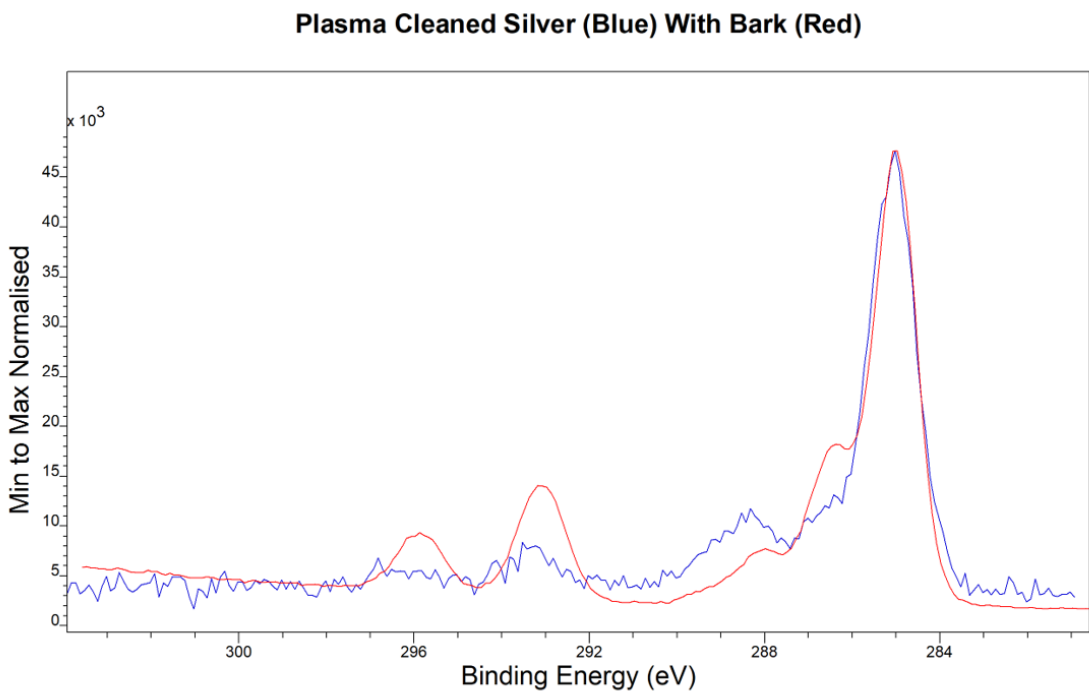


Figure 5.5: Min-to-max normalised comparison of two examples of C 1s spectra of plasma cleaned Ag Control (Blue) and plasma cleaned Ag with bark incubation (Red), which indicate the emergence of two peaks attributable to the bark extract at 293.0eV, and 296.0eV.

### 5.3.2 Adsorption characteristics of bark-derived dissolved organic matter on photoaged polymer surfaces

From the wide scans observed below it was clear that, in general, the incubation with bark-derived DOM did not lead to significant adsorption in the wide scans for any of these materials; the pristine and aged surfaces behaved almost identically. These wide spectra correlate strongly with the ‘Long’ photoaged reference spectra collected in chapter 4. The only notable result from these data is that the ‘Long’ photoaged PS surfaces showed a consistent calcium peak, visible in figure 5.6 at 348.0eV. This is evidence that the highly-oxidised PS surfaces could be leading to sorption of positively-charged ions, such as  $\text{Ca}^{2+}$  ions (identified as a trace element of the bark extract in table 5.1), which would be reasonable given that oxygen-based functional groups such as carbonyl and carboxyl groups are typically highly polar, and have a  $\delta^-$  charge associated with them. However, the overall sorption observed is still fairly low, and only correlates with this one ion. Based on the representative wide survey scan of the dried extract this is to be expected, as whilst trace elements were observed, they were in low concentrations. It is also clear that, as these spectra strongly reflect the highly photoaged surfaces observed in section 4.3.2, any surface conditioning films formed as a result of this incubation are very thin, leading to no clear obscuration. The ‘Short’ and ‘Medium’ breakpoints were also analysed, however data from these samples are not reported here because those data were consistent with the observations made for ‘Long’ aged samples, but with even fewer noticeable changes.

Because the characteristic bark spectrum (figure 5.4) contains a sharp carbon peak, C 1s spectra were investigated for evidence of CF formation in the narrow carbon signal. For all three polymers investigated, both the pristine and aged surfaces treated with a bark extract look similar to the coreline spectra detailed in section 4.3.2, as shown in figures 5.9 - 5.14. These overlays also indicate that the surface aging, even in the more dramatically oxidised PS surface, did not appear to have a significant effect on adsorption when compared to the pristine polymer treatments. There is some peak broadening and dampening of the peaks after the bark extract treatment. However, no new peaks attributable to the reference spectrum obtained in figure 5.5 appear, indicating that overall these materials did see a significant sorption of carbon-based DOM species, or a qualitatively significant shift with photoaging. Figure 5.10 indicates some decrease in the peak around 289eV. It is possible that the bark treatment is removing part of the oxidised layer, as washing of surfaces is known to be able to change surface chemistry and remove some oxygen-carbon functionalities [49].

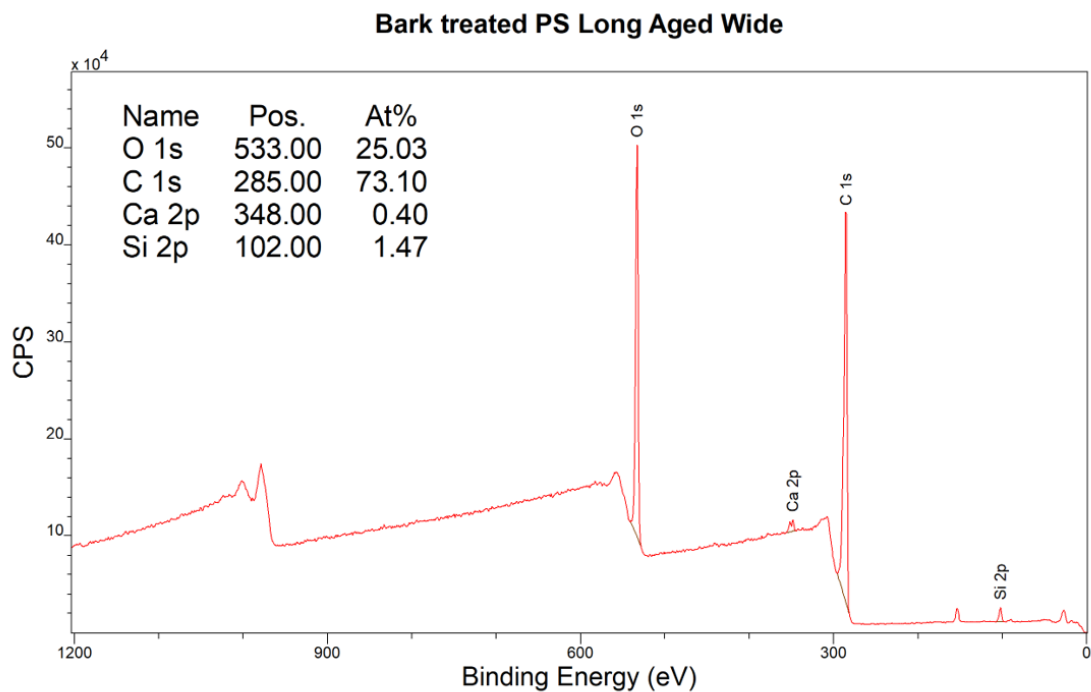


Figure 5.6: A long-exposure photoaged PS representative wide scan treated with bark extract. This wide scan shows an oxygen peak of 25.03%, and a carbon peak of 73.10%, making it comparable to the reference spectra seen in chapter 4. There is also the addition of a calcium peak (0.40% at 348.00 eV) and a silicon peak (1.47% at 102.00 eV), indicative of limited but measurable sorption from the mixture.

### Bark Treated LDPE Long Aged Wide

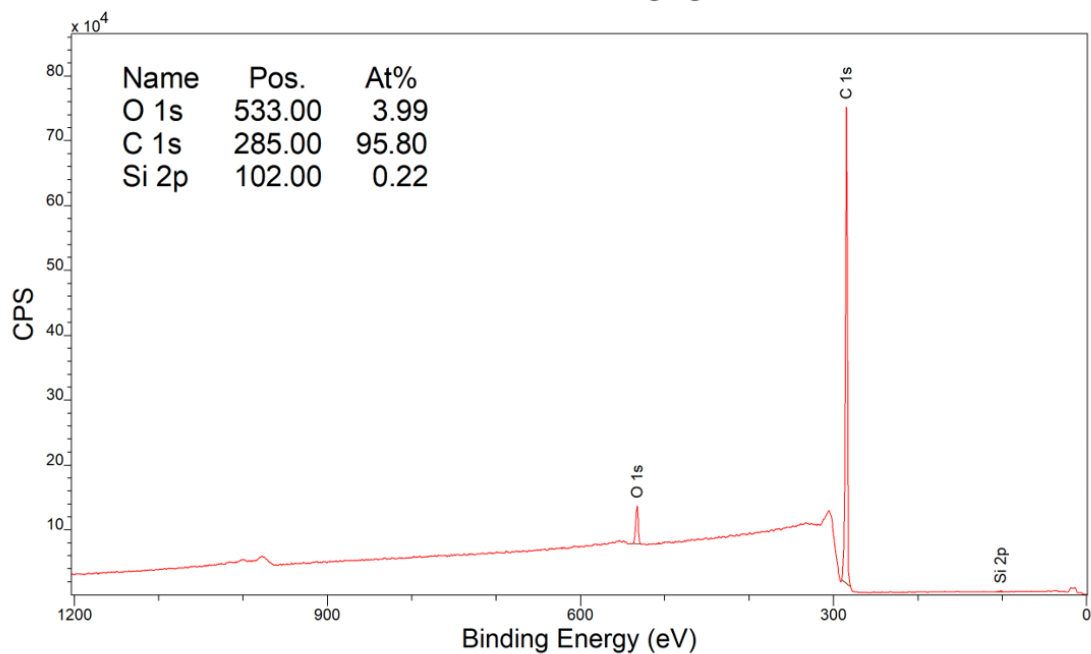


Figure 5.7: A long-exposure photoaged LDPE representative wide scan treated with bark extract. Similarly to those analysed in chapter 4, this long-exposure photoaged LDPE samples has a relatively low level of oxidation compared to the plasma-aged surfaces, and to PS. This sample has only 3.99% surface oxygen, which is assessed to be attributed to the aged material. There is a small amount of silicon adsorbed to the surface (0.22%), but overall it has not changed meaningfully with treatment.

### Bark Treated PLA Long Aged Wide

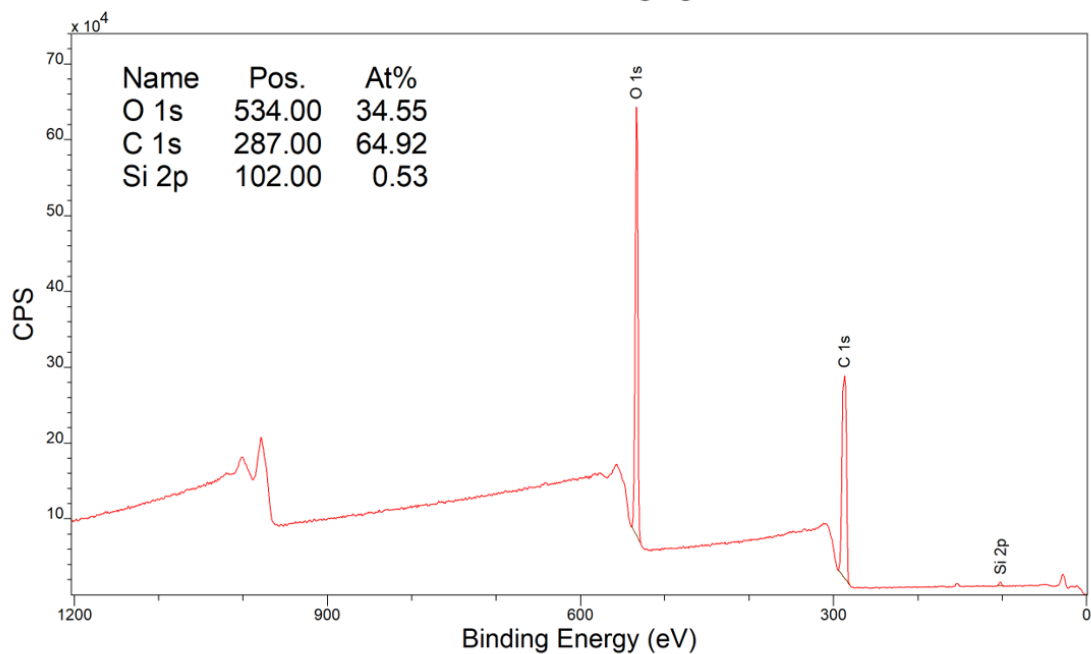


Figure 5.8: A long-exposure photoaged PLA representative wide scan treated with the bark extract. The resulting scan similarly showcases a high-quality PLA spectrum, with only 0.53% of non-PLA elements in silicon, indicating minimal sorption from the extract.

### PS Control (Red) With Bark Treatment (Blue)

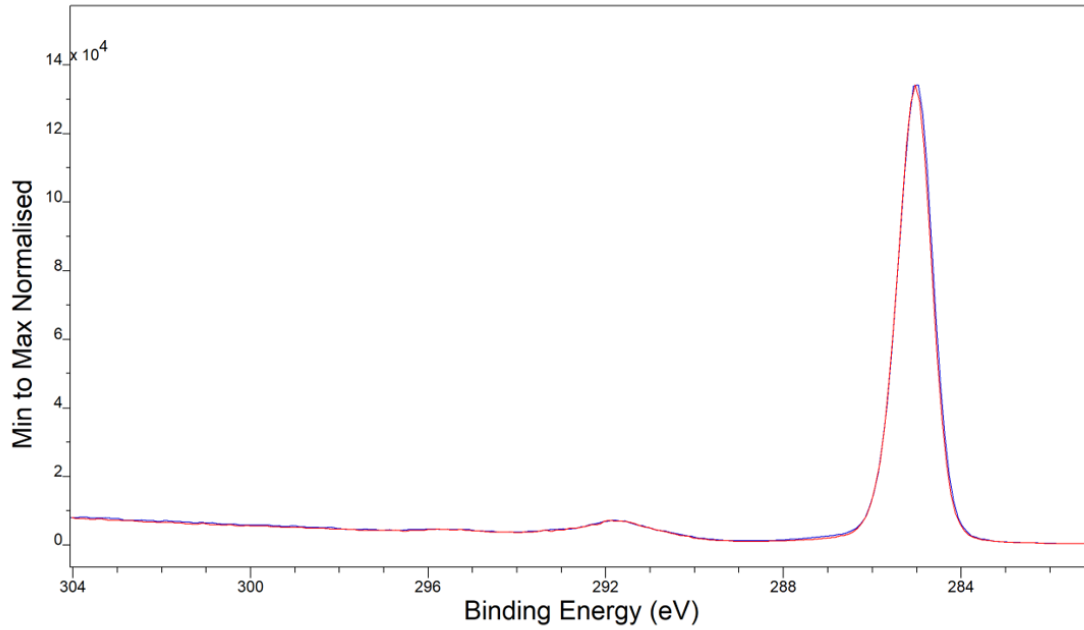


Figure 5.9: A min-to-max normalised overlay of control PS samples without (Red) and with (Blue) bark extract treatment, indicating no noticeable differences with treatment. This means that there was no noticeable sorption of carbon-based species from the treatment.

### PS Long Aged (Red) with Bark Treatment (Blue)

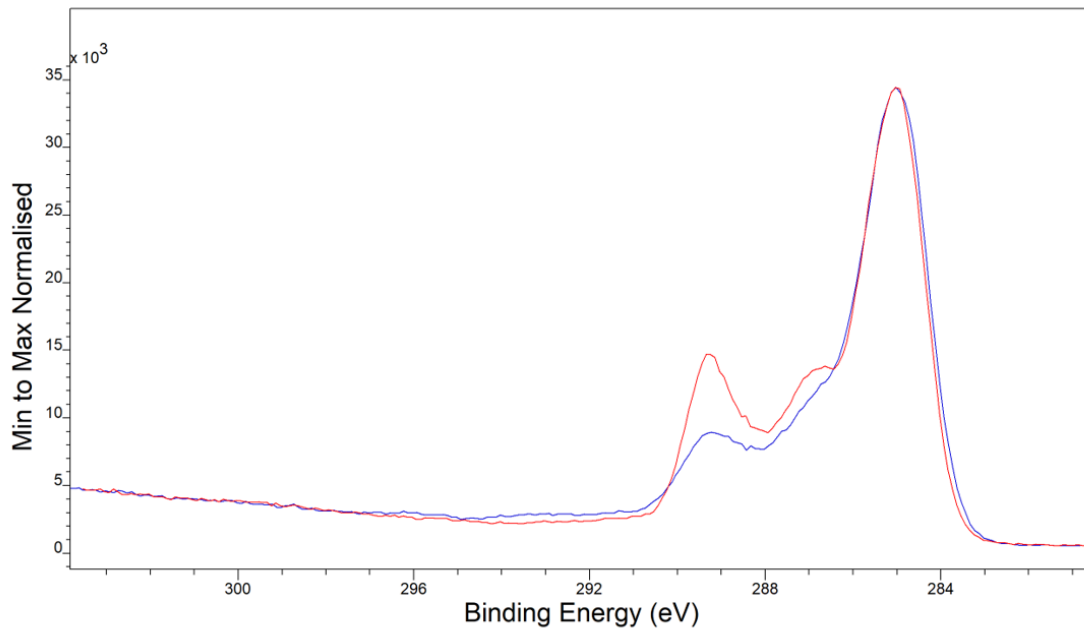


Figure 5.10: A min-to-max normalised overlay of Long Photoaged PS without (Red) and with (Blue) bark extract treatment, indicating minimal differences with treatment.

**LDPE Control (Red) With Bark (Blue)**

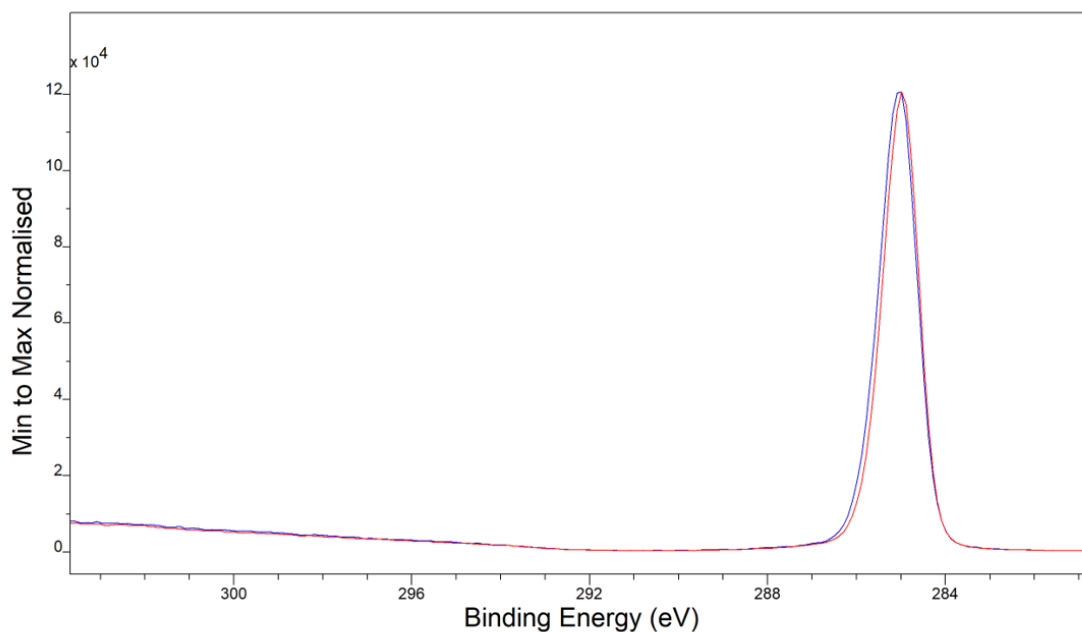


Figure 5.11: A min-to-max normalised overlay of the non-aged Control LDPE without (Red) and with (Blue) bark extract, highlighting that no significant differences were observed in the coreline C1s when treated.

**LDPE Long Aged (Red) with Bark Treatment (Blue)**

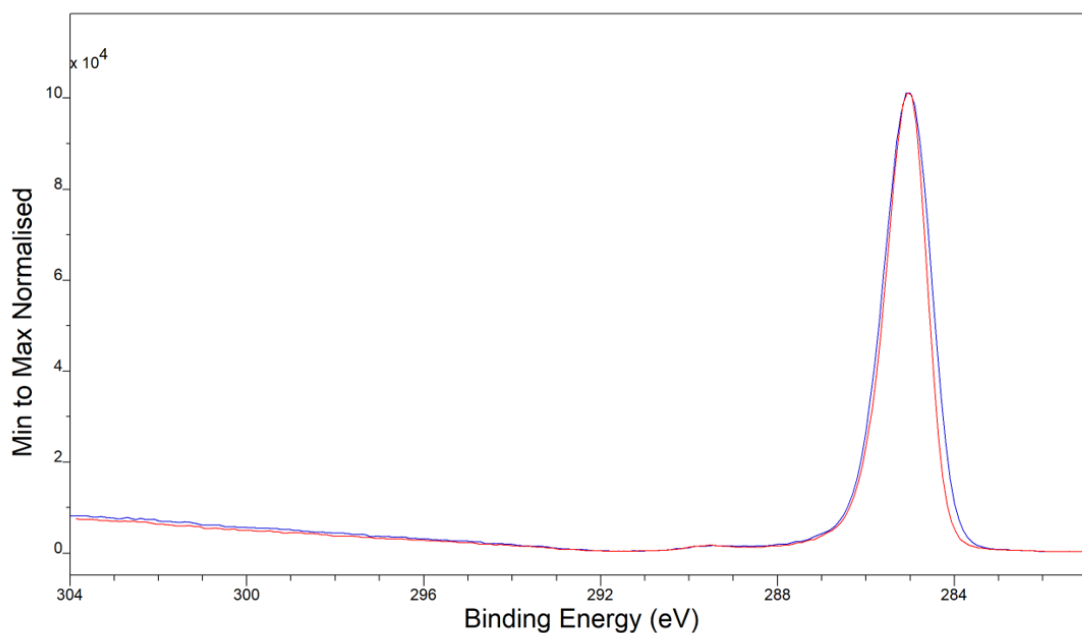


Figure 5.12: A min-to-max normalised overlay of Long Photoaged LDPE without (Red) and with (Blue) bark extract, highlighting that no significant differences were observed in the coreline C1s when treated.

### PLA Control (Red) With Bark Treatment (Blue)

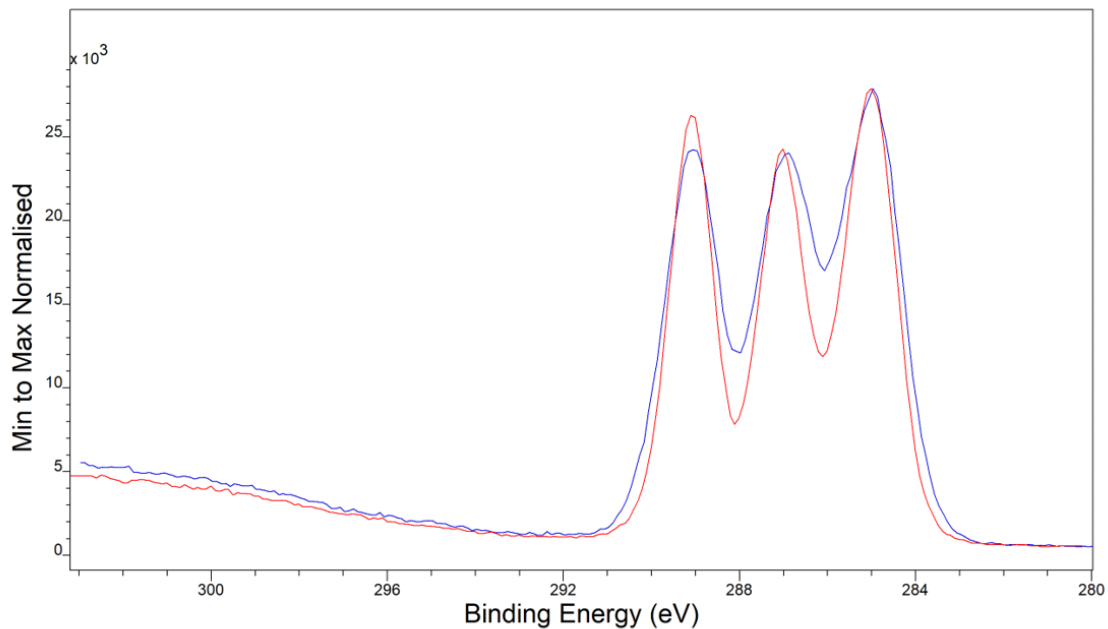


Figure 5.13: A min-to-max normalised overlay of the non-aged Control PLA without (Red) and with (Blue) bark extract, highlighting some peak broadening occurring.

### PLA Long Aged (Red) With Bark Treatment (Blue)

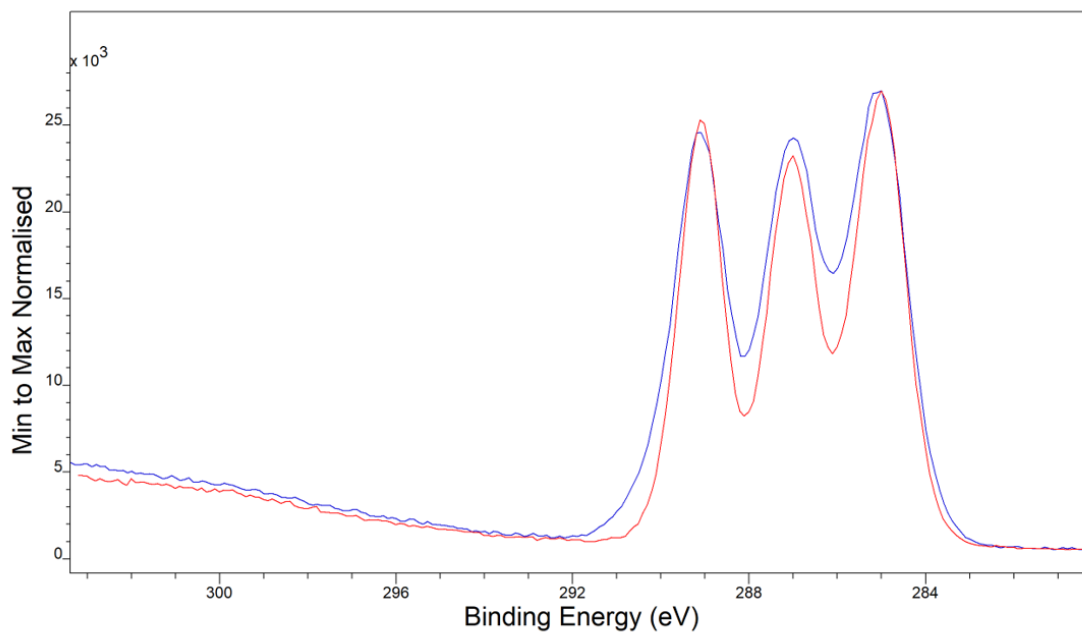


Figure 5.14: A min-to-max normalised overlay of the Long Aged PLA without (Red) and with (Blue) bark extract, highlighting some peak broadening occurring that looks comparable to that seen in the control PLA samples in figure 5.13.

### 5.3.3 Phosphate adsorption analysis

For the higher concentration solutions reported in this chapter ( $1000\text{mgPL}^{-1}$ ) all pristine materials showed only trace levels of sodium and phosphate adsorption, indicating that all three of the pristine polymers were resistant to the sorption of chemical species. However, after simulated aging significant differences were observed. All three polymers tested showed a large increase in positively-charged and negatively-charged adsorbed species, as summarised in Table 5.2. These results were largely consistent between replicates, and almost all of these results were significant to a p-value of  $\leq 0.05$  indicating that surface aging leads to a clear increase in affinity of these nutrient ions towards aged polymer surfaces. There was material-specific variation with respect to which ions sorbed to which surfaces. PS showed statistically significant sorption ( $p \leq 0.05$ ) of  $\text{PO}_4^{3-}$ , but not of  $\text{Na}^+$ . Assuming perfect dissolution, the stoichiometric ratio of ions in solution is 2 : 1 for  $\text{Na}^+$  and  $\text{PO}_4^{3-}$  ions in  $\text{Na}_2\text{HPO}_4$ , and both aged LDPE and PS showed adsorption ratios close to this, at 2.3 : 1.0 and 2.2 : 1.0 respectively, indicating that these surfaces showed little preference for positively or negatively charged species. The aged PLA surface however showed a stronger affinity for the positively-charged sodium ions in greater proportion, with the Na:PPO<sub>4</sub> ratio increasing to 3.3 : 1.0.

Overall ratios of Na and P on all pristine samples differed markedly between materials, and compared to their aged counterparts, as seen in table 5.3. However, due to the exceptionally low overall adsorption for the pristine samples, a direct comparison of these results needs to be undertaken with extreme caution, and is not explored further here.

At the lower and more environmentally-realistic concentration of  $1\text{mgPL}^{-1}$  no noticeable adsorption of any ions was seen on the pristine materials, and only trace levels of sorption of  $\text{Na}^+$  ions were observed for the aged LDPE, and the aged PS surfaces (average peak areas of  $0.05 \pm 0.08$  and  $0.08 \pm 0.07$  respectively). There was also no observed phosphate adsorption at lower concentrations outlined in table 5.2. This is consistent with the above observations, indicating that both aged PS and LDPE have a greater affinity for adsorption of this ion in general, and a greater overall affinity for the positively-charged ions.

Table 5.2: Relative peak areas for sodium and phosphate ion adsorption onto pristine and plasma-aged polymer surfaces. Asterisks (\*) reflect a significant result of  $p \leq 0.05$  compared to the respective control materials.  $n=3$ .

Polymer	Nutrient	Concentration	Peak	Average Peak % (pristine)	Average Peak % (Aged)
LDPE	$\text{Na}_2\text{HPO}_4$	$1000\text{mgPL}^{-1}$	Na1s	$0.09 \pm 0.02$	$7.96 \pm 0.16$ *
			P2p	$0.01 \pm 0.01$	$3.41 \pm 0.18$ *
PLA	$\text{Na}_2\text{HPO}_4$	$1000\text{mgPL}^{-1}$	Na1s	$0.09 \pm 0.09$	$2.97 \pm 0.31$ *
			P2p	$0.00 \pm 0.00$	$0.89 \pm 0.30$ *
PS	$\text{Na}_2\text{HPO}_4$	$1000\text{mgPL}^{-1}$	Na1s	$0.10 \pm 0.09$	$4.92 \pm 3.66$
			P2p	$0.00 \pm 0.00$	$2.22 \pm 0.56$ *
LDPE	$\text{Na}_2\text{HPO}_4$	$1\text{mgPL}^{-1}$	Na1s	$0.00 \pm 0.00$	$0.05 \pm 0.08$
			P2p	$0.00 \pm 0.00$	$0.00 \pm 0.00$
PLA	$\text{Na}_2\text{HPO}_4$	$1\text{mgPL}^{-1}$	Na1s	$0.00 \pm 0.00$	$0.00 \pm 0.00$
			P2p	$0.00 \pm 0.00$	$0.00 \pm 0.00$
PS	$\text{Na}_2\text{HPO}_4$	$1\text{mgPL}^{-1}$	Na1s	$0.00 \pm 0.00$	$0.08 \pm 0.07$
			P2p	$0.00 \pm 0.00$	$0.00 \pm 0.00$

Table 5.3: Ratios of sodium and phosphate ion adsorption onto pristine and plasma-aged polymer surfaces.  $n=3$ .

Polymer	Nutrient	Concentration	Na:P Ratio (pristine)	Na:P Ratio (Aged)
LDPE	$\text{Na}_2\text{HPO}_4$	$1000\text{mgPL}^{-1}$	9.0 : 1.0	2.3 : 1.0
PLA	$\text{Na}_2\text{HPO}_4$	$1000\text{mgPL}^{-1}$	1.0 : 0.0	3.3 : 1.0
PS	$\text{Na}_2\text{HPO}_4$	$1000\text{mgPL}^{-1}$	(Undefined)	2.2 : 1.0
LDPE	$\text{Na}_2\text{HPO}_4$	$1\text{mgNL}^{-1}$	(Undefined)	1.0 : 0.0
PLA	$\text{Na}_2\text{HPO}_4$	$1\text{mgNL}^{-1}$	(Undefined)	(Undefined)
PS	$\text{Na}_2\text{HPO}_4$	$1\text{mgNL}^{-1}$	(Undefined)	1.0 : 0.0

### 5.3.4 Nitrate adsorption analysis

At the higher concentration of  $1000\text{mgNL}^{-1}$ , all pristine materials showed inconsistent, trace levels of sodium adsorption, and no detectable nitrate adsorption, indicating that all three of the pristine polymers were resistant to the sorption of these chemical species. However, after simulated aging significant differences were found. All three polymers tested showed a noticeable increase in both positively-charged and negatively-charged adsorbed species, as outlined in Table 5.4. These results were largely consistent between replicates, indicating that surface aging leads to a substantial increase in the affinity between polymer surfaces and these ions. There was also material-specific variation with respect to which ions sorbed to which surfaces. Assuming perfect dissolution, the stoichiometric ratio of sodium to nitrate ions in solution is 1 : 1 for  $\text{NaNO}_3$ . LDPE and PS showed adsorption ratios just over double this at 2.3 : 1.0, indicating that these surfaces showed a preference for positively-charged sodium ions over the negatively-charged nitrate ions. Aged PLA showed a more balanced affinity of both species compared to the other 2 polymers at 1.4 : 1.0.

Again, at the more realistic lower concentration adsorption of the negatively-charged ions was no longer observed across all three materials, with LDPE and PS showing very low (but measurable) levels of adsorption of sodium ions with average peak areas of  $0.25 \pm 0.24$  and  $0.07 \pm 0.08$  respectively, but again no results that were statistically significant to a p-value of  $\leq 0.05$ . This is consistent with the observations seen in the phosphate analysis.

Table 5.4: Relative peak areas for sodium and nitrate ion adsorption onto pristine and plasma-aged polymer surfaces. Asterisks (\*) reflect a significant result of  $p \leq 0.05$  compared to the respective control materials.  $n=3$ .

Polymer	Nutrient	Concentration	Peak	Average Peak % (pristine)	Average Peak % (Aged)
LDPE	NaNO <sub>3</sub>	1000mgNL <sup>-1</sup>	Na1s	0.12 ± 0.03	2.41 ± 0.28 *
			N1s	0.00 ± 0.00	1.07 ± 0.52 *
PLA	NaNO <sub>3</sub>	1000mgNL <sup>-1</sup>	Na1s	0.02 ± 0.03	3.03 ± 0.46 *
			N1s	0.00 ± 0.00	2.15 ± 0.35 *
PS	NaNO <sub>3</sub>	1000mgNL <sup>-1</sup>	Na1s	0.20 ± 0.08	2.78 ± 0.21 *
			N1s	0.00 ± 0.00	1.22 ± 0.39 *
LDPE	NaNO <sub>3</sub>	1mgNL <sup>-1</sup>	Na1s	0.00 ± 0.00	0.25 ± 0.24
			N1s	0.00 ± 0.00	0.00 ± 0.00
PLA	NaNO <sub>3</sub>	1mgNL <sup>-1</sup>	Na1s	0.00 ± 0.00	0.00 ± 0.00
			N1s	0.00 ± 0.00	0.00 ± 0.00
PS	NaNO <sub>3</sub>	1mgNL <sup>-1</sup>	Na1s	0.00 ± 0.00	0.07 ± 0.08
			N1s	0.00 ± 0.00	0.00 ± 0.00

Table 5.5: Ratios of sodium and nitrate ion adsorption onto pristine and plasma-aged polymer surfaces.  $n=3$ .

Polymer	Nutrient	Concentration	Na:NO <sub>3</sub> Ratio (pristine)	Na:NO <sub>3</sub> Ratio (Aged)
LDPE	NaNO <sub>3</sub>	1000mgNL <sup>-1</sup>	1.0 : 0.0	2.3 : 1.0
PLA	NaNO <sub>3</sub>	1000mgNL <sup>-1</sup>	1.0 : 0.0	1.4 : 1.0
PS	NaNO <sub>3</sub>	1000mgNL <sup>-1</sup>	1.0 : 0.0	2.3 : 1.0
LDPE	NaNO <sub>3</sub>	1mgNL <sup>-1</sup>	(Undefined)	1.0 : 0.0
PLA	NaNO <sub>3</sub>	1mgNL <sup>-1</sup>	(Undefined)	(Undefined)
PS	NaNO <sub>3</sub>	1mgNL <sup>-1</sup>	(Undefined)	1.0 : 0.0

### 5.3.5 Ammonium adsorption analysis

Unlike both of the other inorganic nutrient adsorption tests, the application of both the concentrated nutrient mixture ( $1000\text{mgNL}^{-1} \text{NH}_4\text{Cl}$ ) and the more realistic dilute mixture ( $1\text{mgL}^{-1}\text{-N NH}_4\text{Cl}$ ) for ammonium showed minimal permanent surface sorption. There was some evidence that the positively-charged ammonium ions showed a slightly greater affinity for sorption to aged surfaces, as there was measurable levels of N in the wide spectra for aged PLA and aged PS surfaces. However, these peak areas were low and inconsistent at  $0.24\% \pm 0.34\%$  and  $0.10\% \pm 0.18\%$  respectively for the higher concentration mixture, and  $0.33\% \pm 0.29\%$  for the aged PLA surface only at lower concentrations. This conflicts with what was observed in the two previous sections when comparing at phosphate and nitrate adsorption, indicating sorption to aged polymer surfaces is highly species specific. Ammonium is a relatively volatile ion when compared to phosphate and nitrate, so this could possibly be explained by the ultra-high vacuum applied within the XPS being able to desorb ammonium from the surface of these materials. Ammonium is also extremely soluble in water, as a result of its ability to form strong hydrogen bonds in solution. Therefore these observations are also possibly explained by the ammonium salt having an understandably higher affinity for the water it was dissolved in compared to the other nutrient salt solutions.

Table 5.6: Relative peak areas for ammonium and chloride ion adsorption onto pristine and plasma-aged polymer surfaces. Asterisks (\*) reflect a significant result of  $p \leq 0.05$  compared to the respective control materials.  $n=3$ .

Polymer	Nutrient	Concentration	Peak	Average Peak % (pristine)	Average Peak % (Aged)
LDPE	NH <sub>4</sub> Cl	1000mgNL <sup>-1</sup>	Cl2p	0.00 ± 0.00	0.00 ± 0.00
			N1s	0.00 ± 0.00	0.00 ± 0.00
PLA	NH <sub>4</sub> Cl	1000mgNL <sup>-1</sup>	Cl2p	0.00 ± 0.00	0.00 ± 0.00
			N1s	0.00 ± 0.00	0.24 ± 0.34
PS	NH <sub>4</sub> Cl	1000mgNL <sup>-1</sup>	Cl2p	0.00 ± 0.00	0.00 ± 0.00
			N1s	0.00 ± 0.00	0.10 ± 0.18
LDPE	NH <sub>4</sub> Cl	1mgNL <sup>-1</sup>	Cl2p	0.00 ± 0.00	0.00 ± 0.00
			N1s	0.00 ± 0.00	0.00 ± 0.00
PLA	NH <sub>4</sub> Cl	1mgNL <sup>-1</sup>	Cl2p	0.00 ± 0.00	0.00 ± 0.00
			N1s	0.00 ± 0.00	0.33 ± 0.29
PS	NH <sub>4</sub> Cl	1mgNL <sup>-1</sup>	Cl2p	0.00 ± 0.00	0.00 ± 0.00
			N1s	0.00 ± 0.00	0.00 ± 0.00

Table 5.7: Ratios of ammonium and chloride ion adsorption onto pristine and plasma-aged polymer surfaces.  $n=3$ .

Polymer	Nutrient	Concentration	N:Cl Ratio (pristine)	N:Cl Ratio (Aged)
LDPE	NH <sub>4</sub> Cl	1000mgNL <sup>-1</sup>	(Undefined)	(Undefined)
PLA	NH <sub>4</sub> Cl	1000mgNL <sup>-1</sup>	(Undefined)	1.0 : 0.0
PS	NH <sub>4</sub> Cl	1000mgNL <sup>-1</sup>	(Undefined)	1.0 : 0.0
LDPE	NH <sub>4</sub> Cl	1mgNL <sup>-1</sup>	(Undefined)	(Undefined)
PLA	NH <sub>4</sub> Cl	1mgNL <sup>-1</sup>	(Undefined)	1.0 : 0.0
PS	NH <sub>4</sub> Cl	1mgNL <sup>-1</sup>	(Undefined)	(Undefined)

### 5.3.6 G6P adsorption analysis

The G6P sorption experiment resulted in no measurable level of phosphorus on the surface of any of the pristine or aged polymers used in this study. G6P is a much larger molecule compared to the inorganic nutrients, but only has one phosphate group, which takes up a relatively smaller share of the molecular weight when compared to the inorganic phosphorus example tested (36.5% mass compared to 66.9%). It is possible that the mechanism by which these compounds are adsorbing to the surface is therefore resulting strongly from the ionic component of the molecules rather than arising from Van-der Waals (VdW) interactions, as larger molecules would have greater potential for VdW interactions, and less potential for ionic attraction on a per-molecule basis. It is also reasonably explained by the large number of hydroxyl groups in the G6P molecule showing a greater affinity for the water when compared the polymer surfaces, resulting in no permanent binding to the polymer material surface.

These results give a further strong indication that sorption to polymer surfaces is highly nutrient-specific, and even a significantly oxidised polymer surface is not necessarily enough to lead to permanent and measurable surface sorption in an aqueous context. These data highlight that caution should be taken when making broad generalisations about the sorption dynamics of aged polymer surfaces.

### 5.3.7 Spectral analysis of concentrated nutrient sorption on Pristine and Plasma-aged polymer surfaces

Figures 5.15 through 5.23 showcase representative spectra for pristine and aged polymers included in this study post immersion in each of the three high concentration inorganic salt solutions:  $\text{Na}_2\text{HPO}_4$ ,  $\text{NaNO}_3$ , and  $\text{NH}_4\text{Cl}$  (at  $1000\text{mgPL}^{-1}$  or  $1000\text{mgNL}^{-1}$  respectively). The spectral signature peaks for each of the respective nutrient salts are highlighted on the spectra. Overall, these results clearly demonstrate that this approach using XPS leads to high-resolution results that can be used to give a strong indication of surface sorption dynamics, as the underlying polymer wide spectra are clearly resolvable as the polymer substrate spectra identified in section 4.3.2. Additionally, for these polymers and nutrient salts, all of the nutrient peaks stand far apart from the peaks present in the polymer spectrum, meaning that any adsorption of these nutrients can be clearly identified and resolved. This means that any analysis of relative peak % will be accurate for all three polymers.

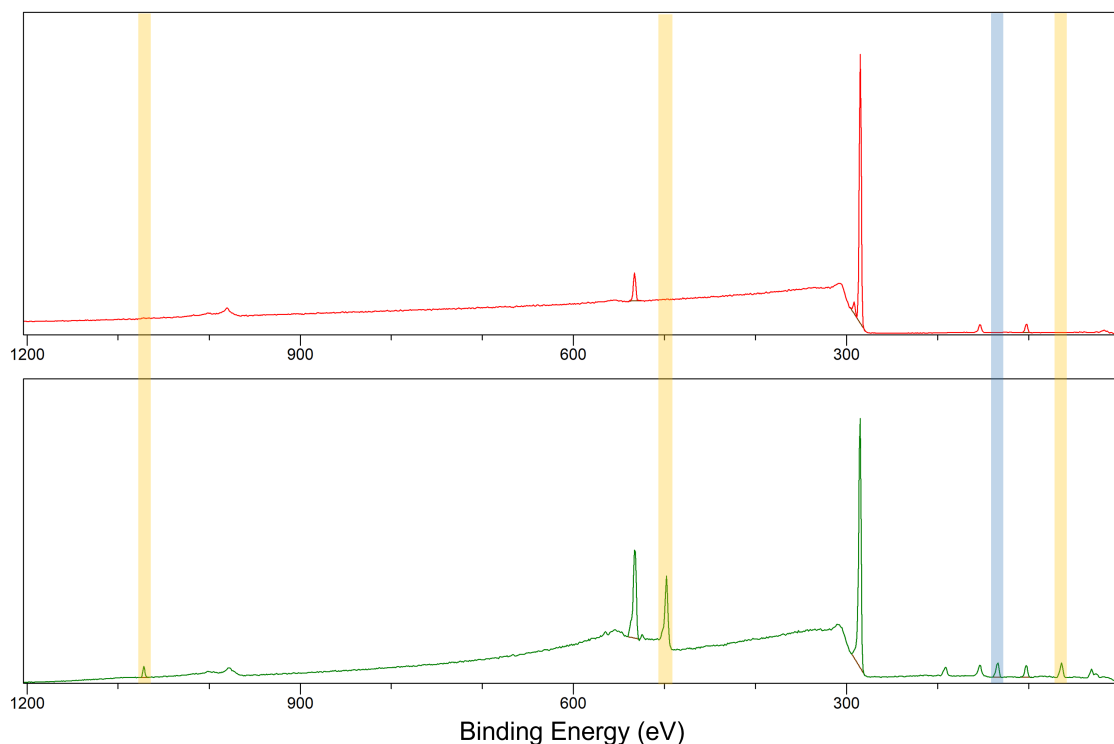


Figure 5.15: Offset overlay for pristine (top) and plasma aged (bottom) representative PS spectra treated with  $1000\text{mgPL}^{-1}$   $\text{Na}_2\text{HPO}_4$ , with sodium (yellow), and phosphorus (blue) spectral lines highlighted.

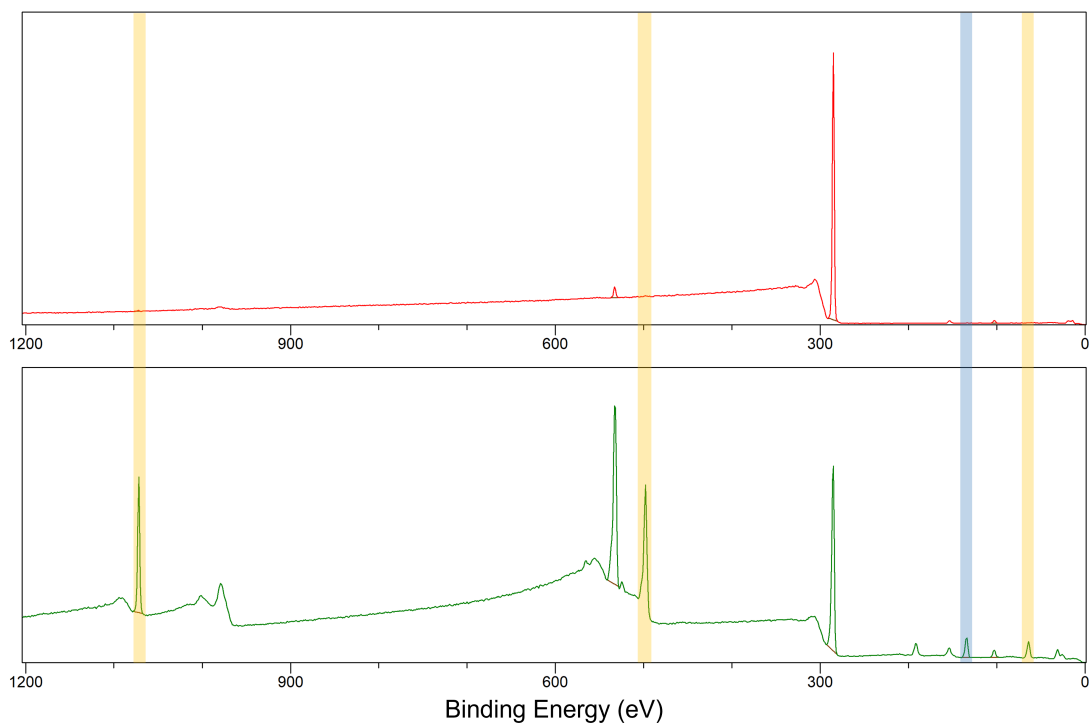


Figure 5.16: Offset overlay for pristine (top) and plasma aged (bottom) representative LDPE spectra treated with  $1000\text{mgPL}^{-1}$   $\text{Na}_2\text{HPO}_4$ , with sodium (yellow), and phosphorus (blue) spectral lines highlighted.

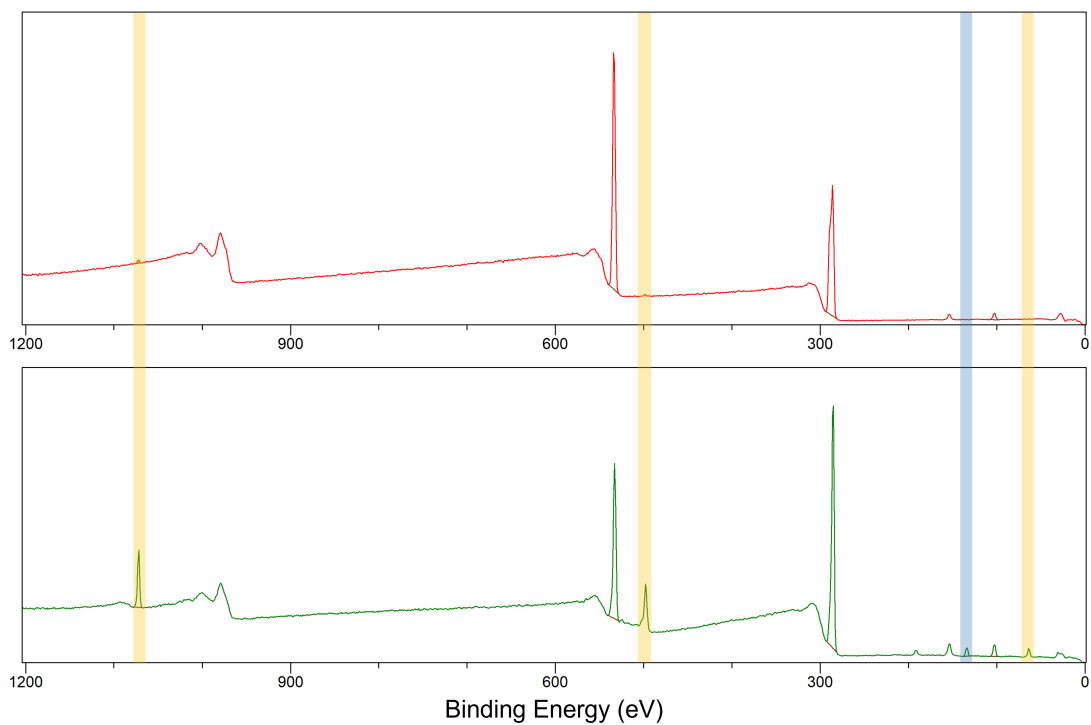


Figure 5.17: Offset overlay for pristine (top) and plasma aged (bottom) representative PLA spectra treated with  $1000\text{mgPL}^{-1}$   $\text{Na}_2\text{HPO}_4$ , with sodium (yellow), and phosphorus (blue) spectral lines highlighted.

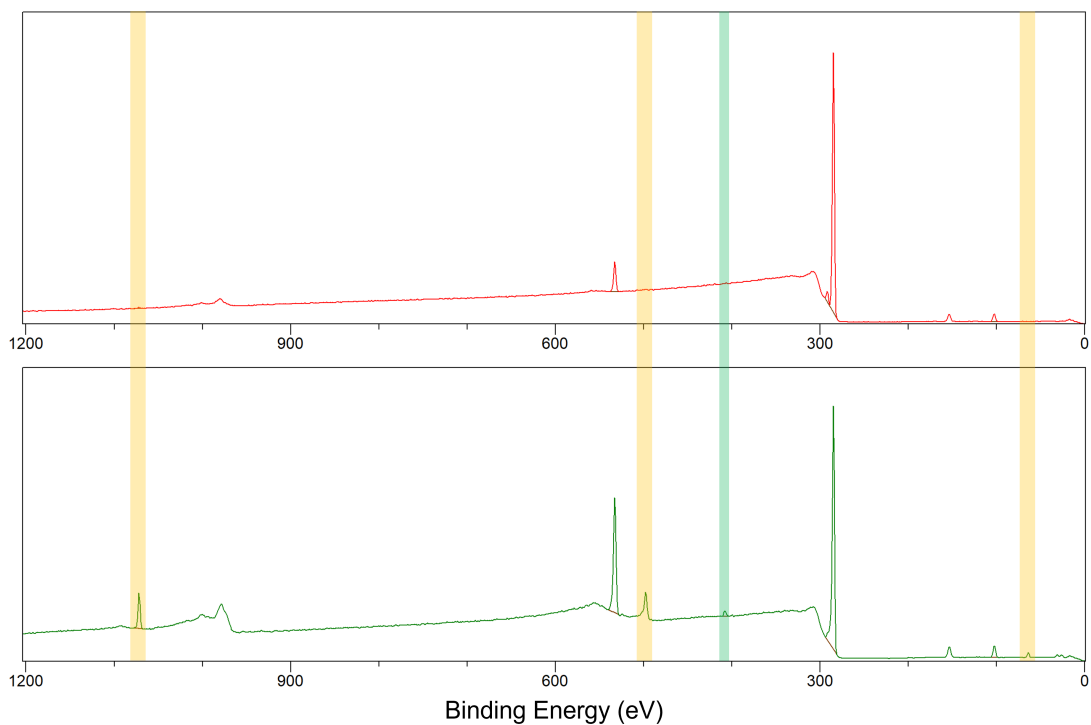


Figure 5.18: Offset overlay for pristine (top) and plasma aged (bottom) representative PS spectra treated with  $1000\text{mgNL}^{-1}$   $\text{NaNO}_3$ , with sodium (yellow), and nitrogen (green) spectral lines highlighted.

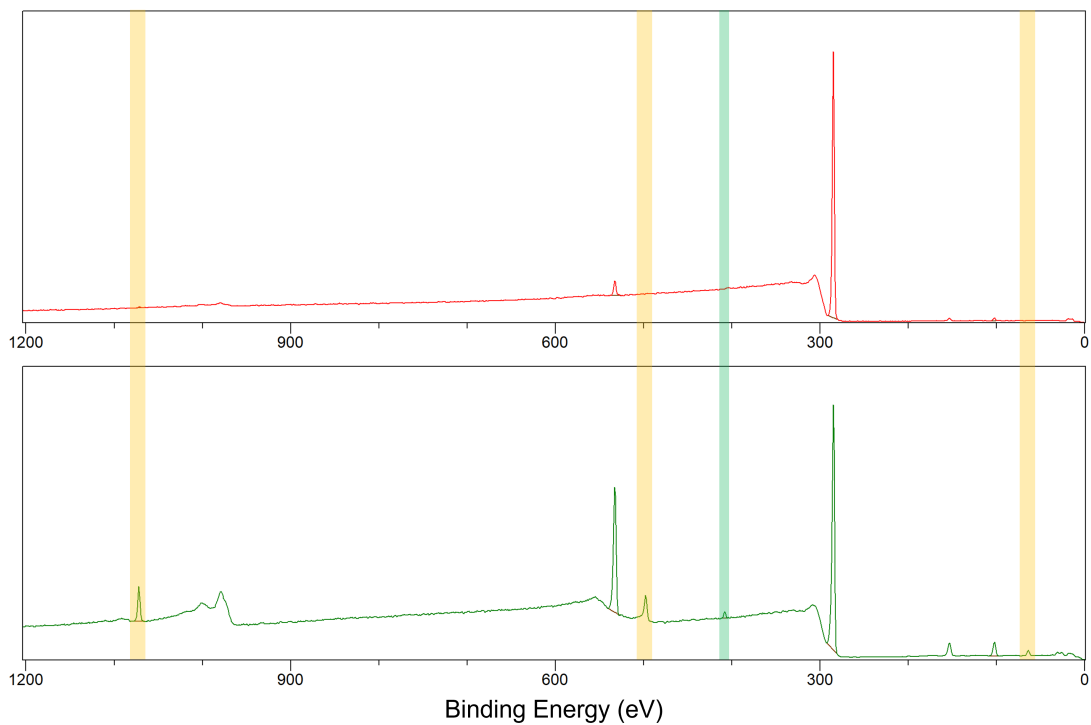


Figure 5.19: Offset overlay for pristine (top) and plasma aged (bottom) representative LDPE spectra treated with  $1000\text{mgNL}^{-1}$   $\text{NaNO}_3$ , with sodium (yellow), and nitrogen (green) spectral lines highlighted.

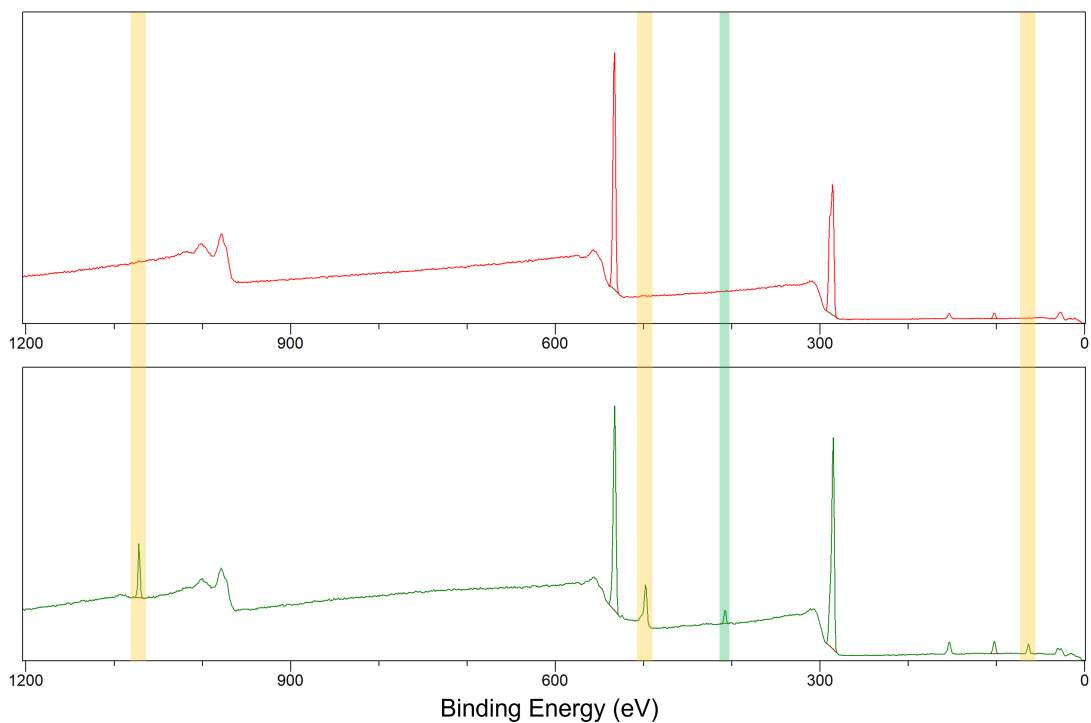


Figure 5.20: Offset overlay for pristine (top) and plasma aged (bottom) representative PLA spectra treated with  $1000\text{mgNL}^{-1}$   $\text{NaNO}_3$ , with sodium (yellow), and nitrogen (green) spectral lines highlighted.

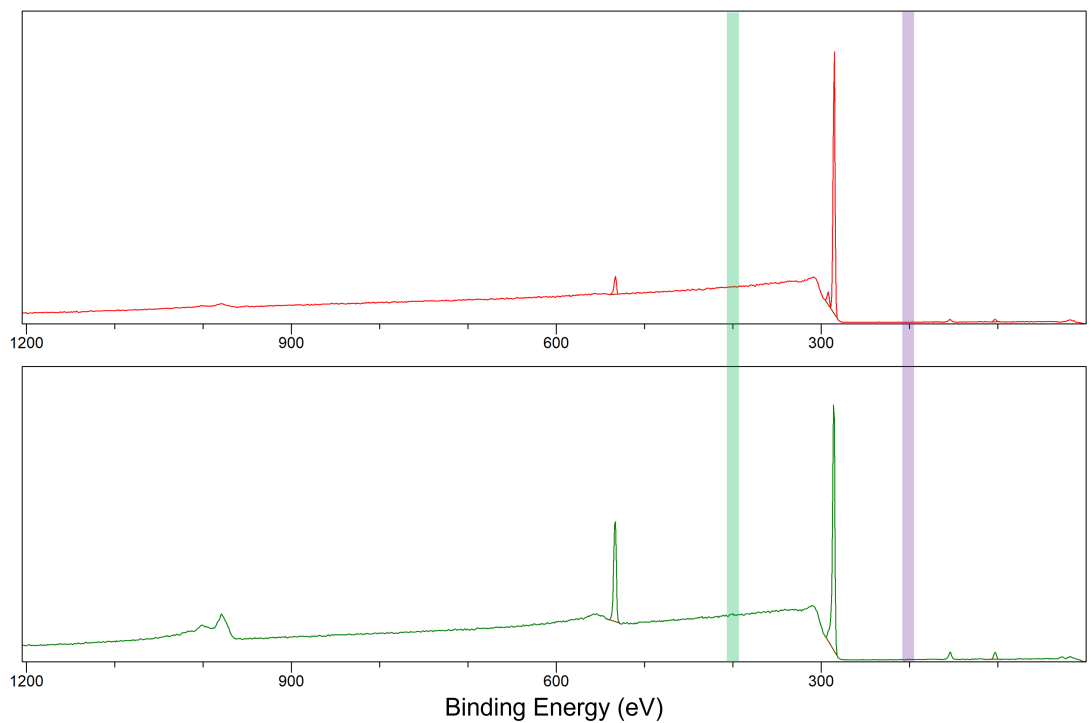


Figure 5.21: Offset overlay for pristine (top) and plasma aged (bottom) representative PS spectra treated with  $1000\text{mgNL}^{-1}$   $\text{NH}_4\text{Cl}$ , with chlorine (purple), and nitrogen (green) spectral lines highlighted.

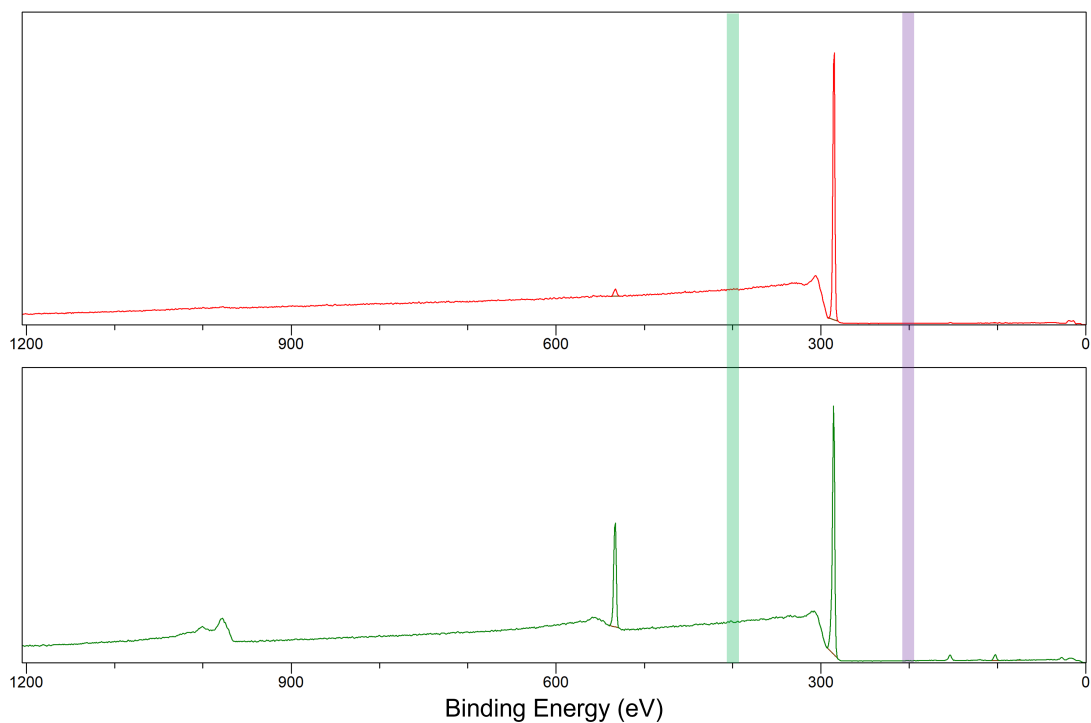


Figure 5.22: Offset overlay for pristine (top) and plasma aged (bottom) representative LDPE spectra treated with  $1000\text{mgNL}^{-1}$   $\text{NH}_4\text{Cl}$ , with chlorine (purple), and nitrogen (green) spectral lines highlighted.

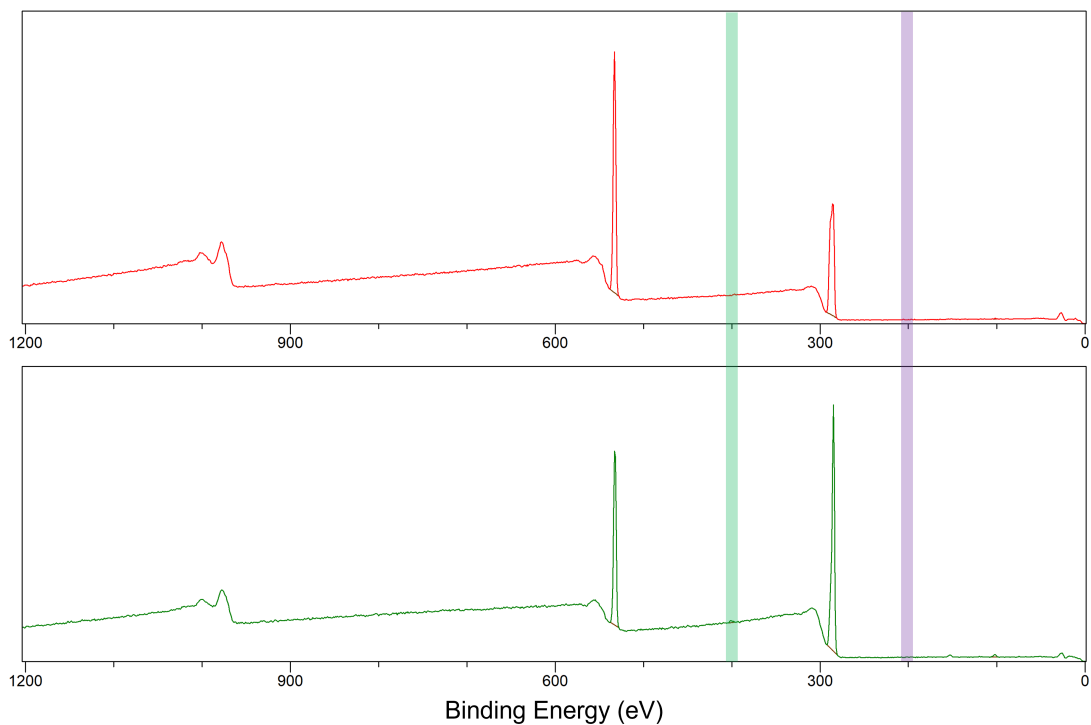


Figure 5.23: Offset overlay for pristine (top) and plasma aged (bottom) representative PLA spectra treated with  $1000\text{mgNL}^{-1}$   $\text{NH}_4\text{Cl}$ , with chlorine (purple), and nitrogen (green) spectral lines highlighted.

## 5.4 Conclusion

Overall, the results presented in this chapter indicate that the aging of polymer surfaces can lead to variation in the permanent surface sorption of environmentally-relevant chemical species, such as DOM and concentrated solutions of nutrient salts under certain conditions. Because of the high degree of surface sensitivity of XPS, any consistent layering should strongly attenuate the signature spectrum for each of the polymers in this study. However, for the durations tested, the formation of thick or consistent surface conditioning films was not observed, as indicated by the strong polymer signals that continue to be visible after immersion of the polymer treatments in all solutions tested. This is a strong evidence that aged polymer surfaces do not form thick ‘hard’ conditioning films based solely on their surface chemistry, and that aged plastics do not appear to become immediately biofouled by DOM alone. This is an important observation, as plastic pollution is often moving through, and interacting with, environmental matrices via water, and this means that it is possible that the base substrate will continue to be accessible to the environmental matrix.

Future studies should look to widen this approach further by assessing microbial adhesion to aged surfaces, deepen this approach by testing more polymers, aging protocols (including methods that combine other degradation steps such as mechanical degradation, which would result in changes to surface roughness), and a variety of other relevant nutrient mixtures. This could be further expanded by testing if truly realistic surface conditioning, with molecules and detritus larger than the  $0.2\mu\text{m}$  filtered solution used in this study, could lead to a hard conditioning film that might attenuate the extent of surface-nutrient interactions, and therefore affect the sorption of nutrients to polymer surfaces. These experiments could be further complemented in future work by using other analyses, such as Bradford Assays, to test soft coronae formation by measuring protein sorption onto pristine and aged polymer surfaces.

It is also clear that the increased presence of oxygen-containing functional groups due to simulated environmental aging can lead to increased sorption of nutrient ions to the surface. These results were shown to strongly relate to the chemical species in question, and to their concentration, with immersion in high concentration solutions of  $\text{Na}_2\text{HPO}_4$  and  $\text{NaNO}_3$  leading to significant sorption of phosphate, nitrate and their respective counter ions to aged surfaces for all three plastics tested. However, for  $\text{NH}_4\text{Cl}$  and G6P these trends were not observed. These results highlight that the aging of polymer

surfaces can lead to significant and measurable levels of permanent association of nutrient ions with plastics surfaces. Further work is needed to confidently ascertain if these results could lead to the immobilisation of nutrients species in environmental matrices as a result of increasing levels of plastic pollution.

## Chapter 6

# Investigating the impact that surface aging of microplastics has on key soil health metrics

### Graphical Abstract

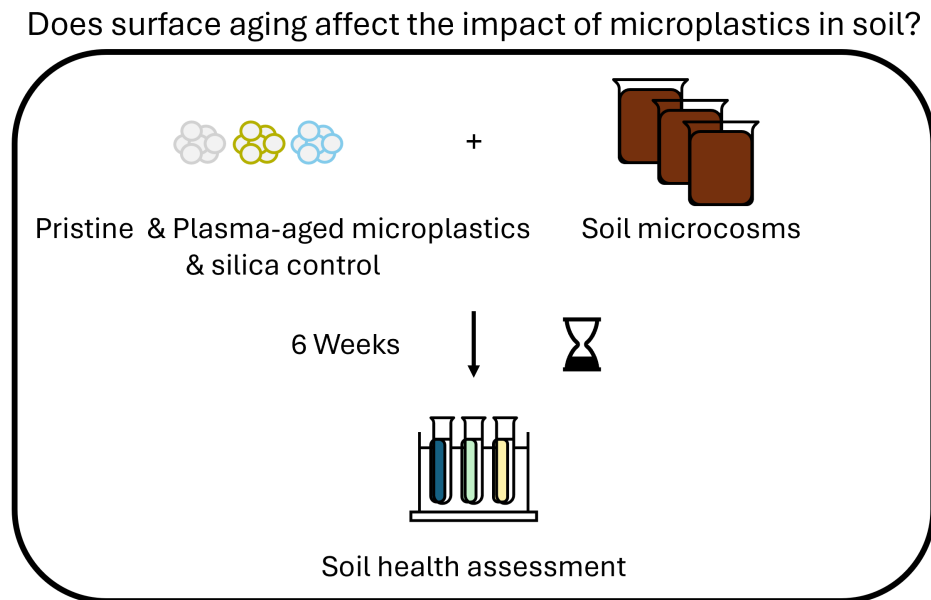


Figure 6.1: A visualisation of the research hypotheses investigated in this research chapter

## Abstract

In this paper, an assessment of the impact of microplastic aging on key soil health parameters was conducted. By using a rapid plasma-aging protocol optimised for microplastics research combined with a cryomilling protocol highly aged polystyrene, low-density polyethylene, and polylactic acid powders were generated. This study was carried out with a negative soil-only control, and a positive control formed from cryomilled silica glass beads. Soils were incubated with 0.25% w/w concentration of each amendment for a 6-week incubation. Results indicate some material-specific significant differences in some of the response variables, including significant changes in EC and pH as a result of polylactic acid amendments. such as a measured pH change associated with the advanced aged PLA treatment, in which the pH decreased from  $8.45 \pm 0.02$ , down to  $8.17 \pm 0.12$  (compared to the ‘soil only’ controls). Additionally, polylactic acid notably showed significant differences in the stability of aggregates formed, and in general all polymeric amendments significantly affect measured phosphate levels, with the advanced aged PLA leading to a measured value of  $187.1 \pm 5.6 \text{ PO}_4^{3-} \text{ mg kg}^{-1}$ , almost double the values recorded for the ‘soil only’ and silica controls of  $99.1 \pm 3.7 \text{ PO}_4^{3-} \text{ mg kg}^{-1}$  and  $101.0 \pm 2.9 \text{ PO}_4^{3-} \text{ mg kg}^{-1}$  respectively. Overall, these data indicate that microplastic pollution, even at 0.25% w/w can lead to significant, measurable changes in key soil health parameters, and these effects appear to be dominantly driven by material type.

## 6.1 Introduction

Microplastic pollution has become well documented in soil matrices across the world in recent decades [167][168][23], and understanding the impacts of microplastic pollution within soils is emerging as a key priority within microplastics research [169], as highlighted in chapter 3. Plastics are introduced into soils both deliberately, through the use of farming equipment and mulch films, but also indirectly via atmospheric deposition [170], sewage sludge [69], littering and improper handling of plastic waste [65]. Because the vast majority of plastics are designed to be resilient, are generally resistant to water and microbial degradation, and formed from very long polymer chains, these materials are expected to persist in soils [171]. Over time these materials disintegrate and fragment into microplastics [24], after which they become all but impossible to remove from soils, making their long-term resilience a real concern. Further to this, their expanded use in agricultural practices is leading to their accumulation in agricultural soils [172]. This could be highly disruptive to soil ecosystems for the reasons outlined

in chapter 3. As almost all chemicals that could fall under the umbrella of ‘polymer’ or ‘plastic’ are not found in nature, there is no good natural analogue to point towards for understanding how soils will respond to this novel pollutant. Rapidly assessing the outcomes of increasingly polluted soils is essential to understanding any potential harms.

There are many ways microplastics could present mechanisms for disruption within soils. Firstly, they have the potential to alter the physical characteristics of soils. Machado et al have already demonstrated some evidence that microplastics can affect some physical and structural properties of soils, such as the ability to influence soil bulk density, hydraulic conductivity, and water holding capacity [112]. Further still, there are other physical properties that could hypothetically be affected by the presence of plastic pollution, such as soil aggregation. The aggregate stability of a soil matrix is considered to be a key marker of soil quality [173], and the stabilisation of soil aggregates is significantly affected by the composition of a given soil [174]. As plastic particles become a persistent part of the soil fraction, they could either negatively affect soil aggregation, because of their typical hydrophobic properties (which are in turn further influenced by how aged the materials are) which could affect the ability for water to bind aggregates together with plastic particles, or they could positively affect soil aggregation, by acting as substitutes of other persistent binding agents (such as recalcitrant humic materials [174]) necessary for aggregate formation.

Beyond physical soil impacts, the presence of microplastics could theoretically lead to changes in the chemical properties of soils. Plastics are excellent substrates for sorption [159], and because of this it is reasonable to hypothesize that the introduction of these pollutants could lead to noticeable changes in soil properties such as pH and soil electrical conductivity. The electrical conductivity (EC) of a soil is a measure of how many dissolved ions are released into solution from the soil matrix, and the introduction of microplastics, which have a high capacity to adsorb chemical compounds, could result in a change in these properties. It is also possible that the addition of plastic pollution could affect pH and EC indirectly through longer-term mechanisms, such as influencing soil microbial communities which regulate soil nutrients.

The potential to alter the microbial community within a soil is itself a key way in which soils may respond differently with plastic pollution, which could have a drastic impact on the overall health of a soil as microbial communities regulate nutrient cycling (such as the carbon cycle) within these

matrices, affect soil aggregation, and soil hydraulic properties [175]. These processes are essential to enabling plants to grow (the basis of agricultural food production), and balancing atmospheric carbon and oxygen levels. Research has emerged in recent years clearly demonstrating that plastics form unique microbial assemblages in the environment compared to their surroundings [101], and a more recent study has demonstrated that environmental microcosms containing plastics can alter the biogeochemical cycles of carbon and nitrogen by stimulating the degradation of buried organic nutrients [9], therefore expecting microplastic pollution to have an impact on the microbial response of a soil is reasonable. However, studies examining the ability for microplastic pollution to affect these processes in soils are still largely missing.

One significant limitation of existing studies investigating plastics in soils is that they have largely focused on the impact of pristine (i.e. new, out of the factory) materials [112][113][136][137]. However, this understanding is important because it is well known that plastics found in the environment are often highly degraded [145]. Mechanistically, material aging could plausibly change how soils respond to plastic pollution, as typical aging of polymers leads to an increase in more active functional groups on their surfaces such as carbonyl and carboxyl groups (as observed in chapter 4), as well as shortening of the polymer chains, as low molecular weight intermediates are more susceptible to microbial assimilation [176]. In order to properly assess the impacts of plastic pollution on soil ecosystems, research is urgently required that addresses how material aging influences these impacts. However as discussed in detail in chapter 4, aging plastics is a slow process, with even the fastest commonly-used methods at present taking several days to several weeks to age samples [50]. This is a significant barrier to research seeking to address these issues, therefore the use of far more rapid methods is desired.

This research chapter focuses in on these issues by performing analyses of key soil health parameters in response to microplastic pollution. The chief aim of this study is to understand how soils respond to the addition of microplastic pollution at a realistic concentration of 0.25% w/w. Then, the impact of material aging on these response values is tested through the use of the novel microplastic aging protocol demonstrated in chapters 4 and 5. This method is far more rapid, with highly-aged surfaces being achieved within minutes, and this study is the first to apply it as an aging protocol to an incubation of microplastics in soils. By shedding light on key physical, chemical, and microbial processes it is possible to rapidly build a critical starting point of the impact that surface aging may have on the effects of microplastic pollution in soils. In this study, a soil incubation was established using

a realistic concentration of plastic found in the environment, for the three environmentally-relevant polymers chosen in this thesis, at 0.25% w/w. In the past some studies have used exceptionally high values when evaluating the impact of microplastics on soils with some studies going as high as 28% w/w [177]. Studies like this help to build a picture of the upper limit of unconstrained plastic pollution, but they do not allow for the assessment of the immediate impact of microplastic pollution on soil health at present concentrations. The rates of microplastics in typical agricultural soils right now is well documented, as outlined in section 3.2.2. This makes a rate of 0.25% w/w a meaningful ratio for use in this study, as it reflects the impact that microplastic pollution is having on soils right now.

In order to create a broad reflection on the impact of microplastic pollution on soil health a wide range of commonly-used soil parameters were chosen, spanning physical metrics (slow and fast wetting aggregate stability), soil chemistry (pH, EC, available ammonium, available nitrate, available phosphate), and parameters related to the soil microbial community (microbial activity). To ensure that any observed differences are arising from the polymers and from changes in polymer chemistry, a positive control of silica beads, milled to the same size distribution as the microplastics, was used as a positive control. Because silica is often found naturally in the environment as sand and quartz, it is an excellent positive control for the research questions in this chapter. Previously, in key research studies positive controls have not been used [112][113], however given that microplastics present a physical change to the soil composition, as well as their novel chemistry, this is a highly desired addition when addressing these research questions. The presence of chemical additives in plastics can impact soils as well, itself a critical emerging research topic [178]. As such, the highest purity options available for procurement were selected for this study, in order to minimise the impact that additives could have on the research outcomes.

## 6.2 Methodology

### 6.2.1 Soil preparation

A sandy loam topsoil was sourced from Bailey's Of Norfolk. This soil was sieved through a 4.75mm sieve to remove larger aggregates, stones, flora, fauna, and roots, ensuring consistency between replicates. In order to assess the water holding capacity (WHC) of the soil, approximately 100g of the soil was decanted into three foil trays, dried at 105°C for 24h, then weighed to assess the dry weight equivalent

of the soil. In parallel, three replicates of approximately 100g of the same soil were loaded into identical bottomless plastic containers with identical filter papers fixed to their base, saturated from the base in a tray of water, and then loaded onto a tension table set to -3cm, left overnight, and then reweighed. These measurements were used to generate estimates for the 100% and 0% WHC limits of the soil.

Additionally, in order to understand the rate of ambient soil drying in the laboratory, three replicates of 100g of the same fresh soil were taken and left to dry in ambient conditions over the duration of a week. These samples had their mass measured periodically to observe changes in mass due to evaporation. Then a 1st-order polynomial was modelled to these data in order to yield a coarse estimate of the drying characteristics of the soil, in order to inform soil maintenance procedures during the 6-week incubation.

### **6.2.2 Microplastic and positive control materials**

Four materials were processed for use as soil amendments in the research reported in this chapter: silica glass beads, Low Density Polyethylene (LDPE), Polylactic Acid (PLA), and Polystyrene (PS) nurdles. These materials were all procured from Goodfellow Cambridge Ltd. The highest purity options available for procurement were selected for this study to minimise the impact that additives could have on the outcomes. Each of the 4 amendments were then cryomilled using a Retsch Cryomill. Further details on cryomilling parameters are reported in section 2.6. The milled materials were sieved in a stack of 10cm diameter sieves of mesh size 125 $\mu\text{m}$ , 250 $\mu\text{m}$ , 500 $\mu\text{m}$ , and 1000 $\mu\text{m}$ . Particles retained in the 125-500 $\mu\text{m}$  size range were then separated and mixed together. This size range formed the basis of the amendments used in the research reported here.

### **6.2.3 Plasma aging of microplastics**

The microplastics (PLA, LDPE and PS) retained in the size range of 125-500 $\mu\text{m}$  were then separated into three groups: Pristine (P), Lightly Aged (L), and Advanced Aged (A). Groups L and A were loaded into a Diener Plasma Technology Zepto Plasma Cleaner. Samples were loaded within high-walled aluminium foil boats, to minimise disruption or spilling caused by surface charging of these light particles, then mounted via a metal loading plate. These powders were spread as thinly as possible within the boats to ensure even surface degradation. The equipment was pumped down to base pressure (nominal value of 5.00x10<sup>-3</sup> Pa) prior to loading samples, and after samples had been

loaded, to minimise contamination. Air was then passed into the chamber to reach stable pressures of  $\sim 10 - 15$  Pa. This air flow was ignited into a plasma with 100W input power for durations of 5s (L) and 60s (A). The chamber was then vented slowly to minimise potential disruption of these light samples. These powders were shaken and re-aged for the same durations respectively once more to ensure even surface aging of the powders. These powders were characterised using XPS, and these spectra can be found in section 4.3.7.

#### **6.2.4 Soil sample preparation & incubation**

New, 150mL Pyrex beakers were washed overnight in approximately 10% Decon 90 soap solution to remove any possible contaminants. Beakers were rinsed with tap water, and then rinsed a second time with Milli-Q water prior to incubation, and shaken dry. The small amount of water left in the beaker was accounted for, and formed part of the added water mass when the soils were hydrated up to 70% WHC. 6 replicates for each treatment was maintained, to enable nondestructive and destructive analyses to be completed in triplicate without affecting results. Each of the soil amendments were mixed into a subsample of the sieved soil, equal to 6 x 0.175g of each amendment and 6x70g dry weight of soil for each subsample, as this formed the basis of the 6 replicates for a given treatment, with great care taken to ensure each amendment was gently but thoroughly distributed through the soil matrix. This was achieved by shaking a small portion of the milled material onto the soil surface, folding over freshly sieved soil, mixing the soil, and repeating until a fully incorporated and visually mixed distribution was achieved. Each soil amendment was incorporated at a concentration of 0.25% w/w to the dry-weight equivalent of the soil. Subsequently, 70g dry weight-equivalent of each treatment was then gently decanted into the pyrex beakers using a spatula, with care taken to avoid damaging aggregates. To prevent cross-contamination, each soil treatment was prepared independently, within separate mixing trays, and tools used were washed in a 10% Decon 90 soap solution, rinsed, dried, and further rinsed down with Milli-Q water between treatments. The mixed soil contained within each of the individual 250mL beakers was then raised to 70% WHC of the soil, as measured by the weight of the microcosm, using a squeeze dispensing bottle filled with Milli-Q water, and covered with identical breathable dust-free optical lens cloths, and kept in a dry, temperate soil laboratory. Soil moisture contents were monitored three times a week for the duration of the 6-week incubation, with care taken to keep them at approximately 70% WHC. In the 4th week, the soils were exposed to a 'dry down' period to simulate natural variation in soil moisture conditions. The soils were first raised to

100% WHC, and then left to dry out for two weeks under ambient conditions, where the soil moisture contents dropped to approximately 20% WHC. Once this condition was met, the soils were raised back to 70% WHC and maintained there for the remainder of time (approximately 1 week). During the incubation, a Mini-Diver data logger was programmed in order to track the ambient temperature and pressure within the laboratory.

### **Post-incubation analysis**

In the post-incubation phase, eight analyses were conducted to assess the impact of the soil amendments on key soil parameters. Each analysis was completed in a timely manner, with all analyses completed as quickly as possible, with more time-sensitive analyses prioritised for completion first.

#### **6.2.5 EC and pH measurements**

EC and pH measurements were conducted using a Mettler Toledo FiveEasy EC probe set, and a Mettler Toledo SevenCompact pH probe set. 10g (fresh weight) of each treatment was added to a labelled 50mL centrifuge tube, mixed with 25mL of deionized water, shaken on an orbital shaker for 30 minutes, then left to settle for 30 minutes. The pH and EC of the solution were then measured by dipping the probes into the tubes, gently stirring, and measuring just above the settled soil-water interface.

#### **6.2.6 Aggregate stability**

A standardised aggregate stability analysis was performed using ‘fast wetting’ and ‘slow wetting’ protocols adapted from Le Bissonais’ methodology [179]. Soil was prepared by air drying for 1 week, loosely covered over in a temperate laboratory with a breathable cloth. This soil was then sieved in the region of 2mm to 4.75mm, and the size fraction in this range was retained. The retained aggregates were transferred to a foil dish and placed in an oven at 40°C until they reached constant matric potential (>24h).

##### **Fast wetting preparation**

To test fast wetting 5.0±0.1g of aggregates were placed in 50mL centrifuge tubes and 50mL of deionised water was gently decanted into the tubes, added slowly to a tilted tube in order to avoid damaging the aggregates, and left to rest for 10 minutes. After this time the excess water was removed using

a pipette, and the wetted aggregates were then transferred to a 50 $\mu\text{m}$  sieve immersed in ethanol in a fume hood, and the post-wetting protocol outlined below was followed.

#### **Slow wetting preparation**

A tension table was set to -3cm. 5.0 $\pm$ 0.1g mass of aggregates were gently placed onto Whatman 42 ashless filter papers, and left to soak on the tension table for 30 minutes. These slow wetted aggregates were then transferred to a 50 $\mu\text{m}$  sieve immersed in ethanol in a fume hood, and the post-wetting protocol outlined below was followed.

#### **Post-wetting processing**

Each respective soil treatment was placed onto the 50 micron immersed sieve, and then gently shaken whilst remaining submerged in order to separate the aggregates in the <50 $\mu\text{m}$  range. The sieve was then lifted, and the retained aggregates (greater than 50 microns in size) were carefully decanted into an aluminium foil dish, and left to dry open in a fume hood overnight. These dried aggregates were then transferred to an oven set to 105°C, and left to dry for 24h. These oven dried aggregates were transferred to a stack of 20cm diameter sieves in the following descending mesh range: 2000 $\mu\text{m}$ , 1000 $\mu\text{m}$ , 500 $\mu\text{m}$ , 200 $\mu\text{m}$ , 100 $\mu\text{m}$ , 50 $\mu\text{m}$ , and gently sieved by hand. The mass of soil retained on each sieve mesh was then separately transferred to an A3 piece of paper to avoid loss of light aggregates, gently decanted into a weighing dish, and weighed. Once all of the weigh fractions were summed, it was assumed that any mass loss from the original 5g aggregate mass was attributed as the <50 $\mu\text{m}$  fraction. These masses were then used to calculate the aggregate mass distribution and the Mean Weight Diameter (MWD) of these treatments.

### **6.2.7 Microbial activity assessment**

A coarse test for overall microbial activity was adapted from [180], using Fluorescein Diacetate (FDA) hydrolysis as an proxy for microbial activity. FDA is a non-fluorescent molecule that can be hydrolysed by living cells, generating fluorescein as a byproduct. Fluorescein is a fluorescent dye that strongly fluoresces at 490nm. The more microbial activity in a soil, the more FDA is hydrolysed, and the more fluorescein will be available to absorb 490nm photons when analysed on a spectrophotometer. This method is visualised in figure 6.2.

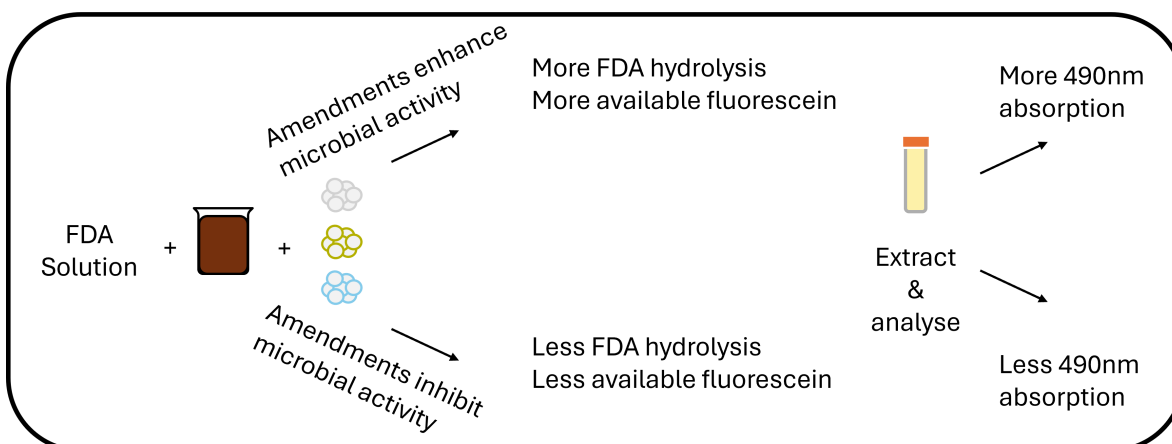


Figure 6.2: A flow diagram visualising and explaining how microbial activity in a soil can be assessed by this method

This method involved preparing centrifuge tubes with  $0.60 \pm 0.01\text{g}$  air dried soil. A pH buffer solution was prepared from sodium phosphate dodecahydrate tribasic and hydrochloric acid until a pH of  $7.60 \pm 0.01$  was reached, measured using a pH probe. 30mL of the buffer solution was decanted into each of the centrifuge tubes. An FDA substrate solution was prepared by mixing 15mg of FDA into 30mL of acetone. 0.3mL of this substrate solution was then added to each of the centrifuge tubes. Each tube was then shaken by hand in order to ensure the FDA was well mixed with the soil. The centrifuge tubes were then placed inside a water bath at  $37^{\circ}\text{C}$  for 3 hours. After this incubation, 1.2mL of acetone was added to each tube to terminate hydrolysis, then each tube was centrifuged at room temperature at 4000rpm for 10 minutes using a Sorvall ST 40R Centrifuge, and solutions were then filtered through Whatman Grade 42 filter papers. The resultant filtrate was stored in a fridge at  $3^{\circ}\text{C}$  ready for analysis. The analysis was conducted by loading each filtered sample into a new disposable cuvette, and measuring the absorbance of the solution at a wavelength of 490nm. The spectrophotometer (Jenway 6300 Visible Spectrophotometer) was calibrated using a blank solution of 30mL of the same pH buffer solution mixed with 1.5mL acetone (i.e. the same solution medium minus the active components), which set the zero point reference for absorbance before any measurements were made. Additionally, 3 blanks (same method and treatment but minus the soil) were ran in parallel to control for any background microbial activity arising from contamination through the process. The mean of this absorbance was then subtracted from the final results, in order to show the ‘true’ absorbance arising from microbial activity from each studied treatment.

### 6.2.8 Available nitrogen analysis

Soil available inorganic nitrogen ( $\text{NH}_4^+$ ,  $\text{NO}_3^-$ ) was tested using standard protocols. This was conducted by mixing 5g (fresh weight) of each soil treatment with 25mL 2M KCl, shaking on an orbital shaker for 1h, leaving to settle for 30 minutes, and then filtering through a Whatman Grade 42 filter paper. Samples were then deep frozen at  $-20^\circ\text{C}$ , and subsequently analysed on a SEAL Analytical AA3 Auto Analyser. A stock standard solution was used to calibrate the measurements; this was made up of 0.472g ammonium sulphate, and 0.722g potassium nitrate made up to 100mL using Milli-Q water. This was then diluted down in volumetric glassware to standards of 1, 2, 3, 4, 5 ppm of  $\text{NH}_4^+$ ,  $\text{NO}_3^-$  respectively. Blank (i.e. reagent only) and drift (periodic measurements during operation) measurements were also evaluated to ensure no contamination had occurred.

### 6.2.9 Available phosphorus analysis

In order to test inorganic phosphorus availability a similar process was undertaken using 2g (fresh weight) of each soil treatment added to 40mL  $\text{NaCHO}_3$ . Then mixture was then shaken on an orbital shaker for 30 minutes, left to settle for 30 minutes, and filtered through a Whatman Grade 42 filter paper. Samples were then deep frozen at  $-20^\circ\text{C}$ , and analysed on a SEAL Analytical AA3 Auto Analyser. A stock standard solution was used to calibrate the measurements; this was made up of 0.4394g potassium dihydrogen phosphate made up to 100mL using Milli-Q water. This was then diluted down in volumetric glassware to standards of 1, 2, 3, 4, 5 ppm of  $\text{PO}_4^{3-}$ . Blank (i.e. reagent only) and drift (periodic measurements during operation) measurements were also evaluated to ensure no contamination had occurred.

### 6.2.10 Statistical analysis

All t-tests conducted in this chapter were completed as two-tail tests at a p value of  $\leq 0.05$ . These tests were performed using Python 3.9 via modules in the Anaconda distribution package (Pandas, SciPy). In this chapter, where results differ significantly from the negative soil control ('CTR-N') to a p value of  $\leq 0.05$  the data is annotated with an asterisk (\*), and when results differ significantly from the positive soil control ('CTR-P') to a p value of  $\leq 0.05$  the data is annotated with a dagger (†).

## 6.3 Results & Discussion

### 6.3.1 Soil drying characteristics

#### Test soil at 0% WHC and 100% WHC

Results in Table 6.1 report outcomes of the 0% WHC measurements, and results in table 6.2 report outcomes of the 100% WHC measurements. Masses shown are of soil only (i.e. with container weight subtracted). Data from tables 6.1 and 6.2 were used to calculate conversion factors for the fresh soil, in order to estimate the general function of WHC for the soil. From these data the fresh soil was estimated to be at approximately 58.8% WHC before any manipulation of WHC. When normalised to 1.00g, it was estimated that 0.15g of water is needed to wet the dry soil to match the measured fresh WHC of 58.8%, and 0.26g of water is needed to wet it up to 100% WHC. This meant that, for 70g of dry soil mass, the ‘soil only’ weighed 88.2g at 100% WHC, and the soils with 0.25% w/w amendments weighed 88.155g at 100% WHC, as the amendments were assumed to not be able to hold additional water.

Table 6.1: Mass of tested soil at 0% WHC, used to model drying behaviour.

Replicate	Fresh Soil Mass (g)	Fresh Soil Mass at 0% WHC (g)
A	100.0	86.5
B	100.1	86.7
C	100.0	86.7

Table 6.2: Mass of tested soil at 100% WHC, used to model drying behaviour.

Replicate	Fresh Soil Mass (g)	Fresh Soil Mass at 100% WHC (g)
A	99.3	108.3
B	100.4	109.9
C	100.9	110.6

$$M_t = M_0(1 + 0.26W) \quad (6.1)$$

From these data, a general expression (equation 6.1) relating the measured mass WHC of this soil was derived, which was then used monitor the soil mass during the 6-week incubation. In this equation  $M_t$  is the target soil mass,  $M_0$  is the equivalent dry soil mass, and  $W$  is the target water holding capacity (as a fraction of 1). Therefore, at the target WHC of 70% ( $W=0.7$ ) for the soil the desired target soil

mass was 82.708g and 82.740g for the soils with and without amendments respectively.

### Modelling soil drying behaviour

The soil drying data was fitted with a first-order polynomial to estimate the rate of change of WHC from ‘fresh’ to 0% WHC. This yielded the function:

$$M(t) = 99.7 - 0.07t \tag{6.2}$$

Where  $M(t)$  is the function of mass loss in grams for the fresh soil per hour. This indicated that for approximately 100g of fresh soil, the soil lost 0.07g of moisture per hour. This meant that it would take approximately 177 hours (7 days) for the fresh soil (at 58% WHC) to reach dry weight, and 315 hours (13 days) to naturally dry 100g of fresh soil that has been raised to 100% WHC, down to dry weight (figure 6.3). Therefore, monitoring the moisture content 3 times a week for the soils incubation was assessed as appropriate for maintaining constant soil moisture, and a dry down period of two weeks was sensible for simulating natural moisture variation of the soil. All of the data points are plotted in figure 6.3, however because the replicates are very similar to each other, the markers overlap significantly, leading to some of them being less visible. Because the replicates started at 58% WHC, the fit also extrapolates ‘backwards’ in time, modelling the behaviour to the upper limit of 100% WHC.

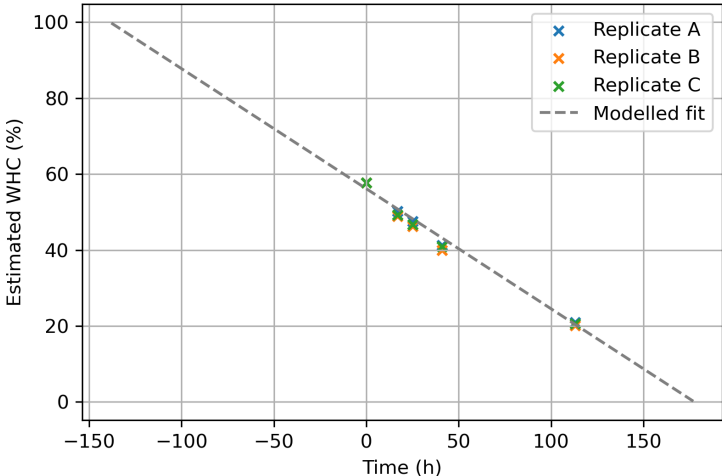


Figure 6.3: Modelled fit of natural drying from 100% WHC to 0% WHC (grey dashed line), with raw data for each replicate plotted on top (green, blue, and yellow dot markers respectively at their equivalent WHCs)

### 6.3.2 EC & pH

Firstly, no significant differences were observed in EC and pH between positive and negative control samples, indicating that the observed significant differences are directly attributable to the microplastics. On the surface, the pH and EC measurements shown below in table 6.3 would indicate a small, but significant deviation between the negative soil-only control and some of the treatments. Small but significant differences (tested to a p value  $\leq 0.05$ ) were found between the negative control, LDPE-P and LDPE-L, but not LDPE-A, for pH measurements only. Significant differences were also found between both of the aged PLA treatments and the negative control, as well as both of the PLA aged treatments and the positive control. For PLA-A this equates to a change of 0.28 on the mean. Because pH is a logarithmic scale, this means that there is almost twice ( $10^{0.28}=1.9$ ) as many H<sup>+</sup> ions in solution compared to the control, a notable difference. No significant differences for either EC or pH were observed when CTR-N and CTR-P replicates were compared to all three of the PS amendments.

Table 6.3: EC and pH measurements of each soil treatment averaged across all replicates (n=3), expressed as  $\pm 1$  standard deviation of this distribution and tested to a p value of  $\leq 0.05$ ; significant differences to negative control are denoted with an asterisk (\*), and significant differences to the positive control are denoted with a dagger (†).

Treatment	pH (Dimensionless)	EC ( $\mu\text{Sm}^{-1}$ )
CTR-N	8.45 $\pm$ 0.02	126 $\pm$ 16
CTR-P	8.42 $\pm$ 0.02	135 $\pm$ 14
PS-P	8.40 $\pm$ 0.03	134 $\pm$ 5
PS-L	8.43 $\pm$ 0.03	140 $\pm$ 29
PS-A	8.43 $\pm$ 0.02	149 $\pm$ 24
LDPE-P	8.38 $\pm$ 0.03 *	155 $\pm$ 4
LDPE-L	8.40 $\pm$ 0.01 *	157 $\pm$ 10
LDPE-A	8.41 $\pm$ 0.05	137 $\pm$ 11
PLA-P	8.35 $\pm$ 0.06	194 $\pm$ 16 †
PLA-L	8.30 $\pm$ 0.02 *†	204 $\pm$ 41 *†
PLA-A	8.17 $\pm$ 0.12 *†	172 $\pm$ 14 *†

For the PLA amendments, it is possible that these changes arise from the partial hydrolysis of the polymer chain. The constituent monomer of PLA is lactic acid. When polymerised, there are no available hydrogen ions or lactate that can freely disperse in solution. However, even partial hydrolysis of the polymer chain could reasonably lead to an increase of these ions in solution, which explains the decrease in pH, and contributes to why the EC increased as well. Additionally, as the pH decreased it is possible that the EC was further altered by a change in the mobility of other ions that could be pH dependent. Given that the application rate was low, and the differences observed are modest, this

explanation seems plausible, as the pH is becoming more acidic as this would predict, and the EC is increasing, as this would also predict.

Unlike PLA, both PS and LDPE do not polymerise from acids. Therefore it is not surprising that the response here was more in line with the observed changes in controls. As the significant changes are observed in the pristine and lightly aged treatments (as opposed to the 'advanced' treatment), it is also unlikely that the observed differences arise from the introduction of carboxylic acid groups formed through oxidation of the polymer chains during aging. It is instead possible that these observations could be a result of subtle changes in microbial activity caused by the addition of LDPE, that is not maintained when this material ages further, such as the fact that plastic pollutants are known to harbour unique microbial assemblages within the environment [101].

### 6.3.3 Soil microbial activity

Each of the soil amendments used for this microbial assay treatment showed no significant differences in FDA hydrolysis, as indicated by no variance in results significant to a p value of  $\leq 0.05$  in the absorbance of their respective solutions at 490nm. This indicates that at 0.25% w/w, none of these treatments were able to significantly alter the overall extent of microbial activity within the soil matrix, as determined via the FDA assay. This also means that the observed pH and EC responses seen in section 6.3.2 are not easily explained by an overall change in microbial activity as determined via the FDA hydrolysis assay.

Table 6.4: Mean absorbance of microbial assay tests for n=3 replicates  $\pm$  standard deviation. Data calibrated with blank values and zeroed to a reagent-only control. Each treatment was tested to a p value of  $\leq 0.05$  with no significant differences found.

Treatment	Adjusted Absorbance (%)
CTR-N	22.1 $\pm$ 3.1
CTR-P	18.2 $\pm$ 6.8
PS-P	20.5 $\pm$ 7.8
PS-L	22.4 $\pm$ 4.4
PS-A	17.5 $\pm$ 1.9
LDPE-P	16.7 $\pm$ 10.3
LDPE-L	12.9 $\pm$ 7.2
LDPE-A	22.6 $\pm$ 2.0
PLA-P	21.5 $\pm$ 1.7
PLA-L	23.8 $\pm$ 0.9
PLA-A	22.9 $\pm$ 2.9

### 6.3.4 Available phosphorus

Figure 6.4 shows how soil available phosphate concentration changes with each of the soil treatments. All of the results were tight, with overall uncertainty in the 3 replicates sampled being a small % of the mean value, therefore these data were analysed with high precision. In general, the addition of any amendment led to a significant increase in phosphate concentrations when compared to both negative and positive controls, with only the Pristine PS showing no significant differences. From these data PLA showed the most significant change compared to the control replicates. In general greater aging of these samples led to a more significant increase compared to the pristine replicates as well.

As the polymers don't contain phosphorus, this increase can't be explained as a direct result of polymer degradation and mineralisation. It is also unlikely to result from the changes in pH or EC affecting nutrient solubility, as significant differences were observed in available phosphorus for all three PS treatments, but not for the pH or EC for the PS treatments. These data could alternatively be explained potentially by a shift in microbial community towards species which are more able to free up phosphate ions in soils. However, further work would be needed to confirm this and to confidently root-cause this result.

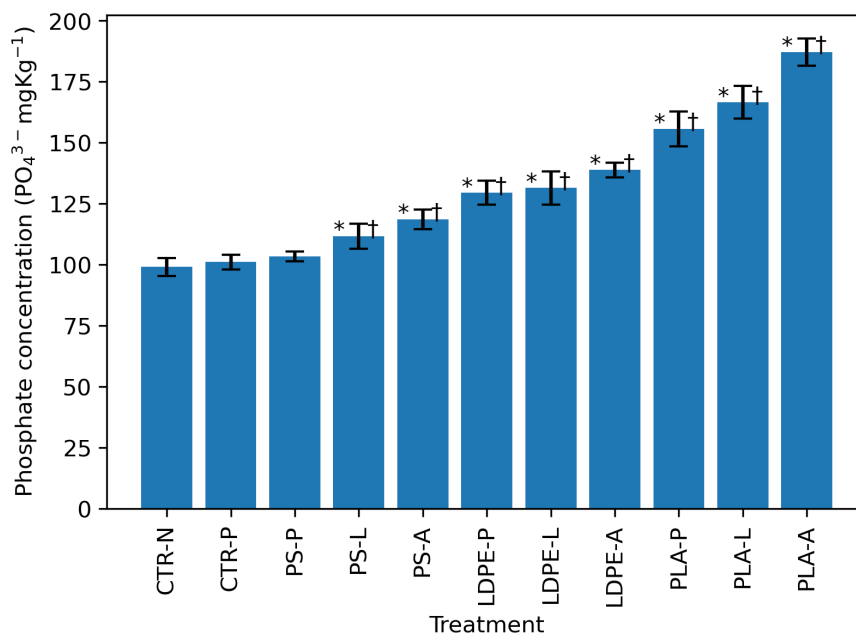


Figure 6.4: Available phosphorus measurements for n=3 replicates. Error bars represent 1 standard deviation from the mean. Significant differences to negative control are denoted with an asterisk (\*, p value  $\leq 0.05$ ), and significant differences to the positive control are denoted with a dagger (†, p value  $\leq 0.05$ ).

### 6.3.5 Available nitrogen

In figure 6.5 a similar trend to the phosphate measurements was observed, with significant differences being found in all of the LDPE samples, and 2/3 of the PLA samples when compared to both positive and negative soil controls and tested to a p value of  $\leq 0.05$ . The advanced aged PLA mean value is also relatively high. However, there was a much larger deviation in the measured values, so this result was not found to be conclusively significant. All three PS treatments showed a significant difference to the positive control, but not to the soil-only control. Additionally, the positive and negative controls are significantly different to each other for this treatment.

Overall these data indicate a material-specific rather than aging-specific variation, as the results show similar statistically significant differences between a given polymer and each of the controls, with very little variation between the aging treatments. Because none of the three polymers contain nitrogen, these differences can't be explained by degradation or mineralisation of the polymers themselves. In general, this provides evidence supporting the same hypothesis, that the addition of certain polymer amendments could be causing a shift in microbial communities, resulting in a difference in nutrient cycling. Further work beyond the scope of this research chapter is needed in order to explore this hypothesis.

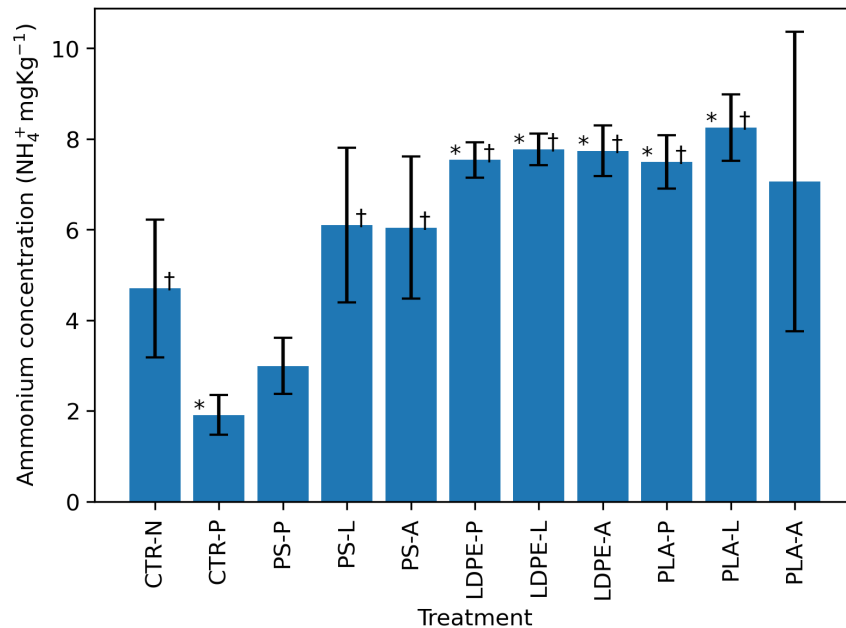


Figure 6.5: Available Ammonium measurements for n=3 replicates. Error bars represent 1 standard deviation from the mean. Significant differences to negative control are denoted with an asterisk (\*, p value  $\leq 0.05$ ), and significant differences to the positive control are denoted with a dagger (†, p value  $\leq 0.05$ ).

Unlike the observed phosphate and ammonium responses, there were no significant differences observed in soil available nitrates due to any of the soil amendments tested in this study.

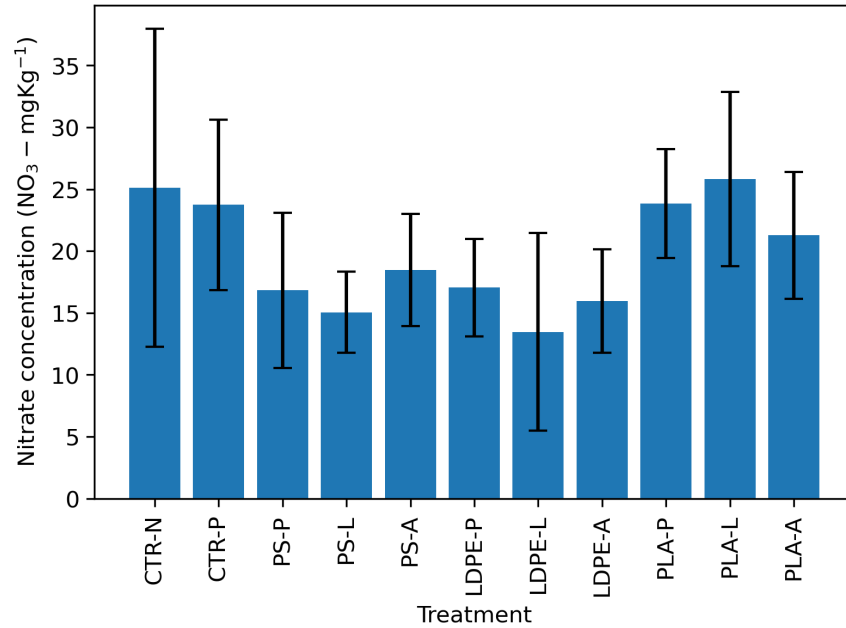


Figure 6.6: Available nitrate measurements for n=3 replicates. Error bars represent 1 standard deviation from the mean. Significant differences to negative control are denoted with an asterisk (\*, p value  $\leq 0.05$ ), and significant differences to the positive control are denoted with a dagger (†, p value  $\leq 0.05$ ).

Across the available nitrogen (as well as the available phosphorus) data, phosphate, nitrate and ammonium levels do not significantly drop with the addition of polymer amendments. This is evidence addressing one of the chief concerns of chapter 5, the possibility of microplastic pollution leading to nutrient immobilisation. One possible explanation for this is that once intimately mixed into a highly heterogeneous matrix such as a soil the surface become highly conditioned by a variety of other macromolecules, meaning that there is very little active surface available for any sorption processes to take effect. It is possible therefore that in sparser environmental matrices such as freshwaters, where microplastic surfaces are continuously washed, those effects may show a greater degree of influence, as was true for the aqueous treatments in chapter 5. Further research is needed to ascertain if this is a concern for aquatic environments.

### 6.3.6 Fast wetting of soil aggregates

It was immediately clear after 10 minutes of immersion that extreme slaking occurred during fast wetting, and that no stable aggregates remained. The result was a complete disaggregation of the soil into its composite particles. The larger particles visible in image 6.7 (highlighted by the red arrows) are stone particles that could not disaggregate further. This outcome was assessed to be a result of the soil type and independent of soil amendment.



Figure 6.7: A photo of a typical treatment after fast wetting

### 6.3.7 Slow wetting of soil aggregates

The data highlighted in figure 6.8 show that specific polymer treatments can have significant effects on the distribution of aggregates within a soil sample. In particular, treatments that included PLA saw a large increase in the % of aggregates appearing in the 1000-2000 $\mu\text{m}$  range compared to CTR-N and CTR-P across all three of the treatments (Pristine, Light and Advanced), indicating that the presence of PLA in soils may be able to influence soil aggregation when finely distributed. One possible explanation of this could be that this is resulting from the size of the microplastic particles themselves, as the data showcased in 2.1 indicates that the PLA particles used would be on the larger end of the distribution, despite being constrained to the narrow range used. However, this hypothesis doesn't hold up to scrutiny, as this would be equally true for LDPE which also had a significant subset of particles in the upper range, and LDPE does not show the same increase in aggregation in the 1000-2000 $\mu\text{m}$  range. Therefore this is a direct result of the amendment. This could plausibly be explained by preferential colonisation of PLA by microbial life, as PLA is a more accessible polymer for microorganisms due to its condensation bond, and microorganisms are known to affect aggregate formation [175]. However, further research is needed to assess microbial adhesion to specific polymer surfaces and if this could be the root cause for the variation in aggregation.

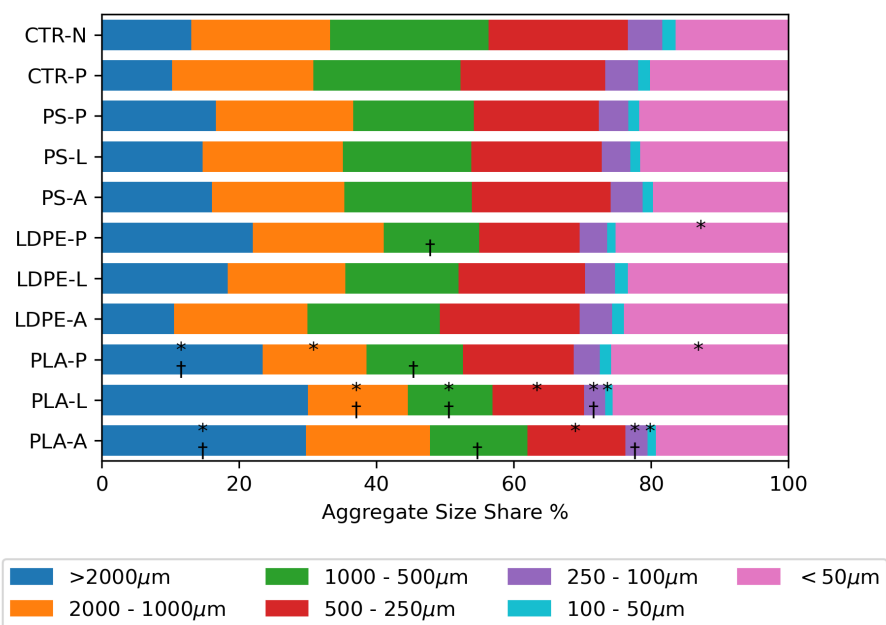


Figure 6.8: Comparison of the aggregate size distributions of different soil treatments after slow wetting; significant differences to negative control are denoted with an asterisk (\*,  $p$  value  $\leq 0.05$ ), and significant differences to the positive control are denoted with a dagger (†,  $p$  value  $\leq 0.05$ ).

Overall, figure 6.9 shows the top-level comparison of aggregate stability resulting from slow wetting with the soil amendments used. Across the three polymer amendments in general, material aging did not lead to any significant difference in MWD values of the soils. Some material-specific significant differences were observed, namely that the pristine PLA led to increased overall aggregate stability. This could be explained similarly as before as a result of differences in microbial adhesion and colonisation affecting aggregation, but further work is needed to assess this hypothesis.

It is unusual at first glance to see that the LDPE-P has a number of significant differences in specific aggregate ranges (figure 6.8), however does not yield a significant difference in MWD. This is an artefact of the aggregation. Because MWD is an aggregated metric, significant differences that oppose each other can cancel out, and insignificant differences that align can add up, shifting the mean in a general direction away from the control. In the LDPE-P individual size fractions data, there is a large value difference between the  $>2000\mu\text{m}$  size range and the  $<50\mu\text{m}$  size range respectively, which are effectively cancelled out when aggregated into MWD. Whereas, for LDPE-A the smaller size fractions are larger, not significantly so individually, but significantly upon aggregation when compared to the positive control. This is one of the challenges of directly comparing aggregated metrics with raw data.

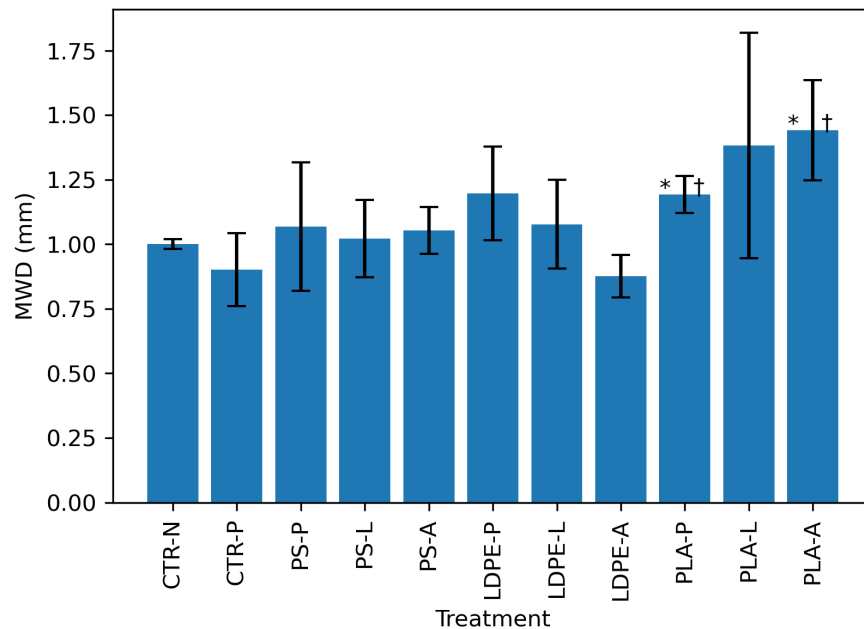


Figure 6.9: MWD values for each slow wetting treatment. Error bars represent 1 standard deviation from the mean. Significant differences to negative control are denoted with an asterisk (\*,  $p$  value  $\leq 0.05$ ), and significant differences to the positive control are denoted with a dagger (†,  $p$  value  $\leq 0.05$ ).

## 6.4 Conclusion

Overall, the results obtained from the experiments analysed in this chapter of results would indicate that at nominally relevant w/w concentrations, across most of the metrics tested, the overall impact of microplastic pollution in soils is primarily driven by the material type, not by aging of the surface. The addition of PLA led to significant changes in pH and EC across all three aging treatments, and the addition of LDPE led to significant differences in pH for pristine and lightly aged treatments.

These data also indicate that the addition of microplastics, when compared to both positive and negative controls, does not significantly alter the magnitude of microbial response as noted in the lack of changes in FDA hydrolysis, but may affect the microbial communities present, as indicated by significant shifts in soil available phosphorus for all polymer treatments other than pristine PS, and significant changes in available ammonium for several treatments. Further research is needed to precisely root cause these variations. Additionally, no evidence was found in this study that would suggest that either microplastic pollution or aging of microplastics leads to nutrient immobilisation in soils, as none of the soil nutrient response variables saw significant negative changes with any of the polymer amendments. Future work should look at the microbial communities present on aged microplastics in soils in order to evaluate this hypothesis.

Significant differences were also observed in soil aggregation as a result of these amendments. Whilst fast wetting led to a complete breakdown of the soil matrix independent of amendment, the aggregate stability in response to slow wetting was affected by the treatments. In particular, all PLA treatments led to notable differences in the size distribution of the aggregates, and pristine and advanced aged PLA treatments led to changes in MWD. It is possible that this results from a preferential colonisation of the PLA substrate, however further work is needed to assess microbial adhesion to different aged polymer surfaces in order to evaluate this.

In closing, several significant results were reported arising from the addition of microplastic treatments to soil matrices. Overall, the size of these effects was relatively small. For soil health this may be perceived as a 'positive' set of results in terms of the risks posed by microplastics, as these concentrations are representative of what is seen typically right now. However, due to the projected increase in the overall production and consumption of plastics, as well as existing in-use stock of plastics transitioning from use to their end-of-life (and possibly ending up as waste entering the environment),

these concentrations will not remain true forever. This overall trajectory indicates that future soils will become more and more polluted with microplastics. Therefore, it is critical that future studies also investigate higher concentrations of both pristine and aged materials that may become present within soil matrices in decades to come to be able to confidently assess if a threshold exists where notably harmful differences begin to appear.

## Chapter 7

# Discussion, conclusion, & further work

Microplastics research is an emerging field of critical importance. Plastic pollution stands as one of the ecological and environmental challenges of our age, and there is now a race against time to understand and address this complex, multifaceted, highly-interdisciplinary problem more deeply, more completely, and with considerable haste. The research outlined in this thesis adds a novel dimension to our understanding of the challenge.

It is clear from the background established in chapter 1 that this issue is complex, and closely intertwined with other major environmental challenges of the Anthropocene, such as the climate crisis. It is highly likely that in the decades to come, should no intervention be taken and we stay the course we're on, that it has the potential to get catastrophically worse in ways that are poorly understood. This is because the legacy of existing plastic pollution is likely to last for some time [138], because the scale of plastic consumption is on track to increase considerably [2][3], and because the well-documented fragmentation of plastics into microplastics [24] makes them all but impossible to remove once dispersed into the natural environment.

Plastic has been demonstrated to pollute the natural environment widely, as evidenced in chapter 3. It has been observed in the oceans [22], in soils of all types and contexts [77][78][79], and in the very air we breathe [181]. Unfortunately, the complexity and depth of this issue will only increase as these

materials break down and degrade in the environment. Their long-term degradation leads to significant physical and chemical changes, making them more chemically active, which emerging evidence and argument suggests affects their behaviour in the environment [164]. But because this process typically occurs incredibly slowly, it is often unrealistic to wait for these materials to age naturally in order to assess their impact. Because of this, accelerated aging techniques are often employed [50], however these techniques can still take considerable time to use. Identifying new approaches and optimising existing methods for this application is an active research topic [50][139].

One possible emerging method is the application of plasma degradation to accelerate microplastic aging [50][144]. To date, only one study has attempted to use this method [144], and it remains largely unproven. In chapter 4 this technique was analysed in detail as a rapid alternative method for the simulation of environmental aging, and tested alongside a far more standard research method in accelerated photodegradation via high-power lamps. This technique was assessed to be broadly fit for purpose as a rapid-aging protocol simulating narrow features of environmental photodegradation. It achieves results at a *significantly* increased rate when compared to other methods, with highly oxidised surfaces reminiscent of photodegradation observed within a minute of treatment. Some specific caveats were made for environmental studies, such as ensuring the correct methodological order when using this technique, and establishing a clear sense of when it is appropriate as a research tool, and when other methods are better suited.

Within this research chapter it was clearly demonstrated that plasma aging has potential as a tool in future microplastics research. Because samples can be significantly aged within minutes, this allows for a vastly improved throughput of sample analysis when compared to the days to weeks seen in other methods [50]. This opens up the potential for a wide array of further work looking to establish a swift assessment of the effects of polymer aging on a variety of test hypotheses within environmental research. Beyond this, plasma treatments come in a wide array of different approaches, and there is significant scope to further develop and optimise these methods for microplastics research through the testing of different reactor builds, inlet gases, and in particular the testing of a wider range of polymers.

This novel rapid aging method was then tested alongside conventional photoaging in the surface-focused sorption study outlined in chapter 5. The hypotheses evaluated in this research stream built

on significant existing research that has explored plastic pollution as a sorption substrate for a wide variety of chemicals, such as POPs, heavy metals, and antibiotics [26][27][28][8], however within the existing research a gap has emerged; these studies generally focused on the ability for microplastics to facilitate bioaccumulation of hazardous chemicals, but this is not the only potential hazard of the high sorption capacity of microplastics. They could also plausibly become sorption sites for nutrients and other chemicals essential to soil health and plant growth, leading to a change in nutrient mobility. By investigating whether commonly polluting plastics, and simulated environmental aging of their surfaces, leads to any noticeable changes in their sorption of DOM, or common nutrient species, this gap was addressed. The initial results outlined here indicated that treatment with DOM for after a lengthy 6-week photoaging protocol led to minimal sorption effects overall, and very little change between pristine and aged surfaces. These results highlight the resilience of plastics in a simulated environmental matrix; they do not form conditioning films from small biological molecules such as DOM easily, with or without photoaging.

A narrower study with plasma aging was then conducted, which observed that, at high concentrations, the aging of polymer surfaces led to sizeable and significant adsorption of phosphate, nitrate, and their respective counter-ions, but pristine surfaces remained largely unchanged. For ammonium however this trend was not continued. At lower, more realistic concentrations these observations largely disappeared, with both control and aged surfaces looking almost pristine, indicating that this effect is observable, but conditional. This immediately highlights that, under certain conditions, the aging of polymer surfaces absolutely has the ability to affect nutrient mobility in a way that pristine polymer surfaces do not. This adds considerable weight to the argument that the surface aging of polymers in the environment is relevant, and that it could affect the way they interact with not only hazardous chemicals, but also key nutrients critical to soil health in the environment.

Further research is needed to expand the depth of the results in this chapter, and to confidently assess if nutrient immobilisation is a real concern when plastic pollution enters into terrestrial or aquatic matrices. Future approaches should look to test changes in a more realistic environmental matrix, and investigate the sorption dynamics of other key biological nutrients, such as larger macromolecules, onto aged polymer surfaces.

Finally, in chapter 6, this research study was extended further into a more realistic and practical setting, in order to identify if surface aging of microplastic particles at realistic concentrations could alter common indicators for soil health, such as pH and aggregate stability. Cryomilling was used to simulate the mechanical degradation of plastics into secondary microplastics, and plasma aging was used to simulate the photodegradation of these microplastics, taking advantage of the technique optimised in chapter 4 to achieve rapid degradation. These materials were then incubated in a 6-week long soil microcosm experiment. Soil samples were maintained at 70% WHC, with a 2-week dry-down period to simulate natural moisture variation. Significant differences were observed in pH, EC, nitrate availability and phosphate availability, with some material-specific and aging-specific variations observed. However, there was no significant difference observed in the overall microbial activity of the soil samples, indicating that the effects were either a direct product of the material or their properties themselves (i.e. from their breakdown), or possibly resulting from a change in microbial communities brought on from their addition.

Further research needs to rapidly continue this inquiry. Assessing whether the aging of polymer surfaces affects their colonisation by microbial life, or whether its aging affects the microbial community that colonise the plastic substrate itself, or how the microbial community mature in the surrounding soil environment would shed much additional light on these results. Beyond this, only three polymers were tested in this study, but there is a huge variety of other polymers that pollute the natural environment, and at widely different concentrations, that will only increase should trends continue. Therefore future studies need to also assess a wider range of polymer concentrations, and ultimately assess if a critical threshold exists wherein plastic pollution has a significant deleterious effect on soil health, that could affect crop quality. Without this knowledge humanity may well accidentally step into a future where plastics alter the sustainability of the world's soils for generations to come.

It is clear that establishing better understanding of the effects of surface aging of plastics within the environment is a relevant, pressing sub-field within microplastic research communities. As the sheer volume of plastic pollution in the environment increases and persists, they will continue to degrade into materials with wildly different properties. This thesis demonstrates that future research needs to take surface aging of plastics into consideration when designing impact studies in terrestrial contexts. However, these observations, and indeed much of the suggested further work, is just as relevant to marine, freshwater and atmospheric environmental matrices. There is significant work still to be done

in order to confidently analyse the overall legacy, and the ultimate fate, that the plastic we use, produce, and discard will have in the decades to come.

The plastic crisis is one *solely* of our own making, and one that is up to us to solve. The research on the ultimate hazard, impact, and fate of these materials may not be fully realised yet, and many unanswered questions remain, but the fact that action is required now is without doubt. There are many tools and mechanisms available to us, both technical and social, however in order to effectively address the plastic crisis a highly-interdisciplinary approach is required, with actions that must be taken at all levels from consumers, to corporations, to governance. These cannot remain abstract or theoretical; our future is shaped by the decisions that we make today. Ultimately, to me, this observation underscores our responsibility to deal more kindly with one another, our duty to preserve the natural environment, and our obligation to safeguard the Earth we inhabit together. The only home we've ever known.

# Appendix A

## A Short Guide To Plastics For SMEs

### Context

This additional body of work was undertaken as part of the Material Social Futures doctoral training program. In this project a conversation was started with a local SME in order to teach them about material sustainability and the use of plastics in their commercial context. Decisions small businesses make with respect to the materials they use were assessed in the context of the plastic crisis, possible solutions were discussed, leading to the independent writing of this white paper.

### Introduction

The connection we have with the materials that make up our world is changing. In recent decades some remarkable materials have emerged that have fundamentally changed how we live and work. However, our understanding of their impact, and how to use them sustainably and responsibly, has increasingly come into focus. Several emerging ecological crises, such as unprecedented environmental pollution and climate change, continue to present important, and difficult questions about how we use and value these materials. Successfully addressing these challenges requires us to reconsider our consumption practices and values, how we choose products to sell, and how we deliver consumer goods. At the very heart of this issue is plastic.

## What is plastic?

Plastics are modern-day super materials. They are robust, highly adaptable, and cheap to produce [19], leading them to serve a wide variety of applications across all aspects of society, from military radars, to musical records [18]. They facilitate a number of irreplaceable roles in various fields, such as readily enabling sterile environments in medical technology [20], that would be virtually impossible to replicate with other materials. Well over 360 million tonnes of plastic get produced every year [2], and it is projected to increase significantly in the decades to come [182].

Plastic is a broad umbrella term for a very wide range of different materials that begin with a type of chemical called a ‘polymer’, and often contain other chemicals called ‘additives’ [10]. Polymers are long chains of molecules built up of small, often simple, units that repeat (‘monomers’). Virtually all everyday plastics are made of carbon and hydrogen, with some small quantities of other elements, meaning that by weight they are mostly carbon. It is relatively easy to make adjustments to their chemical structure, leading them to have an unmatched ability to adapt to different purposes when compared to other materials. This is then further expanded by the addition of additives. The term additive represents a wide array of chemicals, and in almost all cases they are loosely bound to the polymer [11]. Additives can enhance or augment the properties of a plastic, such as making them more resistant to heat or light, make them more visually attractive, reinforce them, and make them cheaper to manufacture [11].

## Understanding common terminology

When understanding plastics, their links with society, and their impact on the environment, there are a number of terms that are important to understand.

### **Conventional**

Most plastics are derived from fossil fuels such as oil. These are far more common than bio-based alternatives, and as such are also often referred to as ‘conventional’ plastics [13].

### **Bioplastic**

Bioplastic is a broad, ill-defined umbrella term that encompasses both bio-based and biodegradable plastics [183]. Both of these terms, and other similar terms, have different meanings, and it is important

to understand the difference. As such, bioplastic is a term that can be misleading; it doesn't necessarily mean that a product is environmentally friendly, or has a reduced impact, and is generally best avoided to minimise confusion.

### **Bio-based**

A polymer is bio-based if the monomers which form it are created from biological resources, such as plant starches [184]. This means that bio-based polymers are (in principle) renewable, as most biomass sources would be from crops that could be readily grown again. It does not mean that the resulting polymer shares the properties of its feedstock, e.g. a plastic derived from potato starch is very unlikely to have the same material properties as a potato. This means that it should not be inferred that a bio-based polymer is in any way biodegradable just because it is derived from biomass.

### **Biodegradable**

In the most fundamental sense, the biodegradability of a chemical is defined by the International Union of Pure and Applied Chemistry (IUPAC) as the altering of a chemical catalysed by enzymes and is separated into three stages: primary biodegradation refers to alterations that lead to the loss of a specific property, environmentally acceptable biodegradation which occurs when the extent of the degradation removes all of its undesirable properties, and finally the ultimate biodegradation as either the full oxidation of a chemical, or its reduction into simple molecules such as carbon dioxide and water [185]. In a recent publication focusing on plastics, researchers have used the definition 'a degradable plastic in which the degradation results from naturally occurring microorganisms such as bacteria, fungi and algae' [184]. It is also important to note, that plastics can be technically biodegradable, but require specific microorganisms that are not necessarily found readily in the environment, or specific conditions that would not necessarily be found in every environmental matrix.

To date, there doesn't appear to be a clear consensus on how 'biodegradable' is applied to plastics in either the UK or the EU, with governing bodies recently consulting for further evidence [186][187]. This means that 'biodegradable' is a tricky word when it comes to describing commercially available plastics and, without clear further explanation, can be misleading.

### **Compostable**

In a recent scientific publication a compostable plastic was defined as 'A plastic that undergoes biological degradation during composting to yield carbon dioxide, water, inorganic compounds, and biomass

at a rate consistent with other known compostable materials and leaves no visually distinguishable or toxic residues' [184]. Effectively, it is biodegradation under managed conditions.

It is not uncommon for households to compost their food waste, so it would be easy to interpret a plastic labelled as, say, a compostable bio-based material derived from sugar as something suitable for a home compost. However, many plastics that are considered compostable require specialised conditions that are only found in industrial composting facilities. Industrial composting is a similar process, but the conditions used in industrial composting facilities are often much different to those in a home compost. For example, some plastics require much higher temperatures to be composted industrially [188].

Similarly to other terms, to date there doesn't appear to be a clear consensus on how 'compostable' is applied to plastics in either the UK or the EU, with governing bodies in both consulting for further evidence [186][187].

### **Oxo-degradable plastic**

Oxo-degradable plastics refers to plastics treated with pro-oxidant additives, which are designed to enable them to breakdown at accelerated rates in the environment; they are not considered biodegradable [184], and they are not necessarily a 'green' or environmentally friendly alternative. They remain controversial for a number of reasons, and have been banned by the European Union [189].

### **Microplastic**

Microplastics are small particles of plastic generally defined as being <5mm in size [190]. When large plastic objects ('macroplastics') are weathered in the environment they fragment into smaller pieces, which in turn can become microplastics. Microplastics are also sometimes directly engineered for products such as cosmetics and toothpaste [191].

## **The impact of plastic**

In recent years plastic pollution has emerged as an increasingly visible ecological crisis. Stories of beached whales which have swallowed disturbingly large amounts of plastic are commonplace [60],

and the build up of plastic pollution has become a widely documented issue by journalists [192]. Plastics are persistent by design, however their persistence is key to them being a serious environmental contaminant. They have been described as poorly reversible pollutants [31], meaning that once they are introduced to the environment it is hard to clean them up or remove them. Once plastics start to form microplastics they become difficult to identify, sort and remove, and become highly mobile within the environment. As plastic particles continue to fragment they can even form much smaller particles known as nanoplastics, where they become very difficult to detect, as most existing techniques have a minimum detectable size limit of a few micrometres [29]. Micro- and nano-sized plastic particles present a range of poorly understood interactions within the environment, including the ability to transport toxic chemicals [26], threats to biodiversity [193], as well as concerns that they might be able to alter biogeochemical cycles [9].

Plastic pollution is also a major public health concern. It is widely acknowledged that microplastics are now a part of modern-day diets, with foods such as table salt, beer, and drinking water containing measurable quantities of these materials [194][195][196]. Whilst exposure can vary considerably, some researchers estimate that humans may be ingesting tens of thousands, even millions, of particles per person per year [197]. In the last two years alone stories have emerged of microplastics being found in human blood, human lung tissue, and even in human placenta [198][199][7]. Plastic particles have also been shown to be able to internalise into human cells under certain conditions [200]. It is not clear at this stage where the safe threshold of consumption is, or what the consequences of chronic microplastic exposure will be [6].

## **How can businesses use plastics sustainably?**

Identifying the most sustainable and environmentally friendly products for a business is tricky, but it is important. It reinforces a company's values, helps to show customers what is important to the business and what they can expect from its products. It also communicates to producers that these products are desirable, and that there is a need to see (and buy) more of them. Making a good decision about these things is hard, and there's rarely a clear 'right' answer. Almost all material choices have advantages and drawbacks, and fundamentally, a company has to be profitable in order to operate.

But for a company to thrive as an ethical and responsible enterprise it needs to acknowledge that there is a triple-bottom line; commercial, environmental, and social obligations that all have to be met in order to thrive as a business [201]. Not all products have desirable alternatives to plastics, and not all of the obvious solutions can apply to all plastic products. Fundamentally, the products still have to work! With all this in mind, there are some ways to start to take action:

### **Some helpful ideas to start**

- Find ways to incentivise customers to reuse suitable containers, or to bring their own, to minimise waste and unnecessary plastic use
- Opt for products that are clear about what they are made of, ideally of a single continuous material that is easily recyclable
- Ensure products are well-labelled, so that the consumer clearly understands what the material is made from, and how to recycle it
- Where products must be composite, it is highly desirable that consumers can easily separate the materials into clearly labelled components that are individually recyclable
- When using products designed to be composted, it is critical to communicate if these materials require industrial composting facilities, and how to get the waste to these facilities; this prevents consumers mistaking these materials as home compostable
- Where possible opt to work with suppliers that care about these issues and have a vision for addressing them
- Communicate to customers and to suppliers that these issues matter, and that it is important to see more sustainable products in the future

## **Conclusion**

Across their brief history plastics have transformed modern life, but now present humanity with a number of difficult questions about how sustainably we live, and how we treat our environment, that need to be addressed. To alleviate the worst impacts of the plastic crisis consumers, businesses and governments all need to play a role. Ultimately, if we can drastically improve some of the choices we

make with plastics, such as when we use them, how much we use, and how we manage their end of life, then plastics may well be a highly sustainable option in the future.

## Appendix B

# Understanding the role of Corporate Social Responsibility in addressing the plastic crisis

### Context

This additional project was undertaken as part of the Material Social Futures doctoral training program. This white paper was independently written as part of a collaboration with the Lancaster University Management School in order to connect the research conducted during this PhD to the broader societal and business context.

### Introduction

Businesses have a complicated relationship with plastics. Through their meteoric rise across the 20th century these exciting new materials have helped commercial enterprise to usher in unprecedented prosperity, convenience, and wide-ranging consumer products. They are ubiquitous across all aspects of modern-day life, from their applications in packaging, to vehicles, to medical technology [202], and humanity's appetite for plastic has skyrocketed through the last century to an estimated worldwide production of 368 million tonnes in 2019 alone [2]. It is difficult to imagine life without them, and

even more difficult to live without them.

Plastic is the generic term for a truly staggering variety of different materials built on a backbone of hydrogen and carbon. Everything from food packaging to furniture to medical devices are made of some type of plastic material, with polymers such as polyethylene (PE) and polyvinyl chloride (PVC) being among the most common [2]. Modern plastics are generally synthesised from petrochemicals like oil, but they can be made from plant-based stocks as well, such as corn and sugar [203]. Plastics are cheap, versatile, and readily adaptable with the help of chemical additives, which can augment the properties of the materials in almost any way seen desirable to consumers, including the addition of colour, heat resistance, and antimicrobial properties. As a result plastics serve almost every material need, from being lightweight alternatives to glass, to mimicking the natural beauty of pearl and tortoiseshell [17].

But this wave of innovation has introduced an entirely new ecological crisis. Plastics are, by design, persistent materials. Even polymers marketed as biodegradable can persist for long periods of time under certain circumstances, and whilst biodegradability standards have been established, they are still open to much criticism for their efficacy [204][205]. Often, creatures mistake plastic particles as a source of food [206], and they have repeatedly been shown to have a range of negative effects on marine life [207]. Over time, plastics left in the environment have also been shown to fracture and fragment into smaller particles known as microplastics [24]. These scraps may seem harmless, but they become virtually impossible to detect and to clean up, and are expected to have severe negative effects on life [208]. Perhaps most concerningly, there is speculation and emerging evidence that the sheer volume of plastics introduced into the environment could influence the biogeochemical cycles that keep the planet running [9].

This has raised some challenging questions for the businesses that produce, supply, and rely on them. As scientists begin to fully understand the impacts of these materials, and consumers start to engage with these issues more, does the current convenience model of plastics within business need to change, and what role should commercial enterprise have in the solution of this problem?

## **Beyond Profits: Do businesses have a responsibility to solve this issue?**

To what extent businesses should directly be responsible for enacting social change is a hotly debated topic across sociology and business management literature. It is self-evident that for some issues, such as the marketing of plastic products, corporations that manufacture and supply these goods to consumers have a lot of control in what and how their customers shop. They choose which products are available to buy, they choose which new products are worth investing in, and they (to a large extent) choose how these products are advertised. Ultimately, the decision to buy a product is with the consumer and it is reasonable at first glance to expect that if a customer doesn't agree with a product that they won't buy it. This argument is challenging with plastics however, because for many plastic products there are currently no alternatives in stores for market forces to take hold, and the alternatives that do exist have their own nuanced and complex challenges [204]. This can significantly impact the rates at which consumers can select out products that they disagree with. One way to address this hurdle is for businesses to proactively step in and take responsibility for the choice and impacts of the plastics within their supply chain.

### **What is Corporate Social Responsibility?**

Corporate Social Responsibility (CSR) is by no means a novel concept. It has evolved steadily over time as thinking, laws, and businesses have changed, with its routes being traced back hundreds of years in the industrial powerhouses of the UK and the US alone [209][210]. Some of the key concepts of modern CSR can be seen embedded within US businesses as early as the 1900s, but up until the 1950s business executives tended to favour philanthropic gestures over largescale business practices [210]. In contemporary literature CSR has many definitions [211]. For the purpose of this article the definition presented by McWilliams et al is appropriate, stating it as “actions which appear to further some social good, beyond the interests of the firm and that is required by law” [212]. In essence, CSR may not necessarily be profitable for a company directly, but be desirable (or even necessary) for the health and wellbeing of citizens and the environment.

## **Do businesses have a responsibility to act sustainably?**

Businesses are set up and operated in order to be profitable. No-one starts a business aiming to lose money. Within the framework of CSR this is sometimes referred to as the bottom of the pyramid [213]. In order to even consider making positive decisions that are not directly aligned with a company's profit margins, the company has to have a profitable business model. This is easily understandable, as without this it doesn't matter how inspirational or popular a company will be, it will eventually go bust. The company also has to observe its legal responsibilities in order to ensure that it doesn't get closed down. It is only from here that a business can explore its role in society.

*“[The responsibility of a corporate executive]...is to conduct the business in accordance with [the shareholders'] desires, which generally will be to make as much money as possible while conforming to the basic rules of the society, both those embodied in law and those embodied in ethical custom.”*

*Milton Friedman [214]*

For some economists, most notably the Nobel Prize-winning economist Milton Friedman who is widely considered the most influential thinker on this stance [215], undertaking more extensive CSR clashes with the role business plays in society. From Friedman's perspective, giving a business a social conscience and using it to address social issues amounted to “preaching pure and unadulterated socialism” [214]. He goes on to argue that this is not to say that businesses can't be used to for social good, but that the executive's key objective is to serve the needs of its employer (its owners & shareholders), and for businesses this overwhelmingly is to turn a profit. From his perspective, if an individual feels social responsibilities, it is with their own time, money and energy that they should serve that purpose, that if a social cause is in the interest of an individual, it is with their own resources that they should push market forces, rather than using a business to effect a tax on its stakeholders [214].

Friedman's stance has some attractive elements to it, such as its simplicity. If business can rely on the law as its ethical framework, it has a very clear set of rules to play by, and rules that it can reasonably assume are desirable to the society in which it operates. Governments additionally have

the ability to raise funds to meet a need, whereas a business acting alone is limited to the point where a decision is no longer profitable. This means that, particularly for problems that have unclear, long term, or negligible returns on investment governments, in theory, have more agency to solve the issues. This can make governments better suited to solving some broad societal issues.

But there are a number of complications. Compared to Friedman's era, companies are far more global than ever before. This means that they simultaneously have to make decisions across the often very different legal and cultural landscapes of different nations [216]. This can sometimes lead to companies having complex roles within different nations, as the minimal legal standard for some activities across different nations can vary wildly. This means a purely profit-driven stance can lead to highly undesirable outcomes, such as environmental catastrophe and human rights abuses, when operating across national borders [217]. Friedman's profit-oriented approach also neglects that sometimes the legal pathways that allow a company to maximise profit can undermine a government's ability to act, and a citizen's ability to effect change. Businesses can lobby governments, run marketing campaigns, and buy media outlets in order to protect their financial interests, to the detriment of society. Some of these speculated actions are already well documented in other industries [218].

*“ .. What responsibility to society may businessmen reasonably be expected to assume? What tangible benefits might result if the concern of many businessmen about the social implications of their work were spread widely through their business structure? ..”*  
*Howard Bowen, Social responsibilities of the businessman (Preface) [219]*

Friedman's perspective is sometimes referred to as the argument for “narrow CSR”, as he does not completely rule out that businesses have *some* level of contextual social responsibility [220]. The broader social perspective as a result is sometimes dubbed “broad CSR” [215][221]. Broad CSR diverges from Friedman's stance in a wide variety of ways, and has several different approaches, but largely shares the sentiment of Bowen's pioneering book *Social responsibilities of the businessman* (regrettably published in an era when women were less well represented within business). Bowen raised the issue that businesses have an inextricable link with society, and he penned that decisions made by business can directly lead to wealth inequality, the depletion of natural resources, and even impact international

relations (p4) [219]. From Bowen's perspective, it is unethical for a business to neglect this, and as a result they have a responsibility to act. In broad CSR frameworks businesses favour looking beyond their immediate narrow financial priorities, and towards the broad ethical and philanthropic obligations that they perceive their business to hold.

Further, it is argued in contemporary literature that modern society actually expects its companies to go beyond the bare minimum and have some degree of ethical agenda, and desirably to build on that a philanthropic purpose, with ethical behaviour permeating throughout [222]. This means that broad CSR frameworks can be seen as a popular strategy for businesses to improve their brand perception. As Werther et al note, strong brands cultivate the image of quality, consistency and security, and help to secure repeat customer business that can be particularly volatile in affluent markets where the costs of brand switching is low [223]. By making decisions that align with the needs, values, and aspirations of their customers, businesses give their customers reasons to continue to shop with them over their competitors.

Within this space, businesses take on a lot more responsibility. Often, these colossal obligations may be difficult, expensive, and unrealistic to meet, particularly on smaller scales. Not all CSR activities can contribute to business growth for small-medium enterprises (SMEs), and often the research exploring CSR may not hold equally true for SMEs [224][225]. In the context of plastic for example, if a small business relies on a product that is made from a cheap petrochemical-based non-renewable plastic (such as the simple takeaway coffee cup) and there's no alternative, it is reasonable to expect them to not be able to fund the research and development necessary to meet their CSR. This can leave them in the position of saying one thing, and doing another, which could be detrimental for their brand, particularly if larger competitors can afford to meet the challenge. Additionally, in SMEs there may simply not be enough time to effectively manage CSR amongst their other responsibilities due to their small number of employees and managers, and their ability therefore to be aware of (and act on) additional responsibilities may be low [225]. Due to these factors, favouring societal change with CSR could be disproportionately beneficial to companies that are already profitable and well-established, leaving startups and SMEs to struggle.

Many technologies of the future require safeguards and regulations that cannot be expected to exist today. Plastics were introduced long before we understood the damage they could cause. In this

instance, a purely profiteering company would have little financial incentive to act when the issue becomes apparent, even if this issue is dangerous. This is particularly concerning in cases where the technology or supply chain behind a product is complex, and where the expertise of the business itself is best suited to understanding a hazardous decision, as is arguable for the manufacturing and supply of plastic products. In the face of the plastic crisis, businesses who rely on these materials may end up exacerbating known harms, and propagating further unknown problems, should a purely profit-driven approach be considered. CSR has potential to help to address the plastic crisis, and some authors have already specifically investigated mechanisms for CSR in the governance of marine plastic debris, citing that contemporary local and international law is just insufficient in dealing with this issue [226].

## **How are businesses responding to the plastic crisis?**

Recent decades have seen significant progress in the battle against unnecessary and hazardous plastic waste supplied by businesses operating in the UK through both direct actions and through government regulation. In 2011 the Welsh government introduced the first plastic bag tax across the UK, in which a 5p charge was levied against single-use plastic carrier bags, with the rest of the UK following suit by 2015 [227]. This change to the way that supermarkets have dealt with carrier bags has led to a significant and steady decrease in the number of plastic bags used, and has raised tens of millions of pounds in funds for charitable sectors [228]. By making this step optional for smaller enterprises, the government potentially helped to sidestep issues arising from expensive step transitions for SMEs, and by making this step broad the government helped to minimise the commercial disadvantage that might have arisen from the change in customer experience for any one retailer. This year, the initiative has been shown to be so successful and impactful that the levy has been increased from 5p to 10p [228], although it is reasonable to expect that this will have less of an impact on consumer behaviour, as consumers are known to behave differently when products are free, indicating that perhaps this strategy does still need to evolve [229].

The overwhelming success of the government-sponsored plastic bag tax does provide strong evidence that, at least in part, government regulation is capable of stepping in and making social progress on this issue without business having to rise to the responsibility. Friedman and other proponents of narrow CSR frameworks may have seen this as government fulfilling its duty, and business responding to its legal obligation as defined by government.

But whilst this was a charge imposed on businesses, rather than a decision made proactively by them, it was a decision that appears to have been supported by businesses across the UK, and resulting actions have since superseded this start. Without regulatory prompt, major companies have started to respond to the plastic crisis. Tesco, the UK's largest supermarket chain, has taken further action such as no longer offering carrier bags as part of their online deliveries, which they estimate will eliminate 250 million new bags from circulation each year [230]. Asda has trialled the use of reusable bags for loose produce over single-use plastic bags [231]. Morrison's have trialled the introduction of reverse vending machines to encourage plastic recycling [232]. Sainsbury's are looking to trial a 'pre-cycle' area, in which customers can remove packaging they don't want to take with them in store, and leave it to be recycled [233]. These actions are a few examples of the fairly extensive reforms addressing the plastic crisis available to see within the CSR reports of the big 4 retailers, and many smaller companies in the sector have shown similar eagerness [234][235].

In the same decade, a large collection of businesses operating in the UK have united with the charity WRAP to take on several truly ambitious goals within a project dubbed the UK Plastic Pact. The plastic pact has several key aims: (1) to completely remove problematic single-use plastics from the supply chain; (2) to ensure that 100% of plastics are reusable, recyclable, or compostable; (3) for at least 70% of plastic packaging to be effectively recycled or composted; (4) for 30% of the content of plastic packaging on average to be recycled material. All by 2025 [34]. All of the UK's major grocery retailers are signatures to this proposal, as well as several suppliers and smaller businesses. This agreement tackles the plastic crisis whilst supporting businesses in a number of powerful ways. By working with a specialised charity, smaller and less knowledgeable businesses gain access to guidance and expertise that help to simplify and support their decision making. Businesses alleviate potential commercial disadvantages that could arise from unprofitable decisions, whilst retaining the positive brand reflection, as their competitors choose to act by the same rules. As product suppliers can work with multiple retailers, approaching CSR with industry-wide inclusion enables suppliers and manufacturers to make systematic changes that would be challenging if different companies took different approaches and prioritised different changes. Widespread action through the plastic pact presents a consistent message to customers, which reinforces the importance and gravity of the issues at the heart of this agenda.

This proactive step would suggest that not only does this action, which aligns with a broad CSR identity, lead to significant change, but that all of the big 4 major retailers, and many smaller businesses, see effective action as critical to their fight for market share. They are trying to enact innovative change around plastic to fight to be the market leader on this issue.

## **Conclusion**

Friedman and Bowen may have had differing perspectives on the role of business in society, but it is clear that in the decades that have followed CSR has taken off in the boardroom. Whilst it is still unclear exactly how effective this societal shift has been so far, within the recent decade alone this has not stopped many key players in commercial enterprise from embracing change, and trying to beat their competitors to a stronger stance on plastic waste. This new-found passion could be further channelled into more specific, measurable and achievable solutions, mirroring the actions taken in the UK Plastic Pact, to pave an ambitious path forward into a truly successful strategy to tackle plastic pollution.

Businesses have the ability to effect changes that governments do not, and governments can effect changes that businesses cannot. Ultimately, for society to continue to address the huge issues surrounding our consumption of plastic in the modern day, it is clear that governments, citizens, scientists, and businesses need to work hand-in-hand to solve this crisis, utilising the strengths and mechanisms available to each sector. Plastics are complex materials with complex chemistry and complex supply chains. They are capable of fulfilling roles and needs that would be all but impossible to replace with other materials. But in order to stay with us the way we consume these materials does need to change. To address the existing crisis and to minimise future harms, we need to find the right uses, the right place, for plastics in our society.

## Appendix C

# Web Of Science Queries

The following queries were designed to search the Web Of Science (WOS) database for the literature quantification analysis seen in chapter 3:

- ‘TS=(\*plastic? AND pollution)’; used to assess total papers published in this field
- ‘TS=(\*plastic? AND pollution AND (soil OR terrestrial))’; used to assess literature related to terrestrial matrices
- ‘TS=(\*plastic? AND pollution AND (marine OR ocean OR sea OR aquatic OR freshwater))’; used to assess literature related to aquatic environments
- ‘TS=(\*plastic? AND pollution AND (air OR atmospher\*))’; used to assess literature related to microplastics in the atmosphere

Please note that in WOS queries an asterisk (\*) is used to denote additional ‘wildcard’ characters, meaning that it captures literature using ‘microplastic’ or ‘microplastics’ interchangeably, and a question mark (?) denotes one additional ‘wildcard’ character. The terms were tailored to avoid studies from other fields that were not concerning microplastic pollution (e.g. microplasticity in metals). Due to the evolving and maturing nature of this subfield of research, terms have changed over time as more concrete definitions (such as ‘microplastic’) have been adopted, meaning these queries are not a perfect capture of all relevant studies, instead a reflection of the general trends seen in the research.

# Bibliography

- [1] S. L. Lewis and M. A. Maslin, “Defining the anthropocene,” *Nature*, vol. 519, no. 7542, pp. 171–180, 2015.
- [2] PlasticsEurope, *Plastics - the facts 2020 an analysis of european plastics production, demand, and waste data*, 2020.
- [3] E. MacArthur *et al.*, “The new plastics economy - rethinking the future of plastics,” 2016.
- [4] T. Wang, L. Qu, D. Luo, *et al.*, “Microplastic pollution characteristics and its future perspectives in the tibetan plateau,” *Journal of Hazardous Materials*, p. 131 711, 2023.
- [5] C. L. Waller, “Microplastics in the antarctic marine system: An emerging area of research,” *The Science of the Total Environment*, vol. 598, pp. 220–22, 2017.
- [6] S. L. Wright and F. J. Kelly, “Plastic and human health: A micro issue?” *Environmental science & technology*, vol. 51, no. 12, pp. 6634–6647, 2017.
- [7] A. Ragusa, A. Svelato, C. Santacroce, *et al.*, “Plasticenta: First evidence of microplastics in human placenta,” *Environment international*, vol. 146, p. 106 274, 2021.
- [8] T. S. Galloway, M. Cole, and C. Lewis, “Interactions of microplastic debris throughout the marine ecosystem,” *Nature ecology & evolution*, vol. 1, no. 5, pp. 1–8, 2017.
- [9] C. Sanz-Lázaro, N. Casado-Coy, and A. Beltrán-Sanahuja, “Biodegradable plastics can alter carbon and nitrogen cycles to a greater extent than conventional plastics in marine sediment,” *Science of The Total Environment*, vol. 756, p. 143 978, 2021.
- [10] M. Vert, Y. Doi, K.-H. Hellwich, *et al.*, “Terminology for biorelated polymers and applications (iupac recommendations 2012),” *Pure and Applied Chemistry*, vol. 84, no. 2, pp. 377–410, 2012.

- [11] J. N. Hahladakis, C. A. Velis, R. Weber, E. Iacovidou, and P. Purnell, “An overview of chemical additives present in plastics: Migration, release, fate and environmental impact during their use, disposal and recycling,” *Journal of hazardous materials*, vol. 344, pp. 179–199, 2018.
- [12] A. Jenkins, P. Kratochvil, R. Stepto, and U. Suter, “Glossary of basic terms in polymer science (iupac recommendations 1996),” *Pure and applied chemistry*, vol. 68, no. 12, pp. 2287–2311, 1996.
- [13] J. Song, R. Murphy, R. Narayan, and G. Davies, “Biodegradable and compostable alternatives to conventional plastics,” *Philosophical transactions of the royal society B: Biological sciences*, vol. 364, no. 1526, pp. 2127–2139, 2009.
- [14] J. Pang, M. Zheng, R. Sun, A. Wang, X. Wang, and T. Zhang, “Synthesis of ethylene glycol and terephthalic acid from biomass for producing pet,” *Green Chemistry*, vol. 18, no. 2, pp. 342–359, 2016.
- [15] D. Taufik, M. J. Reinders, K. Molenveld, and M. C. Onwezen, “The paradox between the environmental appeal of bio-based plastic packaging for consumers and their disposal behaviour,” *Science of the total environment*, vol. 705, p. 135 820, 2020.
- [16] H. V. Ford, N. H. Jones, A. J. Davies, *et al.*, “The fundamental links between climate change and marine plastic pollution,” *Science of The Total Environment*, vol. 806, p. 150 392, 2022.
- [17] L. Siegle, *Turning the Tide on Plastic: How Humanity (And You) Can Make Our Globe Clean Again*. Hachette UK, 2018.
- [18] “A history of plastics.” (2021), [Online]. Available: [https://www.bpf.co.uk/plastipedia/plastics\\_history/Default.aspx](https://www.bpf.co.uk/plastipedia/plastics_history/Default.aspx). Last accessed 2021-05-24.
- [19] A. L. Andrady and M. A. Neal, “Applications and societal benefits of plastics,” *Philosophical Transactions of the Royal Society B: Biological Sciences*, vol. 364, no. 1526, pp. 1977–1984, 2009.
- [20] B. Joseph, J. James, N. Kalarikkal, and S. Thomas, “Recycling of medical plastics,” *Advanced Industrial and Engineering Polymer Research*, vol. 4, no. 3, pp. 199–208, 2021.
- [21] E. J. Carpenter, S. J. Anderson, G. R. Harvey, H. P. Miklas, and B. B. Peck, “Polystyrene spherules in coastal waters,” *Science*, vol. 178, no. 4062, pp. 749–750, 1972.
- [22] L. Lebreton, B. Slat, F. Ferrari, *et al.*, “Evidence that the great pacific garbage patch is rapidly accumulating plastic,” *Scientific reports*, vol. 8, no. 1, pp. 1–15, 2018.

- [23] F. Büks and M. Kaupenjohann, “Global concentrations of microplastics in soils—a review,” *Soil*, vol. 6, no. 2, pp. 649–662, 2020.
- [24] D. K. Barnes, F. Galgani, R. C. Thompson, and M. Barlaz, “Accumulation and fragmentation of plastic debris in global environments,” *Philosophical transactions of the royal society B: biological sciences*, vol. 364, no. 1526, pp. 1985–1998, 2009.
- [25] D. M. Mitrano, P. Wick, and B. Nowack, “Placing nanoplastics in the context of global plastic pollution,” *Nature Nanotechnology*, vol. 16, no. 5, pp. 491–500, 2021.
- [26] Y. Mato, T. Isobe, H. Takada, H. Kanehiro, C. Ohtake, and T. Kaminuma, “Plastic resin pellets as a transport medium for toxic chemicals in the marine environment,” *Environmental science & technology*, vol. 35, no. 2, pp. 318–324, 2001.
- [27] L. A. Holmes, A. Turner, and R. C. Thompson, “Adsorption of trace metals to plastic resin pellets in the marine environment,” *Environmental Pollution*, vol. 160, pp. 42–48, 2012.
- [28] J. Li, K. Zhang, and H. Zhang, “Adsorption of antibiotics on microplastics,” *Environmental Pollution*, vol. 237, pp. 460–467, 2018.
- [29] W. J. Shim, S. H. Hong, and S. E. Eo, “Identification methods in microplastic analysis: A review,” *Analytical methods*, vol. 9, no. 9, pp. 1384–1391, 2017.
- [30] C. M. Rochman, M. A. Browne, B. S. Halpern, *et al.*, “Classify plastic waste as hazardous,” *Nature*, vol. 494, no. 7436, pp. 169–171, 2013.
- [31] M. MacLeod, H. P. H. Arp, M. B. Tekman, and A. Jahnke, “The global threat from plastic pollution,” *Science*, vol. 373, no. 6550, pp. 61–65, 2021.
- [32] W. J. Sutherland, S. Broad, S. H. Butchart, *et al.*, “A horizon scan of emerging issues for global conservation in 2019,” *Trends in ecology & evolution*, vol. 34, no. 1, pp. 83–94, 2019.
- [33] N. Pettorelli, N. A. Graham, N. Seddon, *et al.*, “Time to integrate global climate change and biodiversity science-policy agendas,” *Journal of Applied Ecology*, vol. 58, no. 11, pp. 2384–2393, 2021.
- [34] WRAP, *A roadmap to 2025 - the uk plastics pact*, 2020.
- [35] “Science to enable sustainable plastics: A whitepaper from the 8th chemical sciences and society summit(cs3),” 2020.

- [36] J. Rockström, W. Steffen, K. Noone, *et al.*, “A safe operating space for humanity,” *nature*, vol. 461, no. 7263, pp. 472–475, 2009.
- [37] P. Villarrubia-Gómez, S. E. Cornell, and J. Fabres, “Marine plastic pollution as a planetary boundary threat—the drifting piece in the sustainability puzzle,” *Marine policy*, vol. 96, pp. 213–220, 2018.
- [38] H. Serrano-Ruiz, L. Martin-Closas, and A. M. Pelacho, “Biodegradable plastic mulches: Impact on the agricultural biotic environment,” *Science of The Total Environment*, vol. 750, p. 141 228, 2021.
- [39] E. Syranidou, K. Karkanorachaki, F. Amorotti, *et al.*, “Biodegradation of weathered polystyrene films in seawater microcosms,” *Scientific reports*, vol. 7, no. 1, p. 17 991, 2017.
- [40] G. J., *Mineralogy of Quartz and Silica Minerals*. MDPI, 2018.
- [41] L. Yang, Y. Zhang, S. Kang, Z. Wang, and C. Wu, “Microplastics in soil: A review on methods, occurrence, sources, and potential risk,” *Science of the Total Environment*, vol. 780, p. 146 546, 2021.
- [42] J. Chastain and R. C. King Jr, “Handbook of x-ray photoelectron spectroscopy,” *Perkin-Elmer Corporation*, vol. 40, p. 221, 1992.
- [43] D. Briggs and G. Beamosn, *High Resolution XPS Of Organic Polymers: The Scienta ESCA 300 Database*. American Chemical Society (ACS), 1992, vol. 92.
- [44] P. K. Chu and X. Lu, *Low temperature plasma technology: methods and applications*. CRC press, 2013.
- [45] F. L. Tabares and I. Junkar, “Cold plasma systems and their application in surface treatments for medicine,” *Molecules*, vol. 26, no. 7, p. 1903, 2021.
- [46] B. Chapman and J. Vossen, *Glow discharge processes: Sputtering and plasma etching*, 1981.
- [47] D. Mariotti and R. M. Sankaran, “Perspectives on atmospheric-pressure plasmas for nanofabrication,” *Journal of Physics D: Applied Physics*, vol. 44, no. 17, p. 174 023, 2011.
- [48] T. Von Woedtke, H.-R. Metelmann, and K.-D. Weltmann, “Clinical plasma medicine: State and perspectives of in vivo application of cold atmospheric plasma,” *Contributions to Plasma Physics*, vol. 54, no. 2, pp. 104–117, 2014.

- [49] R. M. France and R. D. Short, "Plasma treatment of polymers effects of energy transfer from an argon plasma on the surface chemistry of poly (styrene), low density poly (ethylene), poly (propylene) and poly (ethylene terephthalate)," *Journal of the Chemical Society, Faraday Transactions*, vol. 93, no. 17, pp. 3173–3178, 1997.
- [50] P. Liu, Y. Shi, X. Wu, *et al.*, "Review of the artificially-accelerated aging technology and ecological risk of microplastics," *Science of the total environment*, vol. 768, p. 144 969, 2021.
- [51] ASTM. "Standard practice for fluorescent ultraviolet (uv) lamp apparatus exposure of plastics." (), [Online]. Available: <https://www.astm.org/d4329-05.html>. [Online; Last accessed 2022-07-25].
- [52] K. Zhu, H. Jia, Y. Sun, *et al.*, "Long-term phototransformation of microplastics under simulated sunlight irradiation in aquatic environments: Roles of reactive oxygen species," *Water Research*, vol. 173, p. 115 564, 2020.
- [53] R. Mao, M. Lang, X. Yu, R. Wu, X. Yang, and X. Guo, "Aging mechanism of microplastics with uv irradiation and its effects on the adsorption of heavy metals," *Journal of hazardous materials*, vol. 393, p. 122 515, 2020.
- [54] L. Cai, J. Wang, J. Peng, Z. Wu, and X. Tan, "Observation of the degradation of three types of plastic pellets exposed to uv irradiation in three different environments," *Science of the Total Environment*, vol. 628, pp. 740–747, 2018.
- [55] K. M. Krishnan, *Principles of materials characterization and metrology*. Oxford University Press, 2021.
- [56] D. Y. Kwok and A. W. Neumann, "Contact angle measurement and contact angle interpretation," *Advances in colloid and interface science*, vol. 81, no. 3, pp. 167–249, 1999.
- [57] A. Ahmed, R. Sanedrin, T. Willers, and P. R. Waghmare, "The effect of dynamic wetting pressure on contact angle measurements," *Journal of Colloid and Interface Science*, vol. 608, pp. 1086–1093, 2022.
- [58] P. He, L. Chen, L. Shao, H. Zhang, and F. Lü, "Municipal solid waste (msw) landfill: A source of microplastics?-evidence of microplastics in landfill leachate," *Water research*, vol. 159, pp. 38–45, 2019.
- [59] R. Geyer, J. R. Jambeck, and K. L. Law, "Production, use, and fate of all plastics ever made," *Science advances*, vol. 3, no. 7, e1700782, 2017.

- [60] T. Guardian. “Whale dies from eating more than 80 plastic bags.” (), [Online]. Available: <https://www.theguardian.com/environment/2018/jun/03/whale-dies-from-eating-more-than-80-plastic-bags>. Last accessed 2022-05-31.
- [61] N. Rangel-Buitrago and W. J. Neal, “A geological perspective of plastic pollution,” *Science of the Total Environment*, vol. 893, p. 164 867, 2023.
- [62] F. A. Santos, G. R. Diório, C. C. F. Guedes, *et al.*, “Plastic debris forms: Rock analogues emerging from marine pollution,” *Marine pollution bulletin*, vol. 182, p. 114 031, 2022.
- [63] P. M. Kopittke, N. W. Menzies, P. Wang, B. A. McKenna, and E. Lombi, “Soil and the intensification of agriculture for global food security,” *Environment international*, vol. 132, p. 105 078, 2019.
- [64] P. Smith, M. R. Ashmore, H. I. Black, *et al.*, “The role of ecosystems and their management in regulating climate, and soil, water and air quality,” *Journal of Applied Ecology*, vol. 50, no. 4, pp. 812–829, 2013.
- [65] M. Bläsing and W. Amelung, “Plastics in soil: Analytical methods and possible sources,” *Science of the total environment*, vol. 612, pp. 422–435, 2018.
- [66] P. J. Kole, A. J. Löhr, F. G. Van Belleghem, and A. M. Ragas, “Wear and tear of tyres: A stealthy source of microplastics in the environment,” *International journal of environmental research and public health*, vol. 14, no. 10, p. 1265, 2017.
- [67] M. A. Browne, P. Crump, S. J. Niven, *et al.*, “Accumulation of microplastic on shorelines worldwide: Sources and sinks,” *Environmental science & technology*, vol. 45, no. 21, pp. 9175–9179, 2011.
- [68] F. Murphy, C. Ewins, F. Carbonnier, and B. Quinn, “Wastewater treatment works (wwtw) as a source of microplastics in the aquatic environment,” *Environmental science & technology*, vol. 50, no. 11, pp. 5800–5808, 2016.
- [69] P. van den Berg, E. Huerta-Lwanga, F. Corradini, and V. Geissen, “Sewage sludge application as a vehicle for microplastics in eastern spanish agricultural soils,” *Environmental Pollution*, vol. 261, p. 114 198, 2020.
- [70] M. C. Rillig, L. Ziersch, and S. Hempel, “Microplastic transport in soil by earthworms,” *Scientific reports*, vol. 7, no. 1, pp. 1–6, 2017.

- [71] M. Kooi, E. H. v. Nes, M. Scheffer, and A. A. Koelmans, “Ups and downs in the ocean: Effects of biofouling on vertical transport of microplastics,” *Environmental science & technology*, vol. 51, no. 14, pp. 7963–7971, 2017.
- [72] J. Brahney, M. Hallerud, E. Heim, M. Hahnenberger, and S. Sukumaran, “Plastic rain in protected areas of the united states,” *Science*, vol. 368, no. 6496, pp. 1257–1260, 2020.
- [73] S. Allen, D. Allen, V. R. Phoenix, *et al.*, “Atmospheric transport and deposition of microplastics in a remote mountain catchment,” *Nature Geoscience*, vol. 12, no. 5, pp. 339–344, 2019.
- [74] S. Veerasingam, M. Saha, V. Suneel, *et al.*, “Characteristics, seasonal distribution and surface degradation features of microplastic pellets along the goa coast, india,” *Chemosphere*, vol. 159, pp. 496–505, 2016.
- [75] C. Schmidt, T. Krauth, and S. Wagner, “Export of plastic debris by rivers into the sea,” *Environmental science & technology*, vol. 51, no. 21, pp. 12 246–12 253, 2017.
- [76] S. Fuller and A. Gautam, “A procedure for measuring microplastics using pressurized fluid extraction,” *Environmental science & technology*, vol. 50, no. 11, pp. 5774–5780, 2016.
- [77] M. Scheurer and M. Bigalke, “Microplastics in swiss floodplain soils,” *Environmental science & technology*, vol. 52, no. 6, pp. 3591–3598, 2018.
- [78] S. Abbasi, A. Turner, M. Hoseini, and H. Amiri, “Microplastics in the lut and kavir deserts, iran,” *Environmental Science & Technology*, vol. 55, no. 9, pp. 5993–6000, 2021.
- [79] E. da Silva Paes, T. V. Gloaguen, H. d. A. da Conceição Silva, *et al.*, “Widespread microplastic pollution in mangrove soils of todos os santos bay, northern brazil,” *Environmental Research*, vol. 210, p. 112 952, 2022.
- [80] S. J. Cusworth, W. J. Davies, M. R. McAinsh, and C. J. Stevens, “Sustainable production of healthy, affordable food in the uk: The pros and cons of plasticulture,” *Food and Energy Security*, vol. 11, no. 4, e404, 2022.
- [81] C. Maraveas, “Environmental sustainability of plastic in agriculture,” *Agriculture*, vol. 10, no. 8, p. 310, 2020.
- [82] I. Blanco, R. V. Loisi, C. Sica, E. Schettini, and G. Vox, “Agricultural plastic waste mapping using gis. a case study in italy,” *Resources, Conservation and Recycling*, vol. 137, pp. 229–242, 2018.

- [83] D. Briassoulis and A. Giannoulis, “Evaluation of the functionality of bio-based plastic mulching films,” *Polymer Testing*, vol. 67, pp. 99–109, 2018.
- [84] Z. Steinmetz, C. Wollmann, M. Schaefer, *et al.*, “Plastic mulching in agriculture. trading short-term agronomic benefits for long-term soil degradation?” *Science of the total environment*, vol. 550, pp. 690–705, 2016.
- [85] Y. Huang, Q. Liu, W. Jia, C. Yan, and J. Wang, “Agricultural plastic mulching as a source of microplastics in the terrestrial environment,” *Environmental Pollution*, vol. 260, p. 114 096, 2020.
- [86] J. Zhou, R. Jia, R. W. Brown, *et al.*, “The long-term uncertainty of biodegradable mulch film residues and associated microplastics pollution on plant-soil health,” *Journal of Hazardous Materials*, p. 130 055, 2022.
- [87] A. Rafique, M. Irfan, M. Mumtaz, and A. Qadir, “Spatial distribution of microplastics in soil with context to human activities: A case study from the urban center,” *Environmental Monitoring and Assessment*, vol. 192, pp. 1–13, 2020.
- [88] Y. Su, Z. Zhang, D. Wu, L. Zhan, H. Shi, and B. Xie, “Occurrence of microplastics in landfill systems and their fate with landfill age,” *Water research*, vol. 164, p. 114 968, 2019.
- [89] V. Yadav, M. Sherly, P. Ranjan, *et al.*, “Framework for quantifying environmental losses of plastics from landfills,” *Resources, Conservation and Recycling*, vol. 161, p. 104 914, 2020.
- [90] S. Loppi, B. Roblin, L. Paoli, and J. Aherne, “Accumulation of airborne microplastics in lichens from a landfill dumping site (italy),” *Scientific reports*, vol. 11, no. 1, p. 4564, 2021.
- [91] X. Lim *et al.*, “Microplastics are everywhere—but are they harmful,” *Nature*, vol. 593, no. 7857, pp. 22–25, 2021.
- [92] R. Menezes, M. A. da Cunha-Neto, G. C. de Mesquita, and G. B. da Silva, “Ingestion of macroplastic debris by the common dolphinfish (*coryphaena hippurus*) in the western equatorial atlantic,” *Marine pollution bulletin*, vol. 141, pp. 161–163, 2019.
- [93] J. Rivers-Auty, A. L. Bond, M. L. Grant, and J. L. Lavers, “The one-two punch of plastic exposure: Macro-and micro-plastics induce multi-organ damage in seabirds,” *Journal of Hazardous Materials*, vol. 442, p. 130 117, 2023.
- [94] M. C. Blettler and C. Mitchell, “Dangerous traps: Macroplastic encounters affecting freshwater and terrestrial wildlife,” *Science of the Total Environment*, vol. 798, p. 149 317, 2021.

- [95] D. Honingh, T. Van Emmerik, W. Uijttewaal, H. Kardhana, O. Hoes, and N. Van de Giesen, “Urban river water level increase through plastic waste accumulation at a rack structure,” *Frontiers in earth science*, vol. 8, p. 28, 2020.
- [96] E. Fries and R. Sühling, “The unusual suspects: Screening for persistent, mobile, and toxic plastic additives in plastic leachates,” *Environmental Pollution*, vol. 335, p. 122 263, 2023.
- [97] K. Fikarová, D. J. Cocovi-Solberg, M. Rosende, B. Horstkotte, H. Sklenářová, and M. Miró, “A flow-based platform hyphenated to on-line liquid chromatography for automatic leaching tests of chemical additives from microplastics into seawater,” *Journal of Chromatography A*, vol. 1602, pp. 160–167, 2019.
- [98] J. Oehlmann, U. Schulte-Oehlmann, W. Kloas, *et al.*, “A critical analysis of the biological impacts of plasticizers on wildlife,” *Philosophical Transactions of the Royal Society B: Biological Sciences*, vol. 364, no. 1526, pp. 2047–2062, 2009.
- [99] K. Gunaalan, E. Fabbri, and M. Capolupo, “The hidden threat of plastic leachates: A critical review on their impacts on aquatic organisms,” *Water Research*, vol. 184, p. 116 170, 2020.
- [100] S. W. Kim, W. R. Waldman, T.-Y. Kim, and M. C. Rillig, “Effects of different microplastics on nematodes in the soil environment: Tracking the extractable additives using an ecotoxicological approach,” *Environmental Science & Technology*, vol. 54, no. 21, pp. 13 868–13 878, 2020.
- [101] E. R. Zettler, T. J. Mincer, and L. A. Amaral-Zettler, “Life in the “plastisphere”: Microbial communities on plastic marine debris,” *Environmental science & technology*, vol. 47, no. 13, pp. 7137–7146, 2013.
- [102] S. Oberbeckmann, B. Kreikemeyer, and M. Labrenz, “Environmental factors support the formation of specific bacterial assemblages on microplastics,” *Frontiers in microbiology*, vol. 8, p. 2709, 2018.
- [103] H.-Q. Li, Y.-J. Shen, W.-L. Wang, H.-T. Wang, H. Li, and J.-Q. Su, “Soil ph has a stronger effect than arsenic content on shaping plastisphere bacterial communities in soil,” *Environmental Pollution*, p. 117 339, 2021.
- [104] M. Basili, G. M. Quero, D. Giovannelli, *et al.*, “Major role of surrounding environment in shaping biofilm community composition on marine plastic debris,” *Frontiers in Marine Science*, vol. 7, p. 262, 2020.

- [105] M. Arias-Andres, U. Klümper, K. Rojas-Jimenez, and H.-P. Grossart, “Microplastic pollution increases gene exchange in aquatic ecosystems,” *Environmental pollution*, vol. 237, pp. 253–261, 2018.
- [106] R. I. Aminov, “Horizontal gene exchange in environmental microbiota,” *Frontiers in microbiology*, vol. 2, p. 158, 2011.
- [107] M. C. Rillig, A. Lehmann, A. A. de Souza Machado, and G. Yang, “Microplastic effects on plants,” *New Phytologist*, vol. 223, no. 3, pp. 1066–1070, 2019.
- [108] Y. Qi, X. Yang, A. M. Pelaez, *et al.*, “Macro-and micro-plastics in soil-plant system: Effects of plastic mulch film residues on wheat (*triticum aestivum*) growth,” *Science of the Total Environment*, vol. 645, pp. 1048–1056, 2018.
- [109] Y. Qi, A. Ossowicki, X. Yang, *et al.*, “Effects of plastic mulch film residues on wheat rhizosphere and soil properties,” *Journal of Hazardous Materials*, vol. 387, p. 121 711, 2020.
- [110] Q. Hu, X. Li, J. M. Gonçalves, H. Shi, T. Tian, and N. Chen, “Effects of residual plastic-film mulch on field corn growth and productivity,” *Science of the Total Environment*, vol. 729, p. 138 901, 2020.
- [111] Y. Xiang, L. Jiang, Y. Zhou, *et al.*, “Microplastics and environmental pollutants: Key interaction and toxicology in aquatic and soil environments,” *Journal of Hazardous Materials*, vol. 422, p. 126 843, 2022.
- [112] A. A. de Souza Machado, C. W. Lau, J. Till, *et al.*, “Impacts of microplastics on the soil biophysical environment,” *Environmental science & technology*, vol. 52, no. 17, pp. 9656–9665, 2018.
- [113] A. A. de Souza Machado, C. W. Lau, W. Kloas, *et al.*, “Microplastics can change soil properties and affect plant performance,” *Environmental science & technology*, vol. 53, no. 10, pp. 6044–6052, 2019.
- [114] J. Zhou, Y. Wen, M. R. Marshall, *et al.*, “Microplastics as an emerging threat to plant and soil health in agroecosystems,” *Science of the Total Environment*, vol. 787, p. 147 444, 2021.
- [115] M. C. Rillig, *Microplastic disguising as soil carbon storage*, 2018.
- [116] C. P. Ward, C. J. Armstrong, A. N. Walsh, J. H. Jackson, and C. M. Reddy, “Sunlight converts polystyrene to carbon dioxide and dissolved organic carbon,” *Environmental science & technology letters*, vol. 6, no. 11, pp. 669–674, 2019.

- [117] S.-J. Royer, S. Ferrón, S. T. Wilson, and D. M. Karl, “Production of methane and ethylene from plastic in the environment,” *PloS one*, vol. 13, no. 8, e0200574, 2018.
- [118] M. C. Rillig, E. Leifheit, and J. Lehmann, “Microplastic effects on carbon cycling processes in soils,” *PLoS Biology*, vol. 19, no. 3, e3001130, 2021.
- [119] A. Göpferich, “Mechanisms of polymer degradation and erosion,” *Biomaterials*, vol. 17, no. 2, pp. 103–114, 1996.
- [120] N. S. Allen, “Recent advances in the photo-oxidation and stabilization of polymers,” *Chemical Society Reviews*, vol. 15, no. 3, pp. 373–404, 1986.
- [121] G. Grause, M.-F. Chien, and C. Inoue, “Changes during the weathering of polyolefins,” *Polymer Degradation and Stability*, vol. 181, p. 109364, 2020.
- [122] B. Singh and N. Sharma, “Mechanistic implications of plastic degradation,” *Polymer degradation and stability*, vol. 93, no. 3, pp. 561–584, 2008.
- [123] D. Feldman, “Polymer weathering: Photo-oxidation,” *Journal of Polymers and the Environment*, vol. 10, pp. 163–173, 2002.
- [124] P. Gijsman, “A review on the mechanism of action and applicability of hindered amine stabilizers,” *Polymer Degradation and Stability*, vol. 145, pp. 2–10, 2017.
- [125] A. T. N. Do, Y. Ha, and J.-H. Kwon, “Leaching of microplastic-associated additives in aquatic environments: A critical review,” *Environmental Pollution*, p. 119258, 2022.
- [126] V. R. Hebert and G. C. Miller, “Depth dependence of direct and indirect photolysis on soil surfaces,” *Journal of agricultural and food chemistry*, vol. 38, no. 3, pp. 913–918, 1990.
- [127] J. Moalli, *Plastics Failure - Analysis and Prevention*. Plastics Design Library, 2001.
- [128] K. Liu and M. Piggott, “Fracture failure processes in polymers. i: Mechanical tests and results,” *Polymer Engineering & Science*, vol. 38, no. 1, pp. 60–68, 1998.
- [129] E. Yousif and R. Haddad, “Photodegradation and photostabilization of polymers, especially polystyrene,” *SpringerPlus*, vol. 2, no. 1, pp. 1–32, 2013.
- [130] A. Winkler, N. Santo, M. A. Ortenzi, E. Bolzoni, R. Bacchetta, and P. Tremolada, “Does mechanical stress cause microplastic release from plastic water bottles?” *Water research*, vol. 166, p. 115082, 2019.

- [131] D. L. Kaplan, R. Hartenstein, and J. Sutter, “Biodegradation of polystyrene, poly (methyl methacrylate), and phenol formaldehyde,” *Applied and environmental microbiology*, vol. 38, no. 3, pp. 551–553, 1979.
- [132] Y.-N. Han, M. Wei, F. Han, *et al.*, “Greater biofilm formation and increased biodegradation of polyethylene film by a microbial consortium of arthrobacter sp. and streptomyces sp.,” *Microorganisms*, vol. 8, no. 12, p. 1979, 2020.
- [133] M. T. Zumstein, A. Schintlmeister, T. F. Nelson, *et al.*, “Biodegradation of synthetic polymers in soils: Tracking carbon into CO<sub>2</sub> and microbial biomass,” *Science advances*, vol. 4, no. 7, eaas9024, 2018.
- [134] M. Vert, “Aliphatic polyesters: Great degradable polymers that cannot do everything,” *Biomacromolecules*, vol. 6, no. 2, pp. 538–546, 2005.
- [135] M. Sander, “Biodegradation of polymeric mulch films in agricultural soils: Concepts, knowledge gaps, and future research directions,” *Environmental science & technology*, vol. 53, no. 5, pp. 2304–2315, 2019.
- [136] B. Boots, C. W. Russell, and D. S. Green, “Effects of microplastics in soil ecosystems: Above and below ground,” *Environmental science & technology*, vol. 53, no. 19, pp. 11 496–11 506, 2019.
- [137] W. R. Waldman and M. C. Rillig, *Microplastic research should embrace the complexity of secondary particles*, 2020.
- [138] A. Chamas, H. Moon, J. Zheng, *et al.*, “Degradation rates of plastics in the environment,” *ACS Sustainable Chemistry & Engineering*, vol. 8, no. 9, pp. 3494–3511, 2020.
- [139] L. Wang, J. Zhang, W. Huang, and Y. He, “Laboratory simulated aging methods, mechanisms and characteristic changes of microplastics: A review,” *Chemosphere*, p. 137 744, 2023.
- [140] P. U. Iyare, S. K. Ouki, and T. Bond, “Microplastics removal in wastewater treatment plants: A critical review,” *Environmental Science: Water Research & Technology*, vol. 6, no. 10, pp. 2664–2675, 2020.
- [141] L. Lei, S. Wu, S. Lu, *et al.*, “Microplastic particles cause intestinal damage and other adverse effects in zebrafish danio rerio and nematode caenorhabditis elegans,” *Science of the total environment*, vol. 619, pp. 1–8, 2018.

- [142] A. Tewari, H. Almuhtaram, M. J. McKie, and R. C. Andrews, "Microplastics for use in environmental research," *Journal of Polymers and the Environment*, vol. 30, no. 10, pp. 4320–4332, 2022.
- [143] P. Liu, L. Qian, H. Wang, *et al.*, "New insights into the aging behavior of microplastics accelerated by advanced oxidation processes," *Environmental science & technology*, vol. 53, no. 7, pp. 3579–3588, 2019.
- [144] L. Zhou, T. Wang, G. Qu, H. Jia, and L. Zhu, "Probing the aging processes and mechanisms of microplastic under simulated multiple actions generated by discharge plasma," *Journal of Hazardous Materials*, vol. 398, p. 122 956, 2020.
- [145] V. Fernández-González, J. Andrade-Garda, P. López-Mahia, and S. Muniategui-Lorenzo, "Impact of weathering on the chemical identification of microplastics from usual packaging polymers in the marine environment," *Analytica Chimica Acta*, vol. 1142, pp. 179–188, 2021.
- [146] A. L. Andrady, S. Hamid, X. Hu, and A. Torikai, "Effects of increased solar ultraviolet radiation on materials," *Journal of photochemistry and photobiology B: Biology*, vol. 46, no. 1-3, pp. 96–103, 1998.
- [147] K. Zhang, A. H. Hamidian, A. Tubić, *et al.*, "Understanding plastic degradation and microplastic formation in the environment: A review," *Environmental Pollution*, vol. 274, p. 116 554, 2021.
- [148] L. C. de Sá, L. G. Luis, and L. Guilhermino, "Effects of microplastics on juveniles of the common goby (*pomatoschistus microps*): Confusion with prey, reduction of the predatory performance and efficiency, and possible influence of developmental conditions," *Environmental pollution*, vol. 196, pp. 359–362, 2015.
- [149] K. Bhagat, A. C. Barrios, K. Rajwade, *et al.*, "Aging of microplastics increases their adsorption affinity towards organic contaminants," *Chemosphere*, vol. 298, p. 134 238, 2022.
- [150] B. Liu, Q. Jiang, Z. Qiu, *et al.*, "Process analysis of microplastic degradation using activated pms and fenton reagents," *Chemosphere*, vol. 298, p. 134 220, 2022.
- [151] C. Xiao, M. Zhang, L. Ding, X. Qiu, and X. Guo, "New sight of microplastics aging: Reducing agents promote rapid aging of microplastics under anoxic conditions," *Journal of Hazardous Materials*, vol. 451, p. 131 123, 2023.

- [152] O. S. Alimi, D. Claveau-Mallet, R. S. Kurusu, M. Lapointe, S. Bayen, and N. Tufenkji, “Weathering pathways and protocols for environmentally relevant microplastics and nanoplastics: What are we missing?” *Journal of Hazardous Materials*, vol. 423, p. 126 955, 2022.
- [153] R. M. France and R. D. Short, “Plasma treatment of polymers: The effects of energy transfer from an argon plasma on the surface chemistry of polystyrene, and polypropylene. a high-energy resolution x-ray photoelectron spectroscopy study,” *Langmuir*, vol. 14, no. 17, pp. 4827–4835, 1998.
- [154] A. Vesel and M. Mozetic, “Surface modification and ageing of pmma polymer by oxygen plasma treatment,” *Vacuum*, vol. 86, no. 6, pp. 634–637, 2012.
- [155] N. Vandencastele and F. Reniers, “Plasma-modified polymer surfaces: Characterization using xps,” *Journal of Electron Spectroscopy and Related Phenomena*, vol. 178, pp. 394–408, 2010.
- [156] G. Kokkoris, N. Vourdas, and E. Gogolides, “Plasma etching and roughening of thin polymeric films: A fast, accurate, in situ method of surface roughness measurement,” *Plasma Processes and Polymers*, vol. 5, no. 9, pp. 825–833, 2008.
- [157] J. F. Friedrich, R. Mix, R.-D. Schulze, A. Meyer-Plath, R. Joshi, and S. Wettmarshausen, “New plasma techniques for polymer surface modification with monotype functional groups,” *Plasma Processes and Polymers*, vol. 5, no. 5, pp. 407–423, 2008.
- [158] A. Andrady, H. Hamid, and A. Torikai, “Effects of solar uv and climate change on materials,” *Photochemical & Photobiological Sciences*, vol. 10, pp. 292–300, 2011.
- [159] F. Wang, Q. Wang, C. A. Adams, Y. Sun, and S. Zhang, “Effects of microplastics on soil properties: Current knowledge and future perspectives,” *Journal of Hazardous Materials*, vol. 424, p. 127 531, 2022.
- [160] B. Gewert, M. M. Plassmann, and M. MacLeod, “Pathways for degradation of plastic polymers floating in the marine environment,” *Environmental science: processes & impacts*, vol. 17, no. 9, pp. 1513–1521, 2015.
- [161] J. P. Rodrigues, A. C. Duarte, J. Santos-Echeandia, and T. Rocha-Santos, “Significance of interactions between microplastics and pops in the marine environment: A critical overview,” *TrAC Trends in Analytical Chemistry*, vol. 111, pp. 252–260, 2019.

- [162] A. Menéndez-Pedriza and J. Jaumot, “Interaction of environmental pollutants with microplastics: A critical review of sorption factors, bioaccumulation and ecotoxicological effects,” *Toxics*, vol. 8, no. 2, p. 40, 2020.
- [163] O. H. Fred-Ahmadu, G. Bhagwat, I. Oluyoye, N. U. Benson, O. O. Ayejuyo, and T. Palanisami, “Interaction of chemical contaminants with microplastics: Principles and perspectives,” *Science of the Total Environment*, vol. 706, p. 135978, 2020.
- [164] L. Fu, J. Li, G. Wang, Y. Luan, and W. Dai, “Adsorption behavior of organic pollutants on microplastics,” *Ecotoxicology and Environmental Safety*, vol. 217, p. 112207, 2021.
- [165] G. Liu, Z. Zhu, Y. Yang, Y. Sun, F. Yu, and J. Ma, “Sorption behavior and mechanism of hydrophilic organic chemicals to virgin and aged microplastics in freshwater and seawater,” *Environmental Pollution*, vol. 246, pp. 26–33, 2019.
- [166] A. W. Wray, D. T. Papageorgiou, R. V. Craster, K. Sefiane, and O. K. Matar, “Electrostatic suppression of the “coffee stain effect”,” *Langmuir*, vol. 30, no. 20, pp. 5849–5858, 2014.
- [167] L. Ramos, G. Berenstein, E. A. Hughes, A. Zalts, and J. M. Montserrat, “Polyethylene film incorporation into the horticultural soil of small periurban production units in argentina,” *Science of the Total Environment*, vol. 523, pp. 74–81, 2015.
- [168] S. J. Cusworth, W. J. Davies, M. R. McAinsh, and C. J. Stevens, “A nationwide assessment of microplastic abundance in agricultural soils: The influence of plastic crop covers within the united kingdom,” *Plants, People, Planet*, 2023.
- [169] A. A. Horton, A. Walton, D. J. Spurgeon, E. Lahive, and C. Svendsen, “Microplastics in freshwater and terrestrial environments: Evaluating the current understanding to identify the knowledge gaps and future research priorities,” *Science of the total environment*, vol. 586, pp. 127–141, 2017.
- [170] J. Brahney, N. Mahowald, M. Prank, *et al.*, “Constraining the atmospheric limb of the plastic cycle,” *Proceedings of the National Academy of Sciences*, vol. 118, no. 16, 2021.
- [171] G. Zhang and Y. Liu, “The distribution of microplastics in soil aggregate fractions in southwestern china,” *Science of the Total Environment*, vol. 642, pp. 12–20, 2018.
- [172] S. Li, F. Ding, M. Flury, *et al.*, “Macro-and microplastic accumulation in soil after 32 years of plastic film mulching,” *Environmental Pollution*, vol. 300, p. 118945, 2022.

- [173] M. A. Arshad and G. M. Coen, "Characterization of soil quality: Physical and chemical criteria," *American Journal of Alternative Agriculture*, vol. 7, no. 1-2, pp. 25–31, 1992.
- [174] E. Amézketa, "Soil aggregate stability: A review," *Journal of sustainable agriculture*, vol. 14, no. 2-3, pp. 83–151, 1999.
- [175] C. D *et al.*, *Fundamentals of Soil Ecology*. London, England: Academic Press, 2018.
- [176] J. P. Eubeler, S. Zok, M. Bernhard, and T. P. Knepper, "Environmental biodegradation of synthetic polymers i. test methodologies and procedures," *TrAC Trends in Analytical Chemistry*, vol. 28, no. 9, pp. 1057–1072, 2009.
- [177] H. Liu, X. Yang, G. Liu, *et al.*, "Response of soil dissolved organic matter to microplastic addition in chinese loess soil," *Chemosphere*, vol. 185, pp. 907–917, 2017.
- [178] X. Cao, Y. Liang, J. Jiang, A. Mo, and D. He, "Organic additives in agricultural plastics and their impacts on soil ecosystems: Compared with conventional and biodegradable plastics," *TrAC Trends in Analytical Chemistry*, p. 117 212, 2023.
- [179] Y. I. Le Bissonais, "Aggregate stability and assessment of soil crustability and erodibility: I. theory and methodology," *European Journal of soil science*, vol. 47, no. 4, pp. 425–437, 1996.
- [180] V. S. Green, D. E. Stott, and M. Diack, "Assay for fluorescein diacetate hydrolytic activity: Optimization for soil samples," *Soil Biology and Biochemistry*, vol. 38, no. 4, pp. 693–701, 2006.
- [181] J. Gasperi, S. L. Wright, R. Dris, *et al.*, "Microplastics in air: Are we breathing it in?" *Current Opinion in Environmental Science & Health*, vol. 1, pp. 1–5, 2018.
- [182] E. MacArthur *et al.*, "Towards the circular economy," *Journal of Industrial Ecology*, vol. 2, no. 1, pp. 23–44, 2013.
- [183] L. Zimmermann, Z. Bartosova, K. Braun, J. Oehlmann, C. Völker, and M. Wagner, "Plastic products leach chemicals that induce in vitro toxicity under realistic use conditions," *Environmental science & technology*, vol. 55, no. 17, pp. 11 814–11 823, 2021.
- [184] S. Lambert and M. Wagner, "Environmental performance of bio-based and biodegradable plastics: The road ahead," *Chemical Society Reviews*, vol. 46, no. 22, pp. 6855–6871, 2017.
- [185] J. H. Duffus, M. Nordberg, and D. M. Templeton, "Glossary of terms used in toxicology, (iupac recommendations 2007)," *Pure and Applied Chemistry*, vol. 79, no. 7, pp. 1153–1344, 2007.

- [186] DEFRA. “Standards for bio-based, biodegradable and compostable plastics.” (), [Online]. Available: [https://assets.publishing.service.gov.uk/government/uploads/system/uploads/attachment\\_data/file/976912/standards-biobased-biodegradable-compostable-plastics.pdf](https://assets.publishing.service.gov.uk/government/uploads/system/uploads/attachment_data/file/976912/standards-biobased-biodegradable-compostable-plastics.pdf). Last accessed 2022-05-31.
- [187] E. Commission, *Bio-based biodegradable and compostable plastics*, [Online; Last accessed 2022-07-25]. [Online]. Available: [https://environment.ec.europa.eu/topics/plastics/bio-based-biodegradable-and-compostable-plastics\\_en](https://environment.ec.europa.eu/topics/plastics/bio-based-biodegradable-and-compostable-plastics_en).
- [188] M. R. Yates and C. Y. Barlow, “Life cycle assessments of biodegradable, commercial biopolymers—a critical review,” *Resources, Conservation and Recycling*, vol. 78, pp. 54–66, 2013.
- [189] W. Abdelmoez, I. Dahab, E. M. Ragab, O. A. Abdelsalam, and A. Mustafa, “Bio-and oxo-degradable plastics: Insights on facts and challenges,” *Polymers for Advanced Technologies*, vol. 32, no. 5, pp. 1981–1996, 2021.
- [190] A. Jahnke, H. P. H. Arp, B. I. Escher, *et al.*, “Reducing uncertainty and confronting ignorance about the possible impacts of weathering plastic in the marine environment,” *Environmental Science & Technology Letters*, vol. 4, no. 3, pp. 85–90, 2017.
- [191] C. T. Madhumitha, N. Karmegam, M. Biruntha, *et al.*, “Extraction, identification, and environmental risk assessment of microplastics in commercial toothpaste,” *Chemosphere*, vol. 296, p. 133976, 2022.
- [192] BBC. “Plastic pollution.” (2022), [Online]. Available: <https://www.bbc.co.uk/news/topics/c61pgw30011t>. Last accessed 2022-07-25.
- [193] D. K. Barnes, “Invasions by marine life on plastic debris,” *Nature*, vol. 416, no. 6883, pp. 808–809, 2002.
- [194] M. E. Iñiguez, J. A. Conesa, and A. Fullana, “Microplastics in spanish table salt,” *Scientific reports*, vol. 7, no. 1, pp. 1–7, 2017.
- [195] G. Liebezeit and E. Liebezeit, “Synthetic particles as contaminants in german beers,” *Food Additives & Contaminants: Part A*, vol. 31, no. 9, pp. 1574–1578, 2014.
- [196] M. Pivokonsky, L. Cermakova, K. Novotna, P. Peer, T. Cajthaml, and V. Janda, “Occurrence of microplastics in raw and treated drinking water,” *Science of the total environment*, vol. 643, pp. 1644–1651, 2018.

- [197] K. D. Cox, G. A. Covernton, H. L. Davies, J. F. Dower, F. Juanes, and S. E. Dudas, “Human consumption of microplastics,” *Environmental science & technology*, vol. 53, no. 12, pp. 7068–7074, 2019.
- [198] H. A. Leslie, M. J. Van Velzen, S. H. Brandsma, A. D. Vethaak, J. J. Garcia-Vallejo, and M. H. Lamoree, “Discovery and quantification of plastic particle pollution in human blood,” *Environment International*, vol. 163, p. 107199, 2022.
- [199] L. F. Amato-Lourenço, R. Carvalho-Oliveira, G. R. Júnior, L. dos Santos Galvão, R. A. Ando, and T. Mauad, “Presence of airborne microplastics in human lung tissue,” *Journal of Hazardous Materials*, vol. 416, p. 126124, 2021.
- [200] A. Ramsperger, V. K. B. Narayana, W. Groß, *et al.*, “Environmental exposure enhances the internalization of microplastic particles into cells,” *Science advances*, vol. 6, no. 50, eabd1211, 2020.
- [201] J. M. Shim, W. S. Lee, J. Moon, and M. Song, “Coffee shop corporate social responsibility (csr) and reuse intention using triple bottom line theory,” *British Food Journal*, 2021.
- [202] British Plastics Federation, *Plastics applications*, Last accessed online 2021-06-09. [Online]. Available: <https://www.bpf.co.uk/plastipedia/applications/Default.aspx>.
- [203] M. Singhvi, S. Zinjarde, and D. Gokhale, “Polylactic acid: Synthesis and biomedical applications,” *Journal of applied microbiology*, vol. 127, no. 6, pp. 1612–1626, 2019.
- [204] T. Iwata, “Biodegradable and bio-based polymers: Future prospects of eco-friendly plastics,” *Angewandte Chemie International Edition*, vol. 54, no. 11, pp. 3210–3215, 2015.
- [205] J. S. Viera, M. R. Marques, M. C. Nazareth, P. C. Jimenez, C. Sanz-Lázaro, and Í. B. Castro, “Are biodegradable plastics an environmental rip off?” *Journal of Hazardous Materials*, vol. 416, p. 125957, 2021.
- [206] R. Steen, C. S. Torjussen, D. W. Jones, T. Tsimpidis, and A. Miliou, “Plastic mistaken for prey by a colony-breeding eleonora’s falcon (*Falco eleonora*) in the mediterranean sea, revealed by camera-trap,” *Marine pollution bulletin*, vol. 106, no. 1-2, pp. 200–201, 2016.
- [207] A. Hernandez-Gonzalez, C. Saavedra, J. Gago, P. Covelo, M. B. Santos, and G. J. Pierce, “Microplastics in the stomach contents of common dolphin (*Delphinus delphis*) stranded on the galician coasts (NW Spain, 2005–2010),” *Marine pollution bulletin*, vol. 137, pp. 526–532, 2018.

- [208] R. Lehner, C. Weder, A. Petri-Fink, and B. Rothen-Rutishauser, “Emergence of nanoplastic in the environment and possible impact on human health,” *Environmental science & technology*, vol. 53, no. 4, pp. 1748–1765, 2019.
- [209] S. O. Idowu, “An exploratory study of the historical landscape of corporate social responsibility in the uk,” *Corporate Governance: The international journal of business in society*, 2011.
- [210] A. B. Carroll, “A history of corporate social responsibility: Concepts and practices,” *The Oxford handbook of corporate social responsibility*, vol. 1, 2008.
- [211] A. Dahlsrud, “How corporate social responsibility is defined: An analysis of 37 definitions,” *Corporate social responsibility and environmental management*, vol. 15, no. 1, pp. 1–13, 2008.
- [212] A. McWilliams, D. S. Siegel, and P. M. Wright, “Corporate social responsibility: Strategic implications,” *Journal of management studies*, vol. 43, no. 1, pp. 1–18, 2006.
- [213] A. B. Carroll *et al.*, “The pyramid of corporate social responsibility: Toward the moral management of organizational stakeholders,” *Business horizons*, vol. 34, no. 4, pp. 39–48, 1991.
- [214] M. Friedman, *A friedman doctrine: The social responsibility of business is to increase its profits*, Accessed online 2021-06-08; originally published in the New York Times September 13th 1970. [Online]. Available: [nytimes.com/1970/09/13/archives/a-friedman-doctrine-the-social-responsibility-of-business-is-to.html](https://www.nytimes.com/1970/09/13/archives/a-friedman-doctrine-the-social-responsibility-of-business-is-to.html).
- [215] M. S. Schwartz and D. Saiia, “Should firms go “beyond profits”? milton friedman versus broad csr 1,” *Business and Society Review*, vol. 117, no. 1, pp. 1–31, 2012.
- [216] D. Jamali, “The csr of mnc subsidiaries in developing countries: Global, local, substantive or diluted?” *Journal of Business Ethics*, vol. 93, no. 2, pp. 181–200, 2010.
- [217] D. Matten and A. Crane, “Corporate citizenship: Toward an extended theoretical conceptualization,” *Academy of Management review*, vol. 30, no. 1, pp. 166–179, 2005.
- [218] K. E. Smith, A. B. Gilmore, G. Fooks, J. Collin, and H. Weishaar, *Tobacco industry attempts to undermine article 5.3 and the “good governance” trap*, 2009.
- [219] H. R. Bowen, *Social responsibilities of the businessman*. University of Iowa Press, 2013, First published 1953.

- [220] J. Salazar and B. W. Husted, "Principals and agents: Further thoughts on the friedmanite critique of corporate social responsibility," *Crane, Andrew; McWilliams, Abigail; Matten, Dirk; Moon, Jeremy*, pp. 137–155, 2008.
- [221] M. Van Marrewijk, "Concepts and definitions of csr and corporate sustainability: Between agency and communion," *Journal of business ethics*, vol. 44, no. 2, pp. 95–105, 2003.
- [222] A. B. Carroll, "Carroll's pyramid of csr: Taking another look," *International journal of corporate social responsibility*, vol. 1, no. 1, pp. 1–8, 2016.
- [223] W. B. Werther Jr and D. Chandler, "Strategic corporate social responsibility as global brand insurance," *Business Horizons*, vol. 48, no. 4, pp. 317–324, 2005.
- [224] C. Stoian and M. Gilman, "Corporate social responsibility that "pays": A strategic approach to csr for smes," *Journal of Small Business Management*, vol. 55, no. 1, pp. 5–31, 2017.
- [225] H. Jenkins, "A critique of conventional csr theory: An sme perspective," *Journal of general Management*, vol. 29, no. 4, pp. 37–57, 2004.
- [226] M. Landon-Lane, "Corporate social responsibility in marine plastic debris governance," *Marine pollution bulletin*, vol. 127, pp. 310–319, 2018.
- [227] The House Of Commons Library, *Plastic bags - the single use carrier bag charge*, Accessed 2021-06-07. [Online]. Available: <https://commonslibrary.parliament.uk/research-briefings/cbp-7241/>.
- [228] UK Government, *Single use carrier bag charge: Data in england for 2019-2020*, Accessed 2021-06-07. [Online]. Available: <https://www.gov.uk/government/publications/carrier-bag-charge-summary-of-data-in-england/single-use-plastic-carrier-bags-charge-data-in-england-for-2019-to-2020>.
- [229] K. Shampanier, N. Mazar, and D. Ariely, "Zero as a special price: The true value of free products," *Marketing science*, vol. 26, no. 6, pp. 742–757, 2007.
- [230] Tesco, *Tesco to remove one billion pieces of plastic from products by the end of 2020*, Last accessed online 2021-06-09. [Online]. Available: <https://www.tescopl.com/news/2019/tesco-to-remove-one-billion-pieces-of-plastic-from-products-by-the-end-of-2020/>.

- [231] ASDA, *Asda removes more than 100m pieces of single use plastic from its stores*, Last accessed online 2021-06-09. [Online]. Available: <https://corporate.asda.com/newsroom/2021/03/18/asda-removes-more-than-100m-pieces-of-single-use-plastic-from-its-stores>.
- [232] Morrison's, *Plastic packaging*, Last accessed online 2021-06-09. [Online]. Available: <https://www.morrisons-corporate.com/cr/policy/plastics/>.
- [233] Sainsbury's, *Sainsbury's to halve plastic packaging by 2025*, Last accessed online 2023-11-18. [Online]. Available: <https://www.about.sainsburys.co.uk/news/latest-news/2019/13-09-2019-sainsburys-to-halve-plastic-packaging-by-2025>.
- [234] Iceland, *Plastic free by 2023*, Last accessed online 2021-06-09. [Online]. Available: <https://about.iceland.co.uk/plastic-free-by-2023/>.
- [235] Waitrose, *Plastics and packaging*, Last accessed online 2021-06-09. [Online]. Available: [https://www.waitrose.com/home/inspiration/about\\_waitrose/the\\_waitrose\\_way/packaging.html](https://www.waitrose.com/home/inspiration/about_waitrose/the_waitrose_way/packaging.html).